

**Synthesis of Stimuli-Responsive Polymers via
Nitroxide Mediated Polymerization and
Characterization in Aqueous and Ionic Liquid Solutions**

Chi Zhang

Doctoral Thesis

Department of Chemical Engineering

McGill University

Montreal, Quebec

April 2014

Thesis submitted in partial fulfillment of the requirements for the degree of Doctor of
Philosophy

© Chi Zhang, 2014. All rights reserved.

Acknowledgements

First and foremost, I would like to express my deepest gratitude towards my supervisor, Prof. Milan Maric, for his constant and invaluable guidance, mentoring and support throughout the course of my Ph.D. program. His emphasis on integrity and diligence will continue to inspire and influence my professional and person development.

I want to thank all my current and past colleagues at McGill University, especially Benoit, for his training and help at the beginning of my program, and Xeniya, Stacey, ZiJun, Keith, and Alex, for the numerous delightful discussions.

I want to thank Frank Caporuscio, Jo-Ann Gadsby, Lou Cusmich, Gerald Lepkyj, Ranjan Roy, Andrew Golsztajn, Emily Musgrave, Melanie Gorman and all other technical and administrative staff of the Chemical Engineering Department, without whom I would not have been able to achieve my research goals. I am also grateful towards Prof. Bruce Lennox, for providing access to his UV-Vis spectrometer and fluorescent spectrophotometer, along with Dr. Paul Goulet for his training on the use of the instruments. I thank the Center for Self-Assembled Chemical Structures (CSACS) for providing access to their equipment and Petr Fiurasek for his training.

I am very grateful for the financial support from McGill University, NSERC Postgraduate Scholarship, NSERC Discovery Grant and Canada Foundation for Innovation New Opportunities Fund. I also thank Arkema, Inc. (Scott Schmidt and Noah Macy) for supplying BlocBuilderTM and SG1.

Last but not least, I want to dedicate my most sincere appreciation for the love and support from my family. I want to thank my loving husband, Erik, for always standing by me and enlightening my life everyday. I want to thank my parents, for their continuous confidence in me, which fostered my independence and courage that help me navigate through this long and adventurous journey far away from home.

Abstract

Stimuli-responsive polymers have been touted as "smart" due to their fast and reversible responses to environmental changes. It is imperative for these polymers to have well-defined structures so that their performance can be consistent and predictable. In order to achieve this, nitroxide mediated polymerization (NMP) was employed as the synthesis technique for the microstructured polymers that form the core of the investigations presented in this thesis. As one of the main controlled radical polymerization techniques, NMP stands out for its simplicity in both required ingredients and purification procedures.

Many known stimuli-responsive polymers are poly(methacrylates). However, homopolymerization of methacrylates has been challenging for NMP mainly due to the large equilibrium constant that resulted in high concentration of active radicals and thus excessive irreversible terminations. By using a small amount of "controlling co-monomer" such as styrene, copolymerizations with methacrylate-rich feeds can be controlled using the commercially available alkoxyamine initiator BlocBuilder™ via NMP, featuring linear increases in number average molecular weight versus conversion, and narrow molecular weight distribution.

In this thesis, two methacrylates, namely 2-(dimethylamino)ethyl methacrylate (DMAEMA) and benzyl methacrylate (BzMA), whose homopolymers exhibit LCST-type phase separation behaviours in aqueous and ionic liquid (IL) solutions, respectively, were copolymerized with various controlling co-monomers by NMP to demonstrate the versatility of NMP in tuning thermo-responsive properties. For both methacrylates,

styrene was initially used as the controlling co-monomer, where about 10 mol% styrene for DMAEMA and 20 mol% styrene for BzMA was found necessary to obtain copolymers with relatively narrow molecular weight distribution ($\overline{M}_w/\overline{M}_n \approx 1.3 - 1.4$) and ability to extend chains to form block copolymers when reinitiated with a fresh batch of monomer. 2-Vinylpyridine (2VP) was then chosen to copolymerize with DMAEMA for its lower hydrophobicity compared to styrene and pH-sensitivity, where about 2 - 5 mol% 2VP was shown sufficient to obtain well-defined DMAEMA/2VP copolymers that can be later used as effective macroinitiators to form block copolymers. For both DMAEMA/styrene and DMAEMA/2VP copolymerizations, a modified alkoxyamine initiator bearing a succinimidyl ester (NHS-BlocBuilder) made by coupling of BlocBuilderTM and *N*-hydroxysuccinimide was used to impart α -functionality to these stimuli-responsive polymers. The succinimidyl ester moiety allows single step conjugation to amine-containing compounds, which was demonstrated by the pre-polymerization coupling of poly(propylene glycol) (PPG) and NHS-BlocBuilder, yielding a macroinitiator that was then used to synthesize doubly thermo-responsive PPG-*b*-DMAEMA/2VP block copolymer. The detailed phase behaviour characterization of these DMAEMA-rich copolymers in aqueous solutions revealed the effects of important factors such as pH, copolymer composition, solution concentration and polymer microstructure, on the tuning of transition temperatures.

For BzMA, 9-(4-vinylbenzyl)-9H-carbazole (VBK) was used as an alternative controlling co-monomer. Controlled and pseudo-“living” copolymerizations were achieved with as little as 2 mol% VBK in the feed, demonstrating significant improvement compared to the BzMA/styrene system. The incorporation of fluorescent VBK resulted in 5-fold

fluorescence enhancement during the phase separation of BzMA/VBK copolymers from IL [C₂mim][NTf₂]. The enhancement resulted from heightened efficiency of the fluorescence resonance energy transfer (FRET) between BzMA and VBK during aggregation. However, the solvophobicity of VBK also significantly reduced the solubility of BzMA/VBK copolymers in the IL and rendered the phase separation irreversible. Further investigation on the effects of solvophilicity and chain mobility on phase separation and reversibility in ILs was carried out by incorporating varying amounts of solvophilic co-monomer, namely methyl methacrylate (MMA) and oligo(ethylene glycol) methacrylate (OEGMA), yielding BzMA/MMA/VBK and BzMA/OEGMA/VBK terpolymers. It was found that molecular weight and solution concentration played important roles on phase separation temperature but sufficiently high solvophilicity (quantified by the concentration of solvophilic group) was essential to facilitate the re-dissolution process after phase separation.

Abrégé

Polymères stimulables ont été célébrés comme «Polymères intelligents» en raison de leurs réponses rapides et réversibles aux changements environnementaux. Il est impératif pour ces polymères d'avoir des structures bien définies afin que leur transformation puisse être bien défini et réversible. Afin d'atteindre cet objectif, la polymérisation médiée par nitroxyde (NMP) a été utilisée comme technique de synthèse des polymères microstructurées et ceci représente la majorité des études et découvertes présentées dans cette thèse. Comme l'une des principales techniques de polymérisation radicalaire contrôlée, l'NMP se distingue par sa simplicité en tant qu'ingrédients nécessaires et de procédures de purification.

De nombreux polymères stimulables qui sont connus sont des poly(méthacrylates). Cependant, l'homopolymérisation de méthacrylates a été difficile par l'NMP principalement en raison de la grande constante d'équilibre qui accompagne une grande concentration de radicaux actifs et ainsi des terminaisons excessives et irréversibles. En utilisant une petite quantité de "co-monomère contrôlant" tel que le styrène, les copolymérisations de polymères riches en méthacrylate peuvent être contrôlées et synthétisées par l'NMP en utilisant l'initiateur alcoxyamine BlocBuilderTM qui est accessible commercialement, donnant comme résultats une augmentation linéaire de la masse moléculaire moyenne en nombre par rapport à la conversion, et une distribution étroite de poids moléculaire.

Dans cette thèse, deux méthacrylates, 2-(diméthylamino)éthyl méthacrylate (DMAEMA) and benzyl méthacrylate (BzMA), dont les homopolymères présentent des comportements de séparation de phase de type LCST dans un liquide aqueux et liquide ionique (IL), respectivement, ont été copolymérisés avec divers monomères contrôlant par l’NMP pour démontrer la polyvalence de l’NMP comme manipulation pour la synthèse de polymères stimulables. Pour les deux méthacrylates, le styrène a été initialement utilisé comme co-monomère de contrôle, où environ 10 % en moles de styrène pour DMAEMA et de 20% en moles de styrène pour BzMA a été trouvé nécessaire d'obtenir des copolymères à distribution de poids moléculaires relativement étroite ($\overline{M}_w/\overline{M}_n \approx 1.3$ à 1.4) et d’avoir la capacité d’être utilisée comme initiateur de nouveaux monomères pour la formation de copolymères à blocs. 2-vinyl-pyridine (2VP) a été ensuite choisie pour copolymériser avec DMAEMA, à cause de son caractère moins hydrophobe par rapport au styrène et sa sensibilité aux pH, où environ 2-5% en moles de 2VP a été montré suffisante pour obtenir des copolymères DMAEMA/2VP bien définies qui peuvent être utilisés comme macroinitiateurs efficaces pour la formation des copolymères à blocs. Pour les deux système de copolymérisations, DMAEMA/styrène et DMAEMA/2VP, un initiateur alkoxyamine modifiée portant un succinimidylester (NHS-BlocBuilder) synthétisé par couplage de BlocBuilderTM et N-hydroxy a été utilisé pour donner α -fonctionnalité de ces polymères stimulables. Le groupement ester de succinimidyle permet la conjugaison avec des molécules qui contient des amines dans une étape, ce qui a été démontré par le couplage de pré-polymérisation de poly(propylène glycol) (PPG) et NHS-Blocbuilder, ce qui donne un macro-initiateur qui a ensuite été utilisé pour synthétiser un polymère doublement thermo-sensible avec

séquencé PPG-b-DMAEMA/2VP. La caractérisation détaillée le comportement de phase de ces copolymères DMAEMA riche en solutions aqueuses révéla les effets des facteurs importants, tels que le pH, la composition du copolymère, la concentration de la solution et de la microstructure du polymère, sur le réglage de la température de transition .

Pour BzMA, 9-(4-vinylbenzyle)-9H-carbazole (VBK) a été utilisé comme une alternative à commander co-monomère. Les copolymérisations contrôlés et « pseudo-vivant » ont été obtenus avec aussi peu que 2 % en moles VBK dans l'alimentation, ce qui démontre une amélioration significative par rapport au système BzMA/styrène. L'incorporation de fluorescence VBK abouti à l'amélioration de la fluorescence de 5 fois au cours de la séparation de phases de copolymères BzMA/VBK dissous dans l'IL [C₂mim][NTf₂]. L'amélioration résulte de l'efficacité accrue du transfert d'énergie de résonance de fluorescence (FRET) entre BzMA et VBK lors de l'agrégation. Cependant, la solvato-phobicité de VBK également réduit de manière significative la solubilité des copolymères de BzMA/VBK dans l'IL et a rendu la séparation de phase irréversible. Les investigations de la solvato-philicity et la mobilité de chaînes pendant la séparation de phase en ajout de la réversibilité thermo-stimulables dans les ILs a été effectuée en incorporant des quantités variables de co-monomère solvato-philic différent de méthacrylate de méthyle (MMA) et de l'oligo(éthylène glycol) méthacrylate (OEGMA), donnant comme résultat BzMA/ MMA/VBK et BzMA/OEGMA/VBK terpolymères. On a trouvé que le poids moléculaire et la concentration de la solution jouée un rôle important sur la température de séparation de phase, mais une quantité suffisamment élevée de monomères solvato-philicity (quantifié par la concentration du groupe

solvatophilic) était essentielle pour faciliter le processus de re-dissolution après séparation des phases.

Contributions of authors

This thesis is manuscript-based and contains 5 manuscripts where I, Chi Zhang, am the first author and have done the majority of the work. In all cases, I conducted all the polymer synthesis, characterization and data analysis. I also wrote all the manuscripts that were then edited and revised by my supervisor Prof. Milan Maric before submitting to peer-reviewed journals. Benoit Lessard, a former Ph.D. student of Prof. Maric, provided me initial training on synthesis techniques and the use of characterization instruments. The manuscripts presented in this thesis are listed below:

- i. **Zhang, C.;** Maric, M. *Polymers* **2011**, *3*, 1398-1422; **(Chapter 3)**
- ii. **Zhang, C.;** Maric, M. *J. Polym. Sci. Part A: Polym. Chem.* **2012**, *50*, 4341-4357; **(Chapter 4)**
- iii. **Zhang, C.;** Lessard, B.; Maric, M. *Macromol. React. Eng.* **2010**, *4*, 415-423; **(Chapter 5)**
- iv. **Zhang, C.;** Maric, M. *J. Polym. Sci. Part A: Polym. Chem.* **2013**, *51*, 4702-4715; **(Chapter 6)**
- v. **Zhang, C.;** Maric, M. *Submitted to Polymer Chemistry, Manuscript ID: PY-ART-02-2014-000300* **2014. (Chapter 7).**

Table of contents

Acknowledgements	ii
Abstract	ivv
Abrégé	vii
Contributions of authors	xii
Table of contents	xiii
List of Tables	xix
List of Figures	xxiii
Chapter 1	1
Introduction	1
1.1 Introduction to smart materials	1
1.2 Ionic liquids and their properties as solvents	2
1.3 Phase separation behaviour of polymers	4
1.3.1 Phase separation in conventional solvents	4
1.3.2 LCST-type phase separation in aqueous and ionic liquid solutions.....	7
1.3.3 Effect of molecular weight distribution on phase separation behaviour	9
1.4 Organization of this thesis	11
Chapter 2	14
Literature Review	14
2.1 Controlled radical polymerization	14

2.2 Nitroxide mediated polymerization.....	15
2.3 Methacrylate polymerization by NMP	17
Chapter 3	22
Controlled Synthesis of Water-soluble and Stimuli-responsive Copolymers	
with Small Amount of Styrene by NMP	22
3.1 Preface.....	22
3.2 Introduction	25
3.3. Results and Discussion	29
3.3.1. Synthesis of statistical copolymers of 2-(dimethylamino)ethyl methacrylate (DMAEMA) and styrene.....	29
3.4 Conclusions.....	52
Chapter 4	54
α-Functional Statistical Copolymers with Dual pH and Temperature	
Responsiveness Made by NMP using 2-Vinylpyridine as “Controlling” Co-	
monomer	54
4.1 Preface.....	54
4.2 Introduction	57
4.3 Results and Discussion	61
4.3.1 Homopolymerization of 2-vinylpyridine (2VP) using NHS-BlocBuilder	62
4.3.2 Statistical copolymerization of 2-(dimethylamino)ethyl methacrylate (DMAEMA) and 2-vinylpyridine (2VP) using NHS-BlocBuilder	64
4.3.4 Temperature and pH sensitivities of the block copolymers	85
4.4 Conclusions.....	90

Chapter 5	93
Controlled Synthesis of Benzyl Methacrylate-rich Copolymer via NMP using Styrene as “Controlling” Co-monomer.....	93
5.1 Preface.....	93
5.2 Introduction	96
5.3 Results and Discussion	99
5.3.1 Effect of Initial Feed Composition on Copolymerization Kinetics	99
5.3.2 Effect of Initial Feed Composition on Molecular Weight Distribution and Copolymer “Livingness”	104
5.3.3 Determination of Copolymerization Reactivity Ratios.....	110
5.4 Conclusion.....	113
Chapter 6	115
Benzyl Methacrylate-rich Copolymers synthesized by NMP that are Fluorescent and Thermo-responsive in an Ionic Liquid	115
6.1 Preface.....	115
6.2 Introduction	118
6.3 Results and discussions.....	121
6.3.1 Effects of feed composition on polymerization kinetics and control	121
6.3.2 Chain extension of BzMA/VBK statistical copolymers	127
6.3.3 Temperature sensitivity and fluorescence properties of statistical copolymers in [C ₂ mim][NTf ₂]	129
6.3.4 Effect of microstructure on fluorescence properties of the block copolymers in [C ₂ mim][NTf ₂]	140
6.4 Conclusions.....	143

Chapter 7	146
Effects of Solvatophilicity of Statistical Terpolymers on Phase Separation and Reversibility in an Ionic Liquid.....	146
7.1 Preface.....	146
7.2. Introduction	149
7.3 Results and Discussion	153
7.3.1 Terpolymerization kinetics and polymerization control	153
7.3.2 Temperature sensitivity and fluorescence properties of terpolymers in [C ₂ mim][NTf ₂].....	157
7.4 Conclusions.....	171
Chapter 8	173
Conclusions.....	173
8.1 Summary	173
8.2 Statement of contributions	176
8.3 Recommendations for future work.....	179
Appendices.....	182
Appendix A.....	183
Controlled Synthesis of Water-soluble and Stimuli-responsive copolymers with small amount of styrene by NMP	183
A.1 Experimental Section	183
A.1.1 Materials.....	183
A.1.2 Synthesis of N-hydroxysuccinimide functionalized BlocBuilder (NHS-BlocBuilder)	183

A.1.3 Synthesis of statistical copolymers of 2-(dimethylamino)ethyl methacrylate and styrene (poly(DMAEMA- <i>stat</i> -styrene)) by NMP.....	184
A.1.4 Polymer characterization using Gel permeation chromatography (GPC) and Nuclear magnetic resonance (NMR).....	186
A.1.5 Transition temperature characterization using UV-Visible spectrometry and Dynamic light scattering (DLS)	187
Appendix B.....	189
α-Functional Statistical Copolymers with Dual pH and Temperature Responsiveness Made by NMP using 2-Vinylpyridine as “Controlling” Co-monomer	189
B.1 Experimental Section	189
B.1.2 Materials.....	189
B.1.3 Homopolymerization of 2-vinylpyridine (2VP) using NHS-BlocBuilder as initiator	189
B.1.2 Statistical copolymerization of 2-(dimethylamino)ethyl methacrylate (DMAEMA) and 2-vinylpyridine (2VP).....	190
B.1.3 Synthesis of poly(propylene oxide)-coupled BlocBuilder (PPO-BB) macroalkoxyamine	192
B.1.4 Synthesis of statistical copolymer of DMAEMA and 2VP using PPO-BB macroalkoxyamine	193
B.1.5 Chain extension experiments	194
B.1.6 Gel permeation chromatography.....	195
B.1.7 Characterization of the aqueous solutions of the statistical copolymers and block copolymers.....	195

B.2 Supporting Information	196
Appendix C	198
Controlled Synthesis of Benzyl Methacrylate-rich Copolymer via NMP using Styrene as “Controlling” Co-monomer	198
C.1 Experimental Section	198
C.1.1 Materials	198
C.1.2 Synthesis of BzMA/Styrene Random Copolymers	198
C.1.3 Chain Extensions with Styrene	200
C.1.5 Characterization	201
Appendix D.....	202
Benzyl Methacrylate-rich Copolymers synthesized by NMP that are Fluorescent and Thermo-responsive in an Ionic Liquid.....	202
D.1 Experimental Section.....	202
D.1.1 Materials.....	202
D.1.2 Statistical copolymerization of benzyl methacrylate (BzMA) and 9-(4- Vinylbenzyl)-9H-carbazole (VBK)	203
D.1.3 Chain extension experiments.....	204
D.1.4 Gel permeation chromatography	206
D.1.5 Characterization of the statistical copolymers and block copolymers in ionic liquid solutions.....	206
D.2 Supporting Information.....	207
Appendix E	211

Effects of solvatophilicity of statistical terpolymers on phase separation and reversibility in an ionic liquid	211
E.1 Experimental section	211
E.1.1 Materials	211
E.1.2 Terpolymerization of benzyl methacrylate (BzMA), methyl methacrylate (MMA) or oligo(ethylene glycol) methyl ether methacrylate (OEGMA) ,and 9-(4-Vinylbenzyl)-9H-carbazole (VBK)	212
E.1.3 Gel permeation chromatography	215
E.1.4 Characterization of the ionic liquid solutions of the terpolymers	216
References.....	217

List of Tables

Table 3-1.	Results of the copolymerizations of 2-(dimethylamino)ethyl methacrylate (DMAEMA) and styrene at 80 °C in bulk using <i>N</i> -hydroxysuccinimidyl-functionalized BlocBuilder as initiator.....	34
Table 3-2.	Summary of the experimental results and polymer properties in the chain extension experiments at 80 °C in bulk.	35
Table 3-3.	Lower critical solution temperature (LCST) of poly(DMAEMA- <i>stat</i> -styrene) at different pH at 0.5 wt% concentration.....	47
Table 4-1.	Molecular weight and composition characterizations of 2VP and DMAEMA homopolymers as well as DMAEMA/2VP statistical copolymers initiated by NHS-BlocBuilder or PPO-BB.....	62
Table 4-2.	Properties of the macroinitiators and chain-extended block copolymers in the chain extension experiments.....	74
Table 4-3.	Comparison of kinetics for DMAEMA/2VP copolymerizations with and without free SG1 nitroxide.	77
Table 4-4.	Cloud point temperature (CPT) of DMAEMA homopolymer and DMAEMA/2VP copolymers at 0.5 wt% concentration and various pH.....	80
Table 5-1.	Propagation Rate Constants and Activation-Deactivation Equilibrium Constants of Styrene and Methacrylates.	97
Table 5-2.	Summary of Benzyl Methacrylate/Styrene Copolymerization Performed in Bulk at 90 °C.....	99

Table 5-3.	Kinetic Parameters Derived from the Semilogarithmic Kinetic Plots for Copolymerization of Benzyl Methacrylate and Styrene in Bulk at 90°C by NMP.	101
Table 5-4.	Kinetic Parameters for Benzyl Methacrylate and Styrene Homopolymerizations.	103
Table 5-5.	Chain Extension with Styrene using Benzyl Methacrylate/Styrene Random Copolymers as Macroinitiator at 110 °C.	109
Table 5-6.	Initial Feed Compositions and Compositions of Benzyl Methacrylate/Styrene Copolymers.	112
Table 5-7.	Monomer Reactivity Ratios for Benzyl Methacrylate (r_1) and Styrene (r_2)	112
Table 6-1.	Summary of polymerizations and molecular properties for the statistical copolymerizations benzyl methacrylate (BzMA or methyl methacrylate (MMA)) with 9-(4-vinylbenzyl)-9 <i>H</i> -carbazole (VBK) via nitroxide mediated polymerization with BlocBuilder.	122
Table 6-2.	Composition and molecular weight characterizations of the macroinitiators and chain extended block copolymers.	128
Table 6-3.	Glass transition temperature (T_g) determined by differential scanning calorimetry (DSC) and cloud point temperature (CPT) of the statistical copolymers in [C ₂ mim][NTf ₂] (3 wt%) measured by UV-Vis spectrometry at two different heating rates.	130
Table 6-4.	Cloud point temperature (CPT) of the block copolymers in [C ₂ mim][NTf ₂] and glass transition temperature (T_g) of the block copolymers.	141

Table 7-1. Summary of characterization data for terpolymers of benzyl methacrylate (BzMA), methyl methacrylate (MMA) or oligo(ethylene glycol)methyl methacrylate (OEGMA) and 9-(4-vinylbenzyl)-9H-carbazole (VBK) synthesized at 90 °C in 20 wt% DMF solution.	153
Table 7-2. Feed composition and the product of average propagation rate constant, $\langle k_p \rangle$, and propagating radical concentration, $[P^\bullet]$, $\langle k_p \rangle [P^\bullet]$, for terpolymerizations of benzyl methacrylate (BzMA), methyl methacrylate (MMA) or oligo(ethylene glycol)methyl methacrylate (OEGMA) and 9-(4-vinylbenzyl)-9H-carbazole (VBK).	155
Table 7-3. Summary of polymer composition, number average molecular weight, glass transition temperature and cloud point temperature (CPT) in $[C_2mim][NTf_2]$ (3 wt% concentration) of the terpolymers.	158
Table A-1. Experimental conditions of the bulk copolymerizations of 2-(dimethylamino)ethyl methacrylate (DMAEMA) and styrene (S) at 80 °C using <i>N</i> -hydroxysuccinimidyl-functionalized BlocBuilder (NHS-BlocBuilder) as initiator.	185
Table A-2. Experimental conditions of the chain extension experiments at 80 °C in bulk.	186
Table B-1. Experimental conditions for the bulk homopolymerization of 2-vinylpyridine (2VP) and 2-(dimethylamino)ethyl methacrylate (DMAEMA) as well as DMAEMA/2VP statistical copolymerizations using NHS-BlocBuilder as the initiator.	192
Table B-2. Experimental conditions of the chain extension experiments.	195

Table D-1. Experimental conditions for statistical copolymerization of benzyl methacrylate (BzMA) (or methyl methacrylate (MMA)) with 9-(4-vinylbenzyl)-9H-carbazole (VBK) in dimethylformamide (DMF) solution at 90 °C and homopolymerization of BzMA in bulk at 80 °C via nitroxide mediated polymerization with BlocBuilder.	204
Table D-2. Experimental conditions for chain extension experiments using selected statistical copolymer of benzyl methacrylate (BzMA) (or methyl methacrylate (MMA)) with 9-(4-vinylbenzyl)-9H-carbazole (VBK) as macroinitiators at 90 °C.....	206
Table E-1. Experimental conditions for terpolymerizations of benzyl methacrylate (BzMA), methyl methacrylate (MMA) or oligo(ethylene glycol)methyl methacrylate (OEGMA) and 9-(4-vinylbenzyl)-9H-carbazole (VBK) in dimethylformamide (DMF) solution at 90 °C via NMP.....	215

List of Figures

- Figure 1-1. Molecular structure of cations and anions in common ionic liquids. 3
- Figure 1-2. A comparison between polymer/solvent systems that exhibit a) an upper critical solution temperature (UCST) and b) lower critical solution temperature (LCST)..... 6
- Figure 1-3. Molecular structures of well-known thermo-responsive polymers in aqueous and ionic liquid solutions..... 9
- Figure 3-1. (a) Kinetic plots of $\ln[(1-\text{conversion})^{-1}]$ versus time for the statistical copolymerizations of 2-(dimethylamino)ethyl methacrylate (DMAEMA) and styrene at 80 °C with initial feed composition with respect to DMAEMA (f_{DMAEMA}) of 80 mol% (\times), 85 mol% (\blacktriangle), 90 mol% (\blacklozenge), and 95 mol% (\blacksquare). (b) Product of average propagation constant, $\langle k_p \rangle$, and concentration of propagating radical, $[P^\cdot]$, $\langle k_p \rangle [P^\cdot]$ (slope of the kinetic plots in Figure 3-1 (a)), versus initial feed composition with respect to DMAEMA (f_{DMAEMA}); error bars represent standard deviations of the slopes from Figure 3-1 (a). 31
- Figure 3-2. (a) Number-average molecular weight (M_n) and (b) dispersity (\mathcal{D}) of poly(DMAEMA-*stat*-styrene) with initial feed composition with respect to DMAEMA (f_{DMAEMA}) of 80 mol% (\times), 85 mol% (\blacktriangle), 90 mol% (\blacklozenge), and 95 mol% (\blacksquare) versus conversion; solid line in (a) represents theoretical trend. M_n determined by GPC calibrated with poly(styrene) standards. 33

Figure 3-3. GPC traces of macroinitiators (dashed line) and chain extended polymers (solid line) for the chain extension of (a) DMAEMA/S-80/20 with a second feed of $f_{DMAEMA} = 95$ mol% and (b) DMAEMA/S-90/10 macroinitiator with a second feed of $f_{DMAEMA} = 90$ mol%. 36

Figure 3-4. Light transmittance as a function of temperature of poly(DMAEMA-*stat*-styrene) copolymers with (a) $F_{DMAEMA} = 96$ mol% (DMAEMA/S-95/5) (b) $F_{DMAEMA} = 89$ mol% (DMAEMA/S-90/10) (c) $F_{DMAEMA} = 84$ mol% (DMAEMA/S-85/15) (d) $F_{DMAEMA} = 81$ mol% (DMAEMA/S-80/20) at 0.1 wt% (dotted line), 0.3 wt% (dashed line) and 0.5 wt% (solid line) in de-ionized water measured by UV-Vis spectrometry..... 40

Figure 3-5. Hydrodynamic radii of copolymers (R_h) as a function of temperature of poly(DMAEMA-*stat*-styrene) copolymers with (a) $F_{DMAEMA} = 96$ mol% (DMAEMA/S-95/5) (b) $F_{DMAEMA} = 89$ mol% (DMAEMA/S-90/10) (c) $F_{DMAEMA} = 84$ mol% (DMAEMA/S-85/15) (d) $F_{DMAEMA} = 81$ mol% (DMAEMA/S-80/20) at 0.1 wt% (\blacktriangle), 0.3 wt% (\blacksquare) and 0.5 wt% (\blacklozenge) in de-ionized water measured by dynamic light scattering..... 41

Figure 3-6. Hydrodynamic radius distribution (using mean % intensity) for 0.3 wt% solution of poly(DMAEMA-*stat*-styrene) with $F_{DMAEMA} = 96$ mol% (DMAEMA/S-95/5) at 40–42 °C..... 42

Figure 3-7. LCST of poly(DMAEMA-*stat*-styrene) as a function of DMAEMA molar composition in the copolymer (F_{DMAEMA}) in de-ionized water at 0.1 wt% (\blacktriangle), 0.3 wt% (\blacksquare) and 0.5 wt% (\blacklozenge) concentration; filled symbols are DLS results and hollow symbols are UV-Vis results..... 44

- Figure 3-8. LCST of poly(DMAEMA-*stat*-styrene) with 96 mol% DMAEMA (DMAEMA/S-95/5, ■), 89 mol% DMAEMA (DMAEMA/S-90/10, ◆), and 84 mol% DMAEMA (DMAEMA/S-85/15, ▲), as a function of solution concentration in de-ionized water; filled symbols are DLS results and hollow symbols are UV-Vis results..... 46
- Figure 3-9. Hydrodynamic radii of particles (R_h) as a function of temperature of poly(DMAEMA-*stat*-styrene) with 96 mol% DMAEMA (DMAEMA/S-95/5, ■) and 89 mol% DMAEMA (DMAEMA/S-90/10, ◆) in pH 10 buffer solution at 0.5 wt% concentration. 48
- Figure 3-10. Hydrodynamic radii of particles (R_h) as a function of temperature of poly(DMAEMA-*stat*-styrene) with 96 mol% DMAEMA (DMAEMA/S-95/5, ■), 81 mol% DMAEMA (DMAEMA/S-80/20, ▲) and block copolymer (D/S80/20-*b*-D/S95/5, ◆) in de-ionized water at 0.1 wt% concentration. 49
- Figure 3-11. Hydrodynamic radii of particles (R_h) as a function of temperature of block copolymer (D/S80-*b*-D/S95, $F_{DMAEMA,overall} = 90$ mol%, $M_n = 27.8$ kg mol⁻¹, ◆), and poly(DMAEMA-*stat*-styrene) (DMAEMA/S-90/10) with $F_{DMAEMA} = 89$ mol% ($M_n = 11.1$ kg mol⁻¹, ▲), and D/S90/10-*b*-D/S90/10 block copolymer with $F_{DMAEMA} = 91$ mol% ($M_n = 26.6$ kg mol⁻¹, ■) in de-ionized water at 0.5 wt% concentration. 51
- Figure 4-1. Bulk homopolymerization of 2VP initiated by NHS-BlocBuilder at 120 °C. (a) Kinetic plot of $\ln[(1-x)^{-1}]$ versus time (x = monomer conversion). (b) Number-average molecular weight (M_n) and dispersity (\mathcal{D}) versus

conversion (M_n relative to poly(styrene) standards). Solid line represents theoretical M_n trend..... 63

Figure 4-2. (a) Kinetic results ($\ln[(1-x)^{-1}]$ versus time) of statistical copolymerization of DMAEMA with 2VP initiated by NHS-BlocBuilder (x = monomer conversion). (b) Product of average propagation rate constant $\langle k_p \rangle$, and propagating radical concentration $[P\bullet]$, $\langle k_p \rangle [P\bullet]$ (slope of the kinetic plots in (a)), versus feed composition with respect to DMAEMA ($f_{DMAEMA,0}$); error bars represent standard deviation of the slopes from (a)..... 65

Figure 4-3. (a) Number-average molecular weight (M_n) and (b) dispersity (\mathcal{D}) of the statistical copolymers of DMAEMA and 2VP measured by GPC relative to poly(methyl methacrylate) standards versus conversion; solid line in (a) represents the theoretical M_n trend expected..... 67

Figure 4-4. (a) Kinetic plot of scaled conversion $\ln[(1-x)^{-1}]$ (x = conversion) versus polymerization time, (b) number-average molecular weight (M_n) and dispersity (\mathcal{D}) of DMAEMA/2VP copolymerization with 95 mol% DMAEMA in the feed initiated by PPO-BB macroalkoxyamine at 80 °C in bulk. M_n and \mathcal{D} were obtained by GPC relative to poly(methyl methacrylate) standards; solid line in (b) represents the theoretical M_n trend..... 70

Figure 4-5. ^1H NMR spectrum of poly(propylene glycol)-*b*-poly(dimethylaminoethyl methacrylate-*stat*-2-vinylpyridine) diblock copolymer (PPO-*b*-P(DMAEMA-*stat*-2VP) in CDCl_3 . Protons P, D, V correspond to the

	labeled protons on the chemical structures for PPO, DMAEMA, 2VP, respectively.....	71
Figure 4-6.	GPC chromatograms of macroinitiator (dashed line) and chain extended polymer (solid line) in the chain extension experiments.....	73
Figure 4-7.	Effect of additional SG1 free nitroxide on (a) number-average molecular weight (M_n , relative to poly(methyl methacrylate) standards) and (b) dispersity (\mathcal{D}) of DMAEMA/2VP statistical copolymers with 95 mol% and 99 mol% DMAEMA in the feed; filled symbols represent results obtained with no free SG1 and open symbols represent results obtained with 10% free SG1, solid line in (a) represents theoretical M_n trend.	75
Figure 4-8.	Cloud point temperature (CPT) of polymers of various compositions versus pH compared to the degree of ionization of PDMAEMA.	81
Figure 4-9.	Hysteresis (difference in temperature at 50% light transmittance during heating and cooling) of polymers with various compositions versus pH of the solutions.....	84
Figure 4-10.	pH titration curve of D2VP-95-2VP diblock copolymer obtained from automatic titration (blue line) and the first derivative of the measured pH (red line).	86
Figure 4-11.	(a) Hydrodynamic radius and (b) dispersity of the particle size distribution (μ_2/Γ^2) of D2VP-95-2VP diblock copolymers determined by dynamic light scattering at room temperature versus pH with solution concentration of 0.5 wt%.....	87

- Figure 4-12. Hydrodynamic radius (R_h) of D2VP-95-2VP diblock copolymer at various pH determined by dynamic light scattering versus temperature. Temperature was increased at a rate about $0.5\text{ }^\circ\text{C min}^{-1}$ 88
- Figure 4-13. Comparison of hydrodynamic radius of poly(propylene glycol) bis(2-aminopropyl ether) (PPO-di-NH₂) and diblock copolymer PPO-D2VP-95 in pH 8 buffer solution measured by dynamic light scattering. Temperature was increased at a rate about $0.5\text{ }^\circ\text{C min}^{-1}$ 90
- Figure 5-1. Plot of $\ln((1-x)^{-1})$ (where x = conversion) versus time for bulk copolymerization at $90\text{ }^\circ\text{C}$ for various initial feed compositions of benzyl methacrylate ($f_{BzMA,0}$). The different $f_{BzMA,0}$ are denoted as followed: $f_{BzMA,0} = 10\%$ (\square), $f_{BzMA,0} = 20\%$ (\blacksquare), $f_{BzMA,0} = 30\%$ (\circ), $f_{BzMA,0} = 40\%$ (\bullet), $f_{BzMA,0} = 50\%$ (Δ), $f_{BzMA,0} = 60\%$ (\blacktriangle), $f_{BzMA,0} = 70\%$ (\diamond), $f_{BzMA,0} = 80\%$ (\blacklozenge), $f_{BzMA,0} = 90\%$ (\times). 101
- Figure 5-2. The product of the average propagation rate constant $\langle k_p \rangle$, and the average equilibrium constant $\langle K \rangle$, $\langle k_p \rangle \langle K \rangle$, for BzMA/styrene copolymerization at $90\text{ }^\circ\text{C}$ in bulk versus initial feed composition of BzMA ($f_{BzMA,0}$) and the best-fit line obtained by non-linear least-square fitting is used as a guide. 102
- Figure 5-3. (a) Number-average molecular weight, M_n (b) and dispersity, \mathcal{D} versus conversion for BzMA/styrene copolymerization; $f_{BzMA,0} = 10\%$ (\square), $f_{BzMA,0} = 20\%$ (\blacksquare), $f_{BzMA,0} = 30\%$ (\circ), $f_{BzMA,0} = 40\%$ (\bullet), $f_{BzMA,0} = 50\%$ (Δ), $f_{BzMA,0} = 60\%$ (\blacktriangle), $f_{BzMA,0} = 70\%$ (\diamond), $f_{BzMA,0} = 80\%$ (\blacklozenge), $f_{BzMA,0} = 90\%$ (\times), straight line in (a) indicates the theoretical trend. 106

Figure 5-4. Gel permeation chromatograms (GPC) for chain extensions of styrene for BzMA/styrene random copolymers with (a) $f_{BzMA,0} = 20\%$, (b) $f_{BzMA,0} = 80\%$, (c) $f_{BzMA,0} = 90\%$ 108

Figure 5-5. Mayo-Lewis plot of copolymer composition with respect to benzyl methacrylate ($F_{BzMA,ini}$) versus monomer feed composition ($f_{BzMA,0}$) using reactivity ratios determined by non-linear least-square fitting of the Mayo-Lewis equation with MatLab. Solid dots are experimental data obtained from random copolymerization of BzMA and styrene in bulk at 90 °C using BlocBuilder and 10 mol% SG1 free nitroxide relative to BlocBuilder. See Table 5-2 for additional characteristics of each of the copolymers. 111

Figure 6-1. Product of average propagation rate constant $\langle k_p \rangle$ and average equilibrium constant $\langle K \rangle$ for copolymerization of benzyl methacrylate (BzMA) with 9-(4-vinylbenzyl)-9H-carbazole (VBK) at 90 °C calculated using the slopes of the kinetic plots in their linear regions in this work (blue circles) compared with the reported $\langle k_p \rangle \langle K \rangle$ values for the copolymerization of BzMA with styrene¹⁴² (red squares), calculated $\langle k_p \rangle \langle K \rangle$ values using a terminal model (TM) for copolymerization of methyl methacrylate with styrene¹⁰⁴ (dashed line) and VBK¹⁴⁷ (solid line) versus initial feed composition of VBK or styrene; the error bars represent standard deviation from the slope calculation. 124

Figure 6-2. Number-average molecular weight (M_n) and dispersity (\mathcal{D}) of statistical copolymers of benzyl methacrylate (BzMA) and 9-(4-vinylbenzyl)-9H-carbazole (VBK) measured by GPC calibrated with poly(methyl

methacrylate) standards (symbols: B/V-2: red squares, B/V-5: blue diamonds, B/V-8: orange circles, B/V-11: green triangles).	126
Figure 6-3. GPC traces of corresponding macroinitiators (dashed lines) and chain extended block copolymers (solid lines) for (a) macroinitiator B/V-5 and block copolymer B/V5-M/S10 and (b) macroinitiator B/V-8 and block copolymer B/V8-M/S10; chromatograms of the chain-extended block copolymers showed no significant changes after fractionation.	129
Figure 6-4. Fluorescence emission spectra ($\lambda_{\text{ex}} = 330 \text{ nm}$) of (a) 3 wt% ionic liquid solution of the statistical copolymer B/V-5, M/V-5 and BzMA homopolymer (PBzMA) at room temperature (b) neat $[\text{C}_2\text{mim}][\text{NTf}_2]$ at	
Figure 6-5. Fluorescence emission spectrum ($\lambda_{\text{ex}} = 330 \text{ nm}$) of 3 wt% ionic liquid solution of BzMA homopolymer (PBzMA) and excitation spectra of 3 wt% ionic liquid solution of BzMA homopolymer (PBzMA) ($\lambda_{\text{ex}} = 350 \text{ nm}$) and 3 wt% ionic liquid solution of the statistical copolymer M/V-5 ($\lambda_{\text{ex}} = 370 \text{ nm}$) at room temperature.	137
Figure 6-6. Fluorescence emission spectra ($\lambda_{\text{ex}} = 330 \text{ nm}$) of (a) 3 wt% ionic liquid solution of the statistical copolymer B/V-5 (CPT = 86 °C) and b) 3 wt% ionic liquid solution of BzMA homopolymer (PBzMA) (CPT ~ 105 °C) at various temperature.	138
Figure 6-7. Raman spectra of (a) 3 wt% ionic liquid solution of BzMA homopolymer (PBzMA) and (b) 3 wt% ionic liquid solution of the statistical copolymer B/V-8 before and after phase separation obtained at 532 nm.	138

- Figure 6-8. Light transmittance (solid lines) and normalized maximum emission (dashed lines, $\lambda_{\text{ex}} = 330 \text{ nm}$) of 3 wt% ionic liquid solutions of statistical copolymers of BzMA and VBK (B/V-5 with $F_{\text{VBK}} = 4 \text{ mol\%}$ and B/V-8 with $F_{\text{VBK}} = 9 \text{ mol\%}$) with heating rate of $1 \text{ }^\circ\text{C min}^{-1}$ 139
- Figure 6-9. Light transmittance (solid lines) and normalized maximum fluorescence (dashed lines, $\lambda_{\text{ex}} = 330 \text{ nm}$) of 3 wt% ionic liquid solutions of block copolymers (a) B/V5-M/S10 (b) M/V5-B/S10 with heating/cooling rate of $1 \text{ }^\circ\text{C min}^{-1}$ 142
- Figure 7-1. Semi-logarithmic kinetic plots of terpolymerization of (a) benzyl methacrylate (BzMA) methyl methacrylate (MMA) and 9-(4-vinylbenzyl)-9H-carbazole (VBK), and (b) benzyl methacrylate (BzMA) oligo(ethylene glycol) methyl ether methacrylate (OEGMA) and 9-(4-vinylbenzyl)-9H-carbazole (VBK) at $90 \text{ }^\circ\text{C}$ via NMP. 154
- Figure 7-2. Number-average molecular weight (M_n) and dispersity (Đ) of terpolymers of (a) benzyl methacrylate (BzMA), methyl methacrylate (MMA) and 9-(4-vinylbenzyl)-9H-carbazole (VBK), and (b) benzyl methacrylate (BzMA) oligo(ethylene glycol) methyl ether methacrylate (OEGMA) and 9-(4-vinylbenzyl)-9H-carbazole (VBK), measured by GPC calibrated with poly(methyl methacrylate) standards. The linear lines in the M_n versus conversion graphs represent the theoretical trends. 156
- Figure 7-3. Light transmittance of 3 wt% terpolymer in ionic liquid solutions of (a) BzMA/MMA/VBK terpolymers, and (b) BzMA/OEGMA/VBK

terpolymers with heating/cooling rate of 1 °C min⁻¹ (heating cycles with hollow symbols and cooling cycles with solid symbols). 161

Figure 7-4. Cloud point temperature of 3 wt% solutions of BzMA/MMA/VBK (blue diamonds) and BzMA/OEGMA/VBK terpolymers (red squares) versus (a) terpolymer composition of MMA (F_{MMA}) or terpolymer composition of OEGMA (F_{OEGMA}); (b) terpolymer composition of MMA (F_{MMA}) or terpolymer composition of ethylene glycol units ($F_{\text{ethylene glycol units}}$, calculated by $(F_{OEGMA} \times 8.5)/(F_{BzMA} + F_{VBK} + F_{OEGMA} \times 8.5) \times 100\%$, 8.5 being the average number of ethylene glycol units in each OEGMA monomer according to the M_n of the monomer). 161

Figure 7-5. Light transmittance of 3 wt% terpolymer in ionic liquid solutions of (a) B60/M30/V10-40 ($F_{BzMA} = 60$ mol%, $F_{MMA} = 22$ mol%, $F_{VBK} = 18$ mol%), and (b) B85/O5/V10-40 ($F_{BzMA} = 86$ mol%, $F_{OEGMA} = 3$ mol%, $F_{VBK} = 11$ mol%) at various solution concentrations (heating cycles with solid lines and cooling cycles with dotted lines). 164

Figure 7-6. Cloud point temperature of 3 wt% solutions in [C₂mim][NTf₂] of B80/M10/V10-10 ($F_{BzMA} = 75$ mol%, $F_{MMA} = 9$ mol%, $F_{VBK} = 16$ mol%), B80/M10/V10-40 ($F_{BzMA} = 74$ mol%, $F_{MMA} = 10$ mol%, $F_{VBK} = 16$ mol%), and B80/M10/V10-80 ($F_{BzMA} = 77$ mol%, $F_{MMA} = 9$ mol%, $F_{VBK} = 14$ mol%) versus M_n relative to PMMA standards. 167

Figure 7-7. Light transmittance of (a) B50/M4/0M10-40 ($F_{BzMA} = 51$ mol%, $F_{MMA} = 29$ mol%, $F_{VBK} = 20$ mol%) and (b) B83/O7/V10-40 ($F_{BzMA} = 81$ mol%, $F_{OEGMA} = 5$ mol%, $F_{VBK} = 14$ mol%) in 3 wt% [C₂mim][NTf₂] solutions

	during 4 consecutive heat/cool cycles (solid line represents heating and dotted line represent cooling).....	169
Figure 7-8.	Normalized maximum fluorescence intensity (excitation at 330 nm) of (a) B50/M40/M10-40 ($F_{\text{BzMA}} = 51$ mol%, $F_{\text{MMA}} = 29$ mol%, $F_{\text{VBK}} = 20$ mol%) and (b) B83/O7/V10-40 ($F_{\text{BzMA}} = 80$ mol%, $F_{\text{OEGMA}} = 8$ mol%, $F_{\text{VBK}} = 12$ mol%) in 3 wt% $[\text{C}_2\text{mim}][\text{NTf}_2]$ solutions during 3 consecutive heat/cool cycles (solid line represents heating and dotted line represent cooling).....	170
Figure B-1.	GPC chromatograms of intermediate samples during the copolymerization of DMAEMA with 2VP initiated by a PPO-BB macroalkoxyamine.....	196
Figure B-2.	Light transmittance of 0.5 wt% solutions of polymers with different compositions in pH 8 buffer measured by UV-visible spectrometry with heating/cooling rate of 0.5 °C min^{-1} ; solid lines are heating cycles and dashed lines are cooling cycles.	197
Figure D-1.	Proton NMR spectrum of a statistical copolymer of benzyl methacrylate (BzMA) and 9-(4-vinylbenzyl)-9 <i>H</i> -carbazole (VBK) (B/V-5 ($F_{\text{VBK}} = 4$ mol%))......	208
Figure D-2.	Semi-logarithmic kinetic plots of statistical copolymerization of benzyl methacrylate (BzMA) and 9-(4-vinylbenzyl)-9 <i>H</i> -carbazole (VBK) at 90 °C via NMP with BlocBuilder TM (symbols: B/V-2 ($f_{\text{VBK},0} = 2$ mol%): red squares, B/V-5 ($f_{\text{VBK},0} = 5$ mol%): blue diamonds, B/V-8 ($f_{\text{VBK},0} = 8$ mol%): orange circles, B/V-11 ($f_{\text{VBK},0} = 11$ mol%): green triangles).	209

Figure D-3. Hydrodynamic radius (R_h , red square) and particle distribution index (μ_s/Γ^2 , blue diamond) versus temperature measured by dynamic light scattering for block copolymer M/V5-B/S10.	210
Figure E-1: ^1H NMR spectrum of (a) B60/M30/V10-40 as an example of BzMA/MMA/VBK terpolymer and (b) B85/O5/V10-40 as an example of BzMA/OEGMA/VBK terpolymer.	214

Chapter 1

Introduction

1.1 Introduction to smart materials

The influence of material technologies on human civilization is unquestionably profound. Starting from the Stone Age, the most advanced materials at the time have been defining the distinct eras of civilization. During the last several decades, the development of synthetic materials, especially polymers, has been almost explosive. Besides low manufacturing costs, the most important advantage of synthetic polymeric materials compared to those used previously used was the vastly different properties and the facile tuning of properties and microstructure by appropriate synthetic methodology and processing techniques. Great efforts on exploiting this potential by numerous researchers have brought us to the door of the “Smart Material Age”.¹

Materials are termed “smart” when they are able to change properties quickly and reversibly in response to external stimuli. Common stimuli include changes in temperature,²⁻⁴ pH,^{3,5} light^{6,7} and CO₂.^{8,9} For instance, photochromic materials change from one color to another as light intensity varies, which can be useful in ink, paint or information recording and processing.¹⁰ Temperature sensitive materials can change solubility, microstructure or shape rapidly as the surrounding temperature varies, which have been applied as food packaging,¹¹ coatings,¹² and drug delivery devices.⁴ The large variety of smart materials developed thus far represents, however, only the embryonic state of the “Smart Material Age”. It is now the imagination that is limiting us from creating materials that have not yet existed.

Among the vast number of possible smart materials, thermo-responsive materials have formed a major category since temperature is one of the most easily manipulated experimental conditions. After Heskins and Guillet demonstrated the temperature sensitivity of poly(*N*-isopropylacrylamide)¹³ in water, the interest in thermo-responsive polymers has been continuously growing. These polymers undergo sharp and often reversible transitions from insoluble to soluble states in certain solvents upon change of temperature. This specific property has resulted in significant advancements in many bioengineering applications such as absorbents for bioseparation and purification,^{14,15} drug delivery devices¹⁶⁻¹⁸ and biocatalysts.¹⁹ Thermo-responsive polymers have also been studied and applied in other media. Recently, serious interests has been shown for the combination of thermo-responsive polymers and a novel solvent called ionic liquid to form highly ion-conductive gels that can be used as a new generation of solid electrolytes for various electrochemical devices²⁰⁻²² without leakage and flammability problems of the current volatile solvent-based electrolytes.²³ The structures and unique properties of ionic liquids are described in Section 1.2.

1.2 Ionic liquids and their properties as solvents

Ionic liquids are molten salts that are liquid at room temperature or near room temperature. They are composed of bulky organic cations such as alkyimidazolium or alkyipyridinium cations and either inorganic or organic anions like BF_4^- , PF_6^- or $(\text{CF}_3\text{SO}_2)_2\text{N}^-$. The molecular structure of cations and anions commonly employed in ionic liquids are shown in Figure 1-1. -1. The replacement of bulky asymmetric organic cations is the main reason for the dramatically reduced melting temperature (for example, the melting temperature for sodium chloride is 803 °C in

comparison to 60 °C for 1-propyl-3-methylimidazolium chloride).²⁴ After convenient synthesis methods were developed about a decade ago,^{25,26} the preparation of ionic liquids with novel structures has been intensively studied.²⁷⁻³¹ There are already more than 500 different ionic liquids that have been synthesized and the number is still rapidly increasing.²⁴

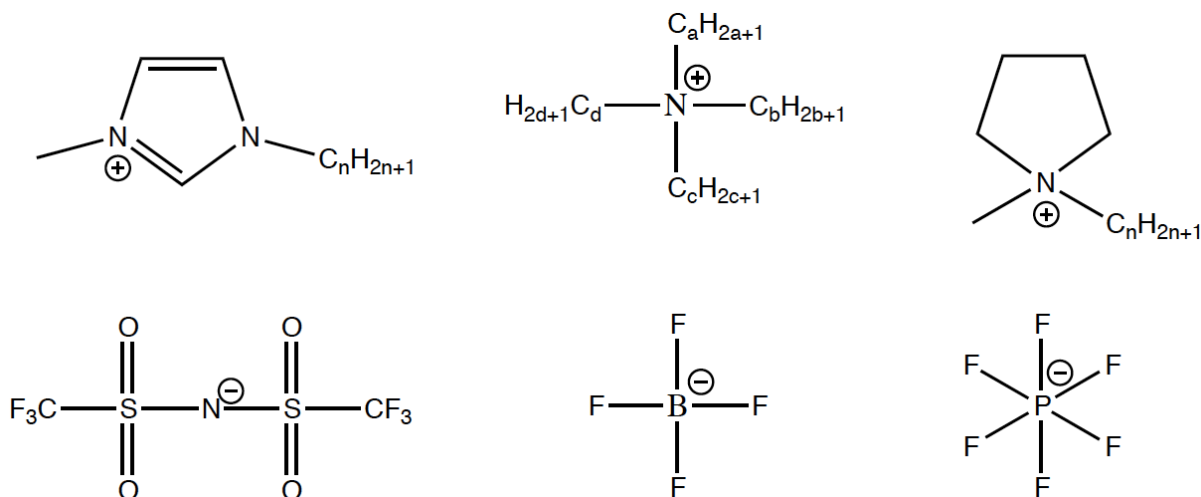


Figure 1-1. Molecular structure of cations and anions in common ionic liquids.

The unique chemical structure of ionic liquids confers them the ability to dissolve a wide range of organic and inorganic compounds with different polarities simultaneously. The ionic interactions due to the charged species in ionic liquids, in addition to the van der Waals, dipole-dipole and hydrogen bonding interactions existing in conventional organic solvents, make ionic liquids miscible with many polar substances. At the same time, ionic liquids can dissolve less-polar substances due to the increased affinity provided by the bulky organic cations.²⁴ It has been also found that substances that are usually poorly soluble in many organic solvent such as cellulosic materials,³²⁻³⁴ wool³⁵ and carbon nanotubes³⁶ can be solubilized or dispersed in selected ionic liquids. The versatility and flexibility of ionic liquids as solvents given by different

combinations of cations and anions has drawn the attention of numerous researchers and given ionic liquids the name “designer solvents”.

Zero vapor pressure is another important property of ionic liquids. The non-volatility of ionic liquids facilitates easy separation of low molecular weight volatile compounds from the catalyst or substrates dissolved in ionic liquids which can be used in subsequent reactions.³⁷ For non-volatile products such as polymers, the unreacted volatile monomers can be recycled by evaporation and the ionic liquid can also be reused after precipitation of polymers and simple purification steps.³⁸ Combining with excellent chemical and thermal stability, ionic liquids have the potential to replace the current volatile organic compounds (VOC) and become a new generation of environmentally friendly solvents.^{21,39-41}

1.3 Phase separation behaviour of polymers

1.3.1 Phase separation in conventional solvents

Polymerizations are often conducted in solutions and solvents which are frequently used to dissolve or recover polymers. Therefore, it is important to be able to predict the dissolution and phase separation (or precipitation) behaviour in polymer/solvent systems. The thermodynamics of phase separation can be described by the Gibbs free energy of mixing, ΔG_m , with its enthalpic and entropic contributions:

Equation 1-1

$$\Delta G_m = \Delta H_m - T\Delta S_m$$

where ΔH_m = enthalpy of mixing, ΔS_m = entropy of mixing and T = absolute temperature.

By assuming purely dispersive interactions, no volume change upon mixing and mean-field conditions, a lattice-based model developed by Flory and Huggins⁴²⁻⁴⁵ can be used to describe ΔG_m in terms of compositions of the polymer/solvent binary system:

Equation 1-2

$$\Delta G_m = kT(\chi_{12}\varphi_1\varphi_2 + \varphi_1 \ln(\varphi_1) + \frac{\varphi_2}{p} \ln(\varphi_2))$$

where k = Boltzmann's constant, φ_1 , φ_2 = volume fractions of solvent and polymer, respectively, χ_{12} = enthalpic interaction parameter = $\Delta H_m / (kT N_1\varphi_2)$ with N_1 = moles of solvent, and p = degree of polymerization of the polymer.

Using the Flory-Huggins equation shown above, one can plot ΔG_m versus composition with a polymer of selected degree of polymerization. At low χ_{12} (or equivalent of high T), $\Delta G_m < 0$ for all compositions, which indicates a single stable phase. As χ_{12} increases (or equivalently the effect of decreasing T) to above a critical point, ΔG_m becomes > 0 for some compositions. These compositions represent unstable compositions at which polymer phase separates from the solvent. The compositions at the minimum ΔG_m at each χ_{12} defines the binodal or coexistence curve. The inflections points for the ΔG_m versus composition curve, or alternatively, the minima of chemical potential with respect to composition, represent the stability limits or the spinodal curve for the mixture. Within the stability limits, the mixture is composed of two separated phases and the mixture is meta-stable at compositions between the binodal and spinodal curves. Once binodal,

spinodal curves and critical points are obtained, complete phase diagrams for the polymer/solvent system can be constructed.

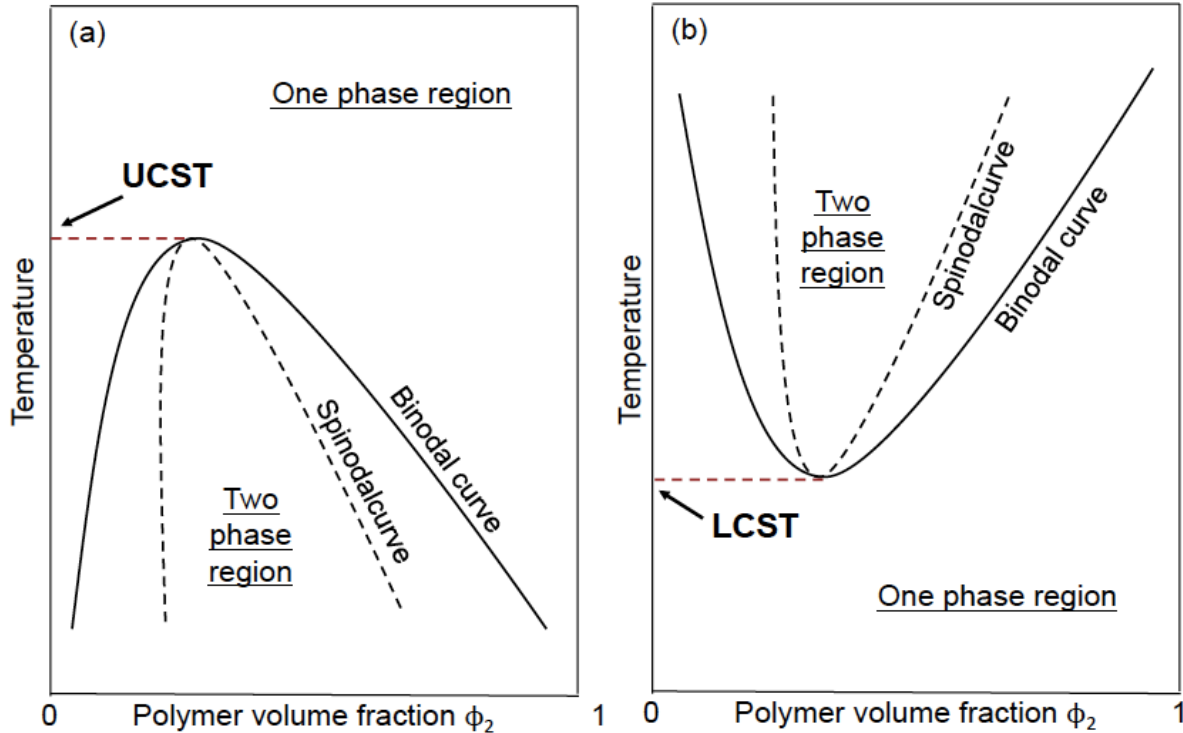


Figure 1-2. A comparison between polymer/solvent systems that exhibit a) an upper critical solution temperature (UCST) and b) lower critical solution temperature (LCST)

The critical temperature above which all compositions are stable as a single phase is defined as an upper critical solution temperature (UCST). There are cases where a single stable phase only exists below a critical temperature. This critical temperature is called a lower critical solution temperature (LCST). A comparison between UCST and LCST-type systems is illustrated in Figure 1-2. The LCST-type behaviours are usually observed in the systems where strong hydrogen bonding or ionic interactions exist. This invalidates the purely dispersive interactions

assumed by Flory-Huggins theory. Examples of LCST-type phase separation behaviours are described in Section 1.3.2.

1.3.2 LCST-type phase separation in aqueous and ionic liquid solutions

In aqueous solutions, the strong hydrogen bonding can sometimes lead to LCST-type phase separation where the polymer solute is soluble below a critical temperature. One example is the aqueous solution of poly(*N*-isopropylacrylamide) (PNIPAm). Hydrogen bonding between water and the isopropyl group in the polymer results in the formation of a layer of a clathrate-like structure which lowers the entropy of mixing.^{21,46} As temperature increases, the bound water is released and the increase of entropy drives phase separation.⁴⁶ Other polymers that are known to exhibit LCST-type phase separation in water include poly(2-(dimethylamino)ethyl methacrylate) (PDMAEMA),^{47,48} poly(oligo(ethylene glycol)methyl methacrylate) (POEGMA),^{49,50} poly(hydroxypropyl acrylate) (PHPA),⁵¹ morpholine-based polymers,^{52,53} and various poly(acrylamide)s.^{54,55} The thermo-responsiveness in aqueous solutions makes these polymers potentially useful for many applications, such as drug/gene delivery, biosensors, bioseparations and tissue engineering.^{3,56,57}

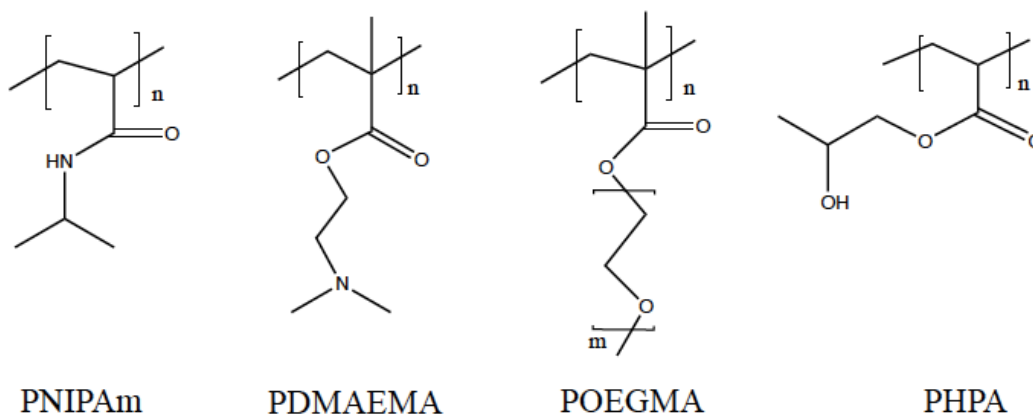
The phase separation behaviour of polymers in ionic liquids has also been a subject of interest because the composite materials of polymer and ionic liquids are attractive candidates as solid electrolytes for various electrochemical devices.⁵⁸⁻⁶⁰ PNIPAm exhibits UCST-type phase separation in a hydrophobic ionic liquid 1-ethyl-3-methyl imidazolium bis(trifluoromethane sulfone)imide ([C₂mim][NTf₂]).⁵⁸ This is a very interesting phenomenon since it is completely opposite to its LCST-type phase separation in aqueous solution as described previously. LCST-

type phase separation behaviour of poly(benzyl methacrylate) (PBzMA)⁵⁸ and its analogue copolymers⁶⁰ is observed in hydrophobic ionic liquids, specifically [C₂mim][NTf₂]. Similar to LCST-phase separation in aqueous solutions, the solvation of PBzMA below its LCST in [C₂mim][NTf₂] was driven by the negative entropy upon mixing.⁶¹ Recent studies claimed that negative entropy was a result of self-organization of the ions of the ionic liquid, where the [NTf₂] anions arrange themselves to the equatorial position of the benzene ring, whereas the imidazolium cations to the electron-rich positions above and below the benzene plane.⁶² Other known polymers that exhibit LCST-type phase separation in ionic liquids include poly(*n*-butyl methacrylate) (PnBMA)⁶³ and poly(ethylene oxide) (PEO).⁶⁴

The Flory-Huggins theory is not sufficient to predict polymer phase separation behaviour in ionic liquids because of the inherently strong interactions in ionic liquids. Studies have shown that the solubility of ionic liquids is mainly governed by their anionic structure.⁶⁵⁻⁶⁸ For example, the ionic liquid 1-alkyl-3-methylimidazolium tetrafluoroborate ([C_nmim][BF₄], 1-alkyl chain ranging from 1 – 9 carbons) is soluble in water while the replacement of (NTf₂)⁻ anion makes the ionic liquid highly hydrophobic. At the same time, an increase of carbon atoms in the alkyl chain of the 1-alkyl-3-methylimidazolium cation strengthens the van der Waals interaction between the ionic liquid and alkyl group in polymers, which has effects on the solubility of the ionic liquid⁶⁸ and the critical temperature for polymer phase separation.⁵⁸

The molecular structures of some well-known polymers that demonstrate LCST-type phase separation in aqueous and ionic liquid solutions are illustrated in Figure 1-3.

LCST-type phase separation in aqueous solutions



LCST-type phase separation in ionic liquid solutions

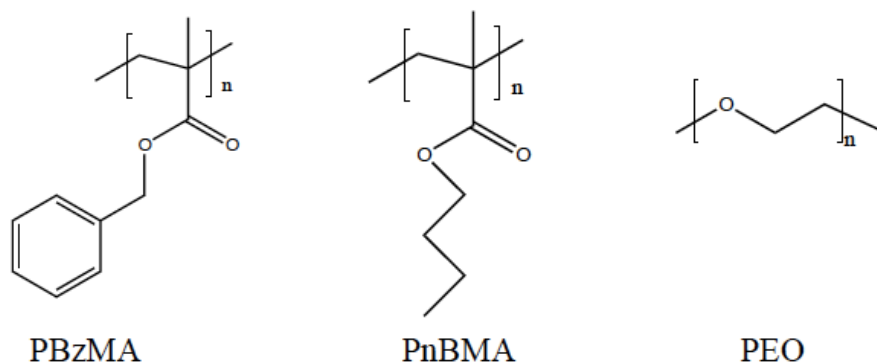


Figure 1-3. Molecular structures of well-known thermo-responsive polymers in aqueous and ionic liquid solutions.

1.3.3 Effect of molecular weight distribution on phase separation behaviour

Phase separation behaviour of polymers in solutions can be affected by many factors such as solution concentration,^{69,70} co-solvent,^{71,72} and the presence of salt.⁷³ However, it is important to point out the effect of molecular weight distribution on the phase separation behaviours here because it set an important criterion for choosing an appropriate synthesis technique for the projects detailed in this thesis.

It is well established that molecular weight has significant effects on the phase separation behaviours of polymers in solutions.^{70,74,75} For LCST-type phase separation, the inverse dependency of LCST on molecular weight was attributed to the increase in polymer molar volume⁷⁴ and decrease in change of entropy of mixing⁷⁰ with increasing polymer chain length. However, polymers are often a mix of chains with different molecular weights. Therefore, it is crucial to characterize the molecular weight distribution (or dispersity \mathfrak{D}) of the polymer. Dispersity is defined as the ratio of the weight-average molecular weight (\overline{M}_w) to the number-average molecular weight (\overline{M}_n) of a polymer, ie. $\overline{M}_w/\overline{M}_n$, where \overline{M}_w and \overline{M}_n are defined by the following equations:

Equation 1-3

$$\overline{M}_w = \frac{\sum N_i M_i^2}{\sum N_i M_i}$$

Equation 1-4

$$\overline{M}_n = \frac{\sum N_i M_i}{\sum N_i}$$

where M_i is the molecular weight of a polymer chain and N_i is the number of chains with molecular weight of M_i .

Dispersity is always greater than or equal to one. A polymer with a dispersity of one consists of chains with equal length. Polymers with low dispersity of about 1.05 – 1.10 can be synthesized using techniques such as anionic polymerization⁷⁶ or controlled radical polymerizations.^{75,77} Polymers synthesized by step polymerization usually have a dispersity of around 2⁷⁸ and those made by conventional free radical polymerization often exhibit dispersities higher than 2.⁷⁹⁻⁸¹

The dispersity of a polymer can significantly affect the phase behavior of the polymer. Although it has been predicted theoretically in 1969⁷⁴ that LCST should decrease with increasing molecular weight, conflicting experimental results have been reported until early 2000. Inverse dependency,^{70,82} direct dependency⁸³ and independent relationship^{81,84} between molecular weight and LCST have been claimed in the early studies of the LCST behaviour of PNIPAm and other poly(acrylamides) in aqueous solutions. Many of these studies employed polymers synthesized by conventional free radical polymerization, which often had high dispersity. The broad molecular weight distribution implies that the reported LCST corresponding to the average molecular weight of the sample could be effectively masked by the lower LCST of the high molecular weight fraction of the sample. In contrast, studies using polymers with narrow molecular weight distribution have consistently reported a trend of sharp decrease in LCST as molecular weight increased followed by a plateau of LCST at high molecular weight.^{75,77,85} Therefore, when studying the thermo-responsiveness of a polymer, it is important to use a synthetic technique that can yield polymers with low dispersity so that representative and consistent results can be obtained.

1.4 Organization of this thesis

Starting with this Introduction, this manuscript-based thesis consists of a total of 8 chapters. In Chapter 2, a brief literature review emphasizing controlled polymer synthesis techniques and nitroxide mediated polymerization (NMP) will be provided. Chapters 3 – 7 are published or submitted manuscripts. Chapter 3 and 4 describe the synthesis and characterizations of polymers

that are stimuli-responsive in aqueous solutions, and Chapter 5 - 7 detail studies of stimuli-responsive polymers in ionic liquid solutions.

Specifically, Chapter 3 is based on a manuscript published in *Polymers*, details the synthesis of pH- and temperature-sensitive statistical copolymers that are rich in 2-(dimethylamino) ethyl methacrylate (DMAEMA), aided with different amounts of styrene as a controlling co-monomer, using NMP. The phase behaviour of these copolymers in aqueous solutions were also characterized and discussed. As a comparison and follow-up study, Chapter 4 is based on a manuscript that details similar synthesis technique of DMAEMA-rich copolymers, with a different controlling co-monomer, 2-vinylpyridine (2VP). This manuscript was published in *Journal of Polymer Science Part A: Polymer Chemistry* and demonstrates the effectiveness of 2VP as a controlling co-monomer for the first time. Chapter 5, a manuscript published in *Macromolecular Reaction Engineering*, details the synthesis of random copolymers of benzyl methacrylate (BzMA) and styrene via NMP. PBzMA is a thermo-responsive polymer in hydrophobic ionic liquids, and this manuscript demonstrates its controlled synthesis via NMP for the first time using styrene as a controlling co-monomer. Chapter 6 details the manuscript published in *Journal of Polymer Science Part A: Polymer Chemistry*, which describes the synthesis of fluorescent and thermo-responsive copolymers of BzMA and 9-(4-vinylbenzyl)-9H-carbazole (VBK) via NMP. The effects of the fluorescent carbazole groups of VBK on the phase transitions of the copolymers in an ionic liquid were emphasized. Chapter 7 presents a manuscript recently accepted to *Polymer Chemistry*. This manuscript investigates the effects of solvatophilicity and chain mobility on phase separation and reversibility using terpolymers consisting of BzMA, VBK and methyl methacrylate (MMA) or oligo(ethylene glycol) methacrylate (OEGMA).

Finally, general conclusions of this thesis will be provided in Chapter 8, followed by a summary of contributions and future work recommendations. The experimental sections and supporting information for each manuscript can be found in the Appendices.

Chapter 2

Literature Review

2.1 Controlled radical polymerization

Conventional radical polymerization is a common technique to prepare high molecular weight polymers in industry and in research laboratories. It is a robust technique, but its slow initiation, along with constant chain transfer and termination side reactions during the polymerization lead to polymer products with broad molecular weight distribution and “dead” chain ends. Polymers are considered “living” if all chains retain the same chain length and the ability to grow without any side-reactions or termination. To synthesize block copolymers and many other polymeric products with well-defined structure, as well as ensure controlled and uniform properties, techniques that are capable of producing living polymers are required.

Since the first proof of living polymerization of styrene by electron transfer initiated by a sodium-naphthalene complex in 1956,⁸⁶ ionic polymerization, especially anionic polymerization, has been applied to polymerize styrene and styrene derivatives,⁸⁷⁻⁹⁰ dienes,⁹¹⁻⁹³ (meth)acrylates⁹⁴⁻⁹⁶ and some other monomers⁹⁷⁻⁹⁹ in a living manner. The initiation in anionic polymerization is assumed to be instantaneous and the propagation is free of termination and chain transfer as long as monomer is available and no impurity is present. The ability to precisely control and predict the structure of the polymeric product is indeed a remarkable advantage of ionic polymerization. However, these systems are highly sensitive to the presence of impurities such as moisture and air. Stringent controls of reagent purity and reaction conditions are required

to achieve desirable results. This makes ionic polymerization relatively expensive and not easily adaptable to industry. In addition, the interference from strong electrophilic groups in monomers such as amino-, carboxyl- or hydroxyl- as well as possible reactions between polar substituents in monomers and the initiator limits the range of monomers that can be polymerized using this technique.¹⁰⁰ Therefore, ionic polymerization may not be the best approach to synthesize affordable well-defined (co)polymers.

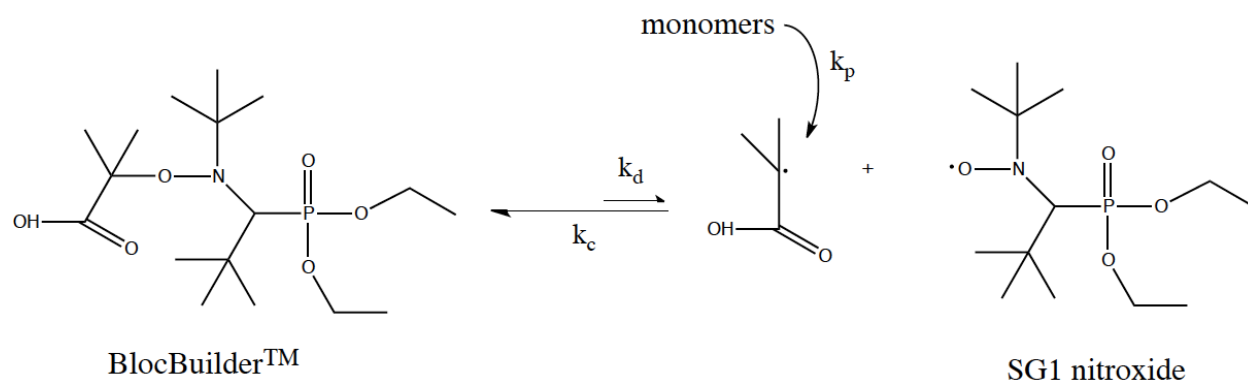
In efforts to combine the robustness of conventional radical polymerization and the control in livingness of ionic polymerization, irreversible termination reactions in conventional radical polymerization were significantly reduced and (co)polymers with designed molecular weight and narrow molecular weight distribution were yielded, which essentially led to the naissance of “living” or controlled radical polymerization (CRP) techniques.¹⁰¹ Being radical polymerizations, CRPs provide simplicity and reaction conditions easily implemented industrially. Excessive purification and strictly controlled apparatus that are necessary for ionic polymerization are not required for CRP. A wider range of monomers as well as numerous combinations of monomers can be (co)polymerized and most importantly, a high level of “livingness” can be retained.¹⁰² The commercial importance of CRP is significant, since the preparation of well-defined polymeric products is now becoming more feasible with economically acceptable manufacturing procedures.

2.2 Nitroxide mediated polymerization

Three major CRP techniques are known as nitroxide mediated polymerization (NMP),¹⁰³⁻¹¹⁰ atom transfer radical polymerization (ATRP)¹¹¹⁻¹¹⁴ and reversible addition-fragmentation transfer

(RAFT).¹¹⁵⁻¹¹⁷ NMP and ATRP control the polymerization by reversible termination. An activation-deactivation equilibrium between a dormant species and propagating radicals is established via coupling to an alkoxyamine initiator for NMP or by ligand coupling to a metal complex (usually a copper-based ligand) for ATRP. RAFT achieves control by a thiocarbonyl ester compound as transfer agent which facilitates reversible chain transfer reactions.

In ATRP, the transition metal catalyst residue can be undesirable, especially for polymers designed for metal-sensitive applications such as electronics. The involvement of a toxic halide initiator in some systems is another drawback of ATRP.¹¹⁸ RAFT can polymerize the widest range of monomers among the three, but the odor and color resulted from the sulphur-based chain transfer agent are problematic in many cases.¹¹⁹ Although the removal of the metal catalyst for ATRP or chain transfer agent for RAFT is possible,¹²⁰⁻¹²² NMP stands out for its simplicity as it requires no additives to achieve controlled polymerization.



Scheme 2-1. The activation-deactivation equilibrium and propagation mechanism of the unimolecular alkoxyamine BlocBuilder™ (k_d = dissociation constant, k_c = recombination constant, k_p = propagation rate constant).

NMP has been successfully utilized in synthesizing styrene-based polymers with a high level of control using the first generation alkoxyamine TEMPO (2,2,6,6-tetramethylpiperidinyl-1-

oxy).^{123,124} The development of so-called second generation acyclic nitroxides such as SG1, or (*tert*-butyl(1-diethoxyphosphoryl-2,2-dimethylpropyl)amino) oxidanyl, has expanded the range of monomers polymerizable by NMP to include acrylates,^{107,125,126} acrylic acid,^{103,127} dienes,¹²⁸ acrylamides^{105,108} and acrylonitrile.^{125,129} The potential of low temperature polymerization (< 90 °C) using NMP¹³⁰ is not only a great advantage to lower energy costs and enhance energy efficiency, but also makes emulsion polymerization possible without the need for high pressure reactors. Scheme 2-1 illustrates the equilibrium between the commercially available unimolecular alkoxyamine BlocBuilderTM and the nitroxide SG1. Because of the absence of additives such as metal catalyst in ATRP or sulphur-based chain transfer agent in RAFT, the purification procedures for NMP often involve a single-step precipitation and for this reason, NMP has been touted as a convenient synthesis technique for non-cytotoxic polymers for biomedical applications or polymers used for metal-sensitive electronics.¹³¹⁻¹³³

2.3 Methacrylate polymerization by NMP

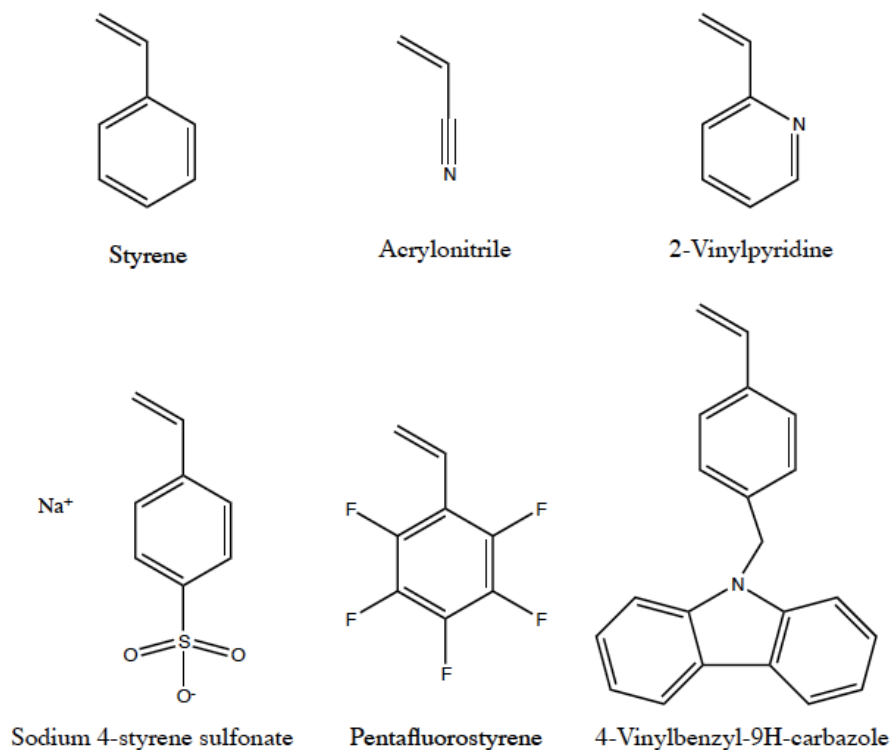
Because of the global production of 2.2 million tonnes per year for poly(methyl methacrylate) (PMMA) alone as of 2001¹³⁴ and steady demand growth for methacrylate polymers due to their use in numerous commercial products in fields such as optics, electronics, and construction,¹³⁵ a robust synthesis technique for poly(methacrylates) is highly desirable. The problematic homopolymerization of methacrylates via NMP (which can be controlled by ATRP or RAFT) is a major drawback of NMP that limits its widespread use.¹³³ The poor control over methacrylate homopolymerization by NMP has been attributed to two main issues: β -hydrogen transfer reaction (or disproportionation) and the large activation-deactivation equilibrium constant, K

($=k_d/k_c$ as shown in Scheme 2-1). Disproportionation produces a non-reactive hydroxylamine and macroradical with an alkene end group, which was blamed as the main cause for uncontrolled polymerization of MMA using TEMPO¹³⁶ or the low conversion during polymerization of MMA with a large excess of SG1.¹³⁷ In some studies with the second-generation acyclic nitroxide such as SG1, disproportionation was not observed and the uncontrolled nature of MMA polymerization was attributed solely to the high K value.^{138,139} The high K value of MMA is mainly the result of slow recombination of nitroxides and the sterically-hindered poly(methacrylate) radicals, which consequently leads to high concentration of active radicals and excessive termination reactions.^{133,139}

The copolymerization of MMA with styrene was first proposed by Charleux et al. as a valid methodology to synthesize methacrylate-rich copolymers using commercially available alkoxyamines.¹⁰⁴ Using both theoretical and experimental approaches, they demonstrated that the average activation-deactivation equilibrium constant, $\langle K \rangle$, can be significantly reduced when there exists a small amount of co-monomer that exhibits a much smaller activation-deactivation equilibrium constant compared to that of methacrylates along with a low cross-propagation rate constant (k_p /reactivity ratio, where k_p is the propagation rate constant).¹⁰⁴ Styrene matches the criteria of a “controlling co-monomer” and it was found that as little as 8.8 mol% styrene in the feed was sufficient to control the MMA/styrene copolymerization and yield MMA-rich copolymers with narrow molecular weight distribution ($\overline{M}_w/\overline{M}_n \approx 1.2 - 1.4$) as well as high level of “livingness”.^{104,130,140} Through ESR studies and PREDICI simulations, it was concluded that the existence of a majority of styrene-terminated with an MMA penultimate unit macroalkoxyamine (MMA-S-SG1) was crucial to achieve both of fast initiation accelerated by the penultimate MMA unit and fast recombination due to the styrene terminal unit, and

consequently the successful SG1-mediated copolymerization of MMA with a small amount of styrene.^{130,140} Meanwhile, numerous NMP studies of copolymerizations of other methacrylates, including ethyl and *n*-butyl methacrylate (EMA and BMA),¹⁴¹ benzyl methacrylate (BzMA),¹⁴² 2-(dimethylamino)ethyl methacrylate (DMAEMA),⁴⁷ and oligo(ethylene glycol) methacrylate (OEGMA),¹³² with a small amount of styrene were published. As researchers examine the robustness and flexibility of this copolymerization approach, the use of alternative controlling co-monomers started to be reported. The molecular structures of some of the effective controlling co-monomers reported are shown in Scheme 2-2. Nicolas et al. showed that a minimal amount of acrylonitrile (2.2 – 8.8 mol% in the feed) was effective in controlling copolymerization feeds that were rich in MMA¹⁴³ and OEGMA.¹³¹ 4-Styrene sulfonate (SS) was demonstrated as an effective controlling co-monomer for methacrylic acid (MAA) in the SG1-mediated copolymerization, yielding water-soluble macroalkoxyamines for the synthesis of amphiphilic block copolymers and nanoparticles.¹⁴⁴ Schubert and coworkers utilized pentafluorostyrene (PFS) as the controlling co-monomer for DMAEMA and OEGMA to yield water-soluble and thermo-responsive copolymers that could undergo “click” reaction, due to the PFS units.¹⁴⁵ Maric and Lessard established the high effectiveness of 9-(4-vinylbenzyl)-9H-carbazole (VBK) as a controlling co-monomer by demonstrating controlled and pseudo-“living” copolymerizations of MMA and VBK with as little as 1 mol% VBK.^{146,147} VBK was then also used to control other methacrylate-rich copolymerizations including DMAEMA,⁴⁸ OEGMA⁵⁰ and BzMA¹⁴⁸ by NMP. Finally, I also demonstrated pH-sensitive 2-vinylpyridine (2VP) to be an effective controlling co-monomer by copolymerizing DMAEMA with as little as 2 mol% 2VP in a controlled manner.¹⁴⁹ It is clear that the copolymerization methodology is an effective and

simple way to produce methacrylate-rich copolymers with possible additional functionality imparted from the co-monomer.



Scheme 2-2. The molecular structures of reported controlling co-monomer for methacrylates by NMP.

On the other hand, attempts have been made to synthesize new alkoxyamines for controlling methacrylate polymerization without any controlling co-monomer via NMP. So far, such efforts have been focused on *N*-phenylalkoxyamines.^{109,150} It was thought that the radical delocalization through the phenyl ring might decrease the spin density on the oxygen atom and thus minimize cross-disproportionation of the nitroxide.^{109,150} Guillauneuf et al. prepared two 2,2-diphenyl-3-phenylimino-2,3-dihydroindol-1-yloxyl nitroxide (DPAIO)-based alkoxyamines, both of which were able to control homopolymerization of MMA at 100 °C up to 60% conversion and yield

PMMA with relatively narrow molecular weight distribution (dispersity $\bar{D} \approx 1.4$).¹⁰⁹ Greene and Grubbs synthesized two *N*-phenylalkoxyamines by the addition of 4-nitrophenyl-2-methylpropionat-2-yl radicals across the double bond of nitrosobenzene.¹⁵⁰ Linear molecular weight increase with conversion up to 49% conversion and low dispersity ($\bar{D} = 1.12 - 1.30$) for MMA homopolymerization were achieved with these new alkoxyamines. However, The DPAIO-based alkoxyamines were not able to initiate polymerization of *n*-butyl acrylate and the *N*-phenylalkoxyamines prepared by Greene and Grubbs could not control synthesis of poly(styrene). The fast recombination of these new nitroxide and propagating radicals was critical in controlling MMA polymerization but at the same time resulted in an equilibrium constant that was too low for monomers that were well controlled by the commercially available nitroxides. The search for a versatile alkoxyamine that can further expand the range of monomers (especially methacrylates) polymerizable in a controlled manner via NMP remains an active research area.

Chapter 3

Controlled Synthesis of Water-soluble and Stimuli-responsive Copolymers with Small Amount of Styrene by NMP

3.1 Preface

This chapter presents an article published in *Polymers* **2011**, 3, 1398-1422. It details the controlled synthesis of copolymers rich in 2-(dimethylamino)ethyl methacrylate (DMAEMA) ($f_{DMAEMA,0} = 80 - 95$ mol%) by nitroxide mediated polymerization (NMP) using styrene as a controlling co-monomer. PDMAEMA is a well known water-soluble polymer that is sensitive to both pH and temperature changes. However, no reports of its controlled synthesis via NMP were found prior to this study.

This work was inspired by the previous success of a number of methacrylate-rich copolymerizations by NMP aided by a small amount of styrene as a controlling co-monomer.^{104,132,141} The copolymerizations in this study were conducted using a modified alkoxyamine initiator functionalized by a succinimidyl ester made by conjugation of commercially available initiator BlocBuilder™ and *N*-hydroxysuccinimide, allowing controlled copolymerizations without aid of excess free SG1 nitroxide. With as little as 5 mol% styrene in the feed, the copolymerizations showed linear growth in molecular weight versus conversion and relatively narrow molecular weight distribution. Selected copolymers were chain-extended to illustrate their effectiveness as macroinitiators and form block copolymers of two DMAEMA/styrene blocks with different compositions. The statistical and block copolymers exhibited LCST-type phase separation in aqueous

solutions, as expected. The effects of polymer composition, solution concentration, pH and polymer microstructure on the phase behaviours of the copolymers were discussed in details. This work expanded the library of poly(methacrylate)s that NMP can synthesize in a controlled fashion with a small amount of styrene. It also illustrated various facile methods to tune the transition temperatures of these copolymers in aqueous solutions. Additionally, these water-soluble copolymers can be later conjugated to nucleophiles including proteins using the succinimidyl ester chain ends from the initiator fragment.¹⁵¹

Synthesis of Stimuli-Responsive, Water-Soluble Poly[2-(dimethylamino)ethyl methacrylate/styrene] Statistical Copolymers by Nitroxide Mediated Polymerization

Chi Zhang and Milan Maric

Department of Chemical Engineering, McGill University,
3610 University Street, Montreal, QC, Canada H3A 2B2

Polymers **2011**, *3*, 1398-1422.

Abstract:

2-(Dimethylamino)ethyl methacrylate/styrene statistical copolymers (poly(DMAEMA-*stat*-styrene)) with feed compositions $f_{DMAEMA} = 80 - 95$ mol%, (number average molecular weights $M_n = 9.5 - 11.2$ kg mol⁻¹) were synthesized using succinimidyl ester-functionalized BlocBuilder alkoxyamine initiator at 80 °C in bulk. Polymerization rate increased three-fold on increasing $f_{DMAEMA} = 80$ to 95 mol%. Linear M_n increases with conversion were observed up to about 50% conversion and obtained copolymers possessed monomodal, relatively narrow molecular weight distributions (dispersity = 1.32 – 1.59). Copolymers with $f_{DMAEMA} = 80$ and 90 mol% were also cleanly chain-extended with DMAEMA/styrene mixtures of 95 and 90 mol% DMAEMA, respectively, confirming the livingness of the copolymers. Copolymer phase behaviour in aqueous solutions was examined by dynamic light scattering and UV-Vis spectroscopy. All copolymers exhibited lower critical solution temperature (LCST)-type behaviour. LCST decreased with increasing styrene content in the copolymer and with increasing solution concentration. All copolymers were completely water-soluble and temperature insensitive

at pH 4 but were more hydrophobic at pH 10, particularly copolymers with $f_{DMAEMA} = 80$ and 85 mol%, which were water-insoluble. At pH 10, LCST of copolymers with $f_{DMAEMA} = 90$ and 95 mol% were more than 10 °C lower compared to their solutions in neutral, de-ionized water. Block copolymers with two statistical blocks with different DMAEMA compositions exhibited a single LCST and no microphase separation apparent between the two blocks.

3.2 Introduction

Stimuli-responsive polymers have sharp and reversible responses to small changes in environmental conditions such as temperature, pH, light, ionic strength, electric and magnetic fields, and they have emerged as a class of materials known as “smart” materials.^{56,152} Water-soluble polymers that can respond to one or more stimuli include poly(*N*-isopropylacrylamide) (PNIPAM), poly(hydroxypropyl acrylate) (PHPA), poly(oligo(ethylene glycol)methyl ether methacrylate) (POEGMEA) and poly(2-(dimethylamino)ethyl methacrylate) (PDMAEMA). These are being extensively studied for numerous potential applications, particularly in the biomedical field, such as drug/gene delivery systems, bioseparations, biosensors, and tissue engineering.^{3,56,57,153-}

155

PDMAEMA is a water-soluble polymer sensitive to both temperature and pH changes. It exhibits a lower critical solution temperature (LCST)-type phase separation upon heating at neutral or basic conditions and is completely water-soluble in acidic media.¹⁵⁶⁻¹⁵⁸ To fine-tune the transition conditions and polymer properties, DMAEMA has been

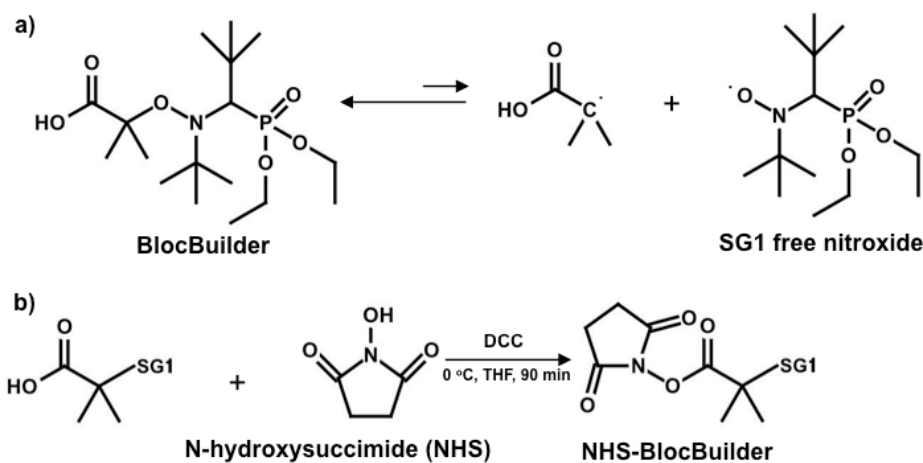
incorporated into block copolymers with various counter blocks such as the pH-sensitive poly(2-vinyl pyridine) to obtain pH-dependent micelles,¹⁵⁶ a temperature-responsive block such as POEGMA¹⁵⁷ and PNIPAM¹⁵⁹ to alter the LCST, and a hydrophobic block such as poly(2-(*N*-carbazolyl)ethyl methacrylate) to make amphiphilic diblock copolymers with hole-transport properties.¹⁶⁰

In order to synthesize well-defined polymers and block copolymers that are crucial to obtain the desired performance, precise controls of molecular weight, block sequence length and molecular weight distribution are required. To achieve these goals with relatively robust experimental conditions, controlled radical polymerization (CRP) techniques like atom transfer radical polymerization (ATRP), reversible addition-fragmentation transfer (RAFT) and nitroxide mediated polymerization (NMP) have emerged.¹⁶¹ For DMAEMA specifically, ATRP¹⁶²⁻¹⁶⁴ and RAFT^{115,157,165} have been successfully applied to obtain well-defined (co)polymers. NMP, being a solely thermal process, does not involve metal catalysts that ATRP requires or bimolecular exchange with sulfur-based agents as in RAFT, which is potentially advantageous for synthesis of non-cytotoxic polymers for biomedical applications^{132,133,151} or electronic applications where metal contamination is undesirable.¹³³ However, controlled polymerizations of methacrylates like DMAEMA is still challenging for NMP because methacrylates have very high equilibrium constant K resulted from slow recombination of nitroxides and sterically-hindered poly(methacrylate) radicals, leading to high concentration of propagating radicals that can promote self-termination, resulting in “dead” polymers at low conversions.^{133,139}

First-generation nitroxide mediators such as TEMPO (2,2,6,6-tetramethylpiperidinyl-1-oxy) limited NMP to mostly styrenic-based monomers.^{123,124,166} Important monomers like acrylates and methacrylates could not be controlled with TEMPO. More recently developed alkoxyamine initiators have opened up possibilities towards accessing (meth)acrylic-based polymers. Aside from the alkoxyamines synthesized specifically for methacrylates,^{109,150} a commercially available SG1-based unimolecular alkoxyamine called BlocBuilder (*N*-(2-methylpropyl)-*N*-(1-diethylphosphono-2,2-dimethylpropyl)-*O*-(2-carboxylprop-2-yl) hydroxylamine; molecular structure of SG1 and BlocBuilder shown in Scheme 3-1 (a)) has achieved controlled polymerization of a range of methacrylates, including methyl,^{104,130} ethyl,¹⁴¹ butyl,¹⁴¹ benzyl¹⁴² and poly(ethylene glycol) methyl ether methacrylates,¹³² with a small amount (4 – 10 mol%) of styrene in the feed and in the presence of about 10% excess of free SG1 relative to the BlocBuilder initiator. The success of such a copolymerization approach was attributed to the low cross-propagation rate constant (k_p /reactivity ratio) and much lower equilibrium constant K of styrene compared to methacrylates,^{104,126,133,167} which dramatically lowers the product of the average propagation rate constant, $\langle k_p \rangle$, and average equilibrium constant, $\langle K \rangle$, $\langle k_p \rangle \langle K \rangle$, which is often used to assess control of such NMP polymerization processes.

Besides controlling polymer microstructure, the alkoxyamine initiator fragment can permit functionalization and derivatization, such as using an initiator bearing an activated ester moiety. *N*-hydroxysuccinimidyl (NHS) esters readily react with nucleophiles in single-step reactions¹⁶⁸ and precursors functionalized by NHS have been reported for ATRP¹⁶⁹ and RAFT¹⁷⁰ to yield α -functional polymers. Vinas *et. al* synthesized the first

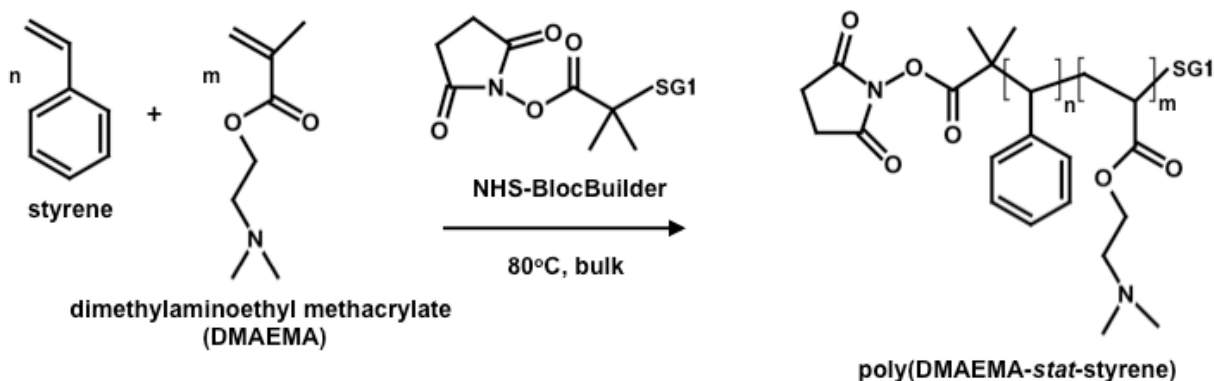
NHS-functionalized initiator for NMP using BlocBuilder.¹⁷¹ The NHS-BlocBuilder (Scheme 3-1 (b)) has been used to effectively control the homopolymerization of styrene and *n*-butyl acrylate, as well as statistical copolymerization of glycidyl methacrylate and styrene without aid of additional free SG1 nitroxide.^{171,172}



Scheme 3-1. (a) Dissociation scheme of BlocBuilder. (b) Synthesis of succinimidyl ester terminated BlocBuilder (NHS-BlocBuilder).

In this study, the NHS-BlocBuilder was used as an initiator to statistically copolymerize DMAEMA with a small amount of styrene as the controlling co-monomer (80 – 95 mol% DMAEMA in the feed) at 80 °C in bulk (Scheme 3-2). The combination of NHS-BlocBuilder with DMAEMA-rich feeds was envisioned to enable the development of a water-soluble PDMAEMA with LCST behaviour that could also later be conjugated to biological compounds or other amine-containing materials. Further, NMP with NHS-BlocBuilder will be tested to see if no additional free SG1 nitroxide was required, as has recently been shown for other methacrylate-rich feeds.¹⁷² The following study details

results concerning the NMP synthesis of DMAEMA-rich copolymerizations (kinetics, level of control and livingness of the copolymers) followed by the responses of the copolymers to temperature and pH changes in aqueous media.



Scheme 3-2. Synthesis of statistical copolymers of 2-(dimethylamino)ethyl methacrylate (DMAEMA) and styrene using *N*-hydroxysuccinimidyl-functionalized BlocBuilder (NHS-BlocBuilder) as the initiator.

3.3. Results and Discussion

3.3.1. Synthesis of statistical copolymers of 2-(dimethylamino)ethyl methacrylate (DMAEMA) and styrene

3.3.1.1 Kinetic results of the statistical copolymerizations

The kinetic results of the copolymerizations of DMAEMA and styrene using *N*-hydroxysuccinimide functionalized BlocBuilder (NHS-BlocBuilder) as initiator are presented in Figure 3-1. All copolymerizations obeyed first order kinetics as described by Equation 3-1 and generated good fits to linear kinetic plots as shown in Figure 3-1 (a).

Equation 3-1

$$\ln \frac{[M]_0}{[M]_t} = \ln \frac{[M]_0}{[M]_0(1 - \text{conversion})} = \ln \frac{1}{1 - \text{conversion}} = \langle k_p \rangle [P\bullet] \times \text{time}$$

In Equation 3-1, $[M]_0$ and $[M]_t$ are concentrations of monomer at time zero and subsequent later time t , respectively; $\langle k_p \rangle$ is the average propagation rate constant; and $[P\bullet]$ is the propagating radical concentration.

The apparent rate constant represented by the slopes of the kinetic plots, $\langle k_p \rangle [P\bullet]$, increased rapidly with the initial DMAEMA feed composition (f_{DMAEMA}), especially when $f_{DMAEMA} \geq 90$ mol%, as shown in Figure 3-1 (b). This result is expected as methacrylates have generally higher k_p and much higher K (defined by Equation 3-2 when SG1 is the nitroxide) compared to styrene.^{126,139,167}

Equation 3-2

$$K = \frac{[SG1\bullet][P\bullet]}{[SG1 - P]}$$

where $[SG1\bullet]$ is the free nitroxide concentration and $[SG1 - P]$ is the concentration of the dormant initiator.

The result is consistent with similar copolymerization studies of methacrylates with styrene using BlocBuilder.^{104,130,132,141,142} The kinetic results showed that the feed composition had a strong effect on the polymerization rate of the DMAEMA-rich

mixtures and the polymerization rate of DMAEMA using NHS-BlocBuilder as the initiator can be controlled with as little as 5 mol% styrene.

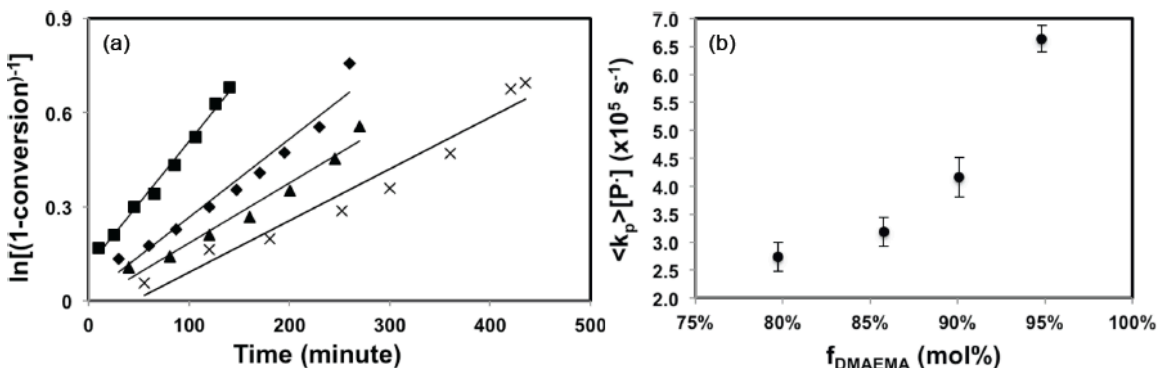


Figure 3-1. (a) Kinetic plots of $\ln[(1-\text{conversion})^{-1}]$ versus time for the statistical copolymerizations of 2-(dimethylamino)ethyl methacrylate (DMAEMA) and styrene at 80 °C with initial feed composition with respect to DMAEMA (f_{DMAEMA}) of 80 mol% (×), 85 mol% (▲), 90 mol% (◆), and 95 mol% (■). (b) Product of average propagation constant, $\langle k_p \rangle$, and concentration of propagating radical, $[P\cdot]$, $\langle k_p \rangle [P\cdot]$ (slope of the kinetic plots in Figure 3-1 (a)), versus initial feed composition with respect to DMAEMA (f_{DMAEMA}); error bars represent standard deviations of the slopes from Figure 3-1 (a).

3.3.1.2 Level of control of the copolymerizations and the livingness of the copolymers

Linear molecular weight increase with conversion and narrow molecular weight distribution of the polymers are characteristics generally associated with controlled polymerizations. In Figure 3-2 (a), number-average molecular weight (M_n) was plotted against conversion for the various copolymerizations. M_n increased linearly with conversion for all copolymerizations up to about 50% conversion. However, the slopes of the increasing trends of the copolymerizations with different compositions varied and differed from the theoretical one as shown in Figure 3-2 (a). For copolymerizations with $f_{\text{DMAEMA}} = 80 - 90$ mol%, the slopes were very similar but slightly smaller than the theoretical one. The small deviation in slopes can be attributed to the differences in

hydrodynamic volumes of the copolymers and that of poly(styrene) standards that used to calibrate the GPC. The copolymerization with $f_{DMAEMA} = 95$ mol%, on the other hand, had a significantly smaller slope than the others, where the difference in hydrodynamic volumes cannot be the sole reason. The copolymerization with $f_{DMAEMA} = 95$ mol% exhibited the most rapid kinetic behaviour as shown in Figure 3-1. The fast kinetics was the result of not only higher $\langle k_p \rangle$, but also likely a comparatively higher $\langle K \rangle$ from the highly methacrylate-rich mixtures.¹⁰⁴ The latter point is particularly important for the level of control because high concentration of propagating radicals favors self-termination and the large K of methacrylates such as methyl methacrylate was claimed to be the main cause for its uncontrolled homopolymerization using nitroxides.¹³⁹ Increase in termination of long chains and initiation of short chains can lower the overall M_n and lead to the decrease in slope for the copolymerization with $f_{DMAEMA} = 95$ mol% as observed in Figure 3-2 (a).

The change in control as a function of feed composition was also reflected in the observed \mathcal{D} s of the copolymers. The copolymer \mathcal{D} s with $f_{DMAEMA} = 80 - 90$ mol% remained relatively constant at about 1.3-1.4 throughout the polymerizations. In contrast, \mathcal{D} s of copolymers with $f_{DMAEMA} = 95$ mol% started at about 1.4 and continued to increase to about 1.6 at 49% conversion. The broadening of the molecular weight distribution is a sign of chain termination events, which is consistent with the results of the M_n trend with conversion.

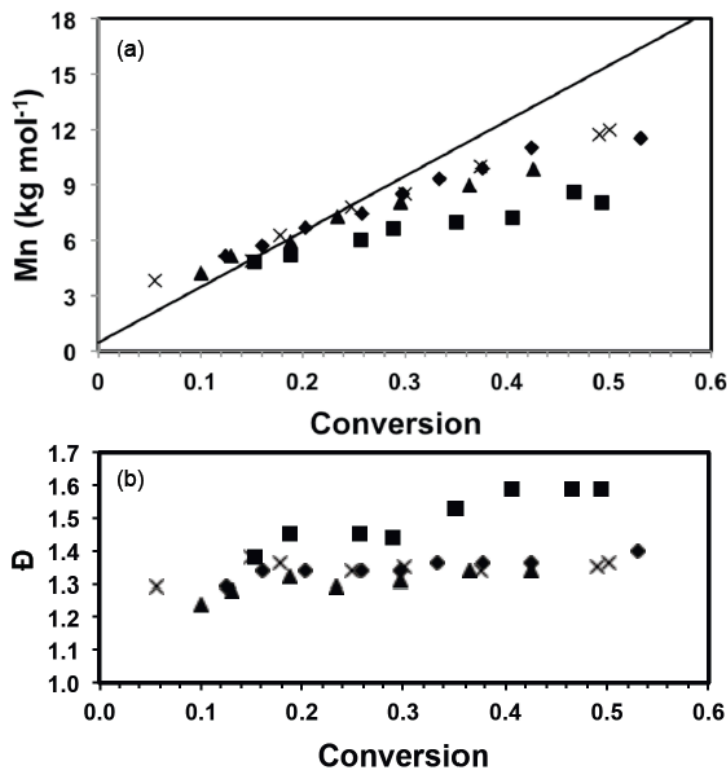


Figure 3-2. (a) Number-average molecular weight (M_n) and (b) dispersity (\bar{D}) of poly(DMAEMA-*stat*-styrene) with initial feed composition with respect to DMAEMA (f_{DMAEMA}) of 80 mol% (x), 85 mol% (▲), 90 mol% (◆), and 95 mol% (■) versus conversion; solid line in (a) represents theoretical trend. M_n determined by GPC calibrated with poly(styrene) standards.

The results of the DMAEMA/styrene statistical copolymerizations using NHS-BlocBuilder as initiator are summarized in Table 3-1. Statistical copolymers had compositions very similar to the feed compositions and copolymers with higher styrene content possessed lower \bar{D} s. The percentage of SG1-capped polymer chains (f_{LC} , Table 3-1) was also examined since the reversible SG1 termination is necessary for the re-initiation of polymer chains. This was the measure of the living fraction of the chains. From the results shown in Table 3-1, copolymers with F_{DMAEMA} up to 89 mol% had more than 80% living chains, whereas the copolymer $F_{DMAEMA} = 96$ mol% had only 69% living

chains. The results of f_{LC} can vary by about $\pm 10\%$ because of the uncertainties in M_n due to different hydrodynamic volumes between the copolymers and poly(styrene) standards. Nonetheless, the f_{LC} results confirm the high level of livingness of the copolymers with F_{DMAEMA} up to 89 mol% and decrease in livingness for the copolymer with $F_{DMAEMA} = 96$ mol%, in agreement with the kinetic data.

Table 3-1. Results of the copolymerizations of 2-(dimethylamino)ethyl methacrylate (DMAEMA) and styrene at 80 °C in bulk using *N*-hydroxysuccinimidyl-functionalized BlocBuilder as initiator.

Exp. ID ^a	Polymerization	Conversion ^b	F_{DMAEMA} ^b		\bar{D} ^c	f_{LC} ^d
	time min		mol%	M_n ^c kg mol ⁻¹		
DMAEMA/S-95/5	140	49%	96%	9.6	1.59	69%
DMAEMA/S-90/10	260	53%	89%	11.1	1.39	106%
DMAEMA/S-85/15	270	43%	84%	9.5	1.36	105%
DMAEMA/S-80/20	435	50%	81%	11.2	1.32	83%

^a The experiment ID donates the molar ratio between DMAEMA and styrene in the feed. ^b Conversion and final DMAEMA molar composition in copolymer determined by ¹H NMR. ^c Number-average (M_n), weight-average (M_w) molecular weight, and dispersity ($\bar{D} = M_w/M_n$) determined by GPC relative to poly(styrene) standards in THF at 40 °C. ^d Percentage of living polymer chains that are capped by SG1, determined by ³¹P NMR using diethyl phosphite as internal standard with experimental errors about $\pm 10\%$.

To further investigate the ability of the copolymers to re-initiate and form block copolymers, two chain-extension experiments were performed using the statistical copolymer synthesized in DMAEMA/S-80/20 ($F_{DMAEMA} = 81$ mol%, $M_n = 11.2$ kg mol⁻¹, $\bar{D} = 1.32$) and DMAEMA/S-90/10 ($F_{DMAEMA} = 89$ mol%, $M_n = 11.1$ kg mol⁻¹, $\bar{D} = 1.39$) as the macroinitiator. The experimental conditions and results of the chain extension experiments are summarized in Table 3-2. With a fresh mixture of 95 mol% DMAEMA, the DMAEMA/S-80/20 macroinitiator with $F_{DMAEMA} = 81$ mol% was extended with a more DMAEMA-rich block with M_n of approximately 16.5 kg mol⁻¹ and the overall

DMAEMA molar composition of the block copolymer was increased from 81 mol% of the macroinitiator to 90 mol%. On the other hand, the DMAEMA/S-90/10 macroinitiator with $F_{DMAEMA} = 89$ mol% was chain-extended with a DMAEMA/styrene mixture of similar composition ($f_{DMAEMA} = 90$ mol%) to obtain a block copolymer that was essentially a statistical copolymer. The two chain extended copolymers were also used to examine the effect of polymer microstructure and molecular weight on LCST behaviour, which will be discussed in section 3.2.5.

The \bar{D} s of the block copolymers (1.91 and 1.70) were significantly higher than that of the macroinitiator (1.32 and 1.39), indicating either termination occurred during the chain extension or some macroinitiator was not initiated.

Table 3-2. Summary of the experimental results and polymer properties in the chain extension experiments at 80 °C in bulk.

Macroinitiator properties			Chain extension conditions		Block copolymer properties			
F_{DMAEMA}^a	M_n^b	\bar{D}^b	f_{DMAEMA}^c	Conv.	Polymer ID	F_{DMAEMA}^a	M_n^b	\bar{D}^b
mol%	kg mol ⁻¹		mol%			mol%	kg mol ⁻¹	
81%	11.2	1.32	95%	40%	D/S80/20-b- D/S95/5	90%	27.8	1.91
89%	11.1	1.39	90%	36%	D/S90/10-b- D/S90/10	91%	26.6	1.70

^a DMAEMA molar composition in the macroinitiator and chain extended block copolymer determined by ¹H NMR. ^b Number-average (M_n), weight-average (M_w) molecular weight, and dispersity ($\bar{D} = M_w/M_n$) determined by GPC relative to poly(styrene) standards in THF at 40 °C.

The results of the chain-extension experiments can be more clearly observed by examining the GPC trace of the macroinitiator compared to the chromatogram of the chain-extended polymer in Figure 3-3. The trace of the chain-extended polymer retained generally its mono-modal nature and has a clear shift to the left, indicating most of the macroinitiators were extended and the level of livingness was high. The tails of chain-

extended copolymers overlap to some degree with the associated macroinitiator traces in both cases, but the tailing was slightly more apparent for the chain extension of the DMAEMA/S-80/20 macroinitiator. From the f_{LC} results listed in Table 3-1, DMAEMA/S-80/20 macroinitiator had a slightly lower percentage of SG1-capped chains than the DMAEMA/S-90/10 macroinitiator but the second batch of monomer was richer in DMAEMA. As noted previously for the statistical copolymer, control was poorer with broader molecular weight distributions when the feed was very rich in DMAEMA ($f_{DMAEMA} = 95$ mol%). This suggested a small amount of “dead” macroinitiator combined with a richer DMAEMA second feed contributed to the broadening of the molecular weight distribution after chain-extension. Baseline drifts immediately after the main peaks were also observed in all traces. To investigate the potential reasons for the drifts, the copolymers were fractionated to remove some low M_n chains and re-examined by GPC. The baseline drift persisted for the fractionated copolymers, indicating adsorption of the polar amine group of PDMAEMA to the GPC column is likely the cause for the baseline drift observed.^{76,162}

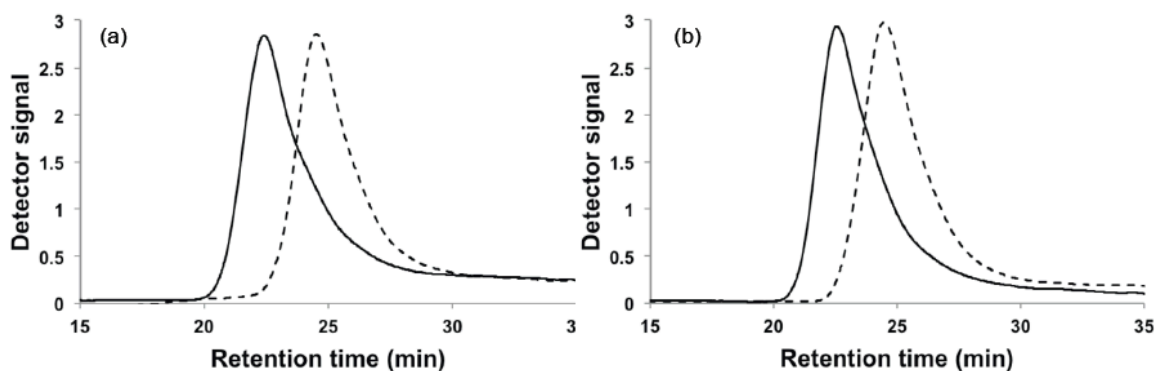


Figure 3-3. GPC traces of macroinitiators (dashed line) and chain extended polymers (solid line) for the chain extension of (a) DMAEMA/S-80/20 with a second feed of $f_{DMAEMA} = 95$ mol% and (b) DMAEMA/S-90/10 macroinitiator with a second feed of $f_{DMAEMA} = 90$ mol%.

In summary, well-defined DMAEMA-rich copolymers capable of initiating a second batch of monomer relatively cleanly were synthesized using NHS-BlocBuilder. To our knowledge, this is the first time such a synthesis using nitroxide-mediated polymerization is reported. Lokaj et al.¹⁷³ attempted to synthesize a block copolymer of styrene and DMAEMA using TEMPO-terminated poly(styrene) macroinitiators. However, conversion stopped increasing after 2 hours of reaction and the final copolymer contained only about 40 mol% DMAEMA. Low conversion and early termination can be results of the slow initiation of poly(styrene) macroinitiator^{130,174} and/or β -hydrogen transfer from the propagating radical to the initiator.^{175,176}

SG1-base initiators such as BlocBuilder have lower activation energy and much higher dissociation rate constant (k_d) compared to TEMPO-based initiators.¹⁷⁷ Additionally, Dire et al.¹³⁷ confirmed that the rate constant for β -hydrogen transfer (k_{tr}) of methyl methacrylate/SG1 system was three orders of magnitude lower compared to a *n*-butyl methacrylate/TEMPO system. As a result, SG1-based initiators can be activated at lower temperatures and allow controlled polymerizations of a wider range of monomers, such as methacrylates, compared to TEMPO. However, when polymerizing non-styrenic monomers using BlocBuilder, additional SG1 nitroxide was required to further reduce polymerization rate and produce well-defined copolymers.^{103,104,110,178}

The k_d of NHS-BlocBuilder measured by Vinas et al. was about 15 times higher than that of BlocBuilder (5 s^{-1} for NHS-BlocBuilder and 0.32 s^{-1} for BlocBuilder) at $120 \text{ }^\circ\text{C}$ in *tert*-butyl benzene.¹⁷¹ Under the same experimental conditions, they also found that the activation energy of NHS-BlocBuilder ($E_a = 105 \text{ kJ mol}^{-1}$) was lower than that of

BlocBuilder ($E_a = 112 \text{ kJ mol}^{-1}$). The high dissociation rate and lower activation energy of NHS-BlocBuilder led to fast initiation and quick release of the regulating SG1 nitroxide, which mimics the situation when additional SG1 free nitroxide is added at the onset to the solution to improve control. Consequently, controlled polymerization of the DMAEMA-rich mixtures without the requirement of additional SG1, as is typical for methacrylate-rich polymerizations by BlocBuilder, was largely accomplished. The results of the DMAEMA/styrene statistical copolymerizations demonstrated that NHS-BlocBuilder was not only is an effective initiator for synthesizing DMAEMA-rich copolymers, but also simplifies polymerization procedures and provides opportunities for further functionalization of the copolymers. Our group earlier noticed similar performance for NHS-BlocBuilder controlled copolymerizations of glycidyl methacrylate with styrene.¹⁷²

3.3.2. Studies of temperature and pH sensitivities of copolymers in aqueous solutions

The sensitivity to both temperature and pH of PDMAEMA in aqueous solution is a hallmark of such materials for applications requiring it as a stimuli-responsive material. The LCST of such a polymer can be affected by many parameters, including molecular weight,^{69,77} polymer composition,^{145,157,179} solution concentration,⁶⁹ and pH^{156,157} in the case of PDMAEMA. Because the DMAEMA/styrene copolymerizations using NHS-BlocBuilder were relatively controlled as demonstrated earlier, final copolymers obtained have similar M_n ($10.4 \pm 0.9 \text{ kg mol}^{-1}$) and \bar{D} (1.42 ± 0.12). Therefore, the second part of this study was to determine the LCST of the copolymers as a function of polymer

composition, solution concentration and pH. This is necessary as the small amount of styrene required as a controlling co-monomer for the BlocBuilder-mediated NMP may affect the LCST compared to that of pure PDMAEMA.

3.3.2.1 LCST-type phase separation illustrated by UV-Visible spectrometry and dynamic light scattering

UV-Visible spectrometry (UV-Vis) and dynamic light scattering (DLS) were used to characterize the phase behaviour of the copolymers. UV-Vis monitored the light transmittance of the solutions as temperature varied. DLS measured the hydrodynamic radius (R_h) distribution of the polymers in solution. Each copolymer was dissolved in de-ionized water at concentrations of 0.1, 0.3 and 0.5 wt% and buffer solutions of pH 4 and 10 at 0.5 wt%. Figure 3-4 and 3-5 shows the changes of light transmittance and R_h with temperature of solutions in de-ionized water, respectively. Copolymers with up to 16 mol% styrene (DMAEMA/S-85/15) were soluble in de-ionized water at all three concentrations. Copolymer with 19 mol% styrene (DMAEMA/S-80/20) was only soluble in de-ionized water at 0.1 wt%.

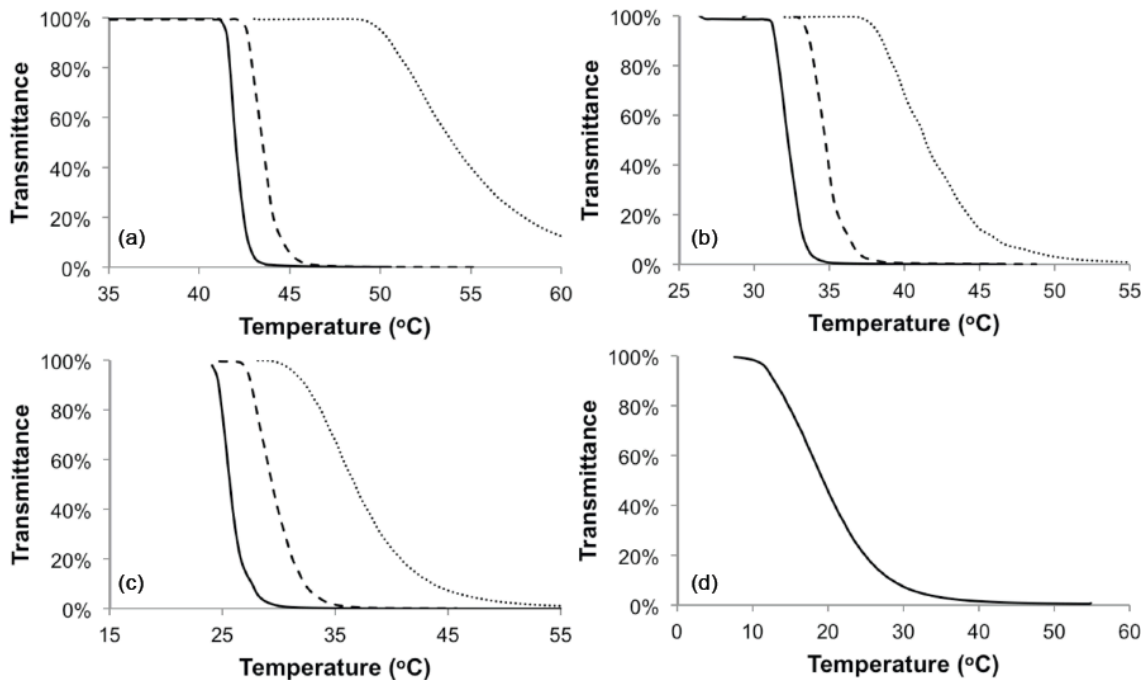


Figure 3-4. Light transmittance as a function of temperature of poly(DMAEMA-*stat*-styrene) copolymers with (a) $F_{DMAEMA} = 96$ mol% (DMAEMA/S-95/5) (b) $F_{DMAEMA} = 89$ mol% (DMAEMA/S-90/10) (c) $F_{DMAEMA} = 84$ mol% (DMAEMA/S-85/15) (d) $F_{DMAEMA} = 81$ mol% (DMAEMA/S-80/20) at 0.1 wt% (dotted line), 0.3 wt% (dashed line) and 0.5 wt% (solid line) in de-ionized water measured by UV-Vis spectrometry.

The light transmittance profiles reflected typical behaviour of LCST-type phase separation, where solutions were 100% transparent at low temperature and became cloudy (0% transmittance) quickly above the critical temperature, illustrating the sudden solubility drop of the polymer in water. The transition temperature decreased as concentration increased. The shapes of the profiles were similar for different copolymers at the same concentration, where the transitions became broader as the concentration decreased from 0.5 wt% to 0.1 wt%.

In the DLS measurements, R_h was below 10 nm at low temperature for all cases and rapidly rose up to about 500 nm for 0.3 and 0.5 wt% solutions and about 100 nm for 0.1

wt% solutions when the critical temperature was reached. It demonstrated the transformation of polymers from small, dispersed unimers¹⁸⁰ to large aggregated particles upon heating. The shifts of critical temperature with concentration were similar to those observed by UV-Vis.

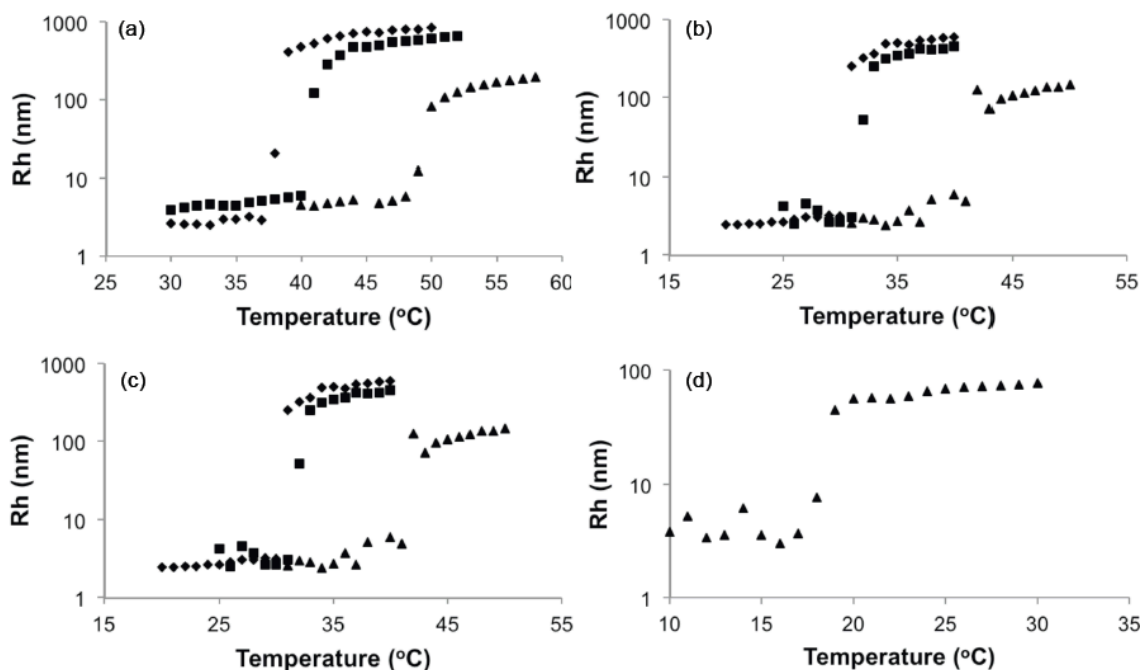


Figure 3-5. Hydrodynamic radii of copolymers (R_h) as a function of temperature of poly(DMAEMA-*stat*-styrene) copolymers with (a) $F_{DMAEMA} = 96$ mol% (DMAEMA/S-95/5) (b) $F_{DMAEMA} = 89$ mol% (DMAEMA/S-90/10) (c) $F_{DMAEMA} = 84$ mol% (DMAEMA/S-85/15) (d) $F_{DMAEMA} = 81$ mol% (DMAEMA/S-80/20) at 0.1 wt% (▲), 0.3 wt% (■) and 0.5 wt% (◆) in de-ionized water measured by dynamic light scattering.

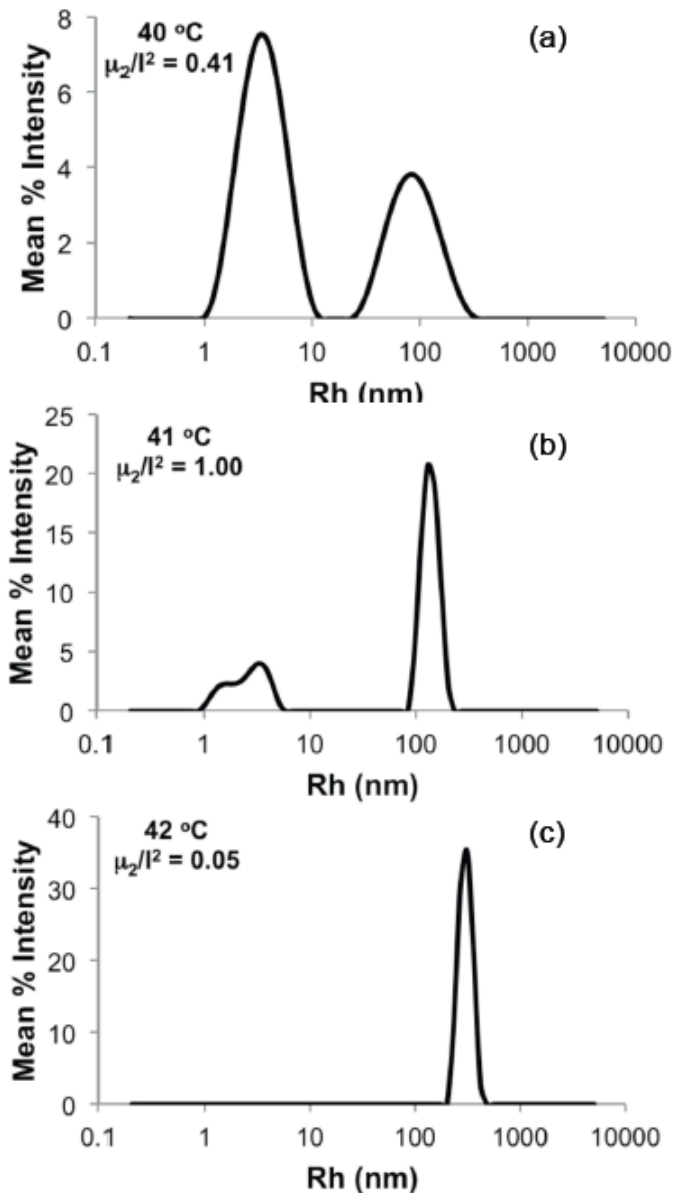


Figure 3-6. Hydrodynamic radius distribution (using mean % intensity) for 0.3 wt% solution of poly(DMAEMA-*stat*-styrene) with $F_{DMAEMA} = 96$ mol% (DMAEMA/S-95/5) at 40–42 °C.

Figure 3-6 shows typical R_h distributions near the critical temperature using the 0.3 wt% solution of poly(DMAEMA-*stat*-styrene) with $F_{DMAEMA} = 96$ mol% as an example. Below LCST (temperature = 40 °C in Figure 3-6), a unimer peak of $R_h < 10$ nm can be observed with a trace amount of loose aggregates. As temperature approached the LCST

(temperature = 41 °C in Figure 3-6), the amount of aggregates increased and the width of the overall distribution (μ_2/Γ^2) became much broader as phase separation started. At temperature = 42 °C in Figure 3-6, the peak corresponding to unimers completely disappeared, leaving only the narrow peak representing large aggregates with μ_2/Γ^2 below 0.1. Because the distributions were intensity-based, the height of the peak is proportional to the corresponding size to the sixth order, according to the Rayleigh approximation.

Therefore, the distribution was heavily biased toward larger sizes as long as peaks of different sizes coexisted. Given this, the LCST was defined as the temperature where the large aggregate peak ($R_h \geq 100$ nm) became the only peak in the distribution (42 °C in Figure 3-6). For UV-Vis, LCST was defined as the temperature where the transmittance dropped to 80%.

3.3.2.2 Effect of polymer composition on LCST

Composition plays an important role on LCST of statistical copolymers with comonomers of different hydrophilicity.¹⁵⁷ Higher content of the less hydrophilic comonomer decreases LCST whereas higher content of the more hydrophilic comonomer increases LCST. Many researchers have fine-tuned the LCST of different copolymers by varying their composition.^{145,157,179} In this study, styrene is a hydrophobic comonomer and it was expected that with more styrene incorporated into the copolymer, the LCST would be lower.

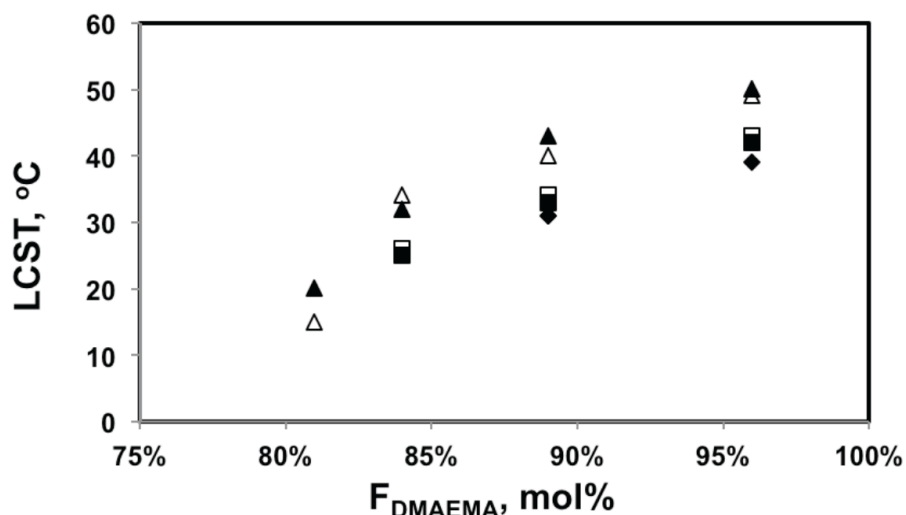


Figure 3-7. LCST of poly(DMAEMA-*stat*-styrene) as a function of DMAEMA molar composition in the copolymer (F_{DMAEMA}) in de-ionized water at 0.1 wt% (▲), 0.3 wt% (■) and 0.5 wt% (◆) concentration; filled symbols are DLS results and hollow symbols are UV-Vis results.

Indeed, the LCST of the statistical copolymers decreased with the higher styrene content in the copolymer as shown in Figure 3-7. The results from DLS and UV-Vis were very similar with the largest difference of 5 °C for the 0.1 wt% solution of the least soluble copolymer with 81 mol% DMAEMA (DMAEMA/S-80/20). Since the copolymer with 81 mol% DMAEMA was not soluble at 0.3 wt% concentration, 0.1 wt% was likely close to its saturation limit at the storage temperature (5 °C). As temperature increased, small amounts of polymer may precipitate before large aggregates could be formed due to a decreasing saturation concentration with temperature. This could introduce errors in its LCST measurements. For copolymers with 84 mol% or more DMAEMA, LCST changed linearly with composition and the slopes of the trends for different concentrations were very similar, which is consistent with the results of other studies.^{145,157,179}

3.3.2.3 Effect of concentration on LCST

The LCST of poly(DMAEMA-*stat*-styrene) copolymer solutions in de-ionized water at 0.1, 0.3 and 0.5 wt% were summarized in Figure 3-8. Overall, LCST decreased as concentration increased, which is consistent with the literature.^{181,182} The LCST decreased by 7 – 10 °C when concentration increased from 0.1 to 0.3 wt%, whereas the LCST for 0.5 wt% solutions were very similar to those for 0.3 wt% solutions, with much smaller differences (0 – 3 °C).

From a thermodynamic perspective, when both the enthalpy (ΔH_m) and entropy (ΔS_m) become negative upon mixing with a dominant entropic term ($\Delta S_m T$), the Gibb's energy of mixing (ΔG_m) becomes negative and a polymer with some solventphobic structures may be solvated below LCST.⁶¹ In aqueous solutions, hydrogen bonding between water molecules and polymer chains can lead to formation of a layer of clathrate-like structures around a hydrophobic structure in a polymer chain which lowers the entropy of mixing and increases the solubility of the polymer in water.^{46,183} As temperature increases above a critical temperature, the ordered water layer is disrupted and the polymer chains collapse and form large aggregates.

It was found that LCST in aqueous solutions was not very concentration-sensitive as long as the solution was not too dilute (typically above 1 wt%).¹⁸²⁻¹⁸⁴ For dilute solutions, large amounts of water molecules are present in between each of the polymer chains, which can increase the energy needed to bring polymer chains together to form aggregates. This explains the broader transitions and smaller aggregate size for 0.1 wt% solutions shown in Figure 3-4 and 3-5. Because the transitions for 0.3 and 0.5 wt%

solutions were very similar in terms of LCST, sharpness of the transition and the size of the aggregates, 0.5 wt% is likely close to the critical concentration, above which LCST is no longer sensitive to concentration.

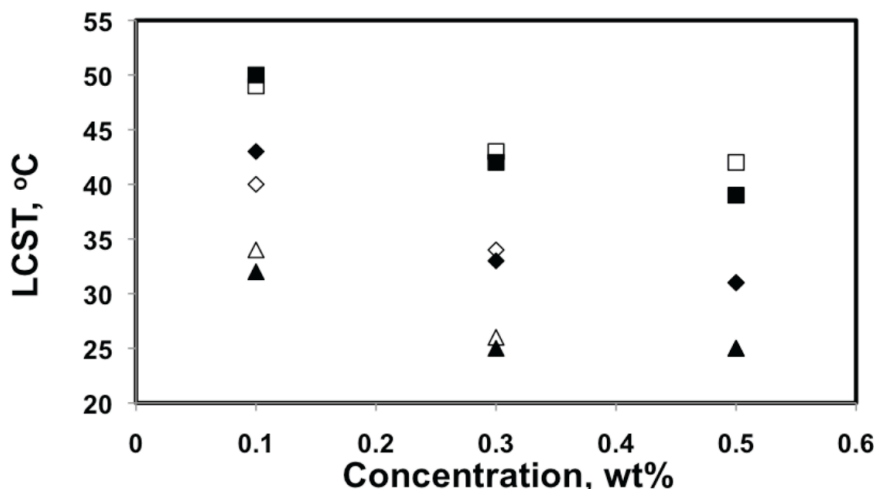


Figure 3-8. LCST of poly(DMAEMA-*stat*-styrene) with 96 mol% DMAEMA (DMAEMA/S-95/5, ■), 89 mol% DMAEMA (DMAEMA/S-90/10, ◆), and 84 mol% DMAEMA (DMAEMA/S-85/15, ▲), as a function of solution concentration in de-ionized water; filled symbols are DLS results and hollow symbols are UV-Vis results.

3.3.2.4 Effect of pH on the solubility of copolymers in aqueous solution

It is known that PDMAEMA is pH sensitive with a pK_a of about 7.3 in water.⁷⁷ To investigate the pH sensitivity of the statistical copolymers, solutions at pH 4 and 10 were prepared and their phase behaviour was compared to that in de-ionized water solutions. The results are summarized in Table 3-3.

All copolymers, including the one with 81 mol% DMAEMA (DMAEMA/S-80/20), which was only soluble at 0.1 wt% in de-ionized water, were soluble at pH 4 at 0.5 wt% and no LCST was observed up to 90 °C. At pH 4, PDMAEMA is completely ionized¹⁵⁶ into a polyelectrolyte. As a result, the solubility of PDMAEMA in water greatly increases

and becomes insensitive to temperature.^{156,157} Because the charged polymer is highly hydrophilic, even with as much as 19 mol% styrene, the copolymer was completely water-soluble at 0.5 wt%.

Table 3-3. Lower critical solution temperature (LCST) of poly(DMAEMA-*stat*-styrene) at different pH at 0.5 wt% concentration.

F _{DMAEMA} ^a mol%	LCST ^b		
	pH 4	~ pH 7 ^c	pH 10
100% [9]		47	35
96%		39	24
89%	soluble ^d	31	18
84%		25	insoluble ^e
81%		insoluble ^e	insoluble ^e

^a DMAEMA molar composition in copolymers. ^b Temperature at which unimer peak completely disappeared in dynamic light scattering. ^c In de-ionized water. ^d No LCST observed from 5 – 90 °C. ^e Insoluble at 5 °C.

At pH 10, LCSTs were observed and decreased with DMAEMA content in the copolymer, similar to the results in de-ionized water solutions. However, the LCST is more than 10 °C lower when comparing the copolymers in the pH = 10 solutions to the neutral, de-ionized water solutions. Additionally, the copolymer with 84 mol% DMAEMA (DMAEMA/S-85/15) that was soluble in de-ionized water was not soluble at pH = 10. In Figure 3-9, the hydrodynamic radii of the copolymers with 96 and 89 mol% DMAEMA (DMAEMA/S-95/5 and DMAEMA/S-90/10, respectively) increased rapidly from below 10 nm to ~ μm at their LCST. Because pH 10 is higher than the pK_a of PDMAEMA, the copolymers were totally deprotonated. As a result, the copolymers became more hydrophobic and easier to precipitate, indicated by the lower LCST at pH 10 than that in neutral water (Table 3-3). These results demonstrated the

DMAEMA/styrene statistical copolymers with 89 and 96 mol% DMAEMA possessed similar pH sensitivity to that expected for PDMAEMA homopolymer.

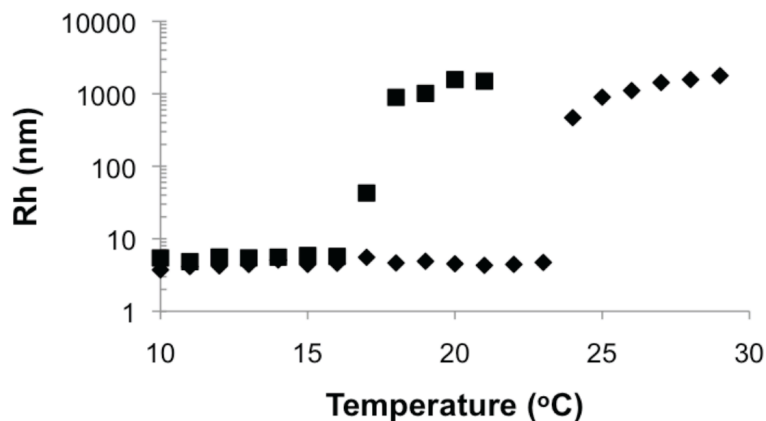


Figure 3-9. Hydrodynamic radii of particles (R_h) as a function of temperature of poly(DMAEMA-*stat*-styrene) with 96 mol% DMAEMA (DMAEMA/S-95/5, ■) and 89 mol% DMAEMA (DMAEMA/S-90/10, ◆) in pH 10 buffer solution at 0.5 wt% concentration.

3.3.2.5 Effect of polymer microstructure and molecular weight on LCST

DMAEMA has been incorporated into various block copolymers to obtain pH and/or temperature induced micelles in aqueous solutions because of the sensitivity to both pH and temperature of PDMAEMA.^{77,156,160,163} In this study, a diblock copolymer (D/S80/20-b-D/S95/5) was synthesized by chain-extending a macroinitiator with 81 mol% DMAEMA (DMAEMA/S-80/20, $M_n = 11.2 \text{ kg mol}^{-1}$) with a fresh mixture of DMAEMA and styrene ($f_{\text{DMAEMA}} = 95 \text{ mol}\%$, $M_{n,2nd \text{ block}} \approx 16.6 \text{ kg mol}^{-1}$, M_n relative to poly(styrene) standards, Table 3-2) and its phase behaviour in water was studied. Since the two blocks have different hydrophilicities as demonstrated earlier, it was anticipated that micellization with a D/S80/20 core and D/S95/5 corona might occur at temperatures

above the LCST of D/S80/20 and below the LCST of D/S95/5, followed by aggregation of entire polymer chains above the LCST of D/S95/5.

In Figure 3-10, the R_h of the block copolymer as a function of temperature was compared to its macroinitiator (DMAEMA/S-80/20, $F_{DMAEMA} = 81 \text{ mol}\%$, $M_n = 11.2 \text{ kg mol}^{-1}$) and the statistical polymers with similar composition and molecular weight as the second block (DMAEMA/S-95/5, $F_{DMAEMA} = 96 \text{ mol}\%$, $M_n = 9.6 \text{ kg mol}^{-1}$). The R_h of the block copolymer remained relatively constant at below 10 nm up to 23 °C with no obvious change at the LCST of the copolymer with $F_{DMAEMA} = 81 \text{ mol}\%$ at 20 °C. Above 23 °C, R_h increased quickly to about 100 nm and stayed constant even above the LCST of the copolymer with $F_{DMAEMA} = 96 \text{ mol}\%$ at 49 °C. These results showed a single step phase separation of the block copolymer similar to the observations of the statistical copolymers was occurring and microphase separation between the two blocks was not observed (i.e. two distinct LCST transitions).

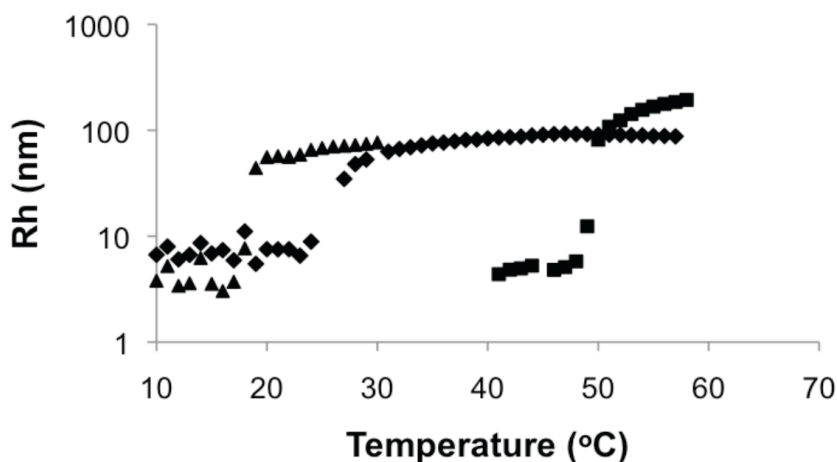


Figure 3-10. Hydrodynamic radii of particles (R_h) as a function of temperature of poly(DMAEMA-*stat*-styrene) with 96 mol% DMAEMA (DMAEMA/S-95/5, ■), 81 mol% DMAEMA (DMAEMA/S-80/20, ▲) and block copolymer (D/S80/20-*b*-D/S95/5, ◆) in de-ionized water at 0.1 wt% concentration.

The reason for the absence of microphase separation was most likely the lack of sufficient solubility difference between the two blocks in aqueous solution. The constituents of the two blocks were essentially the same except for the slightly different compositions. Hence the solubility parameters of the blocks were not sufficiently different to induce micellization. The slightly larger R_h below the LCST of the block copolymer was due to the higher molecular weight ($M_n = 27.8 \text{ kg mol}^{-1}$) of the block copolymer compared to the statistical copolymers ($M_n = 9.6$ and 11.2 kg mol^{-1}). The higher LCST of the block copolymer compared to its DMAEMA/S-80/20 macroinitiator was a result of increased water solubility from the more DMAEMA-rich second block.

Since the D/S80/20-b-D/S95/5 block copolymer synthesized had an overall composition ($F_{DMAEMA,overall}$) of 90 mol% DMAEMA, its phase behaviour was also compared with the statistical copolymers with $F_{DMAEMA} \approx 90 \text{ mol\%}$ that only differ by molecular weight (DMAEMA/S-95/5 and “block copolymer” D/S80/20-b-D/S-90/10, which was essentially as statistical copolymer since the chain extension was done with the same feed composition as the macroinitiator). As shown in Figure 3-11, the block copolymer had a considerably lower LCST compared to the statistical copolymers with similar overall composition. The two statistical copolymers with $F_{DMAEMA} \approx 90 \text{ mol\%}$ had the same LCST despite the difference in M_n , indicating M_n did not influence the LCST of the statistical copolymers significantly in the range of $10 - 30 \text{ kg mol}^{-1}$ and was not the cause for decreased LCST of the block copolymer.

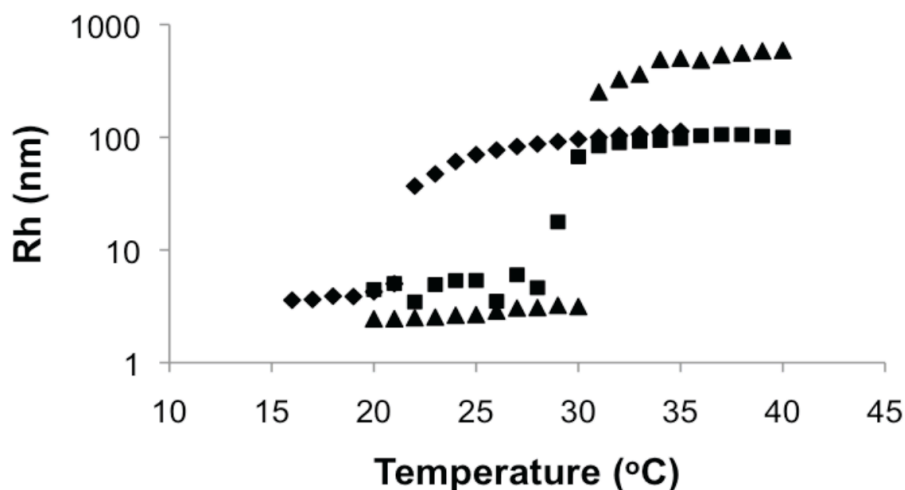


Figure 3-11. Hydrodynamic radii of particles (R_h) as a function of temperature of block copolymer (D/S80-*b*-D/S95, $F_{DMAEMA,overall} = 90$ mol%, $M_n = 27.8$ kg mol⁻¹, ◆), and poly(DMAEMA-*stat*-styrene) (DMAEMA/S-90/10) with $F_{DMAEMA} = 89$ mol% ($M_n = 11.1$ kg mol⁻¹, ▲), and D/S90/10-*b*-D/S90/10 block copolymer with $F_{DMAEMA} = 91$ mol% ($M_n = 26.6$ kg mol⁻¹, ■) in de-ionized water at 0.5 wt% concentration.

The change of LCST probably resulted from the differences in polymer microstructure. As reactivity ratios of methacrylates and styrene are generally similar and less than unity,¹⁸⁵ the distribution of DMAEMA and styrene in the statistical polymers should be relatively random. In the block copolymer, although distinctive microscopic phase separation was not observed, the LCST behaviour became more complicated because DMAEMA was more concentrated in one block than the other.

Park *et al.* reported that gradient copolymers of poly(2-alkyl-2-oxazoline)s showed sharp transitions at their LCST and did not find any evidence of micelle formation.^{186,187} Okabe *et al.* observed gradual phase separation of the gradient copolymer of 2-ethoxyethyl vinyl ether with 2-methoxyethyl vinyl ether, in contrast to the sharp transitions of the corresponding block copolymer.¹⁷⁹ Moreover, the gradient copolymer started phase separation just 3 °C higher than the LCST of the block copolymer. From Figure 3-10, the

block copolymer D/S80/20-b-D/S95/5 had a slightly broader transition compared to the statistical copolymers. Additionally, the LCST of the block copolymer was lower than the statistical copolymers with similar overall composition and close to the micellization temperature (LCST of the D/S80/20 block) if there was one. These observations implied the phase behaviour of D/S80/20-b-D/S95/5 resembled more of what would be expected of a gradient polymer. The exact mechanism of phase separation for such a copolymer was still not clear and should be examined in a more detailed study in the future.

3.4 Conclusions

In this study, DMAEMA was statistically copolymerized with 5 – 20 mol% styrene using NHS-BlocBuilder. Polymerization accelerated with increasing DMAEMA content in the feed as the average propagation rate constant $\langle k_p \rangle$ and average equilibrium constant $\langle K \rangle$ increased. The linear increase of M_n with conversion and successful chain extensions demonstrated the polymerizations were controlled without aid of additional SG1 and the obtained copolymers were living and relatively narrow in molecular weight distribution ($\mathcal{D} = 1.32 - 1.59$). Slight decreases in level of control and livingness were observed for the most DMAEMA-rich copolymer, which is likely attributed to the higher average equilibrium constant $\langle K \rangle$. The copolymers exhibited LCST-type behaviour in aqueous solutions, as expected. The LCST was tuned by varying copolymer composition, solution concentration and pH. The block copolymer of two statistical blocks with different DMAEMA compositions had a single LCST and did not exhibit microphase separation likely due to the lack of sufficient incompatibility between the two blocks. This study

marks the first time that DMAEMA could be polymerized with a small amount of co-monomer by NMP and without any additional free nitroxide, due to the use of the NHS-BlocBuilder initiator. Such water-soluble DMAEMA-rich statistical copolymers and block copolymers could later be conjugated with various nucleophiles using the NHS-fragment from the initiator.

Acknowledgements

The authors are very grateful for the funding support from the NSERC Discovery Grant and Canada Foundation for Innovation New Opportunities Fund.

References

Please refer to the global bibliography at the end of the thesis.

Chapter 4

α -Functional Statistical Copolymers with Dual pH and Temperature Responsiveness Made by NMP using 2-Vinylpyridine as “Controlling” Co-monomer

4.1 Preface

This chapter presents a manuscript published in the *Journal of Polymer Science, Part A: Polymer Chemistry* **2012** (50): 4341-4357. In Chapter 3, the nitroxide mediated polymerization (NMP) of 2-(dimethylamino)ethyl methacrylate (DMAEMA)-rich copolymers was demonstrated to be well controlled when styrene was used as a controlling co-monomer. While styrene has been shown to be effective in achieving controlled synthesis of various methacrylate-rich copolymers via NMP,^{104,132,141,142} the active search for alternative controlling co-monomers has been ongoing to demonstrate the versatility of the methodology,¹⁴³ improve hydrophilicity of the copolymer,¹⁴⁴ or impart additional functionalities to the copolymers.^{145,146}

In this manuscript, 2-vinylpyridine (2VP) was employed as a controlling co-monomer for the first time for methacrylate-rich feeds ($f_{DMAEMA,0} = 80 - 99$ mol%). 2VP was chosen for its reduced hydrophobicity compared to styrene, as well as its pH sensitivity (water-soluble in acidic conditions but hydrophobic in neutral or basic conditions). Similar experimental conditions as the copolymerizations of DMAEMA and styrene presented in Chapter 3 were used so that the two systems can be well compared. With as little as 2 mol% 2VP in the feed, the synthesis of DMAEMA/2VP copolymers was well controlled (linear increase in molecular weight with conversion and relatively narrow molecular weight distribution $\overline{M}_w/\overline{M}_n \approx 1.5 - 1.6$). The

statistical copolymers were completely water-soluble when solution pH was below 7 as DMAEMA was fully protonated; at pH of 7 to 11, the copolymers exhibit LCST behaviour in aqueous solutions with tune-able transition temperatures ranged from 14 to 75 °C.

Block copolymers were also synthesized via two different routes. Chain extension of a DMAEMA/2VP statistical macroinitiator with 2VP yielded a block copolymer that could form pH-induced micelles. The succinimidyl ester-terminated initiator was conjugated to amine-terminated poly(propylene glycol) (PPG), yielding an effective macroinitiator for synthesizing a doubly thermo-responsive PPG-*block*-DMAEMA/2VP block copolymer.

pH and temperature-sensitive statistical copolymers poly[2-(dimethylamino)ethyl methacrylate-*stat*-2-vinylpyridine] with functional succinimidyl-ester chain ends synthesized by nitroxide mediated polymerization

Chi Zhang, Milan Maric

Department of Chemical Engineering, McGill University,

3610 University Street, Montreal, QC, Canada H3A 2B2

Journal of Polymer Science, Part A: Polymer Chemistry **2012** (50): 4341-4357

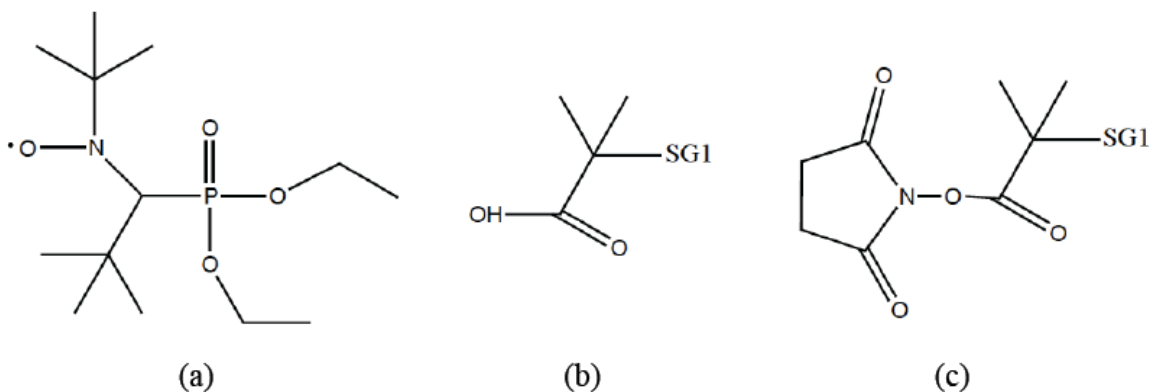
Abstract

Statistical copolymerizations of 2-(dimethylamino)ethyl methacrylate (DMAEMA) with 2-vinylpyridine (2VP) with 80-99 mol% DMAEMA in the feed utilizing a succinimidyl ester-terminated alkoxyamine unimolecular initiator (NHS-BlocBuilder) at 80 °C in bulk were performed. The effectiveness of 2VP as a controlling co-monomer is demonstrated by linear increases in number-average molecular weight versus conversion, relatively low \bar{D} (1.5 - 1.6 with up to 98% DMAEMA) and successful chain extensions with 2VP. Additional free nitroxide does not significantly improve control for the DMAEMA/2VP copolymerizations. The succinimidyl ester on the initiator permits coupling to amine-terminated poly(propylene glycol) (PPG), yielding an effective macroinitiator for synthesizing a doubly thermoresponsive block copolymer of PPG-*block*-P(DMAEMA/2VP). A detailed study of the thermo- and pH-sensitivities of the statistical and block copolymers is also presented. The cloud point temperature of the statistical copolymers is fine tuned from 14 to 75 °C by varying polymer composition and pH.

4.2 Introduction

Polymers that have fast and reversible responses to environmental stimuli such as temperature, pH, light and ionic strength are of great interest for “smart” materials.^{56,152} Poly(2-(dimethylamino)ethyl methacrylate) (PDMAEMA) is a water soluble polymer that is responsive to both temperature and pH.^{156,158,188} It exhibits lower critical solution temperature (LCST)-type phase separation upon heating in aqueous solutions at neutral or basic conditions while it protonates and becomes a polyelectrolyte in acidic media. Such polymers are very attractive for many potential applications, particularly in the biomedical field, such as drug/gene/protein delivery, biosensors, bioseparations, and tissue engineering.^{3,5,56,57}

The properties of a stimuli-responsive polymer such as PDMAEMA are closely related to the polymer microstructure. Traditionally, truly living polymerization techniques such as anionic polymerization¹⁸⁹ were the only approaches to achieve precise control of molecular weight and molecular weight distribution. More recently, controlled radical polymerization (CRP) techniques such as reversible addition-fragmentation transfer (RAFT), atom transfer radical polymerization (ATRP) and nitroxide-mediated polymerization (NMP) were developed to superficially resemble living polymerization with relatively robust reaction conditions.¹⁶¹ For ATRP, metal catalysts are required and RAFT requires sulfur-based bimolecular chain transfer agents. Although these compounds can be removed by post-polymerization modification steps,¹²² NMP requires simple purification procedures, often a single-step precipitation, since it only involves a single initiator for controlling the polymerization. NMP has been touted as a convenient route towards synthesizing non-cytotoxic polymers for biomedical applications.¹³¹⁻¹³³



Scheme 4-1. Structures of (a) SG1 nitroxide (b) BlocBuilder™ (c) *N*-hydroxy succinimidyl ester-coupled BlocBuilder (NHS-BlocBuilder).

However, NMP has not been as successful in controlling homopolymerization of methacrylates such as DMAEMA compared to the other CRP techniques.^{133,190} The very high equilibrium constant *K* of methacrylates that is caused by the slow recombination of nitroxides and the sterically-hindered poly(methacrylate) radicals has been claimed to be the main reason for poorly controlled methacrylate homopolymerizations via NMP.^{133,139} Additionally, other side reactions including irreversible terminations between propagating radicals and/or β -hydrogen transfers between propagating radicals and nitroxides,¹³⁷ chain transfer to solvent/monomers,¹⁹¹ and decomposition of alkoxyamines¹³³ can also deactivate the nitroxide group, limit achievable molecular weight and broaden the molecular weight distribution. Continuous efforts in modifying NMP initiator structures have given rise to alkoxyamines specifically synthesized for methacrylates.^{109,150} However, these alkoxyamines require extensive synthesis steps and lack versatility (eg. they are in some cases difficult to cross-over from one monomer to the other when performing block copolymerizations). Another approach to achieve controlled methacrylate polymerization via NMP is to use a small amount of a controlling co-monomer.¹⁰⁴ With a commercially available SG1-based unimolecular alkoxyamine called BlocBuilder™ (N-

(2-methylpropyl-N-(1-diethylphosphono-2,2-dimethylpropyl)-O-(2-carboxylprop-2-yl) hydroxyl amine, structures of SG1 and BlocBuilderTM shown in Scheme 4-1 (a) and (b)), a range of methacrylates,^{48,104,132,142,143} including DMAEMA,⁴⁸ has been successfully controlled with a small amount (1 – 10 mol%) of co-monomer in the feed and about 10% excess of free SG1 relative to the BlocBuilderTM. While styrene is the most popular choice as a co-monomer,^{104,132,142} acrylonitrile (AN),¹⁴³ sodium 4-styrene sulfonate (SS),¹⁴⁴ 9-(4-vinylbenzyl)-9H-carbazole (VBK),^{48,146} and pentafluorostyrene (PFS)¹⁴⁵ have also been reported as controlling co-monomers for various methacrylates. The key properties of an effective controlling co-monomer are much lower equilibrium constant K and low cross-propagation rate constant (k_p /reactivity ratio) compared to methacrylates.^{126,139,167} For the copolymerization systems of methyl methacrylate (MMA) with less than 10 mol% styrene (S), the favored MMA-S-SG1 chain end formation has been demonstrated critical for controlled SG1-mediated polymerization of MMA.^{130,140} This MMA-S-SG1 formation results in high alkoxyamine dissociation rate at low temperature of about 90 °C due to the penultimate unit effect from MMA and low active radical concentration allowed by the styrene-terminated macroalkoxyamines, ensuring fast initiation and controlled propagation. The same conclusion were also applied for MMA/SS¹⁴⁴ and MMA/AN¹⁴³ copolymerization systems.

When copolymerizing a hydrophilic stimuli-responsive methacrylate with a hydrophobic co-monomer via NMP, the benefits can be expanded from achieving a controlled polymerization to property tuning by simply varying copolymer composition.^{47,48,50,145} However, a hydrophilic poly(methacrylate) can be easily rendered water insoluble when a relatively small fraction of a hydrophobic co-monomer was incorporated. Using specific examples of DMAEMA-rich copolymers, when more than 25 mol% of styrene,⁴⁷ 10 mol% PFS,¹⁴⁵ or as little as 5 mol%

VBK⁴⁸ was copolymerized with DMAEMA, the resulting random copolymer became water-insoluble. This limits the applications of such random copolymers and thus a less hydrophobic controlling co-monomer would be desirable. On the other hand, sodium 4-styrene sulfonate, which was demonstrated to be effective as a co-monomer to control methacrylic acid-rich copolymerizations, is totally water-soluble.¹⁴⁴ However, it has been reported that when LCST-type polymers were copolymerized with hydrophilic co-monomers, the copolymer exhibited incomplete transitions and eventually no transitions as the hydrophilic co-monomer content increased.^{51,192} This phenomena was explained by the dramatic reduction in hydrophobic interactions between the thermo-responsive units above their LCST.

In this work, 2-vinylpyridine (2VP) was chosen as a co-monomer for DMAEMA-rich copolymerizations via NMP as it is structurally similar to styrene but less hydrophobic. Controlled homopolymerization of 2VP has been reported in the presence of TEMPO (2,2,6,6-tetramethylpiperidine-N-oxyl)^{193,194} and the reported kinetics of 2VP polymerization was not significantly different than that of styrene.¹⁹³ We thus expect 2VP to be a suitable controlling co-monomer for methacrylates by NMP. P2VP is also pH-sensitive and becomes a polyelectrolyte in acidic media. Therefore, it can tune the properties of the random copolymer in its neutral form like other hydrophobic co-monomers; it can also become totally water-soluble if it is protonated. Its pH sensitivity and polyampholytic properties have been utilized for pH-dependent micellization^{156,195,196} and forming polymer complexes.¹⁹⁷ By using 2VP as a co-monomer, the resulting copolymer can potentially gain additional functionality besides enabling the controlled polymerization of a functional methacrylate.

Moreover, a modified SG1-based alkoxyamine bearing a N-succinimidyl ester (NHS-BlocBuilder, Scheme 4-1 (c)) was used as the initiator for this work. This alkoxyamine can be

obtained by a single step coupling of BlocBuilder with N-hydroxysuccinimide¹⁷¹ or potentially by a copper metal-mediated reaction of succinimidyl halide with SG1 nitroxide.¹⁹⁸ NHS-BlocBuilder has been shown effective in controlling homopolymerization of styrene and n-butyl acrylate,¹⁷¹ as well as random copolymerization of glycidyl methacrylate with styrene¹⁷² and DMAEMA with styrene⁴⁷ without the aid of additional SG1 nitroxide. The NHS-BlocBuilder is particularly attractive as it can be used for post-polymerization bioconjugation.¹⁵¹

In this paper, the polymerization kinetics, level of control, polymer livingness and the effects of additional SG1 nitroxide on DMAEMA/2VP random copolymerizations initiated by NHS-BlocBuilder will be discussed. The effect of copolymer composition on the pH- and thermo-sensitivities of the copolymers will also be presented. The succinimidyl ester moiety from the NHS-BlocBuilder initiator, since it readily reacts with nucleophiles or amine-containing materials¹⁶⁸ will permit additional functionalization of the copolymer. This will also be demonstrated by the coupling of amine-terminated poly(propylene glycol) to NHS-BlocBuilder to form a macroinitiator for subsequent polymerizations in this work.

4.3 Results and Discussion

The polymerization results and polymer characterizations for homopolymerizations of 2VP and DMAEMA as well as statistical copolymerizations of DMAEMA/2VP are summarized in Table 4-1.

Table 4-1. Molecular weight and composition characterizations of 2VP and DMAEMA homopolymers as well as DMAEMA/2VP statistical copolymers initiated by NHS-BlocBuilder or PPO-BB.

Experiment ID ^a	Polym. Time (min)	Conversion ^b	$f_{\text{DMAEMA},0}^c$ (mol%)	F_{DMAEMA}^b (mol%)	M_n^d (kg mol ⁻¹)	\bar{D}^d
P2VP	180	50%	-	-	15.8	1.29
PDMAEMA	<1	N/A	100%	100%	15.8	2.01
D2VP-99	30	40%	99%	99%	10.1	1.85
D2VP-98	45	43%	98%	95%	14.2	1.63
D2VP-95	80	42%	95%	92%	15.9	1.48
D2VP-90	165	44%	90%	85%	10.7	1.50
D2VP-85	240	44%	85%	81%	11.4	1.48
D2VP-80	295	40%	80%	76%	9.8	1.56
D2VP-95s	160	49%	95%	93%	9.7	1.60
D2VP-99s	65	43%	99%	99%	9.7	1.88
PPO-D2VP-95	60	32% ^e	96%	94% ^e	21.5 ^e	1.78 ^e

^a Experimental identification (ID) for copolymers was given by D2VP-X, where D2VP represent the statistical copolymerization of DMAEMA and 2VP; and X the number abbreviation refers to the feed composition with respect to DMAEMA. D2VP-95s and D2VP-99s were copolymerizations with additional SG1. PPO-D2VP-95 was a statistical copolymerization initiated by PPO-BB macroinitiator. ^b Monomer conversion and copolymer composition with respect to DMAEMA determined by ¹H NMR. ^c Initial feed composition with respect to DMAEMA. ^d Number-average molecular weight (M_n) and dispersity (\bar{D}) determined by GPC relative to poly(styrene) standards for 2VP homopolymer (P2VP) or poly(methyl methacrylate) standards for all other polymers. ^e Monomer conversion from DMAEMA/2VP copolymerization. ^f Composition of the DMAEMA/2VP block. ^g M_n and \bar{D} of the block copolymer relative to poly(methyl methacrylate) standards.

4.3.1 Homopolymerization of 2-vinylpyridine (2VP) using NHS-BlocBuilder

Homopolymerization of 2VP was performed using NHS-BlocBuilder as initiator to examine the level of control and to confirm if 2VP is indeed a good candidate as a controlling co-monomer for this system. The homopolymerization was done in bulk at 120 °C with no additional free SG1 nitroxide.

The kinetic results shown in Figure 4-1 (a) indicate the reaction followed the first order kinetics as expected from a controlled polymerization. The number-average molecular weight (M_n) of the homopolymer increased linearly with conversion and had excellent agreement with the

theoretical prediction as demonstrated in Figure 4-1 (b). The \bar{D} s of the homopolymer remained below 1.30 throughout the reaction. These results illustrated that the 2VP homopolymerization using NHS-BlocBuilder was well controlled.

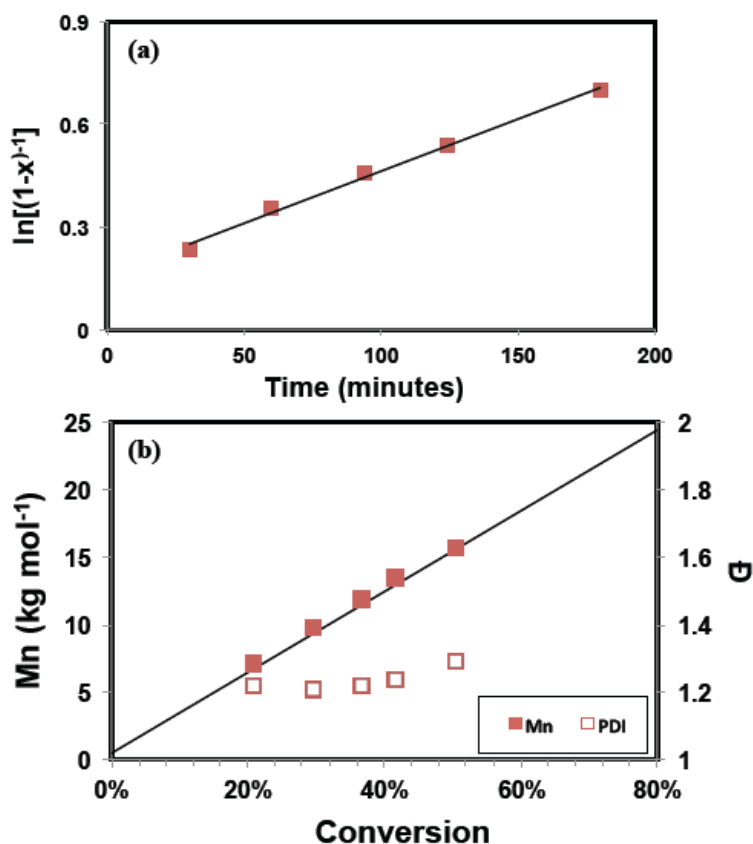


Figure 4-1. Bulk homopolymerization of 2VP initiated by NHS-BlocBuilder at 120 °C. (a) Kinetic plot of $\ln[(1-x)^{-1}]$ versus time (x = monomer conversion). (b) Number-average molecular weight (M_n) and dispersity (\bar{D}) versus conversion (M_n relative to poly(styrene) standards). Solid line represents theoretical M_n trend.

We have previously demonstrated that as little as 5 mol% styrene was effective in controlling 2-(dimethylamino)ethyl methacrylate (DMAEMA) polymerization using NHS-BlocBuilder and producing DMAEMA-rich copolymers capable of re-initiating a second batch of monomer.⁴⁷ In terms of both kinetics and level of control, the 2VP homopolymerization results were very similar to those of styrene homopolymerization initiated by the same alkoxyamine at the same

temperature.¹⁷¹ Therefore, we foresee 2VP as a capable controlling co-monomer for DMAEMA-rich copolymerizations.

4.3.2 Statistical copolymerization of 2-(dimethylamino)ethyl methacrylate (DMAEMA) and 2-vinylpyridine (2VP) using NHS-BlocBuilder

4.3.2.1 Effect of feed composition on polymerization kinetics and control

The homopolymerization of DMAEMA with NHS-BlocBuilder was attempted at 80 °C in bulk. The reaction was highly exothermic and the reaction mixture became very viscous within a minute after the temperature reached 80 °C. The final polymer was shown to have $M_n = 15.8 \text{ kg mol}^{-1}$ and $\bar{D} = 2.01$ when analyzed by GPC relative to poly(methyl methacrylate) standards. The extremely rapid kinetics and broad molecular weight distribution confirmed the uncontrolled nature of the DMAEMA homopolymerization by NMP and the necessity of using a controlling co-monomer with this system (ie. polymerization initiated by NHS-BlocBuilder at 80 °C with a low concentration of a styrenic-type monomer).

For the DMAEMA/2VP statistical copolymerizations performed at 80 °C in bulk initiated by NHS-BlocBuilder, the initial amount of DMAEMA in the feed ($f_{DMAEMA,0}$) was varied from 80 – 99 mol%. All copolymerizations followed first-order kinetics as illustrated by linear kinetic plots presented in Figure 4-2 (a).

The apparent rate constants, indicated by the slopes of the kinetic plots, $\langle k_p \rangle [P\bullet]$ (where $\langle k_p \rangle$ is the average propagation rate constant and $[P\bullet]$ is the propagating radical concentration) were plotted against feed composition in Figure 4-2 (b). The copolymerization rate increased rapidly with increasing amount of DMAEMA in the feed, especially when there was more than 90 mol% DMAEMA in the feed. The $\langle k_p \rangle [P\bullet]$ values were similar to those obtained from the

copolymerization of DMAEMA with styrene ($\langle k_p \rangle [P^\bullet]$) ranged from $2.5 \times 10^{-5} \text{ s}^{-1}$ to $9.2 \times 10^{-5} \text{ s}^{-1}$ when 2VP was used as co-monomer, and ranged from $2.7 \times 10^{-5} \text{ s}^{-1}$ to $6.6 \times 10^{-5} \text{ s}^{-1}$ when styrene was used as co-monomer⁴⁷ as feed composition varied from 80 to 95 mol% DMAEMA).

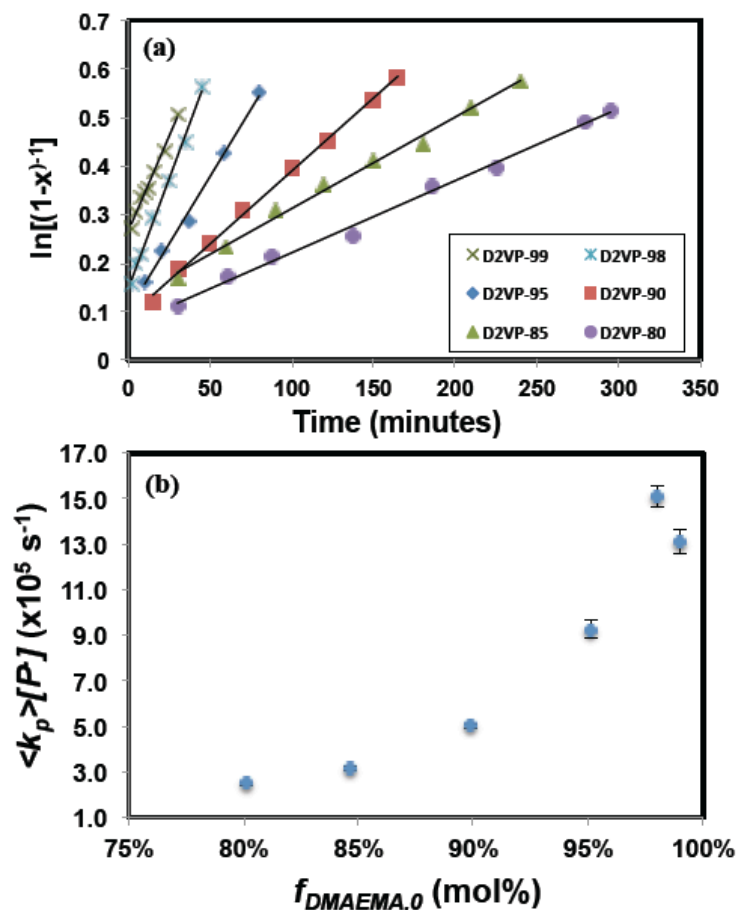


Figure 4-2. (a) Kinetic results ($\ln[(1-x)^{-1}]$ versus time) of statistical copolymerization of DMAEMA with 2VP initiated by NHS-BlocBuilder (x = monomer conversion). (b) Product of average propagation rate constant $\langle k_p \rangle$, and propagating radical concentration $[P^\bullet]$, $\langle k_p \rangle [P^\bullet]$ (slope of the kinetic plots in (a)), versus feed composition with respect to DMAEMA ($f_{DMAEMA,0}$); error bars represent standard deviation of the slopes from (a).

Nitroxide mediated copolymerization kinetics are often expressed as the product of average propagation rate constant $\langle k_p \rangle$ and average equilibrium constant $\langle K \rangle$, $\langle k_p \rangle \langle K \rangle$, which can be

expressed as a function of k_p s, K s and reactivity ratios of both monomers.¹⁰⁴ The equilibrium constant K is defined by Equation 4-1 when SG1 is used as the free nitroxide:

Equation 4-1

$$K = \frac{[SG1\bullet][P\bullet]}{[P-SG1]}$$

where $[SG1\bullet]$ is the free nitroxide concentration and $[P-SG1]$ is the concentration of the dormant initiator.

Methacrylates generally have higher propagation rate constants k_p and much higher equilibrium constants K than styrene.^{126,139,199,200} The values of k_p for 2VP and styrene were similar (96.5 L mol⁻¹ sec⁻¹ for 2VP²⁰¹ and ranged from 77 to 95 L mol⁻¹ sec⁻¹ for styrene,¹⁹⁹ both at 25 °C). To the best of our knowledge, the value of K for 2VP is not available in the literature. We assumed it to be similar to that of styrene considering 2VP homopolymerization had similar kinetics compared to styrene under the same conditions as discussed earlier. Therefore, it was expected that the $\langle k_p \rangle \langle K \rangle$ values and thus the polymerization rates increased rapidly as the feed was enriched with methacrylate, just as in the other cases with methacrylate/styrene copolymerizations controlled by BlocBuilder-type initiators.^{47,104}

As the amount of DMAEMA in the feed was increased from 95 mol% to 98 mol% in this study with 2VP as a controlling co-monomer, the $\langle k_p \rangle [P\bullet]$ values continued to increase sharply. However, a slight decline in $\langle k_p \rangle [P\bullet]$ value was observed for the copolymerization with feed composition $f_{DMAEMA,0} = 99$ mol%. This slight decrease in apparent polymerization rate was not unexpected. In nitroxide-mediated copolymerizations of methacrylates with a very small amount of controlling co-monomer (< 5 mol% in the feed), polymerization rate showed minimal increase^{143,146} or declined slightly^{48,50} with increasing amount of methacrylate in the feed. Note

that in Figure 4-3 (a), the conversion of the first sample for D2VP-99 was 24% at a reaction time of 2 minutes, yet only an increase of 2% in conversion was obtained at 4-minute reaction time for the second sample. With these highly methacrylate-rich feeds, a significant amount of irreversible termination reactions can occur at early stages of the polymerization when the concentration of regulating nitroxide was below its equilibrium value, which leads to non-first-order kinetics, similar to methacrylate homopolymerizations.¹³⁷ Therefore, the apparent rate constant $\langle k_p \rangle [P^\bullet]$ obtained from these higher conversion samples was likely lower than its true value.

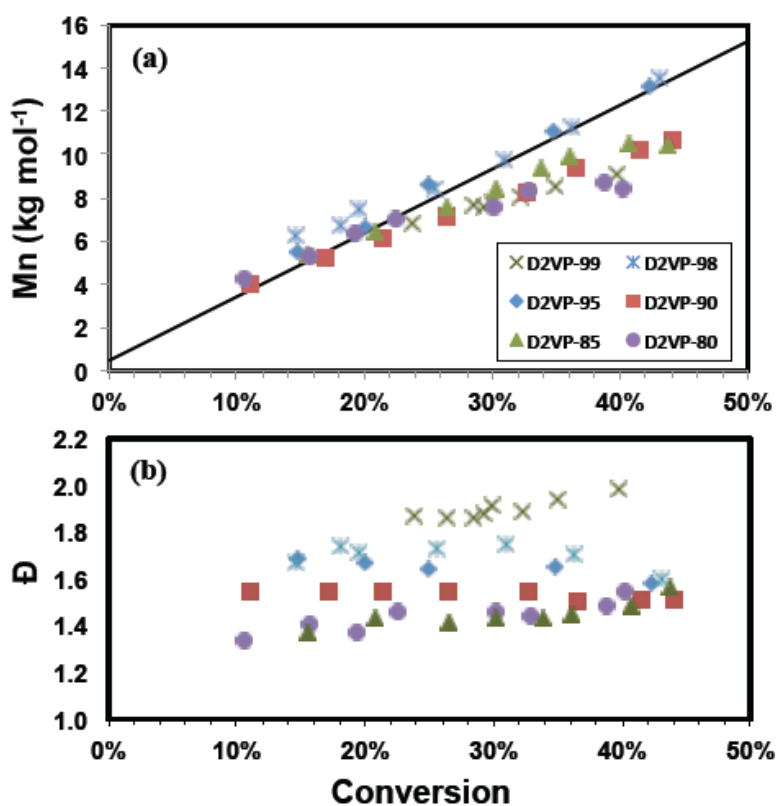


Figure 4-3. (a) Number-average molecular weight (M_n) and (b) dispersity (Đ) of the statistical copolymers of DMAEMA and 2VP measured by GPC relative to poly(methyl methacrylate) standards versus conversion; solid line in (a) represents the theoretical M_n trend expected.

A linear increase of M_n with conversion is one of the signatures of a living polymerization and is often used in the analysis of controlled polymerizations. In all of the copolymerizations of DMAEMA with 2VP with up to 99 mol% DMAEMA in the feed, linear trends of M_n versus conversion were observed up to about 45% conversion, as shown in Figure 4-3 (a). At higher conversions, many of the M_n versus conversion plots of the copolymers still followed the theoretical trend but tended to plateau. This deviation has been observed previously and attributed to the adsorption of PDMAEMA onto the GPC columns.^{162,174} The column adsorption led to an increase in retention time and broadening of peaks which resulted in lower detected molecular weight and higher \bar{D} s. Another possible reason for the $M_n < M_{n,theo}$ behaviour can be related to chain transfer side reactions. Greszta and Matyjaszewski¹⁹¹ showed in their simulations of styrene polymerization in the presence of TEMPO nitroxide that the combination of chain transfer to monomers and alkoxyamine decomposition were the main causes for lower M_n and increasing \bar{D} at high conversions. Zetterlund et al.²⁰² demonstrated experimentally the consequences of chain transfer to monomer with TEMPO and SG1 mediated styrene polymerizations. New chains were created when the radicals transferred to monomer, which could still polymerize in a controlled manner, yet a significant fraction of the new chains remained at low M_n because of the continuous chain transfer. As a result, the overall M_n became lower than the expected values and the distribution broadened. Nonetheless, the deviations of M_n from theoretical values were moderate and the linear increases of M_n versus conversion were evidenced for the controlled nature of the copolymerizations of DMAEMA and 2VP with feed composition up to 99 mol% DMAEMA.

The \bar{D} s of the final copolymers were about 1.5 – 1.6 for copolymerizations with feeds containing up to 98 mol% DMAEMA (Table 4-1) which were comparable to those of the statistical

copolymers of DMAEMA with styrene⁴⁷ and 9-(4-vinylbenzyl)-(9H-carbazole) (VBK)⁴⁸ as controlling co-monomers synthesized with BlocBuilder-type unimolecular initiators. Molecular weight distributions broadened significantly (\bar{D}_s increased from ~ 1.6 to 1.9) when the feed contained more than 98 mol% DMAEMA (Table 4-1) indicating polymerization becoming less controlled. The ability of these statistical copolymers to re-initiate a second batch of monomer was further investigated by experiments discussed in the *Livingness of selected copolymers* section.

4.3.2.2 Statistical copolymerization of DMAEMA and 2VP using PPO-BB macroalkoxyamine

A statistical copolymerization of DMAEMA with 2VP with feed composition $f_{DMAEMA,0} = 95$ mol% was performed using a poly(propylene oxide)-coupled BlocBuilder (PPO-BB) as a macroinitiator at 80 °C in bulk. A linear kinetic plot (Figure 4-4 (a)) was obtained with a slope of $\langle k_p \rangle [P\bullet] = 1.0 \times 10^{-4} \text{ s}^{-1}$, which was similar to the result of the copolymerization with same feed composition initiated by NHS-BlocBuilder ($\langle k_p \rangle [P\bullet] = 9.2 \times 10^{-5} \text{ s}^{-1}$).

M_n of the block copolymers increased linearly with conversion as shown in Figure 4-4 (b) as expected from a controlled polymerization. However, the experimental M_n s were consistently higher than their theoretical values throughout the polymerization. This result is likely due to the combination of slow initiation and low initiating efficiency. Slow initiation in radical polymerization is known to result in higher than expected molecular weight and broad \bar{D}_s .^{101,113} Low initiating efficiency in NMP has been previously reported for copolymerizations with methacrylates (75% at $\sim 60\%$ conversion for MMA/styrene¹⁰⁴ and 50 – 80% at 40% conversion for MMA/VBK¹⁴⁶). The apparent initiating efficiency defined by the value of theoretical M_n

divided by the experimental M_n was about 55% at 32% conversion. These low initiating efficiencies were mainly attributed to incomplete initiation of the alkoxyamine due to irreversible termination of primary and/or oligo-radicals that could not be quantified by GPC.¹⁰⁴ The GPC chromatograms (Figure B-1 in Appendix B) of intermediate samples during the polymerization continued to shift towards lower retention time as reaction proceeded indicating continued increases of M_n with conversion. Small shoulders at about 29 min retention time were evident in all traces which represent a small amount of PPO-di-NH₂ residue that was not removed completely from precipitation, the existence of inactive macroalkoxyamine or/and dead short chains.

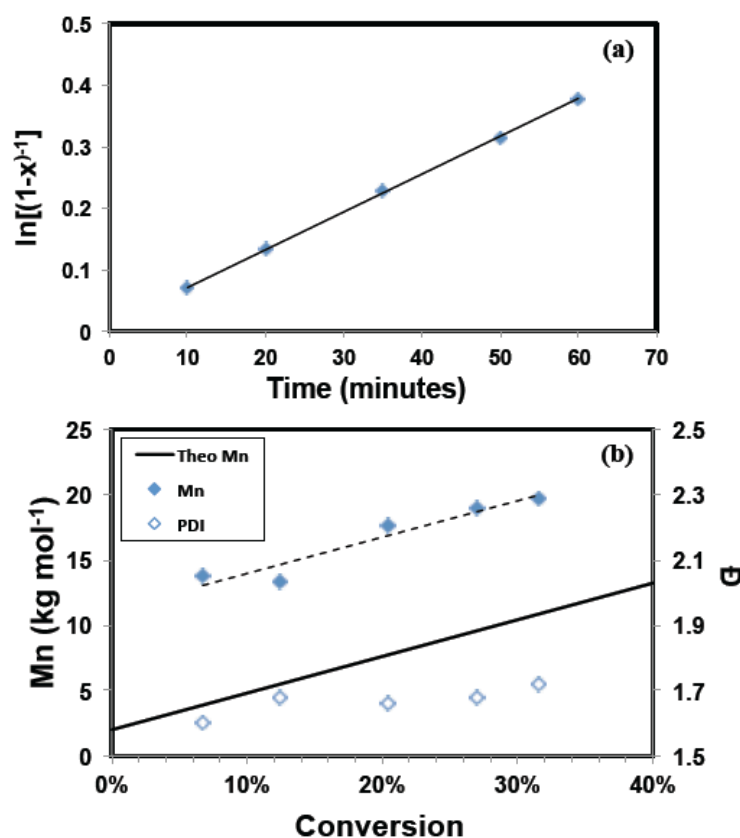


Figure 4-4. (a) Kinetic plot of scaled conversion $\ln[(1-x)^{-1}]$ (x = conversion) versus polymerization time, (b) number-average molecular weight (M_n) and dispersity (\bar{D}) of DMAEMA/2VP copolymerization with 95 mol% DMAEMA in the feed initiated by PPO-BB macroalkoxyamine at 80 °C in bulk. M_n and \bar{D} were obtained by GPC relative to poly(methyl methacrylate) standards; solid line in (b) represents the theoretical M_n trend.

The ^1H NMR spectrum of the final diblock copolymer of PPO-D2VP-95 is presented in Figure 4-5. Degree of polymerization (DP) can be calculated using the PPO protons as a reference since it was known that the M_n of PPO was about 2000 g mol^{-1} (equivalent to DP of about 34, confirmed by ^1H NMR). From the ratios of proton peaks in the NMR spectrum, the DP of DMAEMA was calculated to be about 117 and the DP of 2VP was about 9, giving a DMAEMA/2VP statistical copolymer block of about 19 kg mol^{-1} with 93 mol% DMAEMA. Combined with the 2 kg mol^{-1} PPO block, the M_n of the diblock copolymer was about 21 kg mol^{-1} . This result corresponded well with that obtained from GPC relative to PMMA standards (Table 4-1).

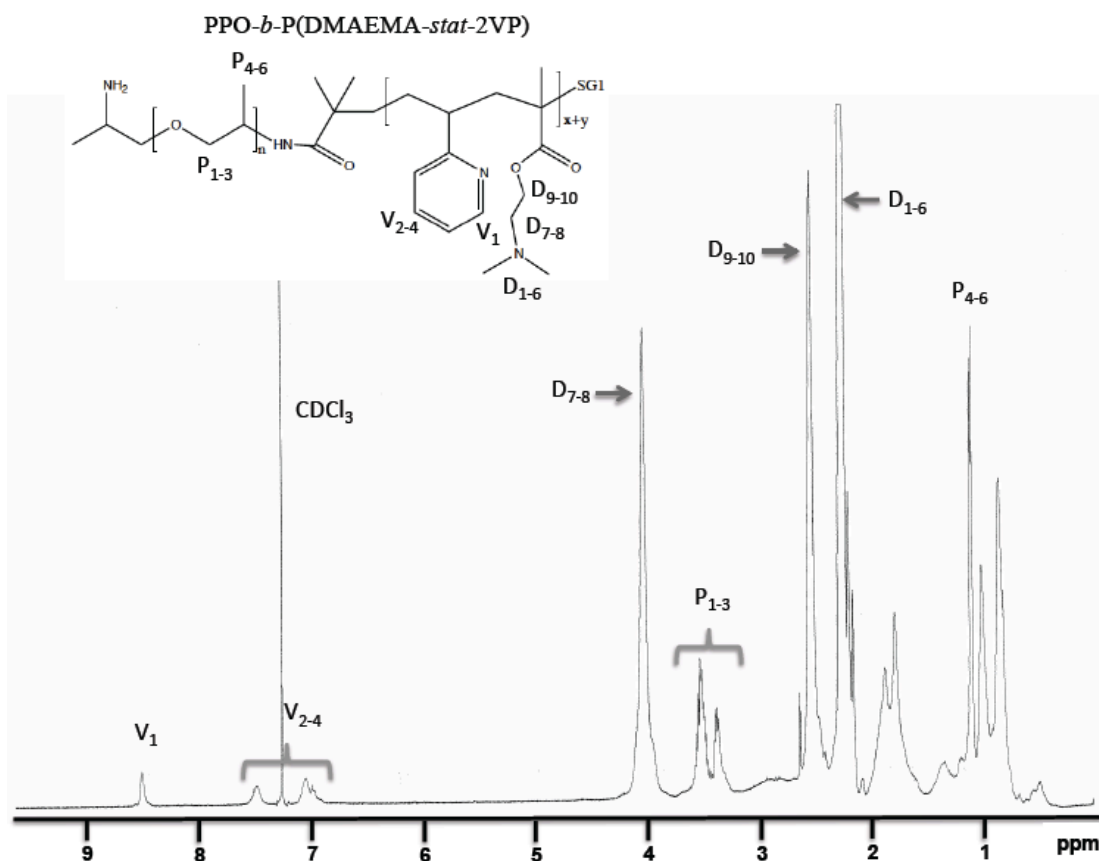


Figure 4-5. ^1H NMR spectrum of poly(propylene glycol)-*b*-poly(dimethylaminoethyl methacrylate-*stat*-2-vinylpyridine) diblock copolymer (PPO-*b*-P(DMAEMA-*stat*-2VP) in CDCl_3 . Protons P, D, V correspond to the labeled protons on the chemical structures for PPO, DMAEMA, 2VP, respectively.

The \bar{D} s of the block copolymers were ~ 1.7 , which was broader than those initiated by NHS-BlocBuilder ($\bar{D} = 1.48$ for D2VP-95, Table 4-1). The broadening of molecular weight distribution may be due to the slow initiation, the incomplete removal of the unreactive PPO-di-NH₂ residue and/or inactive macroalkoxyamine as well as dead oligoradicals. The diblock copolymer was chain extended to further investigate its livingness, which will be discussed in the *Livingness of selected copolymers* section.

4.3.2.3 Livingness of selected copolymers

The statistical copolymers with feed composition $f_{DMAEMA,0} = 95 - 99$ mol% and the diblock copolymer initiated by the PPO-BB macroalkoxyamine were chain extended by 2VP to examine their re-initiation ability. The results were summarized in Table 4-2.

Overall, the percentage of DMAEMA of the chain-extended block copolymers decreased from that of the macroinitiator as expected after the 2VP block was incorporated. M_n of the chain-extended 2VP block was about $15 - 20 \text{ kg mol}^{-1}$ after approximately 3 hours of reaction time. The \bar{D} s of the block copolymers remained nearly the same compared to those of the macroinitiators. These results showed the ability of the macroinitiators to reinitiate a second batch of monomer and continue to polymerize, which is a feature of living polymers.

The chain extension results were also demonstrated in the GPC chromatograms shown in Figure 4-6. The chain-extended block copolymers (shown as solid lines) were all mono-modal and shifted to lower retention times compared to their respective macroinitiators (shown as dashed lines). Low molecular weight tails were observed for all macroinitiators and some of the chain-extended block copolymers. Similar drifting/tailing has been reported previously for

PDMAEMA homopolymer¹⁶² and DMAEMA-rich copolymers^{47,48} and it was attributed to the adsorption of PDMAEMA to the GPC column.¹⁶² The adsorption of the chain-extended products was less significant compared to the DMAEMA-rich macroinitiators as the 2VP concentration increased in the block copolymer composition. The reduced degree of adsorption to the column of the block copolymer compared to the macroinitiator may explain the lower Đs of some of the chain-extended polymer compared to their macroinitiators. For the PPO-D/2VP-95/5 diblock copolymer and its chain-extended triblock copolymer, the small shoulder in the macroinitiator chromatogram became negligible after chain extension, likely due to easier separation of the low molecular weight contaminants (inactive macroinitiator, short dead chains, and/or the unreactive PPO-di-NH₂ residue) from the higher M_n triblock copolymer.

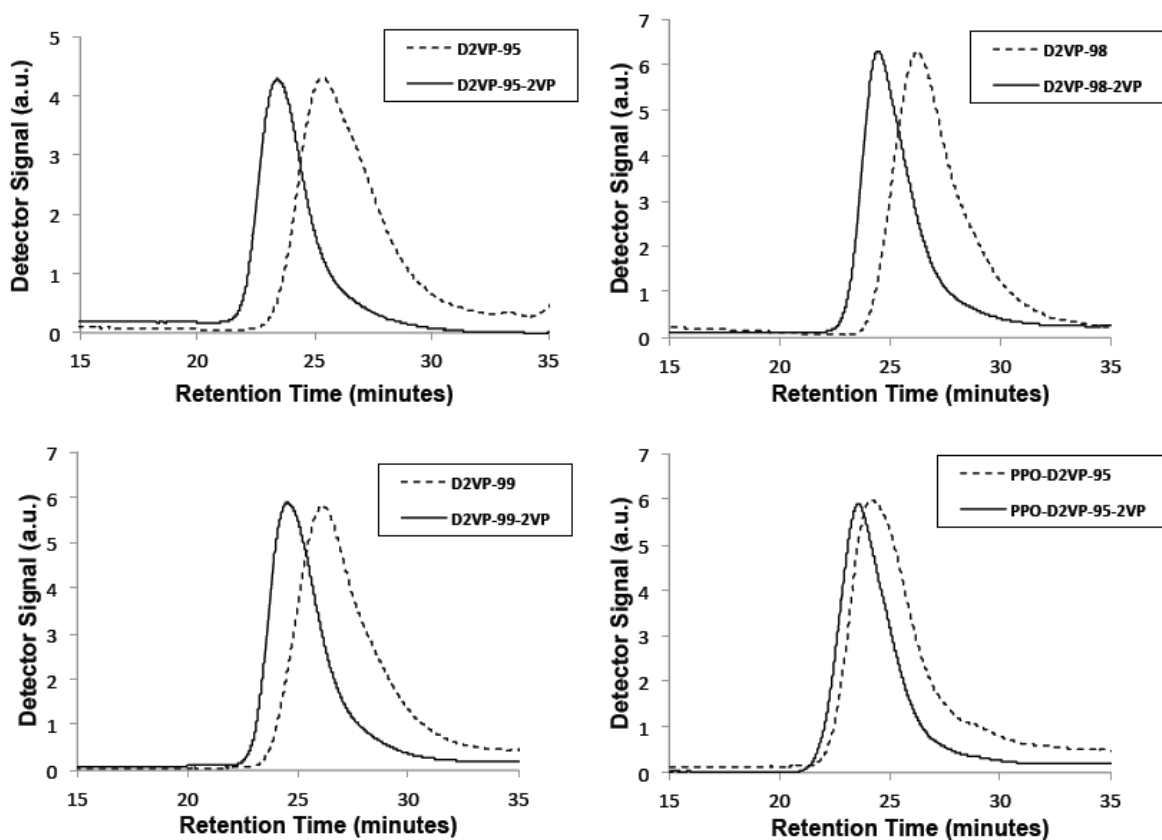


Figure 4-6. GPC chromatograms of macroinitiator (dashed line) and chain extended polymer (solid line) in the chain extension experiments.

Table 4-2. Properties of the macroinitiators and chain-extended block copolymers in the chain extension experiments.

Macroinitiator properties				Block copolymer properties			
Macroinitiator	F _{DMAEMA} (mol%) ^a	M _n (kg mol ⁻¹) ^b	Đ ^b	Block copolymer	F _{DMAEMA} (mol%) ^a	M _n (kg mol ⁻¹) ^b	Đ ^b
D2VP-95	92%	7.8	1.55	D2VP-95-2VP	28%	21.5	1.65
D2VP-98	95%	14.2	1.63	D2VP-98-2VP	33%	30.0	1.60
D2VP-99	99%	10.1	1.85	D2VP-99-2VP	44%	25.6	1.59
PPO-D2VP-95	94%	21.5	1.78	PPO-D2VP-95-2VP	46%	41.7	1.62

^a Overall polymer composition with respect to DMAEMA relative to 2VP determined by ¹H NMR. ^b Number-average molecular weight (M_n) and dispersity (Đ) of the macroinitiator and the block copolymer determined by GPC relative to poly(methyl methacrylate) standards.

4.3.2.4 Effect of additional SG1 free nitroxide

In previous NMP studies with BlocBuilder, a small amount of additional free nitroxide (about 5-10 % relative to the initiator) was beneficial in the reaction mixture with monomers that have relatively high k_p such as acrylates^{110,178,203} and methacrylates^{48,104,132,142} as well as acidic monomers that promote SG1 nitroxide degradation such as acrylic acid¹⁰³ to control the polymerization. The addition of free SG1 reduced the polymerization rate significantly and led to a linear increase in M_n with conversion following the theoretical trend as well as much lower Đs.^{103,110,178,203} As demonstrated in this work and previous studies,^{47,171,172} by using NHS-BlocBuilder as the initiator, additional SG1 was no longer a requirement to achieve controlled polymerization of acrylates¹⁷¹ and more importantly, methacrylates.^{47,172} However, the control in these NHS-BlocBuilder systems was still thought to be able to be improved as the Đs were still relatively high compared to many other controlled polymerization techniques.^{160,204} Therefore, 10% additional free SG1 relative to NHS-BlocBuilder was added in DMAEMA/2VP feeds containing 95 and 99 mol% DMAEMA to examine the effects of excess nitroxide for this system.

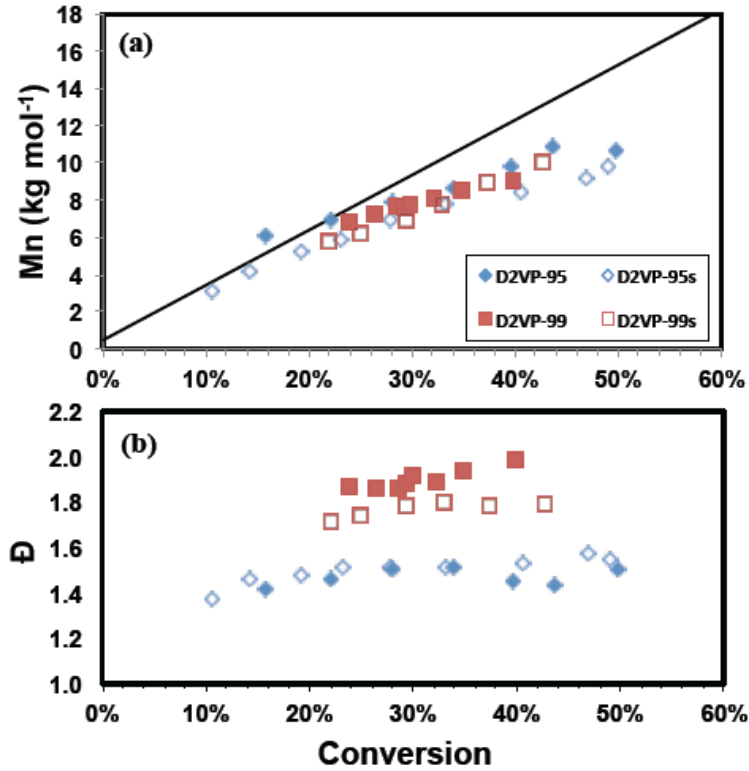


Figure 4-7. Effect of additional SG1 free nitroxide on (a) number-average molecular weight (M_n , relative to poly(methyl methacrylate) standards) and (b) dispersity (\bar{D}) of DMAEMA/2VP statistical copolymers with 95 mol% and 99 mol% DMAEMA in the feed; filled symbols represent results obtained with no free SG1 and open symbols represent results obtained with 10% free SG1, solid line in (a) represents theoretical M_n trend.

In a controlled polymerization, fast initiation and constant chain concentration are often assumed, meaning $[P-SG1] \approx [Initiator]_0$. With the large initial concentration of nitroxide, the nitroxide concentration $[SG1]$ should remain relatively constant, close to its initial value $[SG1]_0$, throughout the polymerization. The product of propagation rate constant k_p and equilibrium constant K , $k_p K$, can then be estimated from the slopes obtained from the kinetic plots and the ratio of initial nitroxide concentration and initiator concentration, r (Equation 4-2):

Equation 4-2

$$k_p K = k_p \frac{[P\bullet][SG1\bullet]}{[P-SG1]} \approx k_p [P\bullet] \frac{[SG1\bullet]_0}{[P-SG1]_0} = k_p [P\bullet] r$$

The kinetic results of the copolymerizations with 10% free SG1 were compared to the ones with no additional SG1 in Table 4-3. The apparent rate constants $\langle k_p \rangle [P\bullet]$ with additional SG1 were lower than those without. This was expected, as the dormant state should be favoured as the nitroxide concentration $[SG1\bullet]$ is increased. $\langle k_p \rangle \langle K \rangle$ values calculated according to Equation 4-2 were very similar to those reported for the DMAEMA/VBK system at the same temperature.⁴⁸

M_n versus conversion was not strongly affected by the addition of free nitroxide, as shown in Figure 4-7. Plateauing at higher conversion still occurred with additional SG1. Further, provided that enough of the controlling co-monomer was added (eg. when $f_{DMAEMA,0} = 95$ mol%), the \mathcal{D} s were not significantly affected by the addition of free SG1. Only in the case when the controlling co-monomer concentration was low ($f_{DMAEMA,0} = 99$ mol%), were slightly lower \mathcal{D} s achieved ($\mathcal{D} \sim 1.8$ with 10% free SG1 versus $\mathcal{D} \sim 1.9$ when no SG1 was added). In summary, at the conditions used, the addition of free SG1 did not improve the control of DMAEMA/2VP copolymerizations significantly.

This result was not totally surprising as NHS-BlocBuilder has a very high dissociation rate constant ($k_d = 5$ s⁻¹ for NHS-BlocBuilder compared to 0.32 s⁻¹ for BlocBuilder at 120 °C in *tert*-butyl benzene¹⁷¹) and relatively lower activation energy ($E_a = 105$ kJ mol⁻¹ for NHS-BlocBuilder compared to 112 kJ mol⁻¹ for BlocBuilder¹⁷¹). The much higher dissociation rate constant for NHS-BlocBuilder provided sufficiently rapid release of the SG1 regulating nitroxide, which mimicked the addition of a small amount of free SG1 at the onset of polymerization when BlocBuilder was used.⁴⁷

Table 4-3. Comparison of kinetics for DMAEMA/2VP copolymerizations with and without free SG1 nitroxide.

$f_{\text{DMAEMA},0}$ (mol%) ^a	No free SG1		With free SG1 ($r = 0.10$) ^d	
	$\langle k_p \rangle [P]$ (s ⁻¹) ^b	$\langle k_p \rangle [P]$ (s ⁻¹) ^b	$\langle k_p \rangle \langle K \rangle$ (s ⁻¹) ^c	$\langle k_p \rangle \langle K \rangle$ (s ⁻¹) ^c
95%	$(9.2 \pm 0.4) \times 10^{-5}$	$(6.2 \pm 0.3) \times 10^{-5}$	$(6.9 \pm 0.3) \times 10^{-6}$	$(6.9 \pm 0.3) \times 10^{-6}$
99%	$(1.3 \pm 0.1) \times 10^{-4}$	$(8.4 \pm 0.4) \times 10^{-5}$	$(8.5 \pm 0.4) \times 10^{-6}$	$(8.5 \pm 0.4) \times 10^{-6}$

^a Feed composition with respect to DMAEMA. ^b Product of average propagation rate constant $\langle k_p \rangle$ and propagating radical concentration $[P]$, obtained from the slopes of the kinetic plots. ^c Product of average propagation rate constant $\langle k_p \rangle$ and average equilibrium constant $\langle K \rangle$, calculated by Equation 4-2. ^d $r = [\text{SG1}]_0 / [\text{NHS-BlocBuilder}]_0$.

In summary, various controlling co-monomers have been previously tested to control methacrylate-rich polymerizations using BlocBuilder-based NMP approach.^{104,143,146} Obviously, minimizing the controlling co-monomer concentration is often viewed as necessary so that the properties of the poly(methacrylates) are not compromised. The minimum amount of controlling co-monomer content has been reported to be 4.4 mol% for MMA/styrene,¹⁰⁴ 2.2 mol% for MMA/acrylonitrile,¹⁴³ ~ 1 mol% for MMA/VBK¹⁴⁶ and ~ 2 mol% for DMAEMA/VBK.⁴⁸ To the best of our knowledge, this is the first time 2VP is reported as a controlling co-monomer for methacrylate-rich polymerizations via NMP and is able to control DMAEMA polymerizations with as little as ~ 2 mol% 2VP in the feed. With only 1 mol% 2VP in the feed, although significant broadening of molecular weight distribution was observed, the copolymer was able to re-initiate to form a block copolymer, indicating its living nature.

Further, we demonstrated that NHS-BlocBuilder could be used without any additional free nitroxide for the controlled NMP of methacrylate-rich compositions. This could simplify greatly the processes for implementation of such polymerizations. Also, NHS-BlocBuilder was shown to be easily conjugated via a single-step coupling to amine-containing compounds, in this case, amine-terminated poly(propylene glycol), and remained an effective macroinitiator for initiating

further polymerizations and yielding a block copolymer. It demonstrated an additional approach to couple different types of polymers to form block copolymers via NMP.

4.3.3 Temperature and pH sensitivities of the statistical copolymers

PDMAEMA is known to be sensitive to both temperature and pH;^{47,48,156,157,160,163} P2VP is water-insoluble at neutral and basic aqueous solutions while highly water-soluble in acidic media.^{156,195,205} It is therefore very interesting to investigate the phase behaviour of the statistical copolymers of DMAEMA with 2VP at different temperatures and pHs, as the 2VP not only can serve as an NMP controlling co-monomer for DMAEMA polymerizations, but also can impart different solution properties to the copolymers, such as tuning of the cloud point temperatures (CPT).

The statistical copolymers were dissolved in buffer solutions from pH 7 to 11 at 0.5 wt% concentration and their thermo-sensitivity was examined by UV-visible spectroscopy. The light transmittance of the solutions decreased sharply from 100% (transparent) to 0% (opaque) once the solution temperature is above a critical value (an example was shown in Figure B-2 in Appendix B), which is typical of a lower critical solution temperature (LCST)-type phase separation. The temperature where light transmittance dropped to 50% during the heating cycle was defined as the CPT. The CPT obtained from turbidity measurements and LCST defined as the onset of particle size increase observed by dynamic light scattering (DLS) by López-Pérez et al.²⁰⁶ can be significantly different in some cases, especially when the polymer consists of a hydrophilic constituent.^{48,206} In cases of DMAEMA-rich copolymers with a small amount of a hydrophobic co-monomer,^{47,48} the reported CPTs and LCSTs have been very similar.

The LCST of a thermo-responsive statistical copolymer can be affected by many parameters such as copolymer composition,^{47,48} molecular weight,^{69,77} solution concentration,^{47,69} and in the case of PDMAEMA, pH.^{47,157} We aimed to focus on examining the effects of pH and copolymer composition on the polymer phase behaviour in aqueous media for this study, thus keeping solution concentration constant at 0.5 wt%. The M_n of the polymers ranged from about 10 to 16 kg mol⁻¹ as listed in Table 4-4. Although the LCST of PDMAEMA has been reported to be M_n -dependent,⁷⁷ it does not differ significantly within our M_n range. Therefore, we assumed the effect of M_n on the aqueous phase behaviour of our polymers to be negligible in our studies. The results demonstrating the thermo- and pH-sensitivities of the copolymers are summarized in Table 4-4.

The pKa values of the polymers shown in Table 4-4 were obtained from titration. The pKa of PDMAEMA in water was reported to be 7.0^{77,207} and pKa of P2VP measured in a mixture of water and ethanol ranged from about 3 to 4 depending on the degree of ionization.²⁰⁸ We obtained a pKa value of 7.0 for the PDMAEMA homopolymer, which was consistent with the literature.^{77,207} For the statistical copolymers with DMAEMA compositions from 76% to 93%, the measured pKas were very similar to the PDMAEMA homopolymer. P2VP is only water soluble when it is 75 – 80% ionized,²⁰⁵ or at pH < 2.5 according to its pKa of 3.0.²⁰⁸ Therefore, the 2VP units in the statistical copolymers likely stayed as a neutral hydrophobic constituent during the titration and did not alter the effective pKa values of the copolymers. It also explains why the measured pHs of all the copolymers dissolved in deionized water were not significantly different.

Table 4-4. Cloud point temperature (CPT) of DMAEMA homopolymer and DMAEMA/2VP copolymers at 0.5 wt% concentration and various pH.

Polymers	F _{DMAEMA} (mol%) ^a	M _n (kg mol ⁻¹) ^b	pK _a ^c	pH in deionized water ^d	CPT (°C) ^e				
					pH 7	pH 8	pH 9	pH 10	pH 11
PDMAEMA	100%	15.8	7.0	8.7	72	49	39	27	31
D2VP-95	93%	11.8	7.0	8.7	75	48	36	26	30
D2VP-90	85%	10.7	7.1	8.8	74	45	33	22	26
D2VP-85	81%	11.5	7.2	8.9	72	42	29	17	20
D2VP-80	76%	9.8	7.2	8.8	71	40	27	14	18

^a Copolymer composition with respect to DMAEMA determined by ¹H NMR. ^b Number-average molecular weight determined by GPC relative to poly(methyl methacrylate) standards. ^c Determined by automatic titration using 0.05 mol L⁻¹ NaOH titrant. ^d pH of 0.5 wt% solutions of the copolymers in deionized water measured by pH probe at room temperature. ^e Cloud point temperature defined by the temperature where light transmittance dropped to 50% when heating at a rate of 0.5 °C min⁻¹.

4.3.3.1 Effect of pH on the LCST of DMAEMA homopolymer

The CPT of the PDMAEMA homopolymer was examined at pHs from 7 to 11 and compared to the literature. As listed in Table 4-4, the CPT decreased sharply from 72 °C at pH 7 to 27 °C at pH 10. These sharp changes in thermo-sensitivity were closely related to the degree of ionization (DI) of the polymer as illustrated in Figure 4-8. As pH increased from 7 to 10, PDMAEMA was largely deprotonated, from about 50% to 0.1% ionized. Meanwhile, the molecular forces controlling chain conformations changed from predominantly repulsive forces between charged units to attractive intermolecular forces between the uncharged side groups,²⁰⁵ causing the polymer chains to become much more compact and hydrophobic. The CPT of 39 °C at pH 9 was consistent with the reported LCST of about 40 °C for PDMAEMA of similar M_n dissolved in water.^{69,77} At pH 10, the DI decreased to below 0.1%, a point at which the polymer can practically be considered neutral. A slight increase in CPT was observed at pH 11, likely due to a relaxation of attractive forces, analogous to pH-induced micelles that became less dense as they passed a critical pH value.¹⁵⁶ These results well demonstrated the interesting combination of

temperature and pH sensitivities of PDMAEMA that make it so attractive for stimuli-responsive materials.

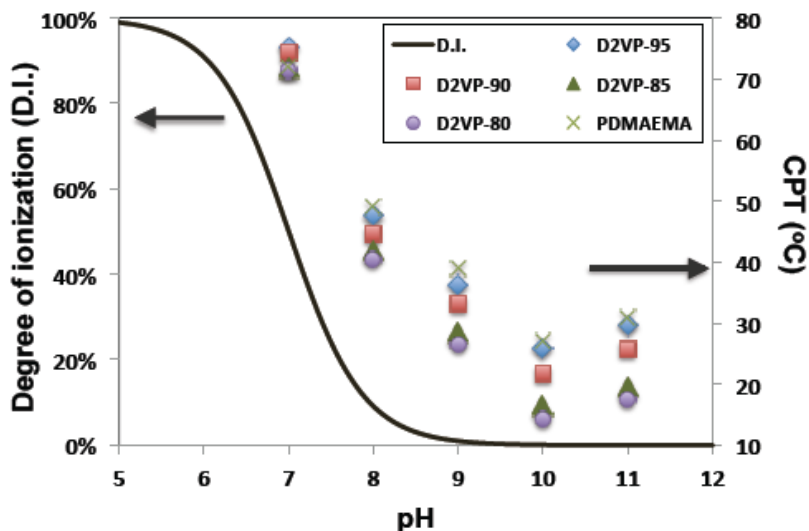


Figure 4-8. Cloud point temperature (CPT) of polymers of various compositions versus pH compared to the degree of ionization of PDMAEMA.

4.3.3.2 Effect of copolymer composition on the LCST of statistical copolymers

The LCST-type phase separation of the statistical copolymers was also investigated at pH 7 to 11. At these conditions, P2VP was totally deprotonated and therefore simply acted as a hydrophobic component of the copolymer. It is known that when DMAEMA is copolymerized with a hydrophobic co-monomer, the CPTs of the resulting statistical copolymer decreases with increasing hydrophobic content.^{47,48} The same is applicable to the DMAEMA/2VP copolymer system, where the CPTs decreased as 2VP content increased in the statistical copolymer as shown in Table 4-4.

Moreover, the effect of copolymer composition on the CPT varied with pH. At pH 10 and 11, the effect of copolymer composition was very similar and the most profound, where the copolymer with 24% 2VP had a CPT 13 °C lower than the PDMAEMA homopolymer. The differences in

CPTs with composition diminished as pH decreased. At pH 7, all copolymers with up to 24% 2VP had similar CPTs to the PDMAEMA homopolymer. These results made good sense if put together with the change in DI of PDMAEMA with pH as shown in Figure 4-8. At pH 10 and above, PDMAEMA is completely deprotonated and no longer sensitive to pH. Therefore, the copolymer composition became the sole variable that affected the CPT, which explains why the changes in CPT at pH 10 and 11 with composition were very similar. As pH decreased below 10, the DMAEMA units started to ionize and the repulsive forces between charged units soon dominated the attractive intermolecular forces from the hydrophobic 2VP units. As a result, the effect of copolymer composition on the cloud point temperatures diminished with decreasing pH.

In previous studies of similar systems where DMAEMA was copolymerized with styrene⁴⁷ and VBK⁴⁸ via NMP, the CPTs of the resulting statistical copolymers were also strongly affected by the copolymer composition. The main difference between those systems and this work is that those copolymers became water-insoluble when DMAEMA content in the copolymer decreased to 81 mol% with styrene⁴⁷ as co-monomer and 87 mol% with VBK⁴⁸ as co-monomer because of the high hydrophobicity of these co-monomers. At pH 10, the DMAEMA/VBK copolymers became water-insoluble even with as little as 2 mol% VBK and the DMAEMA/styrene copolymers were only water-soluble when the copolymer consisted of 89 mol% or more DMAEMA. In comparison, the DMAEMA/2VP copolymers in this study were all water-soluble and exhibited LCST-type phase separation from pH 7 to 11 with up to 24 mol% 2VP in the copolymer. These results demonstrated an obvious advantage of using 2VP as a co-monomer with DMAEMA as compared to the aforementioned systems, as it not only led to controlled polymerization, but also retained the thermo-responsive properties of PDMAEMA and

effectively fine-tuned the CPT of the copolymer in the full range of pH where PDMAEMA was pH sensitive.

4.3.3.3 Effect of composition and pH on reversibility of phase separation

Sharp transitions and reversibility are often cited as the two criteria for “smart” materials. For thermo-responsive polymers such as PDMAEMA, this means the phase separation needs to not only happen quickly at the critical temperature, but also be re-dissolved at the same temperature. Thus, hysteresis was studied and it refers here to a difference in the transition temperature during heating and cooling.

For polymers that exhibit LCST-type phase separation in water, a layer of clathrate-like structures is formed around a hydrophobic group of the polymer via hydrogen bonding between water molecules and a hydrogen-bond acceptor in the polymer (ie. an atom with unpaired electrons, usually nitrogen or oxygen), which increases the solubility of the polymer in water.^{46,183} As temperature increases above a critical point, the ordered water layer is interrupted and the polymer phase-separates from the aqueous solution, undergoing a “coil-to-globule” transition.²⁰⁹ During cooling, the transition from globule to coil is more difficult because of the formation of intra-chain structures in the globule state through intra-chain hydrogen bonding, which retards the re-dissolution of the polymer globule.²⁰⁹

For the DMAEMA/2VP copolymers, 1 to 5 °C of hysteresis was observed as plotted in Figure 4-9. Similar observations were reported for DMAEMA/VBK copolymers that contained only 3 mol% VBK.⁴⁸ Hysteresis increased to as high as 10 °C when VBK content was increased to 7 mol% in the copolymer.⁴⁸ The amplified hysteresis was attributed to the high hydrophobicity of

VBK. In this study, we investigated the effects of both polymer composition and pH on the extent of hysteresis as they both played important roles on the copolymer thermo-responsiveness.

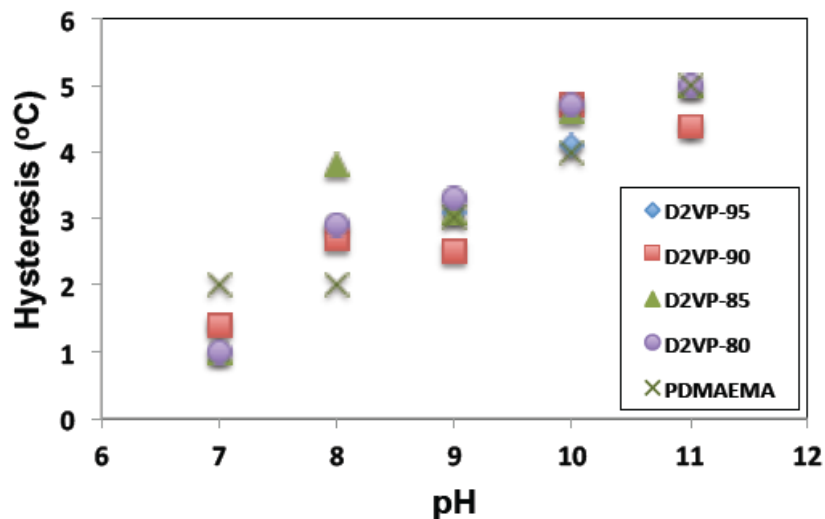


Figure 4-9. Hysteresis (difference in temperature at 50% light transmittance during heating and cooling) of polymers with various compositions versus pH of the solutions.

From Figure 4-9, the extent of hysteresis showed a strong correlation with pH. As discussed before, increasingly more DMAEMA units became charged as pH decreased. These charged units remained in an extended form even at temperatures above the CPT because of the strong electrorepulsive forces. As a result, the polymer chains were less compact when they aggregated at lower pH and easier to be re-dissolved when cooled. Polymer composition did not have a significant impact on the extent of hysteresis according to Figure 4-9 in contrast to DMAEMA/VBK copolymers.⁴⁸ This is likely due to the much lower hydrophobicity of 2VP compared to VBK. In summary, the degree of hysteresis is relatively small for all the DMAEMA/2VP copolymers, indicating good reversibility in phase separation, which is a desirable property for “smart” materials.

4.3.4 Temperature and pH sensitivities of the block copolymers

4.3.4.1 pH-induced micellization at room temperature

Micellization can be induced by changing pH when two ionizable weakly basic (or acidic) polymers of different pK_a^{156,210} or one ionizable block and a water-soluble neutral block¹⁹⁵ are covalently linked in the same molecule as a block copolymer. In this work, a DMAEMA/2VP statistical copolymer with 93 mol% DMAEMA was chain-extended with 2VP to form a block copolymer. The DMAEMA/2VP copolymer had a very similar pK_a as PDMAEMA homopolymer (Table 4-4) and it is known that P2VP had a lower pK_a than PDMAEMA.^{77,207,208} Such a block copolymer should form pH-dependent micelles.¹⁵⁶

The titration curve of the sample D2VP-95-2VP diblock copolymer is presented in Figure 4-10. Because P2VP is only water-soluble when highly protonated at low pH, micelle formation was expected as pH is increased. When titration was started with a pH of about 2, the solution was clear. As pH increased to about 4, the solution developed cloudy domains as the NaOH solution was added to the stirred solution of the block copolymer, indicating initial formation of micelles where local pH was higher. The domains disappeared when the solution became more homogenized, due to more stirring. When solution pH increased to greater than 5, the entire solution suddenly turned translucent, signifying the formation of stable micelles. From the titration curve, a plateau appeared at about pH 5 that coincided with this visual observation of micellar formation. Similar micellization of P2VP-b-poly(ethylene oxide) diblock copolymer was also reported to occur at pH 4.8 using titration.¹⁹⁵

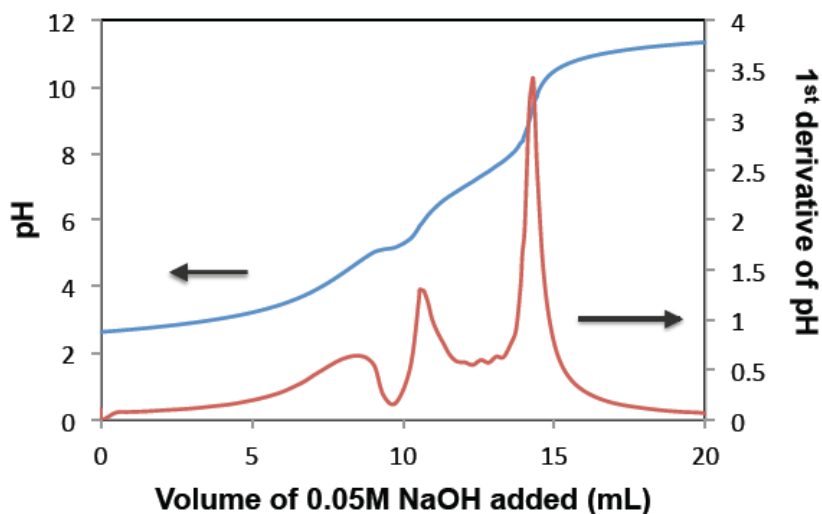


Figure 4-10. pH titration curve of D2VP-95-2VP diblock copolymer obtained from automatic titration (blue line) and the first derivative of the measured pH (red line).

To get better insight of the micellization process, dynamic light scattering (DLS) was used to examine the hydrodynamic radius (R_h) of D2VP-95-2VP diblock copolymer in different buffer solutions. The DLS results are shown in Figure 4-11. The R_h of the diblock copolymer was below 10 nm at pH 4, increased to about 40 nm at pH 5 and reached a plateau at about 60 nm at pH 6. This result demonstrates the transition of the diblock copolymer from well-dispersed unimers at pH 4 to initial micelles at pH 5 and finally stable micelles at pH 6, which agreed well with the observations from titration. Meanwhile, the dispersity of the particle size distribution (μ_2/Γ^2) was about 0.3 at pH 4, indicating loose unimers. The very low μ_2/Γ^2 value of below 0.01 at pH 5 revealed the critical pH where P2VP is completely deprotonated while PDMAEMA is still totally ionized, forming dense micelles.¹⁵⁶ The value of μ_2/Γ^2 relaxed to a relatively constant value of about 0.15 at pH 6 and higher when PDMAEMA became partially deprotonated. These results showed good agreement with a previous study of micellization of PDMAEMA-P2VP diblock copolymer in aqueous solutions.¹⁵⁶

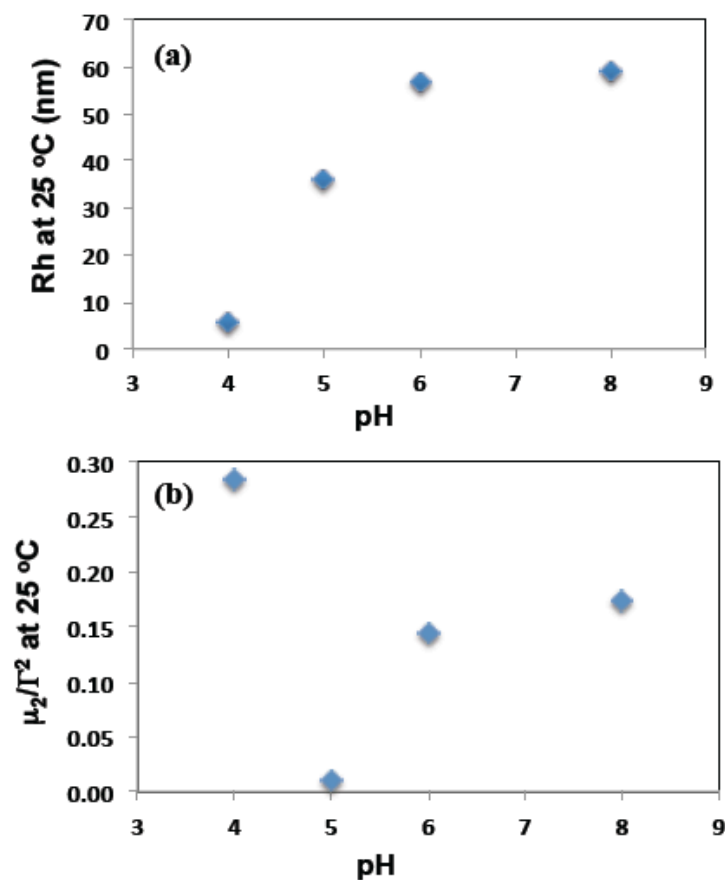


Figure 4-11. (a) Hydrodynamic radius and (b) dispersity of the particle size distribution (μ_2/Γ^2) of D2VP-95-2VP diblock copolymers determined by dynamic light scattering at room temperature versus pH with solution concentration of 0.5 wt%.

4.3.4.2 Temperature sensitivity of D2VP-95-2VP diblock copolymer

The temperature sensitivity of the diblock copolymer D2VP-95-2VP was examined in different pH buffer solutions by DLS and the results are presented in Figure 4-12. Final pHs of the polymer solutions were confirmed using a calibrated pH probe. Surprisingly, some of the solution pHs were not the same as the buffer pHs. Specifically, polymer solutions in pH 3 and 4 buffers appeared to be pH 4 and 5, respectively, at room temperature when measured by a pH probe. It is likely that the basicity of the copolymer overcame the buffering capacity of the pH 3

and 4 buffers. Therefore, the pHs of those two solutions were expected to increase significantly with temperature.

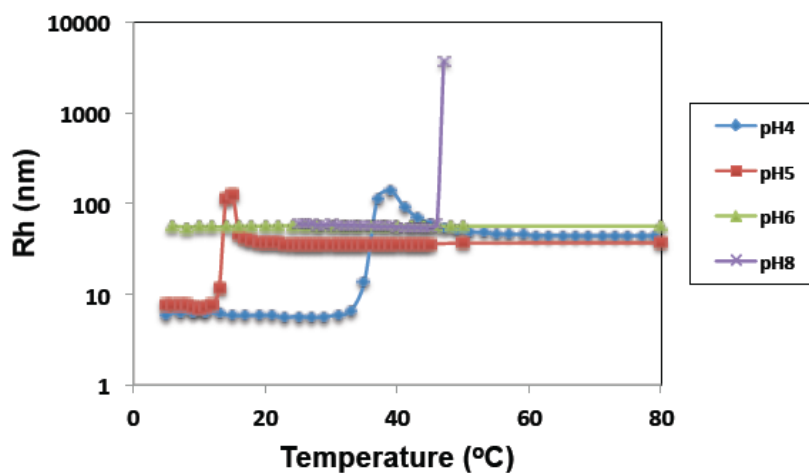


Figure 4-12. Hydrodynamic radius (R_h) of D2VP-95-2VP diblock copolymer at various pH determined by dynamic light scattering versus temperature. Temperature was increased at a rate about $0.5\text{ }^\circ\text{C min}^{-1}$.

From Figure 4-12, well-dispersed unimers with R_h under 10 nm were observed in a pH 4 solution up to about $37\text{ }^\circ\text{C}$ and in a pH 5 solution up to about $10\text{ }^\circ\text{C}$. Again, these pHs only represent the solution pH at room temperature and the true pH varied with temperature. Formation of micelles were evidenced by the sharp increase in R_h to above 100 nm and then dropped to a stable size of about 60 nm in both solutions, indicating a critical pH was reached as temperature increased, consistent with the titration results. For a pH 6 solution, stable micelles were observed from 5 to $80\text{ }^\circ\text{C}$. This is expected because at pH 6 and lower, PDMAEMA is fully protonated and no longer thermo-sensitive. At pH 8, stable micelles were observed up to $47\text{ }^\circ\text{C}$ and then R_h rapidly increased to above 1000 nm, representing collapse of micelles into aggregates. This result is consistent with the CPT of D2VP-95 statistical copolymer at $48\text{ }^\circ\text{C}$ at pH 8 (Table 4-4).

4.3.4.3 *Doubly thermo-responsive block copolymer of poly(propylene glycol)-b-poly(2-dimethylamino ethyl methacrylate-stat-2-vinylpyridine) (PPO-D2VP-95)*

A diblock copolymer consisting of a poly(propylene glycol) (PPO) block and a block of DMAEMA/2VP statistical copolymer with 95 mol% DMAEMA was synthesized using the macroalkoxyamine PPO-BB. It has been previously shown that the solubility of PPO in water decreased with temperature due to diminishing hydrogen bonding between water and PPO.²¹¹ Therefore, the diblock copolymer PPO-D2VP-95 was expected to have additional thermo-sensitivity compared to DMAEMA/2VP statistical copolymers.

Both poly(propylene glycol) bis(2-aminopropyl ether) (PPO-di-NH₂) and the diblock copolymer PPO-D2VP-95 in pH 8 buffers were studied using DLS. As shown in Figure 4-13, PPO-di-NH₂ was found to exhibit LCST-type phase separation in water above a critical temperature of 19 °C. For the diblock copolymer, the R_h increased sharply from below 10 nm to about 100 nm, indicating micelle formation, at 19 °C. The coincidence of transition temperatures implied the PPO block was responsible for the formation of micelles as PPO became water-insoluble. At 41 °C, a second transition was observed, where micelles collapsed and formed large aggregates when the DMAEMA/2VP statistical copolymer segment became insoluble in water. The second transition temperature (41 °C) was lower than the CPT of DMAEMA/2VP statistical copolymer with the same composition (48 °C). This is likely due to the presence of the hydrophobic PPO block rendering the block copolymer more hydrophobic.

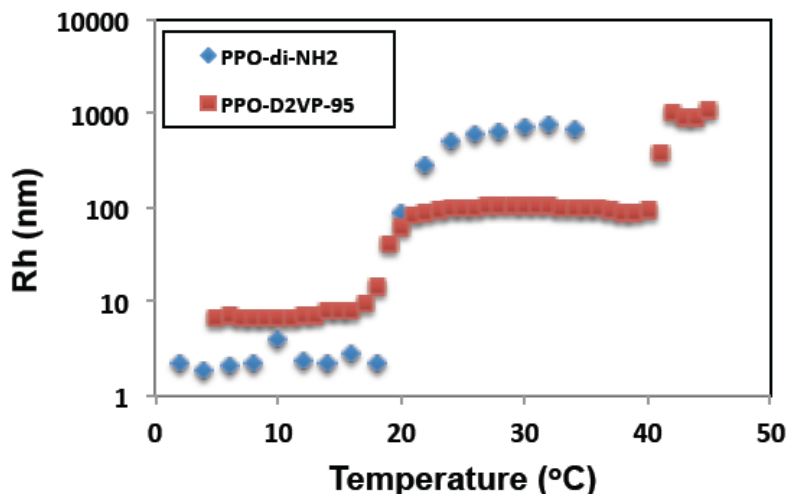


Figure 4-13. Comparison of hydrodynamic radius of poly(propylene glycol) bis(2-aminopropyl ether) (PPO-di-NH₂) and diblock copolymer PPO-D2VP-95 in pH 8 buffer solution measured by dynamic light scattering. Temperature was increased at a rate about 0.5 °C min⁻¹.

These results confirmed the coupling of PPO-di-NH₂ with NHS-BlocBuilder was indeed successful. Vinas et al.¹⁷¹ demonstrated post-functionalization of a NHS-BlocBuilder-initiated polymer with an amine functional compound was also possible. The use of NHS-BlocBuilder opened a new approach for obtaining block copolymers as opposed to the traditional chain extension method. With NHS-BlocBuilder, it is also easy to see how other amine functional materials can be coupled to the polymer chains, as has been demonstrated by bioconjugation of NHS-BlocBuilder to peptides.¹⁵¹

4.4 Conclusions

DMAEMA was copolymerized with 2VP using NHS-BlocBuilder with feed compositions varied from 80 – 99 mol% DMAEMA, producing water-soluble, thermo- and pH-sensitive statistical copolymers. The copolymerization was controlled to relatively high conversions ~ 50% based on the linear increase in M_n versus conversion and monomodal molecular weight distributions with

relatively low Đs. As little as ~ 2 mol% 2VP in the initial composition was demonstrated sufficient in producing controlled, living DMAEMA-rich polymers. Feed containing 1 mol% 2VP yielded DMAEMA/2VP copolymer that was living but had significantly broader molecular weight distribution. With NHS-BlocBuilder, additional SG1 nitroxide was proven unnecessary and pre-functionalization of PPO-di-NH₂ with NHS-BlocBuilder was demonstrated successfully.

The CPTs of the statistical copolymers were tuned in the range of 14 – 75 °C by varying copolymer composition and solution pH. Only 1-5 °C of hysteresis was observed, which indicated good reversibility of the phase separation. The block copolymer obtained by chain extension of DMAEMA/2VP statistical copolymer with 2VP was found to form pH-dependent micelles as expected at a critical pH of 5 at room temperature and collapsed to aggregates at higher temperature at pHs > 8 because of the thermo-responsive DMAEMA/2VP block. The PPO-D2VP-95 diblock copolymer synthesized from the PPO-BB macroalkoxyamine exhibited double thermo-responsiveness at transition temperatures of 19 °C (corresponding to the PPO block) and 41 °C (corresponding to the DMAEMA-rich block).

This study reported for the first time the use of 2VP as a controlling co-monomer for a methacrylate-rich copolymerization without aid of free nitroxide by utilizing NHS-BlocBuilder. We showed that the advantages of 2VP as a co-monomer include a very small amount (~2 mol%) necessary for controlling and low hydrophobicity for tuning LCST while maintaining water solubility within a wide range of pH. The versatility of NHS-BlocBuilder was also demonstrated by producing doubly thermo-responsive block copolymer by pre-functionalization of the NHS-BlocBuilder initiator with PPO-di-NH₂.

Acknowledgements

The authors are very grateful for the funding from the NSERC Postgraduate Scholarship, NSERC Discovery Grant and Canada Foundation for Innovation New Opportunities Fund. They also thank Prof. Bruce Lennox (Dept. of Chemistry, McGill University), for providing access to his temperature modulated UV-vis spectrometer, along with Dr. Paul Goulet for his assistance in training on the use of the instrument. The authors thank Prof. Bernadette Charleux for stimulating conversations regarding the use of vinyl pyridines as controllers for DMAEMA-type monomers and their subsequent properties. We also thank Arkema (Scott Schmidt and Noah Macy) supplying BloBuilder and SG1.

References

Please refer to the global bibliography at the end of the thesis.

Chapter 5

Controlled Synthesis of Benzyl Methacrylate-rich Copolymer via NMP using Styrene as “Controlling” Co-monomer

5.1 Preface

Starting from this chapter, the next three chapters detail the synthesis and characterizations of (co)polymers that are thermo-responsive in ionic liquid (IL) solutions. Chapter 5 presents a manuscript published in *Macromolecular Reaction Engineering*, **2010** (4): 415-423. It details the synthesis of benzyl methacrylate (BzMA)/styrene copolymers by nitroxide mediated polymerization (NMP) using a wide range of feed compositions ($f_{BzMA,0} = 10 - 90$ mol%).

Poly(benzyl methacrylate) (PBzMA) drew our interest because it was known to exhibit LCST-type phase separation in hydrophobic ILs²¹² and it has never been synthesized in a controlled manner via NMP before this manuscript was published. Styrene was used as a controlling co-monomer to significantly reduce active radical concentration and average chain propagating rate, which was confirmed by the exponential-like decrease in $\langle k_p \rangle \langle K \rangle$, the product of average propagating constant and average equilibrium constant, as feed composition of styrene increased. Linear increases in number-average molecular weight with conversion up to 50% and relatively narrow molecular weight distribution ($\overline{M}_w/\overline{M}_n = 1.2 - 1.4$) were achieved for all feed compositions, both of which are features of controlled radical polymerization. Selected copolymers were also chain-extended with a fresh batch of styrene monomer to check their ability to re-initiate and form block copolymers. Copolymers synthesized with up to 80 mol% BzMA in the feed were able to extend their chains, whereas the copolymer made with feed containing 90 mol% BzMA mostly did not re-initiate during chain extension. Lastly, reactivity

ratios of BzMA and styrene were calculated using the Mayo-Lewis equation and the results were comparable with literature values of reactivity ratios for BzMA/styrene system using conventional free radical polymerization.

This manuscript presents the important confirmation that well-defined BzMA-rich copolymers can be synthesized via NMP. This is the first step towards investigations of the LCST-type phase separation behaviours of BzMA-rich copolymers in IL solutions, which will be detailed in Chapter 6 and 7.

Synthesis and Characterization of Benzyl Methacrylate/Styrene Random Copolymers Made by Nitroxide-Mediated Controlled Radical Polymerization

Chi Zhang, Benoit Lessard, Milan Maric*

Department of Chemical Engineering, McGill University,
3610 University Street, Montreal, Quebec, Canada H3A 2B2

Macromolecular Reaction Engineering, **2010** (4): 415-423

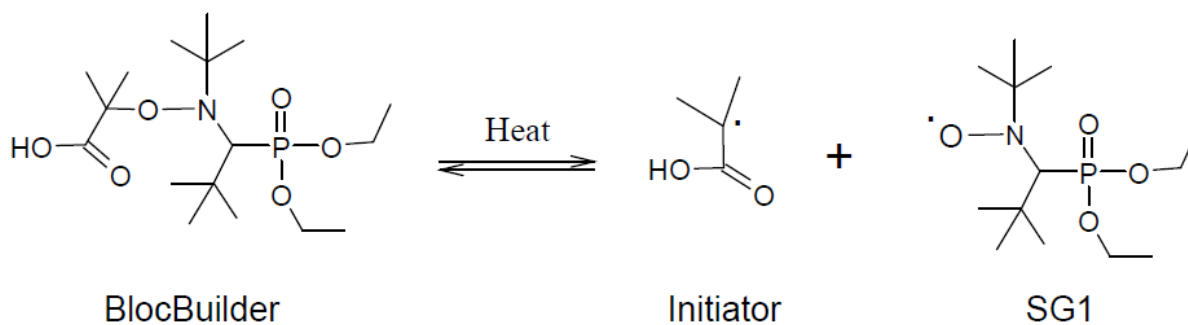
Abstract

Benzyl methacrylate (BzMA) and styrene were randomly copolymerized in bulk at various feed compositions ($f_{BzMA,0} = 10 - 90$ mol% BzMA) at 90 °C by nitroxide mediated polymerization (NMP) with about 10% free SG1 relative to the unimolecular BlocBuilder initiator. Linear molecular weight increase with conversion was observed for all compositions up to conversion of about 50%. Random copolymers with polydispersities $M_w/M_n = 1.1- 1.5$ were obtained. The product of average propagation rate $\langle k_p \rangle$ and average activation-deactivation equilibrium constant $\langle K \rangle$, $\langle k_p \rangle \langle K \rangle$, followed an exponential-like increase with increasing $f_{BzMA,0}$. The extrapolated $\langle k_p \rangle \langle K \rangle$ values for pure BzMA and styrene from experimental data are comparable with literature (K_{MMA} was used as reference since K_{BzMA} is not available). Chain extensions with styrene at 110 °C initiated by selected BzMA/styrene random copolymers showed high levels of “livingness” for macroinitiators possessing up to $f_{BzMA,0} = 80$ mol%. Broad molecular weight distribution and low conversion of the second block was observed for chain extension of macroinitiator with $f_{BzMA,0} = 90$ mol%. Reactivity ratios of the two monomers (r_{BzMA}

= 0.86 ± 0.36 and $r_{styrene} = 0.27 \pm 0.14$) determined from the compositions of the copolymers were within the range reported by conventional radical polymerization.

5.2 Introduction

Nitroxide-mediated polymerization (NMP) is one of the controlled radical polymerization (CRP) techniques that has been successfully utilized in synthesizing polymers. The early NMP using TEMPO (2,2,6,6-tetramethylpiperidiny-1-oxy) as mediator was mainly applied to synthesis of styrenic-based^{123,124} polymers. With the second generation of acyclic nitroxides such as SG1, [*tert*-butyl(1-diethoxyphosphoryl-2,2-dimethylpropyl)amino] oxidanyl (Scheme 5-1), acrylic-based^{107,110,126,203} and acrylamide-based^{105,108,213} polymers can also be synthesized with a high level of control (i.e. narrow molecular weight distribution, linear increase in molecular weight with conversion). However, NMP showed relatively poorer control when used to polymerize methacrylic esters compared to other CRP techniques.²¹⁴



Scheme 5-1. Structure of the unimolecular alkoxyamine BlocBuilder and of the SG1 nitroxide used in this work.

It was found that with TEMPO, β -hydrogen transfer reactions from the propagating radicals to the initiator (also called disproportionation reactions) occurred early during the polymerization

of methacrylic esters.^{139,176,215} These reactions converted the nitroxide to the corresponding hydroxylamine which prevented TEMPO from capping the propagating radicals and resulted in termination at low conversions of the methacrylate monomers.^{139,176} The significance of such disproportionation reactions for SG1-mediated systems was also thoroughly studied in the homopolymerization system of methyl methacrylate (MMA) in the presence of various levels of excess SG1.^{137,215} McHale et al.²¹⁵ demonstrated that with a large excess of SG1 ($\geq 40\%$), the percentage of dead chains formed by disproportionation increased with SG1 concentration and disproportionation became the sole chain-terminating event when more than 177% excess SG1 was used. The rate constant of β -hydrogen transfer from the PMMA propagating radicals to SG1 (k_{bHtr}) obtained by Dire et al.¹³⁷ confirmed the strong contribution of disproportionation to the reduction of living chains during polymerization of MMA; however, the k_{bHtr} was three orders of magnitude lower compared to a *n*-butyl methacrylate/TEMPO system. Besides undesired side reactions, the activation-deactivation equilibrium constants of methacrylates in SG1-mediated polymerization are much greater than that of styrene as illustrated in Table 5-1, using MMA as an example. Coupled with the higher radical propagation constants, k_p , as also shown in Table 5-1, the high concentration of reactive free radicals has caused major challenges to control polymerization of methacrylates via NMP.

Table 5-1. Propagation Rate Constants and Activation-Deactivation Equilibrium Constants of Styrene and Methacrylates.

Monomer	k_p at 90°C L·mol ⁻¹ ·s ⁻¹	K at 90°C ^a L·mol ⁻¹	Ref
styrene	900	4×10^{-10}	126,167
methyl methacrylate	1640	1×10^{-7}	139,167
<i>n</i> -butyl methacrylate	1940	N/A	216
benzyl methacrylate	3000	N/A	216

^a K is the activation-deactivation equilibrium constant for SG1-mediated polymerization.

Poly(benzyl methacrylate) (PBzMA) has attracted a lot of interest lately due to it exhibiting lower critical solution temperature (LSCT)-type phase separation behaviour in common hydrophobic ionic liquids. Sharp and reversible solubility changes in response to changing temperatures were observed for PBzMA-ionic liquid mixtures.^{59,212,217} Ionic liquids are molten salts that have excellent stabilities, negligible vapour pressure and high ionic conductivity, making them candidate “green” solvents and solid state electrolytes, for example.^{39,41,218,219} The reversibly thermosensitive material made from PBzMA and ionic liquids can lead to a new generation of environmentally friendly “smart” materials particularly if the microstructure of PBzMA can be controlled, as suggested by CRP. However, the propagation rate of BzMA is higher than many common methacrylates as shown in Table 5-1 which suggests that controlled homopolymerization of BzMA using NMP will be a formidable challenge. Recent attempts to lower the average activation-deactivation equilibrium constant $\langle K \rangle$ by copolymerizing a low concentration of styrene with methyl methacrylate using SG1-mediated polymerization have shown promising results.^{130,167} Based on this idea, we investigated random copolymerizations of styrene and BzMA at various feed compositions using SG1-mediated polymerization. Our observations of the effects of feed composition on kinetic parameters as well as the characterization of the “livingness” of the copolymers are reported in this paper and will later be used to develop BzMA containing polymers using NMP for ionic gel applications.

5.3 Results and Discussion

5.3.1 Effect of Initial Feed Composition on Copolymerization Kinetics

As summarized in Table 5-2, copolymerization of BzMA and styrene was conducted in bulk at 90 °C with feed compositions ranging from 10 mol% to 90 mol% BzMA (noted as $f_{\text{BzMA},0}$). Some characterization data including final copolymer compositions (noted as $F_{\text{BzMA},\text{fin}}$), and molecular weight distribution of the final copolymers are also listed in Table 5-2. It has been previously shown that addition of free SG1 nitroxide resulted in better controlled polymerization and narrower molecular weight distribution.^{103,110,203} However, large excess of SG1 led to significant amount of disproportionation reactions and thus decreased “livingness” as discussed in *Introduction*. A previous study of a very similar system (copolymerization of methyl methacrylate (MMA) and styrene at 90 °C) used about 10 mol% free SG1 nitroxide relative to the initiator and showed promising results.¹⁶⁷ Therefore, we added 10 mol% excess SG1 nitroxide relative to BlocBuilder for the copolymerization with all feed compositions to decrease the polymerization rate and obtain better control.

Table 5-2. Summary of Benzyl Methacrylate/Styrene Copolymerization Performed in Bulk at 90 °C.

$f_{\text{BzMA},0}$	r^a	Time	Monomer Conversion	$F_{\text{BzMA},\text{fin}}^b$	M_n^c	\mathcal{D}^c
mol %		minute	%	mol %	kg·mol ⁻¹	
10	0.10	440	27	23	7.7	1.24
20	0.13	360	40	32	11.1	1.20
29	0.10	180	58	57	12.4	1.22
40	0.11	120	46	60	11.9	1.24
50	0.09	50	36	61	10.8	1.30
60	0.12	55	55	70	14.7	1.27
70	0.10	22	38	76	12.4	1.40
80	0.10	19	58	75	13.6	1.30
89	0.10	6	52	86	15.6	1.40

^a $r = [\text{SG1}]_0/[\text{BlocBuilder}]_0$. ^b Final BzMA molar composition in copolymer ($F_{\text{BzMA},\text{fin}}$) determined by ¹H nuclear magnetic resonance. ^c Number-average (M_n), weight-average (M_w) molecular weight, and dispersity ($\mathcal{D} = M_w/M_n$) determined by gel permeation chromatography relative to poly(styrene) standards in THF at 40 °C.

As described previously, there exists an equilibrium between the dormant and propagating species in the nitroxide-mediated polymerization.^{103,203}

Equation 5-1

$$\langle K \rangle = \frac{[P\bullet][SG1\bullet]}{[P-SG1]}$$

where $\langle K \rangle$ is the average equilibrium constant, $[P\bullet]$ is the propagating radical concentration, $[SG1\bullet]$ is the free nitroxide concentration and $[P-SG1]$ is the concentration of the dormant species. Since excess free nitroxide was added, $[SG1\bullet] \approx [SG1]_0$. It was also assumed that self-initiation was insignificant and thus $[P-SG1] \approx [BlocBuilder]_0$. By defining $r = [SG1]_0/[BlocBuilder]_0$, the following relationship was deduced:¹⁰³

Equation 5-2

$$\langle k_p \rangle \langle K \rangle \approx \langle k_p \rangle \frac{[P\bullet][SG1]_0}{[BlocBuilder]_0} = \langle k_p \rangle [P\bullet] r$$

where $\langle k_p \rangle$ is the average propagation rate constant.

Figure 5-1 shows the kinetic plots of $\ln[(1-x)^{-1}]$ ($x =$ conversion) versus time for the copolymerization with all feed compositions. The slopes of the plots represent the apparent rate constants $\langle k_p \rangle [P\bullet]$. It was obvious that as the BzMA content in the feed increased, the apparent rate constants increased. The results are in agreement based on the much higher propagation rate of BzMA compared to styrene reported in the literature.^{167,216,220} The experimental values of $\langle k_p \rangle [P\bullet]$ and $\langle k_p \rangle \langle K \rangle$ as well as the standard deviations from the slopes of the kinetic plots are summarized in Table 5-3. We found that an exponential relationship between $\langle k_p \rangle \langle K \rangle$ and the initial feed composition of BzMA best fit our experimental data as shown in Figure 5-2. There are various kinetic models available for fitting and predicting $\langle k_p \rangle \langle K \rangle$ with feed compositions^{130,221,222} which are beyond the scope of this study. The main purpose of the kinetic

study in this case is to confirm the strong influence of feed composition on $\langle k_p \rangle \langle K \rangle$. A more detailed kinetic study for the BzMA/styrene system using electron spin resonance (ESR) will be examined in the near future.

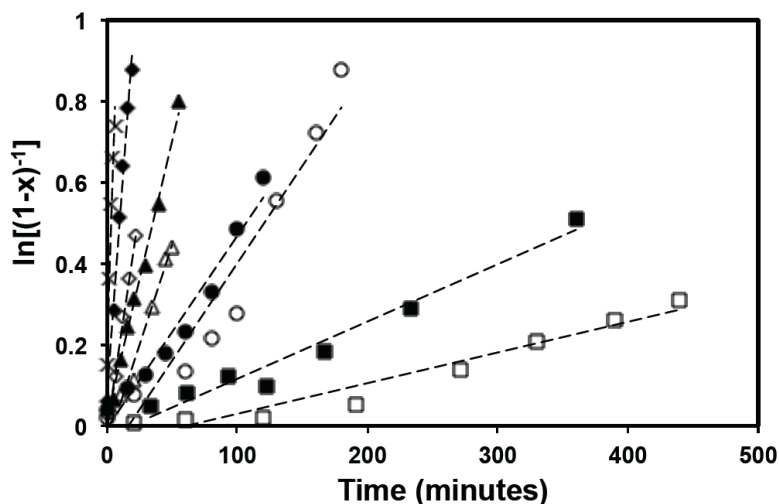


Figure 5-1. Plot of $\ln[(1-x)^{-1}]$ (where x = conversion) versus time for bulk copolymerization at $90\text{ }^{\circ}\text{C}$ for various initial feed compositions of benzyl methacrylate ($f_{BzMA,0}$). The different $f_{BzMA,0}$ are denoted as followed: $f_{BzMA,0} = 10\%$ (\square), $f_{BzMA,0} = 20\%$ (\blacksquare), $f_{BzMA,0} = 30\%$ (\circ), $f_{BzMA,0} = 40\%$ (\bullet), $f_{BzMA,0} = 50\%$ (\triangle), $f_{BzMA,0} = 60\%$ (\blacktriangle), $f_{BzMA,0} = 70\%$ (\diamond), $f_{BzMA,0} = 80\%$ (\blacklozenge), $f_{BzMA,0} = 90\%$ (\times).

Table 5-3. Kinetic Parameters Derived from the Semilogarithmic Kinetic Plots for Copolymerization of Benzyl Methacrylate and Styrene in Bulk at $90\text{ }^{\circ}\text{C}$ by NMP.

$f_{BzMA,0}$ mol%	r^a	$\langle k_p \rangle [P\bullet]$ $\times 10^4\text{ s}^{-1}$	$\langle k_p \rangle \langle K \rangle$ $\times 10^4\text{ s}^{-1}$
10	0.10	0.13 ± 0.01	0.012 ± 0.001
20	0.13	0.24 ± 0.02	0.030 ± 0.003
29	0.10	0.81 ± 0.08	0.083 ± 0.009
40	0.11	0.79 ± 0.06	0.083 ± 0.007
50	0.09	1.30 ± 0.21	0.123 ± 0.020
60	0.12	2.27 ± 0.09	0.283 ± 0.012
70	0.10	3.58 ± 0.37	0.354 ± 0.036
80	0.10	8.16 ± 0.29	0.810 ± 0.029
85	0.10	10.33 ± 0.46	1.012 ± 0.045
89	0.10	21.97 ± 0.88	2.090 ± 0.084

^a $r = [SG1]_0/[BlocBuilder]_0$

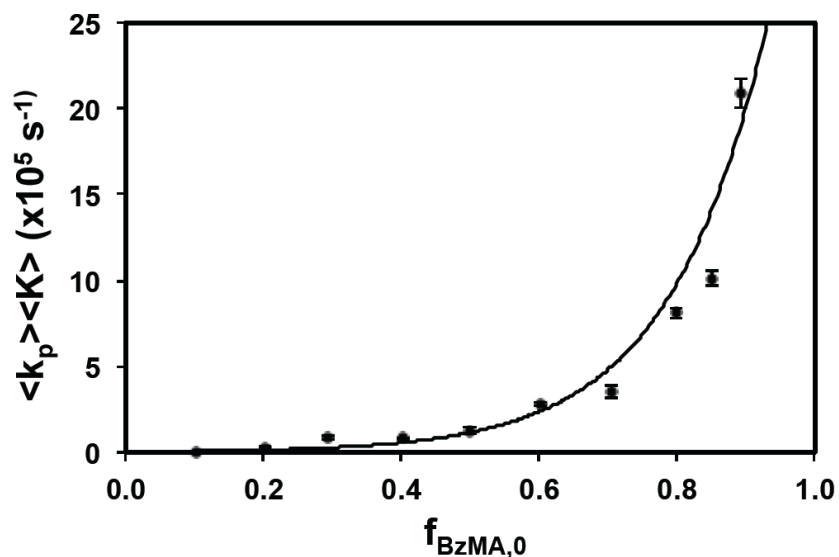


Figure 5-2. The product of the average propagation rate constant $\langle k_p \rangle$, and the average equilibrium constant $\langle K \rangle$, $\langle k_p \rangle \langle K \rangle$, for BzMA/styrene copolymerization at 90 °C in bulk versus initial feed composition of BzMA ($f_{\text{BzMA},0}$) and the best-fit line obtained by non-linear least-square fitting is used as a guide.

The $k_p K$ values for styrene and BzMA homopolymerization at 90 °C were estimated from the best-fit equation and compared with the literature. The comparison is summarized in Table 5-4. The extrapolated $k_p K$ values are $9.0 \times 10^{-7} \text{ s}^{-1}$ and $2.7 \times 10^{-4} \text{ s}^{-1}$ for pure styrene and BzMA, respectively. The k_p values for styrene and BzMA homopolymerization were determined previously by pulsed laser initiated polymerization (PLP).^{199,216} The k_p 's for styrene and BzMA at 90 °C are $9 \times 10^2 \text{ L} \cdot \text{mol}^{-1} \text{ s}^{-1}$ and $3 \times 10^3 \text{ L} \cdot \text{mol}^{-1} \cdot \text{s}^{-1}$ respectively, which were calculated using the Arrhenius parameters reported.^{132,221} Combining with the previously determined equilibrium constant for styrene at 90 °C using a similar alkoxyamine initiator ($K = 4 \times 10^{-10} \text{ mol} \cdot \text{L}^{-1}$),¹²⁶ we obtained a $k_p K$ value of $3.6 \times 10^{-7} \text{ s}^{-1}$ for pure styrene. The calculated $k_p K$ for styrene is lower than our estimated value but within the same order of magnitude. For BzMA, no reported K values were found but the equilibrium constant for MMA ($K = 1 \times 10^{-7} \text{ mol} \cdot \text{L}^{-1}$)²¹⁵ is a reasonable reference because of the structural similarity between the two monomers. Therefore,

we obtained a $k_p K$ value for BzMA of $3.0 \times 10^{-4} \text{ s}^{-1}$ from the reported data which is very close to our estimate from our investigation. These comparisons confirmed that our experimental results were valid representations of the relationship between $\langle k_p \rangle \langle K \rangle$ and feed compositions for the copolymerization of BzMA and styrene.

Table 5-4. Kinetic Parameters for Benzyl Methacrylate and Styrene Homopolymerizations.

	Reported ^{126,167,216}		This work	
	BzMA	Styrene	BzMA	Styrene
k_p at 90°C (L·mol ⁻¹ ·s ⁻¹)	3000	900	N/A	
K at 90°C (L·mol ⁻¹)	1×10^{-7} ^a	4×10^{-10}	N/A	
$k_p K$	3×10^{-4}	3.6×10^{-7}	2.7×10^{-4} ^b	9.0×10^{-7} ^b

^a Equilibrium constant for methyl methacrylate. ^b Extrapolated values from experimental data

With the much higher k_p and the three order of magnitude higher K for BzMA compared to those of styrene, it is not surprising now that the $\langle k_p \rangle \langle K \rangle$ values for the copolymerization increased exponentially with increasing BzMA content in the feed. The high k_p and very high K for methacrylates results in extremely rapid polymerization by NMP and causes major challenges for controlling the polymerization. This is also a key reason why we attempted to copolymerize styrene with BzMA in the first place: to reduce the polymerization rate and acquire better control. The demonstrated dramatic influence of feed composition on $\langle k_p \rangle \langle K \rangle$ confirmed the polymerization rate of BzMA can be significantly reduced by adding a small amount of styrene. It also suggests the control of methacrylate polymerization can be aided in this manner without significantly affecting the properties of the copolymers compared to the PBzMA homopolymer (i.e. very little styrene was needed to induce control). This is a very important confirmation for

our goal to assess BzMA-rich polymers synthesized via NMP for their LCST-type phase separation behaviour in ionic liquids.

5.3.2 Effect of Initial Feed Composition on Molecular Weight Distribution and Copolymer “Livingness”

One of the distinct features of controlled radical polymerization compared to conventional radical polymerization is the linear increase of molecular weight with conversion, which is similar to that of ionic polymerization polymerization or other truly “living” polymerizations. Number-average molecular weight (M_n) and dispersity (\mathfrak{D}) of each sample taken during copolymerization were analyzed by GPC and the relationship of the measured M_n with conversion was compared to the theoretical values ($M_{n,theo}$) as shown in Figure 5-3 (a). M_n 's measured by GPC were based on poly(styrene) standards. The results were then converted to the corresponding copolymer M_n 's based on the initial feed composition and the Mark-Houwink coefficients described in the *Characterization* section. The assumptions used for this M_n conversion are listed in the following equations:

Equation 5-3

$$F_{BzMA} \approx f_{BzMA,0}$$

Equation 5-4

$$K_{PBzMA-PS} \approx f_{BzMA,0} K_{PBzMA} + (1 - f_{BzMA,0}) K_{PS}$$

Equation 5-5

$$\alpha_{PBzMA-PS} \approx f_{BzMA,0} \alpha_{PBzMA} + (1 - f_{BzMA,0}) \alpha_{PS}$$

Equation 5-6

$$K_{PBzMA-PS} M_{n,PBzMA-PS}^{\alpha_{PBzMA-PS} + 1} = K_{PS} M_{n,PS}^{\alpha_{PS} + 1}$$

where F_{BzMA} is the copolymer composition, $K_{PBzMA-PS}$ and $\alpha_{PBzMA-PS}$ are the average Mark-Houwink coefficients for the copolymers with specific compositions.

Overall, the experimental data resembled the theoretical trend with some minor deviations. Higher M_n at low conversion (< 15%) compared to $M_{n,theo}$ resulted mainly from oligomer wash-out during precipitation and decanting. Oligomers make up a significant portion of the polymer chains at low conversions and they are likely partially soluble in the precipitating solvent. Therefore, the loss of some oligomers led to higher apparent M_n and lower apparent \mathcal{D} at low conversions. However, \mathcal{D} seemed to start high for BzMA-rich mixtures as shown in Figure 5-3 (b). As discussed in the kinetics section, polymerization rates increased exponentially with BzMA content in the feed. The equilibrium between the dormant and propagating species could not be established until a much higher conversion was reached for BzMA-rich mixtures. As a result, the polymerization was less controlled at the early stage for BzMA-rich mixtures which led to higher \mathcal{D} at lower conversions compared to polymerizations that had styrene-rich feeds.

As conversion increased, the percentage of oligomers decreased and the effect of wash-out became insignificant. Meanwhile, the measured M_n 's revealed that they followed more closely to the theoretical line and the \mathcal{D} 's started to level out. At high conversion (> 40%), M_n started to deviate downwards from the $M_{n,theo}$ which is an indication of increasing termination rate. Nevertheless, the \mathcal{D} 's remained quite constant at about 1.2 – 1.4 which was interpreted as still being a well-controlled polymerization.

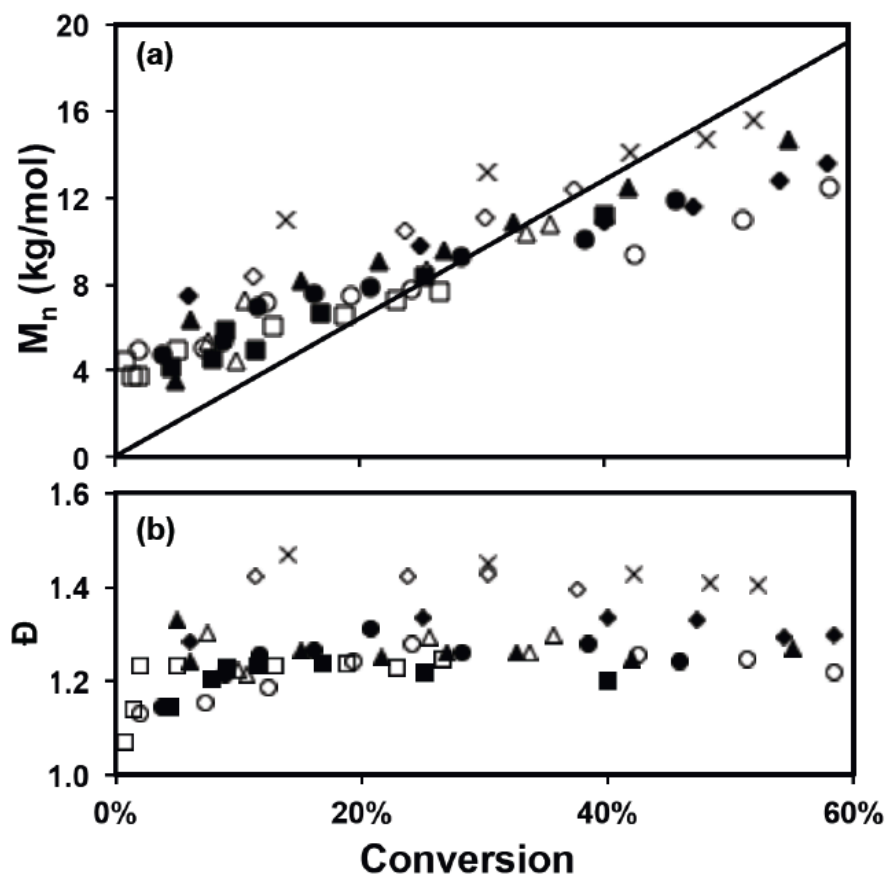


Figure 5-3. (a) Number-average molecular weight, M_n (b) and dispersity, \bar{D} versus conversion for BzMA/styrene copolymerization; $f_{BzMA,0} = 10\%$ (□), $f_{BzMA,0} = 20\%$ (■), $f_{BzMA,0} = 30\%$ (○), $f_{BzMA,0} = 40\%$ (●), $f_{BzMA,0} = 50\%$ (△), $f_{BzMA,0} = 60\%$ (▲), $f_{BzMA,0} = 70\%$ (◇), $f_{BzMA,0} = 80\%$ (◆), $f_{BzMA,0} = 90\%$ (×), straight line in (a) indicates the theoretical trend.

Chain extensions with styrene were performed using selected copolymers as macroinitiators to examine the “livingness” (i.e. ability to cleanly initiate a second batch of monomer) of the copolymers. The chain extensions were conducted using copolymers with $f_{BzMA,0} = 20$ mol%, 80 mol% and 90 mol% (denoted as BS20-fin, BS80-fin and BS90-fin, respectively) as macroinitiators for styrene polymerization at 110 °C for 80 to 110 minutes. The M_n and \bar{D} of the final products were analyzed by GPC and compared to those of the macroinitiators. Details of the experiments are shown in Table 5-5 and the GPC results are illustrated in Figure 5-4. Clear shifts of M_n were observed for both BS20-fin and BS80-fin which implied nearly simultaneous growth

of all chains. However, a slight increase of \bar{D} and downward deviation of M_n from theoretical values for these two copolymers were also observed. It indicates that some chains were terminated during the chain extension which is also illustrated by the tailing of the GPC peaks shown in Figure 5-4 (a) and (b). It should be noted that the BzMA content is not the only difference between the macroinitiators; the “livingness” of the macroinitiators can also be affected by the original monomer conversions during copolymerization. BS20-fin was originally polymerized to a lower monomer conversion during copolymerization than that for BS80-fin which can be deduced from the lower M_n of BS20-fin. The termination rate tends to increase with conversion and thus it was expected that BS80-fin would have more dead chains than BS20-fin. Therefore, the greater deviation of M_n of the chain extended product for BS80-fin compared to BS20-fin is not sufficient evidence for decreased “livingness” due to increased BzMA content, but instead more likely due to the conversion of the macroinitiator.

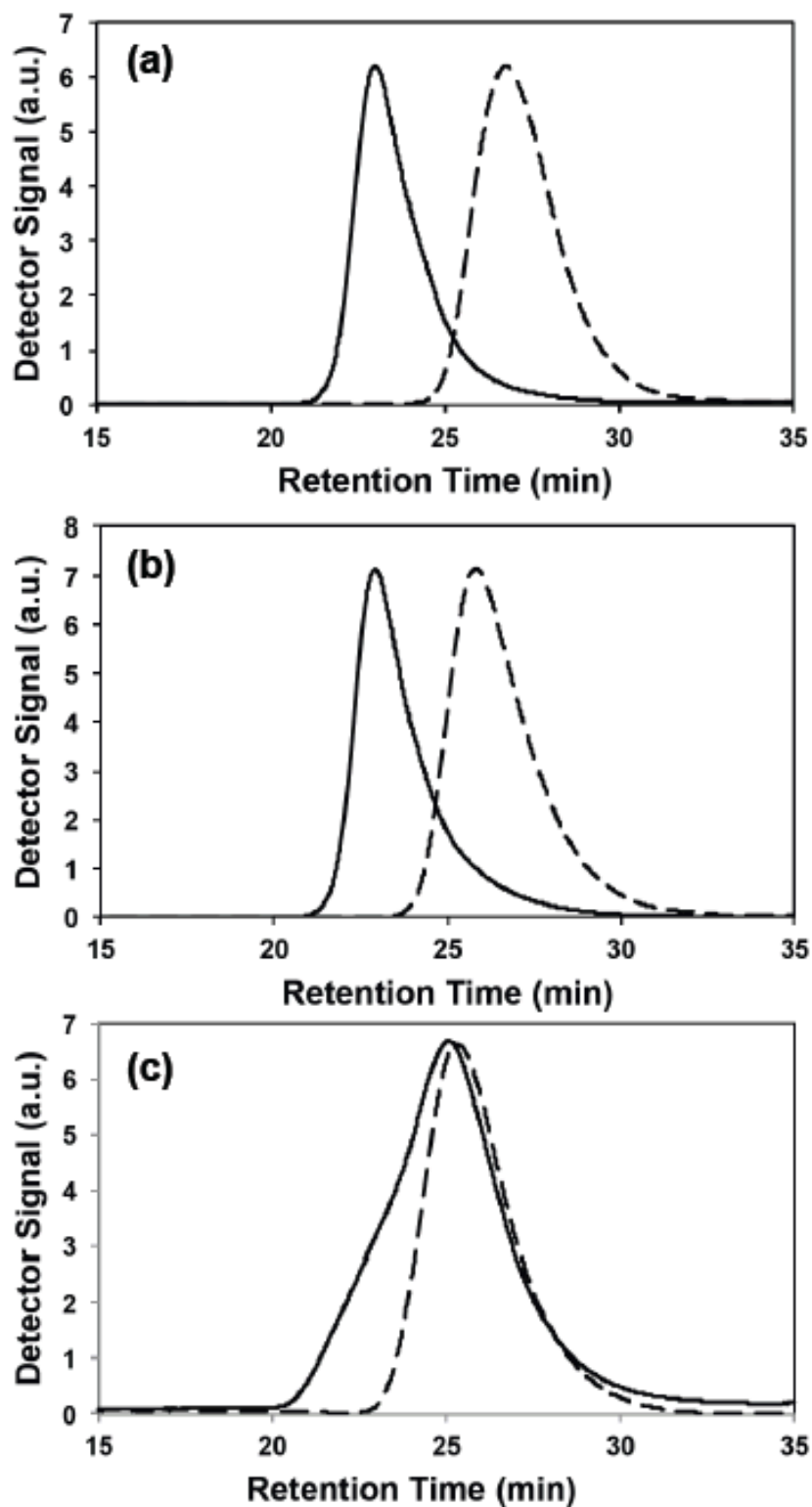


Figure 5-4. Gel permeation chromatograms (GPC) for chain extensions of styrene for BzMA/styrene random copolymers with (a) $f_{BzMA,0} = 20\%$, (b) $f_{BzMA,0} = 80\%$, (c) $f_{BzMA,0} = 90\%$.

However, for BS90-fin, the conversion of the second batch of styrene was a lot lower than the other two copolymers even with about the same reaction time as shown in Table 5-5. M_n of the chain extended product was not significantly higher than that of the macroinitiator while \bar{D} increased considerably. These results imply that only a small portion of the BS90-fin copolymer was able to be reinitiated while most of the BS90-fin copolymers were dead. The low level of livingness was readily seen in the GPC chromatograms where the peak of the chain extended product was broad and mostly overlapped with that of the macroinitiator. The monomer conversion for the initial copolymerization to produce BS90-fin was higher than that for BS80-fin as indicated by the higher M_n of BS90-fin. However, the difference in conversion is not significant enough to cause the dramatic decrease in the “livingness” of the copolymer. Therefore, it was concluded that the increase of BzMA in the copolymer at feed compositions above 80 mol% was the main reason for the decrease in “livingness” of the copolymer. This conclusion can be reaffirmed by the kinetic results where $\langle k_p \rangle \langle K \rangle$ increased dramatically when $f_{BzMA,0} \geq 80$ mol%. The exponential increase of $\langle k_p \rangle \langle K \rangle$ when $f_{BzMA,0} \geq 80$ mol% likely resulted in a much higher propagating radical concentration compared to the dormant species. As a result, the amount of self-termination reactions between the free radicals can increase dramatically.

Table 5-5. Chain Extension with Styrene using Benzyl Methacrylate/Styrene Random Copolymers as Macroinitiator at 110 °C.

Macroinitiator	Macro- initiator M_n $\text{kg}\cdot\text{mol}^{-1}$	Macro- initiator \bar{D}	$m_{\text{initiator}}$ (g)	m_s (g)	Styrene conversion %	$M_{n,\text{theo.}}$ $\text{kg}\cdot\text{mol}^{-1}$	M_n $\text{kg}\cdot\text{mol}^{-1}$	\bar{D}
BS20-fin	8.5	1.23	0.6121	15.67	21	55.3	50.2	1.35
BS80-fin	14.2	1.36	1.0187	15.49	23	63.9	44.6	1.43
BS90-fin	18.7	1.45	1.0552	11.29	5	30.2	20.8	2.06

To maintain control for copolymerization with $f_{BzMA,0} > 80$ mol%, further suppression of reaction rate is necessary. Copolymerization at low temperatures (< 90 °C) has shown positive results for the MMA/styrene system,¹³⁰ which may be a potential solution for BzMA/styrene copolymerization.

5.3.3 Determination of Copolymerization Reactivity Ratios

The compositions with respect to BzMA of BzMA/styrene random copolymers with monomer conversion under 10% (denoted as $F_{BzMA,ini}$) synthesized in bulk at 90 °C were analyzed by ¹H NMR and the results are summarized in Table 5-6. These results were used to determine reactivity ratios of the two monomers by the Mayo-Lewis equation.²²³

Equation 5-7

$$F_1 = \frac{r_1 f_1^2 + f_1 f_2}{r_1 f_1^2 + 2 f_1 f_2 + r_2 f_2^2}$$

The Mayo-Lewis equation relates the copolymer composition F_1 with the initial feed compositions f_1 and f_2 and reactivity ratios r_1 and r_2 . The subscripts “1” and “2” denote the monomer of type 1 (BzMA in this case) and monomer of type 2 (styrene in this case), respectively. Therefore, $f_{BzMA,0}$ and $F_{BzMA,ini}$ listed in Table 5-6 were substituted into the Mayo-Lewis equation as f_1 and F_1 for reactivity ratio determination.

There are various approaches to obtain the reactivity ratios from the Mayo-Lewis equation. Linearization methods such as the Fineman-Ross²²⁴ approach is generally biased since not all data points are weighted equally. The Kelen and Tüdös²²⁵ approach reduces the bias by introducing an adjusting parameter but it still solves the Mayo-Lewis equation indirectly via reduced variables. Non-linear least square fitting using MatLab with 95% confidence bound was

chosen to fit the Mayo-Lewis equation for our data as it should give best estimates without any biasing of the data.²²⁶ The experimental data and the fitting using MatLab are illustrated in Figure 5-5.

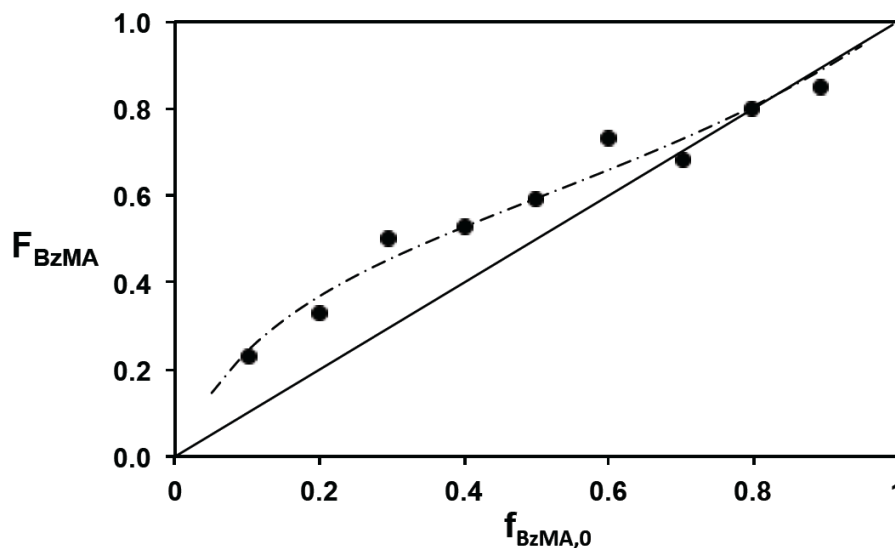


Figure 5-5. Mayo-Lewis plot of copolymer composition with respect to benzyl methacrylate ($F_{BzMA,ini}$) versus monomer feed composition ($f_{BzMA,0}$) using reactivity ratios determined by non-linear least-square fitting of the Mayo-Lewis equation with MatLab. Solid dots are experimental data obtained from random copolymerization of BzMA and styrene in bulk at 90 °C using BlocBuilder and 10 mol% SG1 free nitroxide relative to BlocBuilder. See Table 5-2 for additional characteristics of each of the copolymers.

We found two sets of reactivity ratios for copolymerization of BzMA and styrene in the literature which were both determined from conventional free radical copolymerization using azobisisobutyronitrile (AIBN) as initiator at 60 °C in bulk. The reactivity ratios of styrene and methacrylates are generally about the same and it was expected that r_{BzMA} would be slightly higher than $r_{styrene}$.^{227,228} Table 5-7 summarizes the reactivity ratios we obtained as well as the ones reported for conventional free radical copolymerization.

Table 5-6. Initial Feed Compositions and Compositions of Benzyl Methacrylate/Styrene Copolymers.

$f_{\text{BzMA},0}$	$F_{\text{BzMA},\text{ini}}^{\text{a}}$
mol%	mol%
10	23
20	33
29	50
40	53
50	59
60	73
70	68
80	80
89	85

^a BzMA molar composition in copolymer under 10% conversion ($F_{\text{BzMA},\text{ini}}$) synthesized in bulk at 90 °C determined by ¹H NMR

Table 5-7. Monomer Reactivity Ratios for Benzyl Methacrylate (r_1) and Styrene (r_2)

Initiator/Solvent/Temperature	r_1	r_2	Reference
BlocBuilder/bulk/90°C	0.86 ± 0.36	0.27 ± 0.14	This work
AIBN/bulk/60°C	0.51	0.45	220
AIBN/bulk/60°C	0.53	0.34	221

Uncertainties of the ratios are relatively large due to only nine points being used for the fitting. The difference between our estimates of r_{BzMA} and r_{styrene} is greater than the ones reported. It should be noted that the earlier studies determined the ratios using conventional free radical polymerization at 60 °C whereas we used CRP techniques at 90 °C. In NMP, the polymer chains were reversibly terminated by the nitroxide and therefore, the interaction between the propagating radicals and the nitroxide may play an important role with regard to the relative reactivities. Different chain-end structures have a strong influence on the dissociation energies of the dormant species.²²⁹ The favoured compositions in free radical polymerization may be suppressed by the high dissociation energy of the alkoxyamine chain end in NMP. Nevertheless,

the ratios obtained in the AIBN initiated systems were included in the ranges we determined, and in all cases, both of the reactivity ratios are less than unity and r_{BzMA} is greater than $r_{styrene}$.

5.4 Conclusion

In this study, BzMA and styrene were copolymerized in bulk at various compositions at 90 °C by NMP with about 10% free SG1 relative to the unimolecular BlocBuilder initiator. It was demonstrated that feed composition has a strong influence on $\langle k_p \rangle \langle K \rangle$ which confirmed the polymerization rate of BzMA can be significantly reduced by adding a small amount of styrene. The chain growth during copolymerization followed the theoretical trend expected for controlled radical polymerization and copolymers retained narrow molecular weight distributions ($\mathcal{D} = 1.1 - 1.5$) up to 90 mol% BzMA in the feed. The copolymers were clearly “living” with up to 80 mol% BzMA in the feed according to the GPC results obtained from chain extensions of styrene. However, a large portion of dead chains that could not be re-initiated were observed for copolymer macroinitiator with 90 mol% BzMA. We conclude that the dramatic increase of $\langle k_p \rangle \langle K \rangle$ after $f_{BzMA,0} = 80$ mol% likely resulted in a much higher propagating radical concentration compared to the dormant species. Therefore, the amount of self-termination reactions between the free radicals can increase significantly which leads to the decreased “livingness”. The reactivity ratios determined were similar to those reported for conventional free radical copolymerization with small deviations which may be due to the suppression of termination caused by the nitroxide.

To conclude, the SG1 nitroxide is effective in controlling the random copolymerization of styrene and BzMA even with high BzMA content. The control of BzMA polymerization via

NMP can be aided by adding as little as 10 mol% styrene without significantly affecting the properties of the copolymers compared to the PBzMA homopolymer. This is a very important confirmation that BzMA-rich polymers can be synthesized via NMP and can be further tested as thermosensitive materials with LCST-type phase separation behaviour in ionic liquids.

Acknowledgements

The authors are very grateful for the support of the following funding sources: NSERC Discovery, Canada Foundation for Innovation New Opportunities Fund and the McGill Summer Undergraduate Research Experience (SURE) program.

References

Please refer to the global bibliography at the end of the thesis.

Chapter 6

Benzyl Methacrylate-rich Copolymers synthesized by NMP that are Fluorescent and Thermo-responsive in an Ionic Liquid

6.1 Preface

This chapter presents a manuscript published in *Journal of Polymer Science, Part A: Polymer Chemistry*, **2013** (51): 4702 – 4715. In Chapter 5, controlled synthesis of benzyl methacrylate (BzMA)-rich copolymers via nitroxide mediated polymerization (NMP) was demonstrated when styrene was used as a controlling co-monomer. However, about 20 mol% of styrene was necessary in the feed to attain the “livingness” (ability to continue to extend chains in the presence of monomer) of the BzMA/styrene copolymer. The large amount of styrene needed was not desirable because the high content of solvophobic styrene can easily render the copolymers insoluble in ionic liquid (IL) solutions.

In search of an alternative controlling co-monomer, 9-(4-vinylbenzyl)-9H-carbazole (VBK), a styrenic-based monomer with a carbazole group, was found to be effective in controlling various methacrylate-rich feeds by NMP with as little as 1 - 2 mol% in the feed.^{48,50,146} Moreover, the carbazole-containing VBK also exhibits hole-transport and fluorescent properties. Copolymerizations of BzMA with VBK not only verified if VBK is an effective controlling co-monomer for BzMA-rich feeds, but also provided copolymers useful for studying the effects of electron-donating carbazole groups on phase transitions in IL solutions.

The copolymerizations of BzMA and VBK (2 – 11 mol% VBK in the feed) via NMP was first addressed in the manuscript, followed by characterizations of BzMA/VBK copolymers in IL

solutions. The effectiveness of VBK as a controlling co-monomer was confirmed by dramatic decrease in the values of product of average propagation rate constant and equilibrium constant, $\langle k_p \rangle \langle K \rangle$, compared to those of BzMA/styrene copolymerizations, along with linear increases in molecular weight versus conversion, relatively narrow molecular weight distribution ($\overline{M}_w/\overline{M}_n = 1.34 - 1.42$), and successful chain extensions with a fresh batch of monomers (90 mol% methyl methacrylate and 10 mol% styrene) using the BzMA/VBK macroinitiator synthesized with as little as 2 mol% VBK in the feed. The solubility and LCST of the BzMA/VBK copolymers in IL solutions decreased as VBK content increased, as expected due to the solvophobic nature of VBK. Moreover, the phase separation of the copolymers was found to be totally irreversible. Regarding fluorescence properties, the BzMA/VBK copolymers were not only fluorescent due to the carbazole groups of VBK units, BzMA and VBK were also found to be a pair of fluorescent resonance energy transfer (FRET) donor and acceptor, resulting in 5-fold fluorescence enhancement during phase separation due to the heightened FRET efficiency between BzMA and VBK in close proximity in their collapsed state. The temperature sensitive fluorescence response of these copolymers can be useful for a number of applications but the use is limited by the irreversible nature of the responses. Attempts in restoring reversibility for polymers containing BzMA and VBK are the focus of Chapter 7.

Fluorescent, Thermo-responsive Copolymers Via Nitroxide Mediated Polymerization: Synthesis and Effect of Fluorescent Groups on Phase Transitions in an Ionic Liquid

Chi Zhang, Milan Maric*

Department of Chemical Engineering, McGill University,
3610 University Street, Montreal, QC, Canada H3A 2B2

Journal of Polymer Science, Part A: Polymer Chemistry, **2013** (51):4702 – 4715

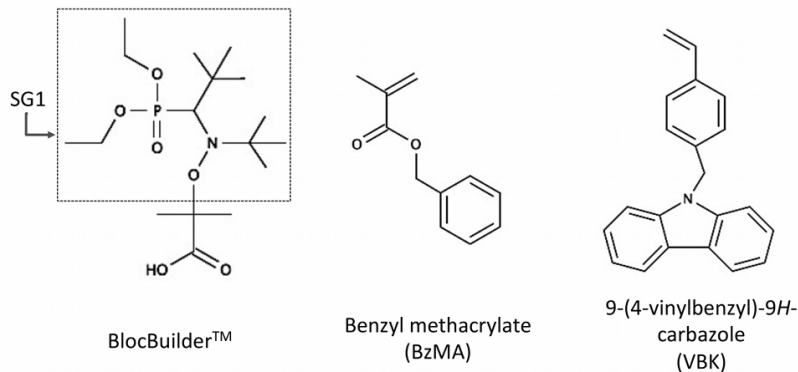
Abstract

Synthesis of poly(benzyl methacrylate) (PBzMA) by nitroxide mediated polymerization with a small fraction of fluorescent, controlling co-monomer, 9-(4-vinylbenzyl)-9*H*-carbazole (VBK, 2-11 mol% in the feed), was studied along with the resulting copolymers' LCST phase behaviour in the ionic liquid (IL) 1-ethyl-3-methylimidazolium bis(trifluoromethane sulfone)imide. The effectiveness of VBK as a controlling co-monomer was demonstrated by a dramatic decrease in the product of average propagation rate constant and average equilibrium constant, $\langle k_p \rangle \langle K \rangle$, compared to BzMA polymerizations with styrene as co-monomer. Linear molecular weight increase with conversion (up to ~ 40% conversion), with polydispersities of about 1.34 - 1.42, and successful chain extensions indicated the copolymerizations were relatively well controlled. The incorporation of fluorescent and solvatophobic VBK units in the BzMA/VBK copolymers not only affected transition temperature and reversibility of the LCST-type phase separation in the IL, but also led to about a 5-fold phase separation-triggered fluorescent enhancements, likely due to enhanced fluorescence resonance energy transfer from BzMA to VBK being in close proximity during aggregation.

6.2 Introduction

Ionic liquids (ILs) are organic salts that are liquid at ambient conditions. Their unique properties such as excellent thermal and chemical stability, high ionic conductivity, compatibility with a wide range of polymeric materials, non-volatility and non-flammability make them excellent candidates as alternatives to conventional organic solvents in chemical synthesis and separation processes^{39,218} or as electrolytes for various electrochemical devices,^{20,21,230} such as dye-sensitized solar cells,^{22,231} and to eliminate the leakage and flammability problems of organic solvent-based electrolytes.²³ Consequently, ionic liquid composites with organic polymers and copolymers (i.e. ionic gels) have been intensely studied by many researchers.^{62,232-235}

In this study, we examined polymers that were fluorescent and thermo-responsive in ionic liquids. More specifically, we focused on the synthesis of statistical copolymers of benzyl methacrylate (BzMA) and 9-(4-vinylbenzyl)-9*H*-carbazole (VBK) (BzMA and VBK structures shown in Scheme 6-1) via nitroxide mediated polymerization (NMP) and the characterization of their phase behaviour as well as fluorescent responses in a hydrophobic ionic liquid, 1-ethyl-3-methylimidazolium bis(trifluoromethane sulfone)imide ([C₂mim][NTf₂]). Carbazole functional ILs have been targeted for application in dye-sensitized solar cells²³⁶ and the photoconductive properties of carbazoles and similar electron-donors like thiophene²³⁷ have been considered for electrochemical/optical applications. Our study attempts to examine the interactions of thermoresponsive carbazole functional copolymers in ILs that could ultimately produce ionic gels of interest for sensor/actuator applications. We are not aware of any studies that have focused on the phase behaviour of carbazole functional (co)polymers in ILs.



Scheme 6-1. Molecular structure of BlocBuilder™, SG1, benzyl methacrylate and 9-(4-vinylbenzyl)-9H-carbazole.

Poly(BzMA) exhibits LCST-type phase separation in hydrophobic ILs.^{61,212} So far, there have been very few reports discussing the phase behaviour of statistical copolymers in ILs. Ueki et al. showed that the incorporation of a solvophilic or solvophobic co-monomer in a random copolymer of BzMA can increase or decrease the LCST in $[\text{C}_2\text{mim}][\text{NTf}_2]$, respectively.²¹² Similar approaches have been used to tune the transition temperature of thermo-responsive polymers in aqueous solutions.^{149,155} The phase behaviour of polymers in ILs was found to be highly sensitive to small changes in the molecular structure of the polymer.²³⁸ The effect of varying copolymer composition on the phase behaviour of the statistical copolymers is however not well known.

Using commercially available initiators such as BlocBuilder[®], NMP has not been as successful in controlling homopolymerization of methacrylates as some other controlled radical polymerization (CRP) techniques mainly due to the high equilibrium constants of methacrylates^{104,130} that consequently led to a high concentration of active radicals favouring irreversible chain self-termination.¹⁰⁴ However, well-defined methacrylate-rich statistical copolymers can be synthesized via NMP when aided with a small amount of controlling co-

monomer.^{50,104,142,143,145,146,149} In comparison to other CRP techniques where additives such as metallic ligands (eg. atom transfer radical polymerization (ATRP)) or sulfur-based chain transfer agents (eg. reversible addition fragmentation transfer polymerization (RAFT)) are required and often need to be removed from the polymer to avoid contamination, NMP employs no additives besides the initiator and thus polymer purification procedures are simple, often involving a single precipitation step. Therefore, NMP can be advantageous when multiple purification steps are not desirable.¹²²⁻³⁰

Recently, VBK was demonstrated as an effective controlling co-monomer for several methacrylate-rich copolymerizations^{48,50,146} via NMP with as little as 1- 2 mol% VBK present in the initial mixture. In addition to controlling highly methacrylate-rich copolymerizations via NMP, the use of the carbazole-containing VBK can also serve as a fluorescent tag for the statistical copolymers as poly(BzMA) phase separates from the IL. The combination of high ionic conductivity of ionic liquids, thermo-sensitivity of poly(BzMA) and fluorescent properties of the carbazole can be very intriguing as these composite materials can be useful for sensing^{239,240} or switching devices.²⁴¹

In this article, the synthesis of BzMA/VBK statistical copolymerizations using BlocBuilder™ (structure shown in Scheme 6-1) as the unimolecular initiator aided with 10% excess free SG1 nitroxide (structure shown in Scheme 6-1) will be first examined in detail. Diblock copolymers with a thermoresponsive block and a solvatophilic block were also synthesized by chain extending selected statistical copolymers as the macroinitiators with a solvatophilic MMA-rich block. The phase behaviour of the synthesized statistical and block copolymers in [C₂mim][NTf₂], including the effects of copolymer composition and heating rates on LCST and reversibility, was then fully addressed. Lastly, an interesting phase separation-triggered

fluorescence enhancement phenomenon due to the presence of the carbazole units will be presented and the possible mechanism for this behaviour will be discussed.

6.3 Results and discussions

6.3.1 Effects of feed composition on polymerization kinetics and control

Firstly, the effectiveness of 9-(4-vinylbenzyl)-9*H*-carbazole (VBK) as a controlling co-monomer for benzyl methacrylate (BzMA)-rich feeds and the effects of feed composition on polymerization kinetics and level of control were examined. Some key results such as conversion, copolymer composition, molecular weight and molecular weight distribution are summarized in Table 6-1.

It is known that controlled homopolymerization of methacrylates via NMP is challenging mainly because of the relatively high equilibrium constant K (defined by Equation 6-1 for a SG1-mediated system where $[P\bullet]$ is concentration of propagating radicals, $[SG1]$ is free SG1 concentration and $[P-SG1]$ is concentration of the dormant species) of methacrylates leading to high concentration of propagating radicals and hence favouring irreversible self-termination.¹⁰⁴

Equation 6-1

$$K = \frac{[P\bullet][SG1\bullet]}{[P-SG1]}$$

Table 6-1. Summary of polymerizations and molecular properties for the statistical copolymerizations benzyl methacrylate (BzMA or methyl methacrylate (MMA)) with 9-(4-vinylbenzyl)-9H-carbazole (VBK) via nitroxide mediated polymerization with BlocBuilder.

Expt. ID ^a	Polym. Time	Conversion ^b	$f_{\text{VBK},0}^c$	F_{VBK}^c	$M_{n,\text{target}}$	M_n^d	\mathcal{D}^d
	min		mol%	mol%	kg mol ⁻¹	kg mol ⁻¹	
B/V-2	120	38%	2%	2%	29.9	17.7	1.42
B/V-5	121	29%	5%	4%	30.0	9.9	1.42
B/V-8	210	26%	8%	9%	29.8	6.7	1.39
B/V-11	360	34%	11%	13%	30.1	12.2	1.35
M/V-5	90	39%	5%	11%	20.1	7.8	1.23
PBzMA	< 5	N/A	0%	0%	20.1	18.0	2.04

^a The experiment ID B/V-X or M/V-X denotes the monomers used in the copolymerization (B for BzMA, M for MMA and V for VBK) and X represents the feed composition of VBK in mol%; ^b Final conversion determined by ¹H NMR; ^c Initial feed composition and final copolymer composition relative to VBK measured by ¹H NMR; ^d Number average molecular weight and dispersity \mathcal{D} of the copolymer measured by GPC relative to poly(methyl methacrylate) standards.

The introduction of a low concentration of controlling co-monomer, which has a lower propagation rate constant k_p and more importantly, a lower K compared to a methacrylate, can dramatically decrease the average equilibrium constant $\langle K \rangle$ and the product of average propagation rate constant $\langle k_p \rangle$ and $\langle K \rangle$. The $\langle k_p \rangle \langle K \rangle$ is often used as a measure of the kinetics and control of the NMP system. The $\langle k_p \rangle \langle K \rangle$ values can be estimated by multiplying the slopes of the semi-logarithmic kinetic plots ($\langle k_p \rangle [P.]$) by the initial feed concentration ratio of SG1 and BlocBuilder ($r = [\text{SG1}]_0 / [\text{BlocBuilder}]_0$, see Equation 6-2). This copolymerization approach has been effective in controlling various methacrylate-rich copolymerizations via NMP,^{47,50,104,142,143,145} yielding methacrylate-rich copolymers with narrow molecular weight distribution that were capable to be re-initiated to form block copolymers.

Equation 6-2

$$\langle k_p \rangle \langle K \rangle \approx \langle k_p \rangle \frac{[P\bullet][\text{SG1}]_0}{[\text{BlocBuilder}]_0} = \langle k_p \rangle [P\bullet]r$$

VBK has been previously shown to be an effective controlling co-monomer for various methacrylates by NMP,^{48,50,146} yielding linear kinetic plots over a substantial conversion range and linear increase in molecular weight versus conversion with as little as 1 to 2 mol% VBK in the feed. In this study, 2 to 11 mol % of VBK was used in the feed with benzyl methacrylate (BzMA) to examine the effectiveness of VBK as a controlling co-monomer for this system.

To evaluate the copolymerization kinetics, the values of $\langle k_p \rangle \langle K \rangle$ for the BzMA/VBK copolymerizations were estimated using the slopes of the kinetic plots in the linear regions (Figure D-2 in Appendix D) and compared with those calculated using a terminal model for SG1-mediated MMA/styrene¹⁰⁴ and MMA/VBK¹⁴⁷ copolymerizations at the same temperature (Figure 6-1). Figure 6-1 illustrates the substantial decrease in $\langle k_p \rangle \langle K \rangle$ with increasing amount of VBK in the feed, which was consistent with other methacrylate-rich copolymerizations using NMP.^{47,104,142,143,146} When comparing the BzMA/VBK with the BzMA/styrene system, the value of $\langle k_p \rangle \langle K \rangle$ with 11 mol% VBK in the feed ($1.98 \times 10^{-6} \text{ s}^{-1}$) is 2 orders of magnitude lower than that with 11 mol% styrene in the feed ($2.09 \times 10^{-4} \text{ s}^{-1}$)¹⁴² at the same temperature with the same initiator. More importantly, the nitroxide-mediated BzMA/VBK copolymerization was relatively well controlled with as little as 2 mol% VBK, in contrast of at least 10 mol% styrene needed to control BzMA/styrene copolymerizations at similar conditions. Thus, incorporation of VBK is useful, particularly if the study of copolymers with low VBK composition is desirable for properties that are highly sensitive to copolymer composition.

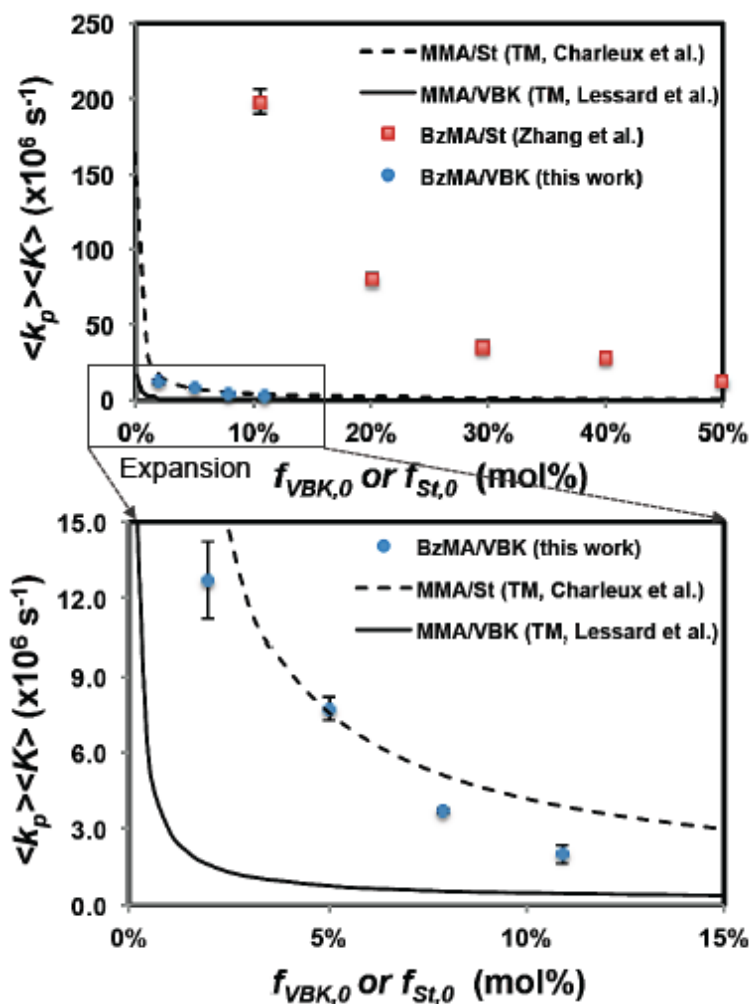


Figure 6-1. Product of average propagation rate constant $\langle k_p \rangle$ and average equilibrium constant $\langle K \rangle$ for copolymerization of benzyl methacrylate (BzMA) with 9-(4-vinylbenzyl)-9*H*-carbazole (VBK) at 90 °C calculated using the slopes of the kinetic plots in their linear regions in this work (blue circles) compared with the reported $\langle k_p \rangle \langle K \rangle$ values for the copolymerization of BzMA with styrene¹⁴² (red squares), calculated $\langle k_p \rangle \langle K \rangle$ values using a terminal model (TM) for copolymerization of methyl methacrylate with styrene¹⁰⁴ (dashed line) and VBK¹⁴⁷ (solid line) versus initial feed composition of VBK or styrene; the error bars represent standard deviation from the slope calculation.

It was also apparent from Figure 6-1 that the nitroxide mediated BzMA/VBK copolymerization behaved more similarly to the MMA/styrene system than that of the MMA/VBK system. We

suspected the main difference between BzMA/VBK system and the other methacrylate/VBK copolymerization systems lied in the reactivity ratios of the two co-monomers.

Recently, for MMA/VBK copolymerizations by NMP, it was shown that the more favourable addition of VBK monomers to the propagating chains compared to MMA monomers ($r_{\text{VBK}} = 2.7$, $r_{\text{MMA}} = 0.24$ ¹⁴⁶) played a major role in the high effectiveness of VBK in controlling MMA polymerization via NMP.¹⁴⁷ It was claimed that the increased concentration of VBK on the terminal unit of propagating chains led to lower $\langle K \rangle$; hence a high level of control can be achieved with minimal amount of VBK at moderate conversions.¹⁴⁷ Although reactivity ratios were not calculated for the DMAEMA/VBK⁴⁸ or OEGMA/VBK⁵⁰ copolymerizations, the preferential addition of VBK during propagation was still apparent when comparing the copolymer compositions with the initial feed compositions. The copolymers formed were comparatively richer in VBK compared to the composition of the initial mixture; for example, for copolymerizations of OEGMA/VBK⁵⁰ with 5 and 10 mol% VBK in the feed, the VBK contents in the copolymers were reported to be 9 and 27 mol%, respectively. However, for the BzMA/VBK copolymerizations, at similar conversions to the other studies, the copolymer compositions were very similar to the feed composition, like the widely studied MMA/styrene copolymerization²²¹ (see Table 6-1). This suggests that the proportion of methacrylate-terminated chains was likely higher during copolymerizations of BzMA with VBK than the other methacrylate/VBK systems, resulting in higher $\langle K \rangle$ and higher probability of irreversible chain termination.

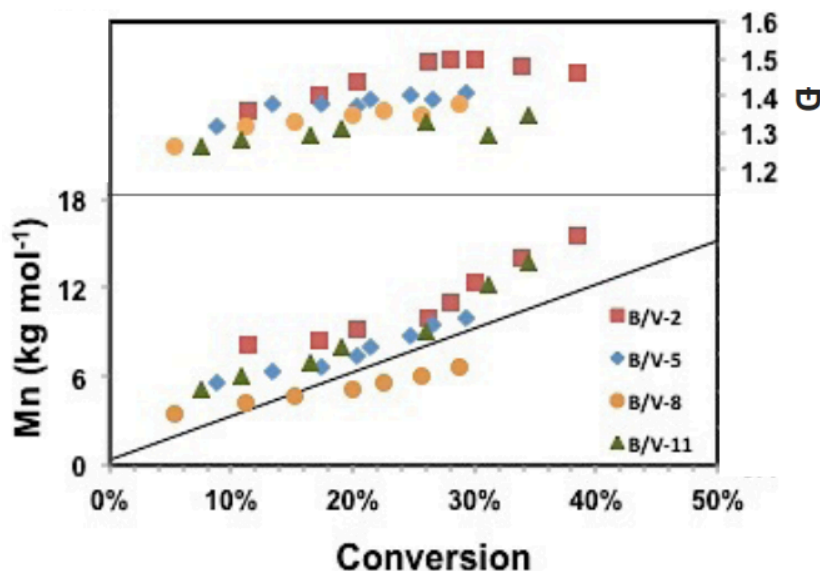


Figure 6-2. Number-average molecular weight (M_n) and dispersity (\bar{D}) of statistical copolymers of benzyl methacrylate (BzMA) and 9-(4-vinylbenzyl)-9H-carbazole (VBK) measured by GPC calibrated with poly(methyl methacrylate) standards (symbols: B/V-2: red squares, B/V-5: blue diamonds, B/V-8: orange circles, B/V-11: green triangles).

Linear increase in molecular weight with conversion and narrow molecular weight distribution are features typically associated with a controlled polymerization. As shown in Figure 6-2, M_n of BzMA/VBK copolymers increased fairly linearly with conversion, closely following the theoretical prediction. M_n drifting upwards was observed in some cases after 30% conversion, which could be a result from the reduction of living chains through mostly bimolecular self-termination. The existence of non-living chains was also observed in the chain extension experiments, which will be discussed in the next section. One may note that all reported M_n s in this report were relative to poly(methyl methacrylate) (PMMA) standards but the possible difference between the reported values and actual M_n of BzMA/VBK copolymers was also considered. The sample M_n s shown in Figure 6-2 were compared to those calculated using universal calibration with Mark-Houwink coefficients for PMMA, PBzMA and PVBK in THF ($K_{\text{PMMA}} = 1.04 \times 10^{-4} \text{ dL g}^{-1}$, $\alpha_{\text{PMMA}} = 0.700$;²⁴² $K_{\text{PBzMA}} = 1.08 \times 10^{-4} \text{ dL g}^{-1}$, $\alpha_{\text{PBzMA}} = 0.635$;²¹⁶ $K_{\text{PVBK}} = 3.2 \times 10^{-5} \text{ dL g}^{-1}$, $\alpha_{\text{PVBK}} = 0.716$ ²⁴³) and the differences were all within 10%. Therefore,

the molecular weight results relative to PMMA standards were concluded to be plausible representations of the actual molecular weight. Molecular weight distribution (or dispersity \bar{D}) was in the range of about 1.4 to 1.5 for the raw copolymers and about 1.3 to 1.4 for purified copolymers.

Overall, the kinetic results and linear increase in M_n with conversion in the range studied demonstrated that the BzMA/VBK copolymerizations were relatively well controlled in that regime with as little as 2 mol% VBK in the feed using BlocBuilderTM as the initiator at 90 °C. Another important feature of controlled polymerization, the ability of the copolymers to be re-initiated and chain-extended to form block copolymers, was also examined.

6.3.2 Chain extension of BzMA/VBK statistical copolymers

Selected statistical copolymers of BzMA/VBK (B/V-5 and B/V-8) were chain extended with a mixture of methyl methacrylate (MMA) and styrene (10 mol% styrene) to examine the “livingness” of these copolymers. The addition of an MMA-rich second block was chosen to obtain diblock copolymers with a thermo-responsive block (BzMA/VBK) and a solvophobic block (MMA/styrene) in the IL. The phase behaviour of these block copolymers in the IL will be discussed in detail later. Some key properties (composition, M_n and \bar{D}) of the macroinitiators and chain-extended block copolymers were summarized in Table 6-2.

Table 6-2. Composition and molecular weight characterizations of the macroinitiators and chain extended block copolymers.

Macroinitiator properties				Block copolymer properties			
Macroinitiator	$F_{\text{VBK}}^{\text{a}}$	M_n^{b}	\bar{D}^{b}	Block copolymer	$F_{\text{BzMA}}/F_{\text{MMA}}^{\text{c}}$	M_n^{b}	\bar{D}^{b}
	mol%	kg mol ⁻¹				kg mol ⁻¹	
B/V-5	4%	9.9	1.42	B/V5-M/S10	0.64/0.36	15.1	1.47
B/V-8	9%	6.7	1.39	B/V8-M/S10	0.61/0.39	14.4	1.56

^a Copolymer composition of VBK of the macroinitiators measured by ¹H NMR; ^b Number average molecular weight and dispersity \bar{D} measured by GPC relative to poly(methyl methacrylate) standards; ^c Molar fractions of benzyl methacrylate relative to that of methyl methacrylate in the block copolymers measured by ¹H NMR, compositions of VBK and styrene were not obtained due to overlapping peaks from their aromatic groups.

After the chain extensions, molecular weight increased in all cases as shown in Table 6-2. Broadening of molecular weight distribution after chain extension was observed, indicating existence of dead chains in the macroinitiator and/or occurrence of termination reactions during the chain extensions. Fractionation was performed for all the block copolymers but the dispersity of the block copolymers was not significantly lower after the fractionation. Nonetheless, the increase in dispersity was relatively minor (from $\bar{D} = 1.42$ to 1.47 for B/V5-M/S10) to moderate (from $\bar{D} = 1.39$ to 1.56 for B/V8-M/S10). The composition of the block copolymers showed evident incorporation of MMA.

The chain extensions are best illustrated by GPC chromatograms. When comparing the GPC traces of the macroinitiators and the chain-extended polymers, as shown in Figure 6-3, one can observe that the chromatograms of both chain-extended block copolymers remained fairly monomodal and shifted to the lower elution volumes compared to their macroinitiator, indicating most chains were able to be re-initiated and grew simultaneously. Small shoulders in the GPC traces after chain extension implied existence of some dead macroinitiator chains. The small shoulders in their GPC traces remained after fractionation was conducted, which indicated the

dead chains and chain-extended species had molecular weights that were too similar to separate easily. Nonetheless, the selected BzMA/VBK copolymers with up to 95 mol% BzMA in the copolymer showed their ability to be re-initiated to form block copolymers in good yield, which was a significant improvement compared to the BzMA/styrene copolymers synthesized in similar conditions where only copolymers with up to 80 mol% BzMA were shown to be able to add a second block in appreciable yield.¹⁴²

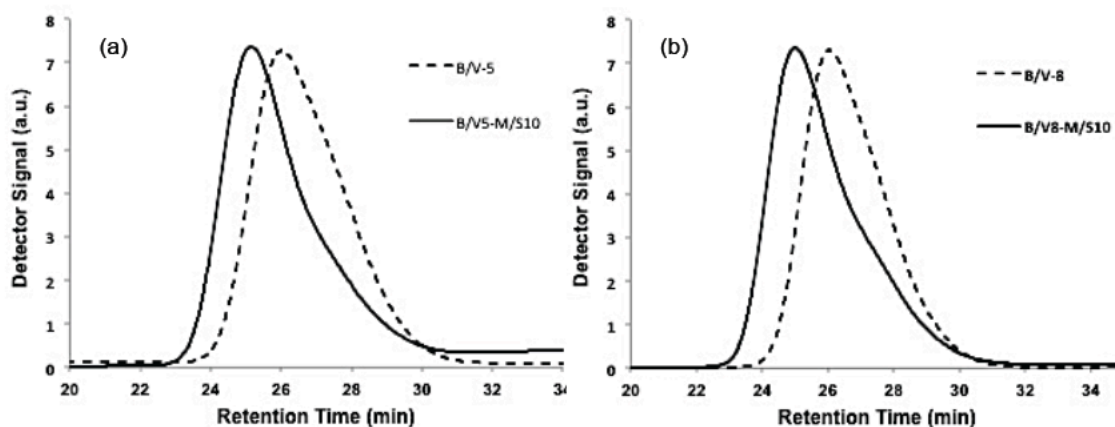


Figure 6-3. GPC traces of corresponding macroinitiators (dashed lines) and chain extended block copolymers (solid lines) for (a) macroinitiator B/V-5 and block copolymer B/V5-M/S10 and (b) macroinitiator B/V-8 and block copolymer B/V8-M/S10; chromatograms of the chain-extended block copolymers showed no significant changes after fractionation.

6.3.3 Temperature sensitivity and fluorescence properties of statistical copolymers in [C₂mim][NTf₂]

It is known that PBzMA exhibits LCST-type phase separation in 1-alkyl-3-methylimidazolium bis(trifluoromethane sulfonyl)imide ionic liquids ([C_nmim][NTf₂]).^{212,238} More specifically, in [C₂mim][NTf₂], PBzMA ($M_n = 28 \text{ kg mol}^{-1}$, concentration = 3wt%) was found to have a cloud point temperature (CPT) of 105 °C.²¹²

Incorporation of hydrophilic or hydrophobic co-monomers in a thermoresponsive polymer is a widely known method to manipulate the transition temperature in aqueous solutions.^{47,50,149} Likewise, the phase separation temperature of polymers in ionic liquids (ILs) can be controlled by copolymerization with solvatophilic or solvatophobic co-monomers.²¹² PVBK was found to be insoluble in [C₂mim][NTf₂]. Therefore, the solubility of the BzMA/VBK copolymers in [C₂mim][NTf₂] was expected to decrease as VBK content increased and hence phase separation should occur at a lower temperature. PVBK is also fluorescent and can serve as a tag for imaging or sensing applications for the BzMA/VBK copolymers, in addition to tuning the transition temperature.^{48,50} Both the thermo-sensitivity and fluorescence properties of the statistical copolymers are discussed in detail in the following section.

Table 6-3. Glass transition temperature (T_g) determined by differential scanning calorimetry (DSC) and cloud point temperature (CPT) of the statistical copolymers in [C₂mim][NTf₂] (3 wt%) measured by UV-Vis spectrometry at two different heating rates.

Polymer ID ^a	F _{VBK}	M _n	T _g	CPT at different heating rates (°C)	
	mol%	kg mol ⁻¹	°C	0.1 °C min ⁻¹	1 °C min ⁻¹
B/V-2	2%	17.7	60	N/A ^b	>99 ^c
B/V-5	4%	9.9	62	86	86
B/V-8	9%	6.7	66	65	68
B/V-11	13%	12.2	74	Insoluble	Insoluble

^a Refer to Table D-1 in Appendix D for synthesis conditions for these copolymers; ^b Not measured; ^c Solution remained transparent up to 99 °C, which was the upper temperature limit of the instrument.

6.3.3.1 Effect of copolymer composition on LCST of the statistical copolymers

Table 6-3 lists all the CPTs measured for the BzMA/VBK copolymers in [C₂mim][NTf₂] at 3 wt% concentration. Among the copolymers, B/V-2 (F_{VBK} = 2 mol%) remained soluble in [C₂mim][NTf₂] up to 99 °C, which was the upper temperature limit of the instrument. Since

PBzMA has a CPT of 105 °C, the CPT of B/V-2 should be in the range of 99 – 105 °C. As VBK content increased in the copolymer, the CPT of the copolymer decreased steeply, indicating reduced solubility. The copolymer CPT decreased by at least 14 °C when F_{VBK} increased from 2 to 4 mol%; about 18 °C when F_{VBK} increased from 4 to 9 mol%; and for B/V-11 ($F_{\text{VBK}} = 13$ mol%), the copolymer was not soluble in the ionic liquid at room temperature. Although the phase separation temperature in ILs was reported to be sensitive to molecular weight for various homopolymers,^{63,64,244} the copolymer composition was considered the dominant factor affecting the transition temperature because the range in molecular weight (ranged from 6.7 to 17.7 kg mol⁻¹) of the BzMA/VBK copolymers studied was fairly limited. A similar conclusion was drawn by Ueki et al.²¹² for BzMA/styrene and BzMA/MMA copolymers, who studied copolymers in the molecular weight range between 13 to 28 kg mol⁻¹.

Similar to PNIPAm in aqueous solutions, the occurrence of LCST-type phase separation in ILs is strongly dependent on the solvophilic and solvophobic balance of the polymer in the solution. It is known that poly(methyl methacrylate) is totally soluble in [C₂mim][NTf₂], whereas poly(styrene) is totally insoluble.²³⁴ Thus, in [C₂mim][NTf₂], the ester groups of PBzMA functions as the solvophilic part and the benzyl group acts as the solvophobic part.²³⁸ In order to solvate PBzMA in [C₂mim][NTf₂], the cation and anion of the ILs position themselves around the benzyl group, resulting in an exothermic ($\Delta H_{\text{mix}} < 0$) process with a negative entropy change (ΔS_{mix}). LCST-type phase separation occurs when the entropy contribution ($\Delta S_{\text{mix}}T$) exceeds ΔH_{mix} . This is analogous to the formation of a layer of clathrate-like structures near the *iso*-propyl groups of PNIPAm in aqueous solutions below the LCST.¹⁸³ However, in contrast to the water-water hydrogen bonding of the water layer facilitating solvation of PNIPAm, the interactions between ILs and PBzMA are mainly relatively weak cation- π interactions and van

der Waals forces.⁶¹ This is reflected in the much smaller magnitudes of the enthalpy and entropy of demixing during phase separation in ionic liquids, as measured by Ueki et al.,⁶¹ compared to those in aqueous solutions. Therefore, the incorporation of a small amount of solvatophobic comonomer can lead to large changes in phase separation temperature or even render the copolymer insoluble.

6.3.3.2 Effects of incorporation of VBK on reversibility of the LCST

Reversibility is an important aspect to examine for any stimuli-responsive polymer because it affects the consistency and repeatability of the material performance. For thermo-responsive polymers, reversibility is often described in terms of hysteresis, which is usually demonstrated by the difference in transition temperatures and profiles during heating and cooling cycles. For the two copolymers that exhibited LCST-type phase separation (B/V-5 and B/V-8) in this study, it was found that the phase separation was not reversible (polymer remained phase-separated from [C₂mim][NTf₂] after cooled to room temperature). This observation can be addressed by comparison to stimuli-responsive polymers in aqueous solution.

In aqueous solutions, PNIPAm is the most well-known polymer that exhibits a significant degree of hysteresis, where a broad transition or slow chain swelling process during cooling was observed in contrast to the very sharp transition or the fast chain contraction when phase separation occurred.^{49,245,246} The hysteresis exhibited by PNIPAm was attributed to the intramolecular hydrogen bonding in the globule state of PNIPAm during the coil-to-globule transition, which acted like “cross-linkers” of the PNIPAm aggregates and retarded redissolution.^{209,245} In IL solutions, however, the existence of hysteresis and non-reversibility are

still not well understood. Kodama et al. observed that although the phase separation of PBzMA in [C₂mim][NTf₂] can be completely reversed, the re-dissolution process required 15 hours at a temperature 10 °C below its CPT with a 3 wt% solution concentration.²³⁸ They also found that the rate of redissolution in ILs was highly dependent on the polymer structure and could be correlated to the difference between the CPT and glass transition temperature (T_g) of each polymer/IL system.²³⁸

With increasing amount of VBK in the copolymer, the T_g of the copolymer increased due to the stiffness of PVBK (Table 6-3) and the CPT of the solution decreased due to the lower solubility of the VBK units in the IL. The difference between CPT and T_g is 24 °C when there was 4 mol% VBK in the copolymer (B/V-5) whereas for the copolymer with 9 mol% VBK (B/V-8), the CPT was almost the same as the T_g of the copolymer. In comparison to the 39 °C difference between CPT and T_g for PBzMA in [C₂mim][NTf₂],²³⁸ it is easy to see that the addition of VBK had adverse effects on the reversibility of the copolymers. In addition to the higher stiffness and lower solubility, the aromatic structure of VBK can complex with the benzyl ring of BzMA via π - π interactions^{247,248} in the collapsed state, further restricting diffusion of the IL into the polymer aggregates and thus rendering the phase separation irreversible.

6.3.3.3 Effects of heating rate on LCST and reversibility

The kinetics of phase separation in ionic liquids was found to be extremely slow compared to that in aqueous solutions, mainly resulting from the much higher viscosity of ionic liquids compared to that of water.⁶¹ In aqueous solutions, it is known that both the transition temperature and sharpness of the LCST transitions were dependent on heating rate.^{53,249} As heating rate

increased, the CPT tended to increase and phase transition became more diffuse⁵³ as the polymer chains had less time to react to the environmental change. In ILs, a heating rate of $\sim 1 \text{ }^\circ\text{C min}^{-1}$ has been most commonly used when studying thermo-responsive polymers.^{60,63,64,212,238} However, Ueki et al. reported the endothermic peak temperature corresponding to the microphase separation of the PBzMA in $[\text{C}_2\text{mim}][\text{NTf}_2]$ continued to depend on heating rate even when it was below $\sim 0.06 \text{ }^\circ\text{C min}^{-1}$.⁶¹ In this study, two heating/cooling rates, $1 \text{ }^\circ\text{C min}^{-1}$ and $0.1 \text{ }^\circ\text{C min}^{-1}$, were applied to examine the effect of heating rate on the phase separation process of these copolymers.

From the results listed in Table 6-3, the CPTs of B/V-5 were the same with the different heating rates whereas the CPT of B/V-8 decreased by $3 \text{ }^\circ\text{C}$ when the heating rate was decreased from $1 \text{ }^\circ\text{C min}^{-1}$ to $0.1 \text{ }^\circ\text{C min}^{-1}$. In ILs, PBzMA was reported to exhibit microscopic phase separation well before macroscopic phase-separation.^{61,62} The microscopic phase separation detected by differential scanning calorimetry⁶¹ or dynamic light scattering⁶² was attributed to the formation of polymer clusters and the solutions remained transparent during this stage. Although the extremely slow kinetics of the microscopic phase separation of PBzMA in ILs was demonstrated,⁶¹ no evidence of slow kinetics for macroscopic phase separation was found. The two samples in this study both showed negligible changes in CPT in response to a variation of heating rates, and thus it suggested that heating rate did not have a significant effect on the CPT and the macroscopic phase separation. Furthermore, by decreasing the heating rate from $1 \text{ }^\circ\text{C min}^{-1}$ to $0.1 \text{ }^\circ\text{C min}^{-1}$, the phase separation for the statistical copolymers was still observed to be irreversible. Indeed, the reduction in heating rate was reported to cause the loss of thermo-reversibility for poly(2-N-morpholinoethyl methacrylate) (PMEMA) in aqueous solutions due to the extended time period PMEMA stayed aggregated above its LCST.⁵³

6.3.3.4 Fluorescence properties of the statistical copolymers

The incorporation of VBK units not only was effective in tuning the phase separation transition temperatures, but also imparted hole transport and fluorescence properties to the BzMA/VBK statistical copolymers due to the carbazole moiety of VBK. Fluorescence spectra with excitation at $\lambda = 330$ nm were obtained for not only the solutions of the BzMA/VBK copolymers in the IL, but also for IL solutions of MMA/VBK copolymer, BzMA homopolymer as well as neat [C₂mim][NTf₂] to examine the fluorescence of VBK, BzMA and IL individually. In Figure 6-4 (a), the emission spectra of B/V-5 ($F_{\text{VBK}} = 4$ mol%), M/V-5 ($F_{\text{VBK}} = 11$ mol%) and BzMA homopolymer (PBzMA) in 3 wt% [C₂mim][NTf₂] solutions were compared. It was found that both PBzMA and MMA/VBK copolymer (VBK was the only potentially fluorescent group in the copolymer) were fluorescent but interestingly the BzMA/VBK copolymers exhibited a major peak at 368 nm and a shoulder at 385 nm when excited at $\lambda = 330$ nm, corresponding to only the carbazole group in the VBK unit.^{48,50} Although weak fluorescence emission was reported for some ILs,²⁵⁰ no significant fluorescence was detected for [C₂mim][NTf₂] from 350 to 450 nm (Figure 6-4 (b)), verifying the fluorescence signal observed for the copolymers was solely from the carbazole groups.

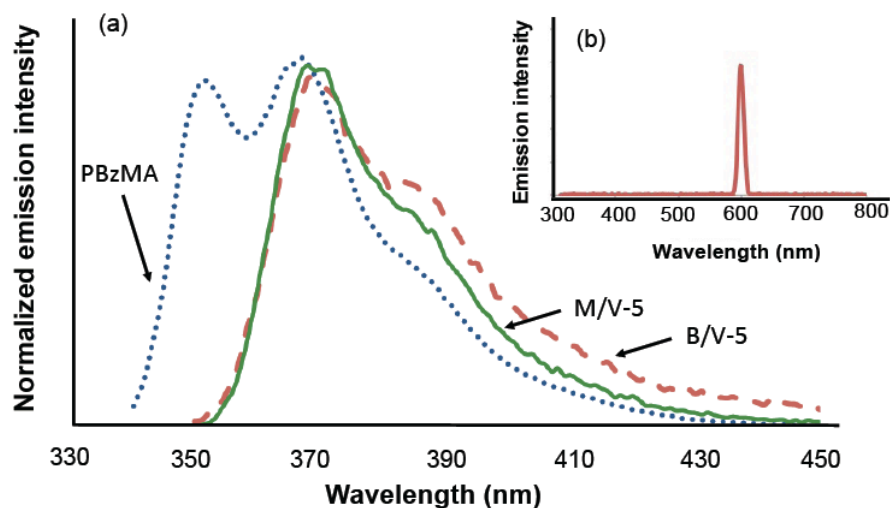


Figure 6-4. Fluorescence emission spectra ($\lambda_{\text{ex}} = 330$ nm) of (a) 3 wt% ionic liquid solution of the statistical copolymer B/V-5, M/V-5 and BzMA homopolymer (PBzMA) at room temperature (b) neat $[\text{C}_2\text{mim}][\text{NTf}_2]$ at room temperature.

To better understand the disappearance of BzMA fluorescence emission in the BzMA/VBK copolymer solutions, the excitation spectra of PBzMA and MMA/VBK (M/V-5) copolymer at their emission maxima ($\lambda_{\text{em}} = 350$ nm for PBzMA and $\lambda_{\text{em}} = 370$ nm for M/V-5) were obtained and compared to the emission spectrum of PBzMA. These spectra are presented in Figure 6-5. From these spectra, it was obvious that there was a high degree of spectral overlap between the excitation spectrum of VBK and the emission spectrum of PBzMA. This led us to deduce that the BzMA/VBK copolymer exhibited fluorescence resonance energy transfer (FRET) where excited benzyl groups in BzMA acted as the donor and transferred the excitation energy in a non-radiative fashion to the VBK, which acted as the acceptor.²⁵¹ FRET is driven by dipole-dipole interactions between two chromophores that are in close proximity and exhibit spectral overlap between donor emission and acceptor absorption, leading to a decrease or quenching of the donor fluorescence,^{251,252} which matched the observations found for the BzMA/VBK copolymers.

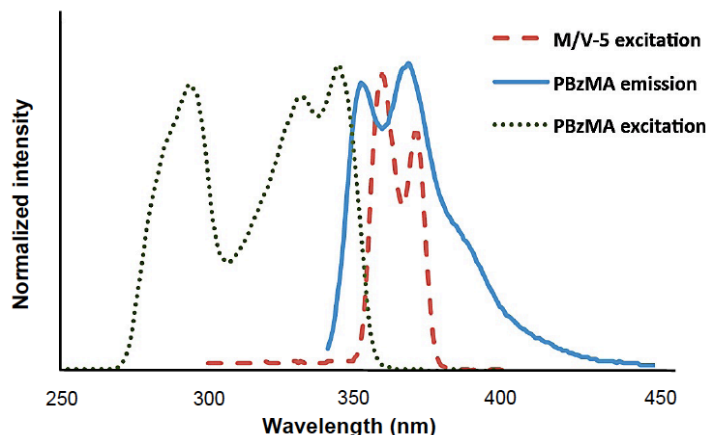


Figure 6-5. Fluorescence emission spectrum ($\lambda_{\text{ex}} = 330 \text{ nm}$) of 3 wt% ionic liquid solution of BzMA homopolymer (PBzMA) and excitation spectra of 3 wt% ionic liquid solution of BzMA homopolymer (PBzMA) ($\lambda_{\text{ex}} = 350 \text{ nm}$) and 3 wt% ionic liquid solution of the statistical copolymer M/V-5 ($\lambda_{\text{ex}} = 370 \text{ nm}$) at room temperature.

The effect of the thermo-sensitivity of PBzMA on the fluorescence properties of the copolymers was then studied. The fluorescence emission of the BzMA/VBK copolymers and BzMA homopolymer in the IL at $\lambda_{\text{ex}} = 330 \text{ nm}$ was monitored as the solution was slowly heated up above their CPTs. In Figure 6-6, the emission spectra of B/V-5 and PBzMA at different temperatures were presented. The fluorescence intensity of PBzMA decreased gradually as temperature increased towards its CPT ($\sim 105 \text{ }^\circ\text{C}$)²¹² and then decreased sharply once temperature was above $105 \text{ }^\circ\text{C}$, as shown in Figure 6-6 (b). Sharp decreases in fluorescence intensity were reported in the literature for other thermo-responsive copolymers with a single fluorophore.^{48,253,254} In the study of poly(2-(dimethylamino) ethyl methacrylate-*ran*-4-difluoro-4-bora-3a,4a-diaza-s-indacene) (poly(DMAEMA-*ran*-BODIPY)), Nagai et al. concluded that the decrease in emission intensity as the copolymer phase separated from aqueous solutions was due to the formation of H-aggregates between the BODIPY planes.²⁵⁴ In the other cases where VBK⁴⁸ or 9,9-dihexyl-2-(4-vinylphenyl)-9H-fluorene (StFI)²⁵³ was incorporated into thermo-responsive copolymers, the decrease in fluorescence intensity during phase separation was

attributed to the suppression of light absorption by the tightly-packed aggregates. In the case of the PBzMA/IL solution, its Raman spectra before and after phase separation were recorded to investigate possible π - π stacking of the aromatic groups. As shown in Figure 6-7 (a), the spectra of the solution before and after phase separation were identical, giving no evidence of any new π - π interaction. Therefore, it was more probable that the collapsed and densely packed polymer chains after phase separation suppressed light absorption of the benzyl moiety, leading to reduced emission intensity.

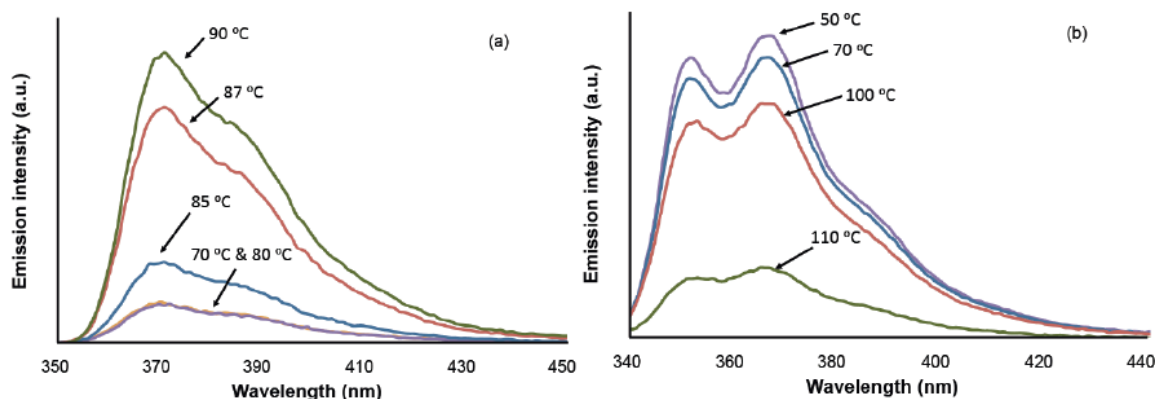


Figure 6-6. Fluorescence emission spectra ($\lambda_{\text{ex}} = 330 \text{ nm}$) of (a) 3 wt% ionic liquid solution of the statistical copolymer B/V-5 (CPT = 86 °C) and (b) 3 wt% ionic liquid solution of BzMA homopolymer (PBzMA) (CPT ~ 105 °C) at various temperature.

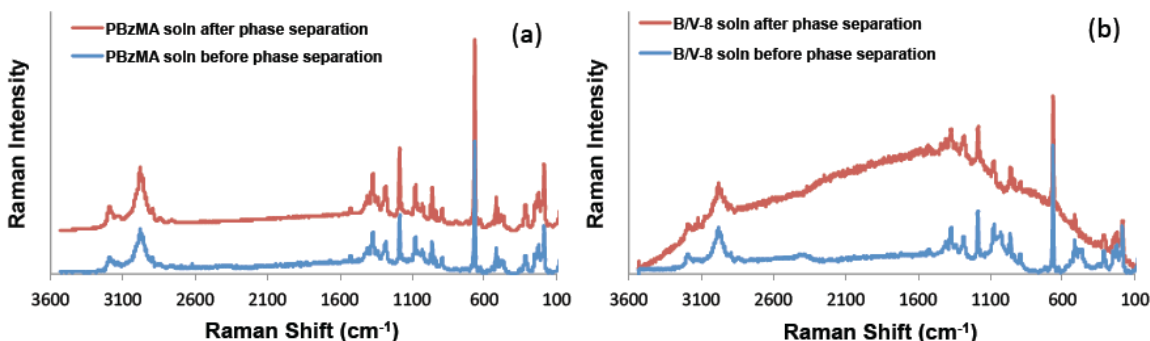


Figure 6-7. Raman spectra of (a) 3 wt% ionic liquid solution of BzMA homopolymer (PBzMA) and (b) 3 wt% ionic liquid solution of the statistical copolymer B/V-8 before and after phase separation obtained at 532 nm.

For BzMA/VBK copolymers, their fluorescence intensity remained relatively constant up to their CPT, after which it increased significantly, as shown in Figure 6-6 (a) using B/V-5 as an example, demonstrating an opposite trend compared to that of the PBzMA/IL solution. To better illustrate this phenomenon, the normalized maximum emission intensity was superimposed with the turbidity measurements for both B/V-5 and B/V-8 in Figure 6-8. An approximate 5-fold increase in fluorescence intensity occurred at a temperature coinciding with the CPT for both B/V-5 and B/V-8. This phase separation triggered fluorescence enhancement was not totally surprising. Since the fluorescence of the copolymers was a result of FRET whose efficiency is strongly dependent on the separation distance between the donor and acceptor pair,²⁵¹ as phase separation occurred, the distance between the benzyl groups of BzMA and carbazole moieties of VBK in the copolymers became much smaller, leading to a greatly enhanced FRET efficiency despite the decrease in emission intensity of PBzMA after phase separation.

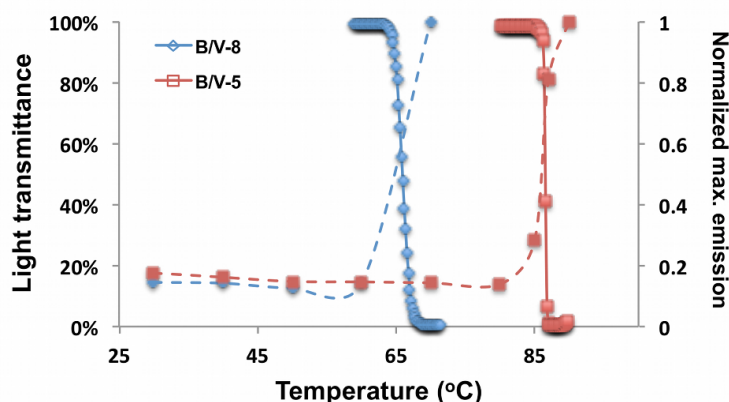


Figure 6-8. Light transmittance (solid lines) and normalized maximum emission (dashed lines, $\lambda_{\text{ex}} = 330 \text{ nm}$) of 3 wt% ionic liquid solutions of statistical copolymers of BzMA and VBK (B/V-5 with $F_{\text{VBK}} = 4 \text{ mol\%}$ and B/V-8 with $F_{\text{VBK}} = 9 \text{ mol\%}$) with heating rate of $1 \text{ }^\circ\text{C min}^{-1}$.

Raman spectra of B/V-8 before and after phase separation were also obtained (Figure 6-7 (b)) to examine any possible formation of H- or J-aggregates between carbazole moieties during phase separation. After phase separation, the enhanced fluorescence emission of the copolymer

strongly interfered with the Raman spectrum and weak peaks were masked. Nonetheless, from the peaks observed, no obvious peak shifts were evident. Therefore, we concluded the higher FRET efficiency at close donor/acceptor proximity after phase separation was the main cause for the enhanced fluorescence emission observed for the BzMA/VBK copolymers.

6.3.4 Effect of microstructure on fluorescence properties of the block copolymers in [C₂mim][NTf₂]

The fluorescence properties of two block copolymers (B/V5-M/S10 and M/V5-B/S10) were examined and compared to investigate the effect of microstructure (whether BzMA and VBK units were in the same block or different blocks) on the fluorescent properties of the block copolymers. As listed in Table 6-4, the two block copolymers were both about 15 kg mol⁻¹ in molecular weight. They both have a BzMA-rich block and a MMA-rich block with the main difference being VBK was in the BzMA-rich block in B/V5-M/S10 while VBK was in the MMA-rich block in M/V5-B/S10; styrene was used as a non-fluorescent controlling monomer for the other methacrylate-rich block. Another difference between the two block copolymers as shown in Table 6-4 was that B/V5-M/S10 had a higher BzMA/MMA molar ratio than that of M/V5-B/S10 ($F_{\text{BzMA}}/F_{\text{MMA}} = 0.64/0.36$ for B/V5-M/S10 and $0.30/0.70$ for M/V5-B/S10). This composition difference was not critical but it affected the glass transition temperature (T_g) of the two block copolymers where M/V5-B/S10 had a higher T_g (90 °C) than that of B/V5-M/S10 (78 °C) as PMMA is stiffer than PBzMA. The cloud point temperatures (CPT) of the two block copolymers were also different. B/V5-M/S10 showed a CPT of 97 °C, significantly higher than its statistical copolymer macroinitiator B/V-5. In addition, the phase separation was reversible as the solution turned from cloudy to clear when the solution was cooled below 81 °C, in contrast to

the irreversibility of the phase separation of the macroinitiator B/V-5. Both the higher CPT and the reversible phase separation were due to the presence of the solvatophilic MMA-rich second block. M/V5-B/S10 had a CPT of 70 °C, much lower than the other block copolymer because of the higher solvatophobic co-monomer content in the BzMA-rich block (10 mol% instead of 5 mol%). Despite the higher MMA/BzMA ratio, the phase transition of M/V5-B/S10 was not reversible like B/V5-M/S10, indicating the stronger effect of the solvatophobic co-monomer within the thermo-responsive BzMA-rich block than that of the presence of a solvetophilic MMA-rich block on the reversibility of the phase transition.

Table 6-4. Cloud point temperature (CPT) of the block copolymers in [C₂mim][NTf₂] and glass transition temperature (T_g) of the block copolymers.

Polymers ^a	F _{BzMA} /F _{MMA} ^b	M _n ^c	CPT ^d	T _g ^e
		kg mol ⁻¹	°C	°C
B/V5-M/S10	0.64/0.36	15.1	97 (81)	78
M/V5-B/S10	0.30/0.70	14.8	70 ^f	90

^a Refer to Table D-2 in Appendix D for synthesis conditions for the block copolymers; ^b Molar fractions of benzyl methacrylate (BzMA) and methyl methacrylate (MMA) in the block copolymers relative to each other measured by ¹H NMR; ^c Number average molecular weight of the block copolymers measured by GPC relative to poly(methyl methacrylate) standards in THF at 40°C; ^d Light transmittance measured by UV-vis spectrometry and cloud point temperature (CPT) defined by the temperature where 50% light transmittance was recorded during heating, the temperature in brackets are CPTs obtained during cooling, all solutions have concentration of 3 wt%, heating rate was 1 °C min⁻¹; ^e Glass transition temperature measured by differential scanning calorimetry; ^f Phase separation not reversible.

The normalized fluorescence intensity of the block copolymers at different temperatures is presented in Figure 6-9. For B/V5-M/S10, the fluorescence intensity of the block copolymer increased sharply as the phase separation of the BzMA-rich block occurred, similar to the statistical copolymers.

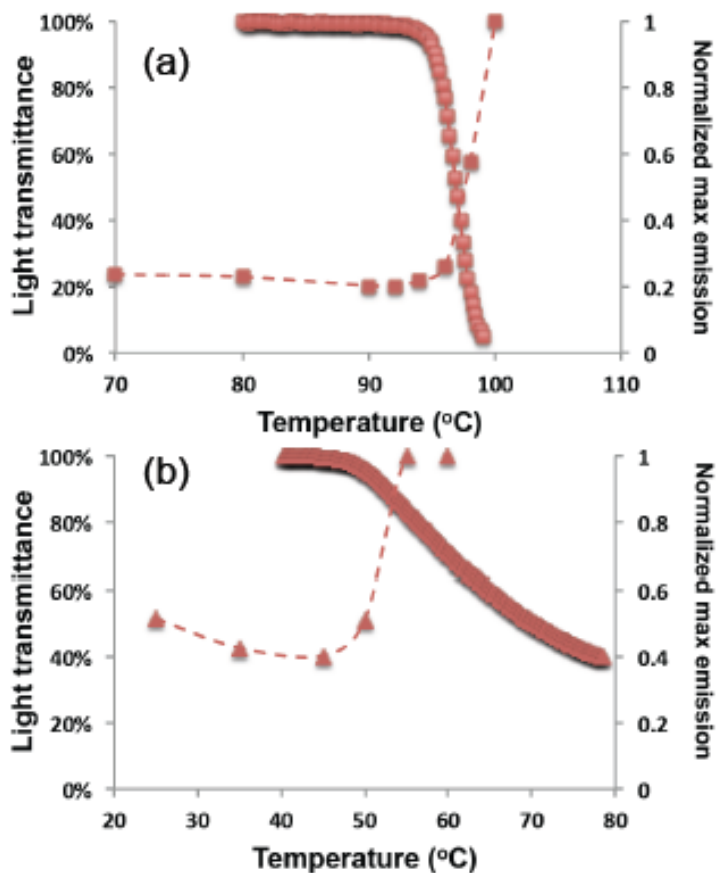


Figure 6-9. Light transmittance (solid lines) and normalized maximum fluorescence (dashed lines, $\lambda_{\text{ex}} = 330 \text{ nm}$) of 3 wt% ionic liquid solutions of block copolymers (a) B/V5-M/S10 (b) M/V5-B/S10 with heating/cooling rate of $1 \text{ }^\circ\text{C min}^{-1}$.

More interestingly, the fluorescence intensity of M/V5-B/S10, where BzMA and VBK units are in separate blocks, also exhibited fluorescence enhancement when the BzMA-rich block phase separated from the IL, as shown in Figure 6-9 (b). Since the fluorescence of the copolymers was due to FRET which is driven by long-range dipole-dipole interactions,²⁵¹ and thus, it was not surprising that fluorescence enhancement can happen even when BzMA and VBK units were in different blocks of a block copolymer. The enhancement observed for M/V5-B/S10 was only about 2-fold instead of about 5-fold when BzMA and VBK units were in the same block, due to the sensitivity to donor/acceptor distance during the FRET process. Particle size distribution for the M/V5-B/S10 block copolymer in the IL was measured by dynamic light scattering as the

solution was heated (more details can be found in Appendix D). Micelle formation was evident as the hydrodynamic radius of the polymer increased from about 10 nm to about 100 nm (Figure D-3 in Appendix D) when the BzMA-rich block phase separated from the solution. Therefore, the energy transfer between VBK and BzMA was further restricted after phase separation as the BzMA units were in the collapsed core while VBK units were in the soluble corona in the IL.

6.4 Conclusions

In this study, well-defined BzMA-rich (with up to 98 mol% BzMA in the copolymer) statistical copolymers were synthesized via NMP when using VBK as a controlling co-monomer. The values of $\langle k_p \rangle \langle K \rangle$ for BzMA/VBK copolymerizations were dramatically lower than those reported for BzMA/styrene copolymerizations via NMP at the same temperature with similar amounts of controlling co-monomer. Within the narrow range of investigated feed composition ($f_{\text{VBK},0} = 2 - 11 \text{ mol\%}$), the addition of VBK to the propagating BzMA/VBK chains was also found to be essentially random, in contrast to the much richer VBK content in the copolymers with other methacrylates such as MMA in comparison to the initial mixture with similar feed compositions. The molecular weight of the copolymers increased linearly with conversion and the copolymers showed narrow molecular weight distributions ($\mathcal{D} = 1.34 - 1.42$), indicating the copolymerizations were relatively well controlled. The capability of the copolymers to be re-initiated to form block copolymers was also demonstrated by chain extension experiments.

LCST-type phase separation in the hydrophobic ionic liquid $[\text{C}_2\text{mim}][\text{NTf}_2]$ was observed for two BzMA/VBK statistical copolymers (B/V-5 and B/V-8). The incorporation of solvatophobic

VBK units was shown to be useful in tuning the transition temperature of the phase separation but it also rendered the phase separation irreversible.

The incorporation of fluorescent VBK units also imparted interesting fluorescence properties to the statistical and block copolymers. It was found that both BzMA and VBK were fluorescent and they were a FRET pair where BzMA was the donor and VBK was the acceptor, leading to quenching of BzMA fluorescence and the copolymer exhibited solely the emission of the carbazole moiety of VBK. The fluorescence intensity of the copolymers were found to enhanced by about 5-fold as phase separation, resulted from the greater FRET efficiency as BzMA and VBK came into close proximity in aggregates. We also showed that the VBK and BzMA units could be in different blocks in a block copolymer to exhibit the phase separation-triggered fluorescence enhancement; yet the enhancement was comparatively smaller. In summary, we were able to synthesizing copolymers via NMP that had thermoresponsive behaviour and exhibited interesting fluorescence properties in an IL. We will continue to examine how to make thermoreversible ion gels with these copolymers.

Acknowledgements

The authors are very grateful for the funding from the NSERC Postgraduate Scholarship, NSERC Discovery Grant and the Canada Foundation for Innovation New Opportunities Fund. The authors thank Prof. Bruce Lennox (Dept. of Chemistry, McGill University) for providing access to his temperature modulated UV-vis spectrometer and fluorescence spectrophotometer. They also appreciate the generosity of Arkema (Scott Schmidt and Noah Macy) for supplying BlocBuilderTM and SG1.

References

Please refer to the global bibliography at the end of the thesis.

Chapter 7

Effects of Solvatophilicity of Statistical Terpolymers on Phase Separation and Reversibility in an Ionic Liquid

7.1 Preface

This chapter presents a manuscript that was submitted to *Polymer Chemistry* in February 2014 and currently under review (manuscript ID: PY-ART-02-2014-000300.R1). In Chapter 6, copolymers of benzyl methacrylate (BzMA) and 9-(4-vinylbenzyl)-9H-carbazole (VBK) were demonstrated to show not only LCST-type phase separation in the ionic liquid (IL) solutions, but also exhibit phase separation-triggered fluorescence enhancement. However, the irreversible nature of the phase separation (and thus the fluorescent response) restricts the number of potential applications these materials can be useful for.

This chapter describes the attempts to improve solubility and restore phase separation reversibility of polymers containing BzMA and VBK by incorporating a solvatophilic comonomer, namely methyl methacrylate (MMA) or oligo(ethylene glycol)methacrylate (OEGMA) to form statistical BzMA/MMA/VBK and BzMA/OEGMA/VBK terpolymers. The solvatophilicity of these terpolymers can be easily adjusted and compared by varying polymer composition if polymer chains were uniform in composition and chain length. The control in chain uniformity was achieved by using nitroxide mediated polymerization (NMP). The well-defined nature of these terpolymers also prevents possible sluggish phase transitions due to broad molecular weight distribution. Features such as linear increase in molecular weight with conversion and narrow molecular weight distribution were presented to confirm the level of

control during synthesis. The phase behaviour of these terpolymers were then characterized in 1-ethyl-3-methylimidazolium bis(trifluoromethane sulfone)imide ($[\text{C}_2\text{mim}][\text{NTf}_2]$), the same IL used in the study presented in Chapter 6, as a function of solvatoophilicity, solution concentration, and the difference in terpolymer chain mobility (via glass transition temperature (T_g) differences due to using MMA versus OEGMA). Restoration of phase separation reversibility was achieved when a minimum amount (about 20 – 30 mol%) of solvatoophilic groups (ester group for MMA and ethylene glycol group for OEGMA) was present in the terpolymers. Solution concentration and molecular weight (or T_g) affected phase separation temperature significantly but did not correlate with reversibility strongly. Lastly, multiple heat/cool cycles were used to demonstrate the consistency of both of the LCST behaviour and fluorescent responses of the terpolymers with sufficiently high solvatoophilicity.

This manuscript provides new insights to the effects of solvatoophilicity of polymers on LCST behaviours, especially the re-dissolution process, in IL solutions, which have not been widely studied. It also demonstrated an intuitive, quantifiable way to adjust solvatoophilicity of polymers, which can be used to not only tune the transition temperature of other thermo-responsive polymers in ILs, but also allow more design possibilities for copolymers with a thermo-responsive constituent and a functional but solvatoophobic co-monomer while maintaining reversibility of the phase separation.

Statistical terpolymers with thermo-responsive fluorescent response in an ionic liquid: Effect of solvatophilicity on LCST phase separation and reversibility

Chi Zhang, Milan Maric*

Department of Chemical Engineering, McGill University,
3610 University Street, Montreal, QC, Canada H3A 2B2

Submitted to *Polymer Chemistry* in **February 2014**. Manuscript ID: PY-ART-02-2014-000300.R1.

Abstract

Well-defined terpolymers of benzyl methacrylate (BzMA), 9-(4-vinylbenzyl)-9H-carbazole (VBK) with either methyl methacrylate (MMA) or oligo(ethylene glycol)methacrylate (OEGMA) were synthesized to study their LCST-type phase behavior (due to BzMA) and fluorescent properties (due to VBK) in a hydrophobic ionic liquid IL, 1-ethyl-3-methylimidazolium bis(trifluoromethane sulfone)imide ($[\text{C}_2\text{mim}][\text{NTf}_2]$) as a function of solvatophilicity and the difference in terpolymer chain mobility (via glass transition differences due to using MMA versus OEGMA). Specifically, MMA and OEGMA provided solvatophilic groups (the ester in MMA or ethylene glycol units in OEGMA) to the terpolymers and their composition was varied to study the effect of solvatophilicity on the terpolymer phase separation and re-dissolution processes in the IL. The concentration of solvatophilic groups in the terpolymer was not only shown to affect phase separation temperature significantly, but also demonstrated to be crucial in driving the re-dissolution process. A minimum concentration of solvatophilic groups to facilitate reversible phase separation was in the range of 20 – 30 mol% for both terpolymer systems. Solution concentration (1 – 10 wt%) also showed significant effects on phase separation

temperature but lower concentration did not guarantee improved re-dissolution. Phase separation temperature was also demonstrated to be inversely proportional to polymer molecular weight ($7.3 - 22.5 \text{ kg mol}^{-1}$). Lastly, the reversibility of phase separation and fluorescent responses in terpolymers with sufficient solvatophilicity was confirmed to be consistent by multiple heating/cooling cycles.

7.2. Introduction

In polymer-solvent systems, some polymers exhibit sharp changes in solubility in response to changes in temperature. Such thermo-responsive polymers in aqueous solutions have been widely studied because of their applicability to controlled drug delivery, bioseparations and tissue engineering.^{4,153,155,255}

Ionic liquids (IL), which are molten organic salts, have drawn serious interest as versatile solvents because of their excellent chemical/thermal stability, ability to dissolve a broad range of compounds, non-volatility and non-flammability.^{39,218,256,257} Numerous polymer/IL composite materials have been created to form ion gels as novel electrolytes for various electrochemical devices, eliminating flammability and leakage problems of conventional volatile solvent-based electrolytes.^{20,21} A number of polymers were reported to be thermo-responsive in different ILs.^{58,63,64,212} Among these polymers, poly(benzyl methacrylate) (PBzMA) was found to exhibit a sharp decrease in solubility upon being heated above a critical temperature (ie. lower critical solution temperature or LCST-type phase separation) in hydrophobic ILs.^{60,212,238} The solvation of PBzMA in ILs was facilitated by spontaneous organization of the IL ions around the solvatophobic benzyl group of the polymer, resulting in a negative change in entropy upon

mixing.^{61,62} As temperature increased above a critical temperature, the ion layer around the benzyl group was disrupted by the increased freedom of motion, leading to phase separation.

To obtain sharp phase transitions and to study the effects of various factors (such as molecular weight and polymer composition) on the phase behavior, the polymer has to be well defined. For this reason, nitroxide mediated polymerization (NMP) was employed for this study. As one of the main controlled radical polymerization techniques, NMP controls polymerization through reversible termination of the propagating chains by the persistent nitroxide radical.^{258,259} It is known that the homopolymerization of methacrylates such as BzMA is challenging for NMP mainly because of the very high equilibrium constant K which leads to large amount of active radicals and excessive termination.^{104,133} Charleux et al.¹⁰⁴ reported that the average equilibrium constant $\langle K \rangle$ could be significantly reduced when methyl methacrylate was copolymerized with a small amount of co-monomer that has a much lower K such as styrene and controlled synthesis of methacrylate-rich copolymers could be achieved using the commercially available initiator BlocBuilderTM. Since then, numerous methacrylate-rich copolymers have been polymerized in controlled manners by NMP using a small amount of styrene and other controlling co-monomers.^{48,132,142,143}

In our previous study,¹⁴⁸ BzMA was combined with a fluorescent co-monomer, 9-(4-vinylbenzyl)-9H-carbazole (VBK), in random copolymers. VBK has been demonstrated previously to be an effective controlling co-monomer for a number of methacrylate-rich copolymerizations via NMP.^{50,53,146} The combination of thermo-responsiveness and fluorescent properties was aimed to create materials potentially useful for sensing, imaging or actuator applications.^{241,260,261} Interestingly, the fluorescence intensity of the BzMA/VBK copolymers in a hydrophobic IL increased sharply 5-fold as phase separation occurred.¹⁴⁸ Emission/excitation

spectra as well as Raman spectra of IL solutions of BzMA homopolymer and BzMA/VBK copolymers indicated that BzMA and VBK were likely a fluorescence resonance energy transfer (FRET) donor and acceptor pair.¹⁴⁸ The increased proximity between BzMA and VBK units during phase separation greatly enhanced FRET efficiency and resulted in fluorescence enhancements.^{148,252} This increase in fluorescence intensity in response to the temperature change made the copolymers interesting candidates as novel fluorescent molecular thermometers.²⁶⁰⁻²⁶³ These molecular thermometers can be used to measure micro-sized areas (eg. biological cells), to map two- or three-dimensional temperature distribution, or to monitor temperature in harsh environments (eg. highly corrosive or high voltage) where conventional thermometers are not practical.²⁶¹⁻²⁶³ To be useful for these applications, the fluorescent response of the system has to be reversible and highly consistent. However, the incorporation of solvophobic VBK in the BzMA/VBK copolymers rendered the phase separation and hence the fluorescence enhancement of the copolymers completely irreversible.

The reversibility of the phase transition of polymer/IL systems has not been studied widely. The phase separation of PBzMA in hydrophobic ILs was reported to be reversible with very slow re-dissolution kinetics.²³⁸ By modifying the polymer structure to adjust the solvophilic/solvophobic balance, Kodama et al. were able to significantly alter the re-dissolution rate.²³⁸ In addition, they also found that a larger difference between phase separation temperature and glass transition temperature (T_g) of the polymer generally led to faster re-dissolution. Their study about the reversibility of the PBzMA and its derivatives in the IL solutions was intriguing but reversibility can be affected by other factors such as molecular weight and solution concentration. Therefore, a more comprehensive study was needed to provide more insight to the re-dissolution process. Also, to tune the solvophilic/solvophobic

balance, instead of modifying each polymer structure, a more intuitive approach would be simply adjusting the composition of a copolymer with a solvophilic and a solvophobic co-monomer. With this approach, the solvophilic/solvophobic ratio of the copolymer can be quantified and finely tuned.

Therefore, in this study, terpolymers consisting of BzMA, VBK and a solvophilic co-monomer with different compositions were synthesized using NMP and their phase behavior was studied in a hydrophobic IL, 1-ethyl-3-methylimidazolium bis(trifluoromethane sulfone)imide ([C₂mim][NTf₂]).

Homopolymers of methyl methacrylate (MMA) and oligo(ethylene glycol) methacrylate (OEGMA) are both known to be soluble in [C₂mim][NTf₂].^{60,234,264} However, PMMA has a higher T_g than PBzMA while the T_g of POEGMA is much lower than that of PBzMA.^{148,242} T_g of a polymer plays an important role in polymer dynamics during the dissolution process and thus also significantly affects the re-dissolution of the phase separated-polymer during cooling.^{238,265} As the content of MMA or OEGMA was increased in the terpolymer, both of the BzMA/MMA/VBK and BzMA/OEGMA/VBK terpolymers should exhibit improving solubility in the IL but the former would have increasing T_g whereas the latter would have decreasing T_g. This study attempts to determine how the T_g of the terpolymers affects their phase behavior and dynamics in the IL, given that solubility is similar. The synthesis of these terpolymers will be first addressed, followed by detailed investigations of the effects of polymer composition, solution concentration, and molecular weight on terpolymer phase behavior and fluorescence responses in the IL.

7.3 Results and Discussion

7.3.1 Terpolymerization kinetics and polymerization control

Terpolymerizations of benzyl methacrylate (BzMA), 9-(4-vinylbenzyl)-9H-carbazole (VBK) and methyl methacrylate (MMA) or oligo(ethylene glycol)methyl methacrylate (OEGMA) were performed with feeds containing fixed amount of VBK (10 mol%) and varying BzMA:MMA (from 80:10 to 50:40) or BzMA:OEGMA (from 87:3 to 80:10) compositions. Results including conversion, composition, molecular weight and dispersity (\bar{D}) were summarized in Table 7-1.

Table 7-1. Summary of characterization data for terpolymers of benzyl methacrylate (BzMA), methyl methacrylate (MMA) or oligo(ethylene glycol)methyl methacrylate (OEGMA) and 9-(4-vinylbenzyl)-9H-carbazole (VBK) synthesized at 90 °C in 20 wt% DMF solution.

Expt. ID ^a	Polym. time	Conv. ^b	F _{BzMA} ^c	F _{MMA} ^c or F _{OEGMA} ^c	F _{VBK} ^c	M _n ^d	\bar{D} ^d
	min		mol%	mol%	mol%	kg mol ⁻¹	
B80/M10/V10-40	245	39%	74%	10%	16%	13.6	1.32
B70/M20/V10-40	243	38%	65%	18%	17%	15.3	1.36
B60/M30/V10-40	261	39%	60%	22%	18%	17.8	1.30
B50/M40/V10-40	245	46%	51%	29%	20%	14.1	1.28
B80/M10/V10-15	258	36%	75%	9%	16%	7.3	1.30
B80/M10/V10-80	360	47%	77%	9%	14%	22.5	1.44
B87/03/V10-40	303	40%	88%	2%	10%	14.3	1.37
B85/05/V10-40	302	37%	86%	3%	11%	13.4	1.33
B83/07/V10-40	304	39%	81%	5%	14%	15.4	1.36
B80/010/V10-40	300	41%	79%	7%	14%	16.0	1.35

^a The experiment ID Bx/My/Vz-m (or Bx/Oy/Vz-m) denotes feed compositions of BzMA (B), MMA (M) or OEGMA (O) and VBK (V) in molar percentage with x, y, z, with respectively, m represents the target molecular weight which is the number average molecular weight at 100% conversion; ^b Final conversion estimated by gravimetry; ^c Final terpolymer composition determined by ¹H NMR; ^d Number average molecular weight and dispersity of the copolymer measured by GPC relative to poly(methyl methacrylate) standards in THF at 40 °C.

VBK was previously reported to be effective in controlling methacrylate-rich copolymerizations via NMP.^{48,50,146} In this study, VBK was not only used as a controlling co-monomer, but also to

impart fluorescent properties to the terpolymer due to its carbazole moiety, which will be discussed in Section 7.3.2.4.

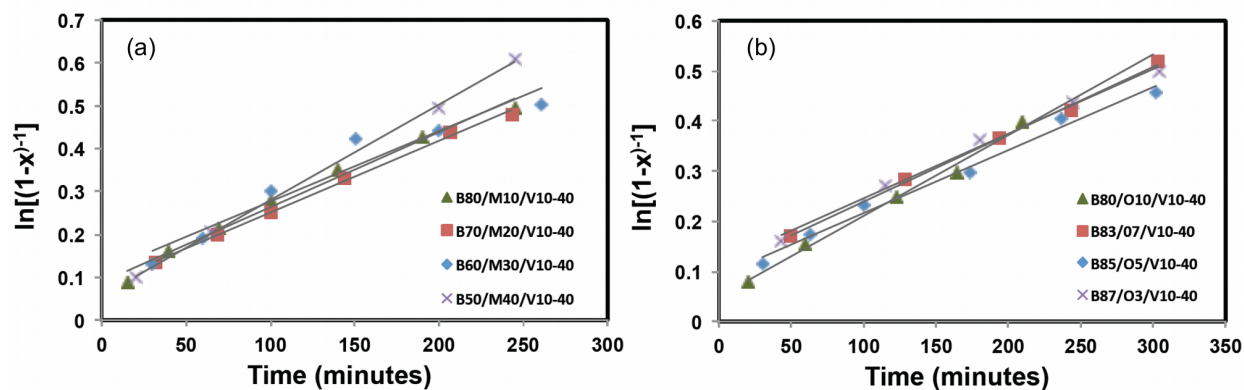


Figure 7-1. Semi-logarithmic kinetic plots of terpolymerization of (a) benzyl methacrylate (BzMA) methyl methacrylate (MMA) and 9-(4-vinylbenzyl)-9H-carbazole (VBK), and (b) benzyl methacrylate (BzMA) oligo(ethylene glycol) methyl ether methacrylate (OEGMA) and 9-(4-vinylbenzyl)-9H-carbazole (VBK) at 90 °C via NMP.

All terpolymerizations were conducted typically for about 4 – 6 hours and the final overall conversion ranged from 36% to 47%. The kinetics of the terpolymerizations was illustrated by semi-logarithmic plots of $\ln[(1-\text{conversion})^{-1}]$ versus time in Figure 7-1. First order kinetics was observed for all terpolymerizations, as expected for controlled polymerizations. Small deviations from the linear trends were observed in some cases. The downward deviations towards the end of the terpolymerizations was also observed for the BzMA/VBK copolymerizations previously reported,¹⁴⁸ which could be due to chain transfer to the monomers or the solvent. A couple of data points from B60/M30/V10-40 also showed deviation from the linear trend, likely resulting from overestimation of conversion when using gravimetry, which is known to cause frequent overestimation of conversions.^{106,141}

The apparent rate constant $\langle k_p \rangle [P\bullet]$, which is the product of average propagation rate constant $\langle k_p \rangle$ and propagating radical concentration $[P\bullet]$, was estimated using the slope from the kinetic

plots and summarized in Table 7-2. For BzMA/MMA/VBK terpolymerizations, their $\langle k_p \rangle [P\bullet]$ ranged from $2.7 \times 10^{-5} \text{ s}^{-1}$ to $3.7 \times 10^{-5} \text{ s}^{-1}$; for BzMA/OEGMA/VBK terpolymerizations, their $\langle k_p \rangle [P\bullet]$ ranged from $2.1 \times 10^{-5} \text{ s}^{-1}$ to $2.7 \times 10^{-5} \text{ s}^{-1}$. There was no obvious correlation between the reaction rate and the feed composition in either case. Feed composition did not affect the kinetics significantly. These results were expected since the reported $\langle k_p \rangle [P\bullet]$ values of the binary copolymerizations of these methacrylates with a small amount of VBK were comparable: $\langle k_p \rangle [P\bullet]_{\text{BzMA/VBK}} = 1.9 \times 10^{-5} \text{ s}^{-1}$ (with $f_{\text{VBK},0} = 11 \text{ mol}\%$),¹⁴⁸ $\langle k_p \rangle [P\bullet]_{\text{MMA/VBK}} = 4.3 \times 10^{-5} \text{ s}^{-1}$ (with $f_{\text{VBK},0} = 5 \text{ mol}\%$),²⁴³ and $\langle k_p \rangle [P\bullet]_{\text{OEGMA/VBK}} = 1.0 \times 10^{-5} \text{ s}^{-1}$ (with $f_{\text{VBK},0} = 10 \text{ mol}\%$),⁵⁰ all estimated at 90 °C in dimethylformamide solutions, which were the same conditions as those used for the terpolymerizations in this study.

Table 7-2: Feed composition and the product of average propagation rate constant, $\langle k_p \rangle$, and propagating radical concentration, $[P\bullet]$, $\langle k_p \rangle [P\bullet]$, for terpolymerizations of benzyl methacrylate (BzMA), methyl methacrylate (MMA) or oligo(ethylene glycol)methyl methacrylate (OEGMA) and 9-(4-vinylbenzyl)-9H-carbazole (VBK).

Expt. ID	$f_{\text{BzMA},0}^a$	$f_{\text{MMA},0}$ OR $f_{\text{OEGMA},0}^a$	$f_{\text{VBK},0}^a$	$\langle k_p \rangle [P\bullet]^b$
	mol%	mol%	mol%	$\text{s}^{-1} \times 10^5$
B80/M10/V10-40	80%	10%	10%	2.92 ± 0.15
B70/M20/V10-40	70%	20%	10%	2.79 ± 0.06
B60/M30/V10-40	60%	30%	10%	2.74 ± 0.37
B50/M40/V10-40	50%	40%	10%	3.71 ± 0.07
B87/03/V10-40	87%	3%	10%	2.15 ± 0.13
B85/05/V10-40	85%	5%	10%	2.09 ± 0.11
B83/07/V10-40	83%	7%	10%	2.24 ± 0.06
B80/010/V10-40	80%	10%	10%	2.69 ± 0.10

^a Feed compositions; ^b Estimated using the slopes of the kinetic plots shown in Figure 1.

The level of control for the terpolymerizations was also illustrated by the linear increase in the number-average molecular weight (M_n) versus conversion shown in Figure 7-2. The dispersity (\mathcal{D}) of the terpolymers was between 1.2 to 1.4.

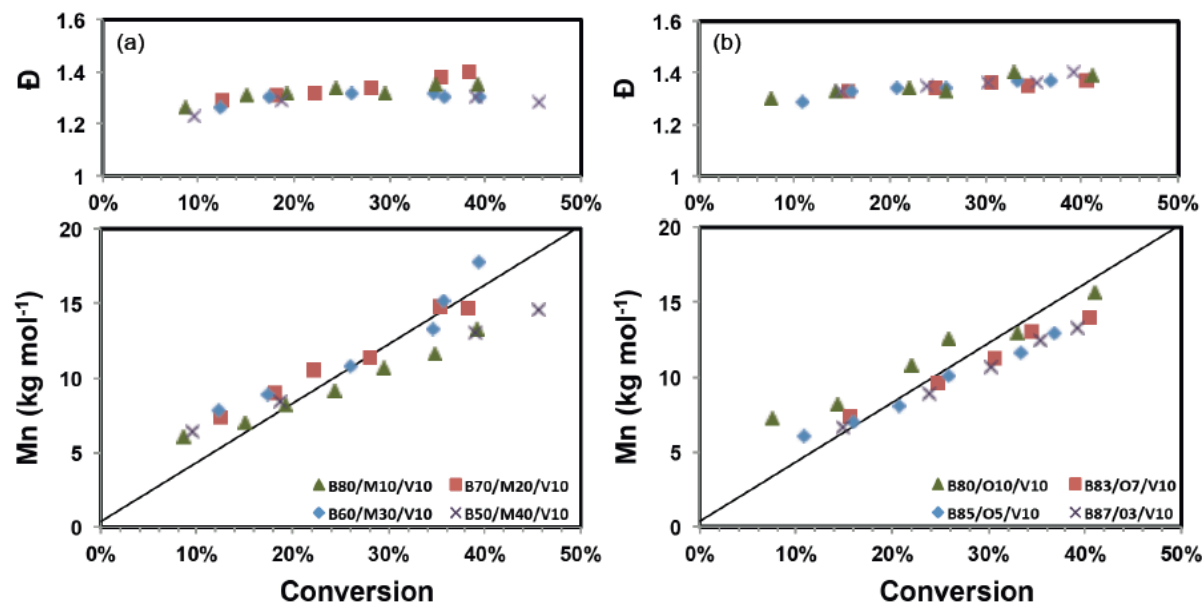


Figure 7-2. Number-average molecular weight (M_n) and dispersity (\mathcal{D}) of terpolymers of (a) benzyl methacrylate (BzMA), methyl methacrylate (MMA) and 9-(4-vinylbenzyl)-9H-carbazole (VBK), and (b) benzyl methacrylate (BzMA) oligo(ethylene glycol) methyl ether methacrylate (OEGMA) and 9-(4-vinylbenzyl)-9H-carbazole (VBK), measured by GPC calibrated with poly(methyl methacrylate) standards. The linear lines in the M_n versus conversion graphs represent the theoretical trends.

It is also interesting to note that the terpolymer compositions were quite different from the feed compositions, especially for BzMA/MMA/VBK terpolymers. The terpolymers were significantly richer in VBK and less rich in MMA compared to their feed compositions, while terpolymer composition and feed composition of BzMA remained similar. While the factors affecting relative reactivities of 3 co-monomers can be complicated, these results were not surprising. VBK was reported to show strong preference to react with its own radical than to MMA radicals

(reactivity ratios of MMA/VBK were calculated to be 0.2 and 2.7, respectively¹⁴⁶). In OEGMA/VBK copolymerizations, copolymer compositions were also measured to be richer in VBK than OEGMA compared to feed compositions as the feed composition was varied between 95 mol% and 80 mol% OEGMA.⁵⁰ On the other hand, significant composition shifts were not observed for BzMA/VBK copolymerizations.¹⁴⁸ The narrow range of feed composition variance for BzMA/OEGMA/VBK may limit the composition shifts for those terpolymerizations as all the feeds were rich in BzMA.

In summary, the kinetics and M_n increases of the terpolymerizations of BzMA/MMA/VBK and BzMA/OEGMA/VBK matched those expected from controlled polymerizations and terpolymer compositions were reasonable based on literature data.

7.3.2 Temperature sensitivity and fluorescence properties of terpolymers in [C₂mim][NTf₂]

One of the main objectives of this study was to comparatively investigate the solution properties of the BzMA/MMA/VBK and BzMA/OEGMA/VBK terpolymers in the IL [C₂mim][NTf₂].

PBzMA is known to exhibit lower critical solution temperature (LCST)-type phase separation in [C₂mim][NTf₂].^{148,212,238} We previously reported that the incorporation of solvophobic VBK in random copolymers with BzMA not only led to decreased solubility and hence lower LCST in the IL as expected, but also rendered the phase separation of the random copolymers irreversible.¹⁴⁸ However, the copolymers of BzMA and VBK exhibited a very interesting fluorescence enhancement triggered by phase separation.¹⁴⁸ In order to restore the reversibility of the thermo-responsiveness of BzMA-rich copolymers while keeping the fluorescence properties of VBK, MMA or OEGMA, whose homopolymers are both completely soluble in

[C₂mim][NTf₂],^{60,234,264} were incorporated to increase the solubility^{50,53} and hence improve reversibility of the terpolymers. The effects of copolymer composition, solution concentration and molecular weight on the phase separation transition and reversibility as well as fluorescence properties of these terpolymers in [C₂mim][NTf₂] will be further discussed in detail in the following sections.

The composition, molecular weight and glass transition temperature of all the terpolymers as well as their cloud point temperature (CPT) were summarized in Table 7-3.

Table 7-3. Summary of polymer composition, number average molecular weight, glass transition temperature and cloud point temperature (CPT) in [C₂mim][NTf₂] (3 wt% concentration) of the terpolymers.

Polymers ^a	F _{BzMA} mol%	F _{MMA or FOEGMA} mol%	F _{VBK} mol%	M _n ^b kg mol ⁻¹	T _g ^c °C	CPT ^d °C
B80/M10/V10-40	74%	10%	16%	13.6	76	62
B70/M20/V10-40	65%	18%	17%	15.3	83	71
B60/M30/V10-40	60%	22%	18%	17.8	85	79
B50/M40/V10-40	51%	29%	20%	14.1	89	95 (82)
B80/M10/V10-15	75%	9%	16%	7.3	67	84
B80/M10/V10-80	77%	9%	14%	22.5	80	55
B87/O3/V10-40	88%	2%	10%	16.0	70	69
B85/O5/V10-40	86%	3%	11%	15.4	64	84 (59)
B83/O7/V10-40	81%	5%	14%	13.4	55	97 (84)
B80/O10/V10-40	79%	7%	14%	14.3	45	N/A ^e

^a Refer to Table E-1 in Appendix E for the synthesis conditions for these terpolymers; ^b Number average molecular weight of the copolymer measured by GPC relative to poly(methyl methacrylate) standards in THF at 40 °C; ^c Glass transition temperature of terpolymers measured by differential scanning calorimetry (DSC); ^d Cloud point temperature (CPT) defined by the temperature where 50% light transmittance was recorded during heating, the numbers in brackets are temperatures where 50% light transmittance was obtained during cooling; phase separation was irreversible if only one temperature was listed; ^e Solution remained clear up to 100 °C (upper temperature limit of the instrument)

7.3.2.1 Effect of varying solvophobic content in terpolymers on transition temperature and reversibility

The effect of varying solvophobic content (ie. F_{MMA} or F_{OEGMA}) on phase separation temperature and reversibility was a key objective of this study. The terpolymers mentioned in this section were all synthesized with the same target molecular weight (40 kg mol^{-1} at complete conversion) and had similar molecular weight (ranged from 13.4 to 17.8 kg mol^{-1}). Therefore, the variation of polymer composition was considered to be the dominant factor affecting the solution properties of these terpolymers. The light transmittance of these terpolymer solutions in $[\text{C}_2\text{mim}][\text{NTf}_2]$ as temperature was varied is shown in Figure 7-3, where 100% light transmittance indicates a transparent solution.

The first observation was that with increasing solvophobic content in the terpolymer, phase separation occurred at higher temperatures. This is consistent with the use of solvophobic co-monomers in a thermo-responsive polymer to increase copolymer solubility and LCST in both aqueous^{50,53} and IL²¹² solutions. The increase in CPT versus terpolymer composition of the solvophobic co-monomer (ie. F_{MMA} or F_{OEGMA} , Figure 7-4 (a)) may appear that MMA and OEGMA had very different impacts on the solvophobicity of the terpolymers. However, one should take note that for each MMA monomer, there is one solvophobic group, namely the ester group,²³⁸ whereas for each OEGMA monomer, there are multiple ethylene glycol (EG) units (~ 8.5 EG per OEGMA monomer in this case based on the average M_n of OEGMA used). Although the correlation between the number of EG units and polymer solubility in ILs has not been comprehensively studied, Horton et al. showed that the higher the number of EG units, the better the solubility of poly(methoxyoligo(ethylene glycol) methacrylates was in $[\text{C}_2\text{mim}][\text{NTf}_2]$ -saturated water.²⁶⁶ It is also well known that poly(ethylene glycol) is completely

soluble in $[\text{C}_2\text{mim}][\text{NTf}_2]$.^{23,267} Therefore, to make a better comparison of solvatophilicity between MMA and OEGMA co-monomers, the effect of terpolymer composition of MMA and that of EG units of the corresponding OEGMA on the cloud points were compared in Figure 7-4 (b). It shows that there exist similar effects of the concentration of solvatophilic groups in a polymer on the solvatophilicity of the overall polymer. This is interesting since one of the reasons why OEGMA and MMA were chosen as the solvatophilic co-monomers was that they have very different glass transition temperatures (T_g). T_g of POEGMA ($\sim -70\text{ }^\circ\text{C}$ ^{178,242}) is much lower compared to PMMA ($105\text{ }^\circ\text{C}$ ²⁴²). T_g of PBzMA is about $54\text{ }^\circ\text{C}$ ²⁴² and a random copolymer of BzMA and VBK with $\sim 10\text{ mol}\%$ VBK had a T_g of about $66\text{ }^\circ\text{C}$.¹⁴⁸ Therefore, the incorporation of MMA increased the overall T_g of the BzMA/MMA/VBK terpolymers (from 76 to $89\text{ }^\circ\text{C}$ as F_{MMA} increased from 10 to $29\text{ mol}\%$) whereas the OEGMA content in the BzMA/OEGMA/VBK decreased the terpolymer T_g (from 70 to $45\text{ }^\circ\text{C}$ as F_{OEGMA} increased from 2 to $7\text{ mol}\%$). Despite the higher T_g of the BzMA/MMA/VBK terpolymers, their CPTs were comparable to those of BzMA/OEGMA/VBK terpolymers with similar concentration of solvatophilic group but lower T_g . It indicated that the concentration of solvatophilic groups was a dominant factor affecting the cloud point of the terpolymer in the solution.

In some cases of thermo-responsive polymers with a solvatophilic co-monomer, the phase separation of the copolymers can become sluggish or the copolymers can even completely lose their thermo-responsiveness.^{48,53,192} With up to $F_{\text{MMA}} = 29\text{ mol}\%$ (B50/M40/V10-40) for the BzMA/MMA/VBK terpolymers or $F_{\text{OEGMA}} = 5\text{ mol}\%$ (or $F_{\text{EG unit}} = 31\text{ mol}\%$, B83/O7/V/10-40) for the BzMA/OEGMA/VBK terpolymers, the decrease in light transmittance as the solutions were heated above the CPT was sharp in all cases. Since the heating rate remained the same, it

means that the introduction of solvatophilic MMA or OEGMA did not significantly affect the aggregation kinetics within the composition range studied.

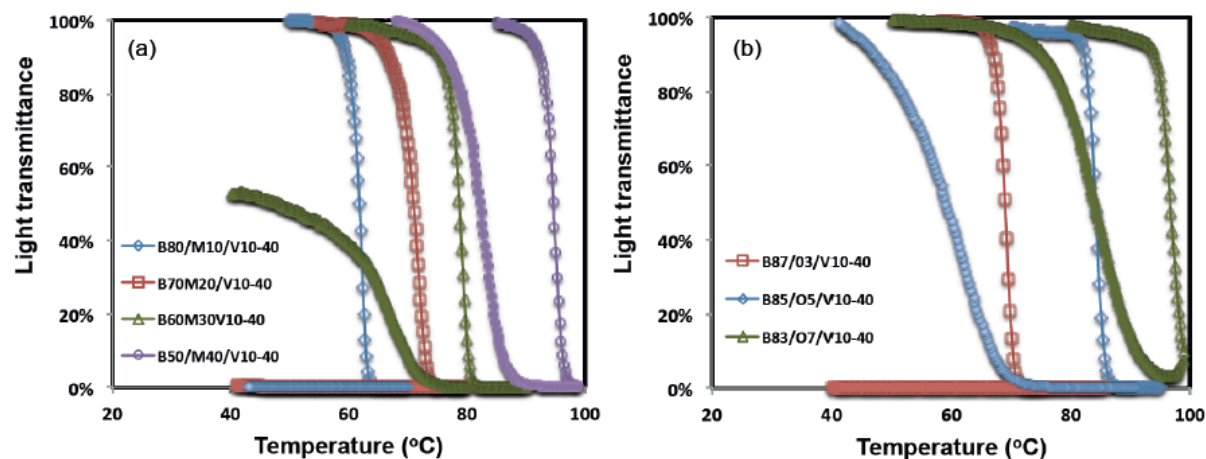


Figure 7-3. Light transmittance of 3 wt% terpolymer in ionic liquid solutions of (a) BzMA/MMA/VBK terpolymers, and (b) BzMA/OEGMA/VBK terpolymers with heating/cooling rate of $1\text{ }^{\circ}\text{C min}^{-1}$ (heating cycles with hollow symbols and cooling cycles with solid symbols).

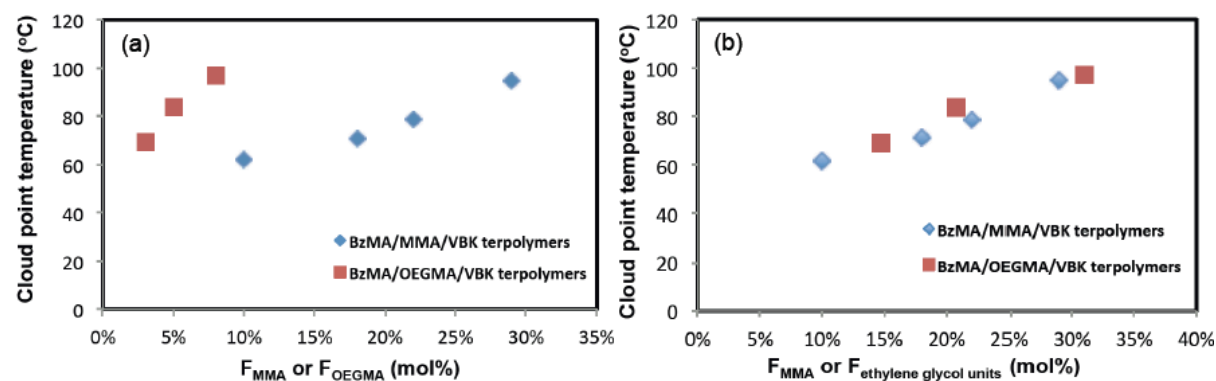


Figure 7-4. Cloud point temperature of 3 wt% solutions of BzMA/MMA/VBK (blue diamonds) and BzMA/OEGMA/VBK terpolymers (red squares) versus (a) terpolymer composition of MMA (F_{MMA}) or terpolymer composition of OEGMA (F_{OEGMA}); (b) terpolymer composition of MMA (F_{MMA}) or terpolymer composition of ethylene glycol units ($F_{\text{ethylene glycol units}}$, calculated by $(F_{\text{OEGMA}} \times 8.5)/(F_{\text{BzMA}} + F_{\text{VBK}} + F_{\text{OEGMA}} \times 8.5) \times 100\%$, 8.5 being the average number of ethylene glycol units in each OEGMA monomer according to the M_n of the monomer).

Regarding reversibility of the phase separation, BzMA/MMA/VBK terpolymers exhibited irreversible phase separation below $F_{\text{MMA}} = 18$ mol% (B70/M20/V10-40). B60/M30/V10-40 with $F_{\text{MMA}} = 22$ mol% showed partial reversibility where the light transmittance of its solution increased up to about 60% after cooling; the phase separation of B50/M40/V10-40 with $F_{\text{MMA}} = 29$ mol% was observed to be completely reversed (ie. the light transmittance was restored to 100% after cooling).

By comparison, for BzMA/OEGMA/VBK terpolymers, the phase separation of B87/O3/V10-40 ($F_{\text{OEGMA}} = 2$ mol% or $F_{\text{EG units}} = 15$ mol%) was totally irreversible. Complete reversal of phase separation was observed for both B8505V10-40 ($F_{\text{OEGMA}} = 3$ mol% or $F_{\text{EG units}} = 21$ mol%) and B83/O7/V10-40 ($F_{\text{OEGMA}} = 5$ mol% or $F_{\text{EG units}} = 31$ mol%). Hysteresis, or the difference between phase separation temperature and re-dissolution temperature, defined as the temperatures where light transmittance was measured to be 50% during heating and cooling, respectively, decreased from 25 °C for B85/05/V10-40 to 13 °C for B83/O7/V10-40. These results indicated that the reversibility of the phase separation for BzMA-rich terpolymers with a highly solvophobic constituent (VBK) can be restored by incorporating sufficient amount of solvophilic group (threshold between about 20 – 30 mol% of solvophilic structure (ie. ester group in MMA or EG units in OEGMA) for both types of terpolymers).

One cannot however explain the restoration of reversibility of phase separation without understanding the mechanism of solvation. The dissolution of PBzMA in the IL was a result of the organization of the $[\text{NTf}_2]$ anions around the equatorial position of the benzene plane of BzMA units and the imidazolium cation above and below the benzene ring's plane,⁶² leading to a negative entropic term during mixing. As temperature rose, the increased kinetic energy of the ions led to liberation of the ions from the polymer, which resulted in phase separation. The

potential π - π interactions between the benzyl group of BzMA units as well as those between BzMA and aromatic groups of VBK in the collapsed state can highly restrict the diffusion of IL ions to the polymers and render re-dissolution of the polymer impossible. A similar explanation is presented for PNIPAM (one of the most widely studied thermo-responsive polymer in aqueous solution), where the intramolecular hydrogen bonding in the globule state of PNIPAM act as “cross-linkers” and slowed re-dissolution.^{209,246}

In this case, the statistically distributed solvophilic groups throughout the terpolymer chains served as “separators” to increase the distance and reduce interactions between like BzMA units and between BzMA and VBK units, therefore making the polymer aggregate less compact and more available for IL diffusion during cooling.¹⁹²

Kodama et al. reported that the rate of re-dissolution of PBzMA and its derivatives in various imidazolium-based ILs could be roughly correlated to the difference between polymer T_g and CPT of each polymer/IL system, ie. $(CPT - T_g)$.²³⁸ The correlation was attributed to an established empirical relation between polymer relaxation time and $(T - T_g)$.^{238,265} This is plausible since when $CPT - T_g \gg$ zero, the polymer chains were flexible when the re-dissolution process started, which can accelerate mutual diffusion between polymer chains and solvent during re-dissolution. For BzMA/OEGMA/VBK terpolymers, complete re-dissolution was observed when $(CPT - T_g)$ increased from -1 to 20 °C and T_g of the terpolymers decreased from 70 to 64 °C. For the BzMA/MMA/VBK terpolymers, the phase separation became reversible when $(CPT - T_g)$ increased from -6 to 6 °C even though T_g of the terpolymers increased from 85 to 89 °C. It appeared that the T_g of the polymer alone was not crucial for re-dissolution to occur, but the polymer needed to be sufficiently solvophilic so that its CPT had to be higher than its T_g to undergo reversible phase separation.

7.3.2.2 Effects of solution concentration on transition temperature and reversibility

To investigate the effects of solution concentration on phase separation temperature and reversibility, a BzMA/MMA/VBK terpolymer (B60/M30/V10-40) and a BzMA/OEGMA/VBK terpolymer (B85/O5/V10-40) were dissolved in $[C_2mim][NTf_2]$ at concentrations varying from 1 to 10 wt%. The light transmittance of these solutions at varying temperature is shown in Figure 7-5. These two specific terpolymers were chosen because their phase separation reversibility was only partially restored at 3 wt% concentration (B60/M30/V10-40 solution showed light transmittance up to 60% during cooling; B85/O5/V10-40 phase separation was completely reversed with a large hysteresis of 25 °C). Therefore, the effects of solution concentration on the re-dissolution properties were likely the most apparent.

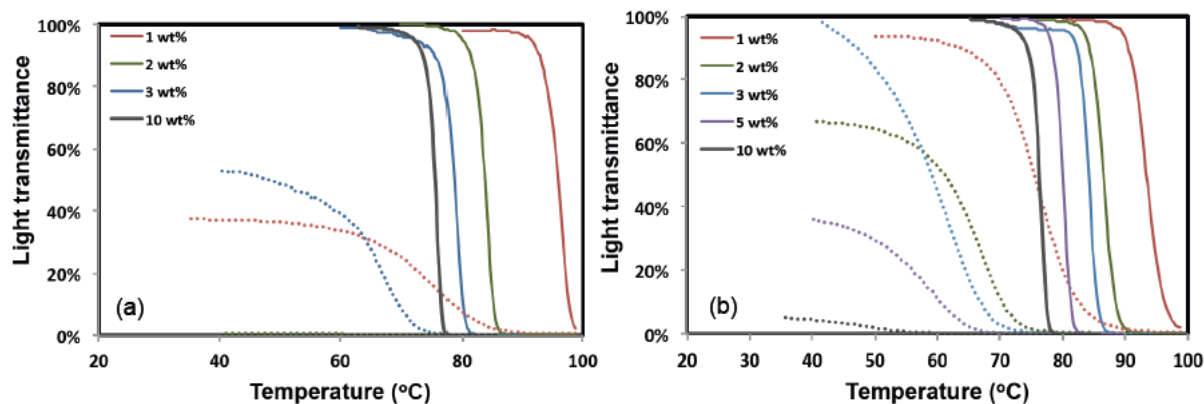


Figure 7-5. Light transmittance of 3 wt% terpolymer in ionic liquid solutions of (a) B60/M30/V10-40 ($F_{BzMA} = 60$ mol%, $F_{MMA} = 22$ mol%, $F_{VBK} = 18$ mol%), and (b) B85/O5/V10-40 ($F_{BzMA} = 86$ mol%, $F_{OEGMA} = 3$ mol%, $F_{VBK} = 11$ mol%) at various solution concentrations (heating cycles with solid lines and cooling cycles with dotted lines).

From Figure 7-5, the most noticeable effect of solution concentration for these two terpolymers was the decreasing CPT with increasing solution concentration. For both terpolymers, CPT decreased by about 20 °C as concentration increased from 1 to 10 wt% (96 to 75 °C for B60/M30/V10-40 and 93 to 76 °C for B85/O5/V10-40). This general trend of decreasing CPT

with increasing solution concentration was consistent with other polymers with LCSTs in both aqueous^{47,182} and IL⁶³ solutions.

It should be noted that there are some differences in the concentration effect between aqueous and IL solutions. In aqueous solutions, the transition temperature is usually only sensitive to concentration in dilute solutions (typically below ~ 1 wt%)^{47,53,183,268} By comparison, in IL solutions, the transition temperature remained sensitive to concentration changes at higher concentrations. In this study, the CPT of the terpolymer solutions decreased continuously with increasing concentration up to 10 wt%. Similarly, Lee et al. reported that the CPT of poly(*n*-butyl methacrylate) solutions in an IL changed gradually by more than 40 °C from 0.25 to 5 wt%.⁶³ Since thermo-responsive polymers were sensitive to a wider range of concentrations in ILs and the change in transition temperature can be substantial, solution concentration can be a very useful tool to fine tune LCST in IL solutions.

For reversibility, it was observed that with lower polymer concentration, a higher degree of re-dissolution, indicated by higher light transmittance after cooling, could be generally achieved. At 10 wt%, both terpolymers showed completely irreversible phase separation. Below 10 wt%, various degrees of reversibility were observed. For B60/M30/V10-40, its solutions at 1 wt% and 3 wt% showed about 40% and 60% light transmittance after cooling, respectively, whereas the solution at 2 wt% exhibited irreversible phase separation. For B85/O5/V10-40, its solution at 1, 2, 3, and 5 wt% showed maximum light transmittance of about 95%, 65%, 100%, 40% after cooling, respectively. Replicates of the 2 and 3 wt% solutions showed that the results of both CPT and light transmittance after cooling were reproducible. Thus, although it is more intuitive to assume polymer in more dilute solution would re-dissolve more readily after phase separation,

solution concentration did not correlate strongly with the extent of re-dissolution in the range of 1 – 5 wt%.

7.3.2.3 Effects of molecular weight on transition temperature and reversibility

The effects of number average molecular weight (\bar{M}_n) on transition temperature and reversibility were illustrated using BzMA/MMA/VBK terpolymers of similar composition ($F_{\text{BzMA}} \sim 75$ mol%, $F_{\text{MMA}} \sim 10$ mol%, $F_{\text{VBK}} \sim 15$ mol%) at three different \bar{M}_n s (7.3, 13.6, 22.5 kg mol⁻¹) in Figure 7-6 (a). These terpolymers were synthesized with the same feed composition (80 mol% BzMA, 10 mol% MMA and 10 mol% VBK, noted as B80/M10/V10-15, B80/M10/V10-40, B80/M10/V10-80 in Table 7-2) and the LCST behaviour of B80/M10/V10-40 was already demonstrated in Figure 7-3. This particular composition was used because CPT could not be obtained for terpolymers with higher MMA content at low $\bar{M}_n \sim 7$ kg mol⁻¹ (ie. no phase separation up to the instrument upper limit, 100 °C).

As \bar{M}_n increased from 7.3 to 22.5 kg mol⁻¹, CPT decreased significantly from 84 to 55 °C. This trend of decreasing CPT with increasing \bar{M}_n is consistent with other thermo-responsive polymers in ILs.^{63,64} The inverse dependency of LCST in aqueous solutions on molecular weight was also well documented.^{70,74,269} Zhu et al.⁷⁰ demonstrated experimentally that the contribution to the entropy of mixing decreased significantly with increasing chain length, which makes dissolution more difficult, or in other words, favors phase separation. It was also shown by Patterson⁷⁴ that LCST is proportional to the critical value of the Flory-Huggins interaction parameter (χ_c), which can be correlated to the ratio of molar volume of polymer to that of the solvent (r):

Equation 7-1

$$\chi_c = \frac{(1 + 1/\sqrt{r})^2}{2}$$

Using Equation 7-1, LCST decreases when r increases. As the molar volume of polymer is proportional to polymer chain length, it is clear that LCST has to decrease with increasing molecular weight.

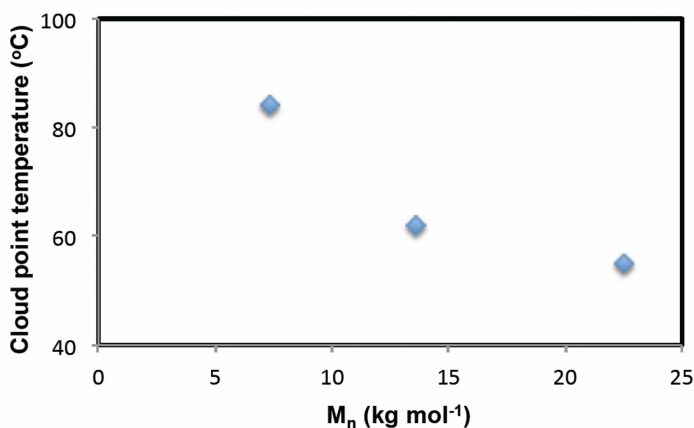


Figure 7-6. Cloud point temperature of 3 wt% solutions in [C₂mim][NTf₂] of B80/M10/V10-10 (F_{BzMA} = 75 mol%, F_{MMA} = 9 mol%, F_{VBK} = 16 mol%), B80/M10/V10-40 (F_{BzMA} = 74 mol%, F_{MMA} = 10 mol%, F_{VBK} = 16 mol%), and B80/M10/V10-80 (F_{BzMA} = 77 mol%, F_{MMA} = 9 mol%, F_{VBK} = 14 mol%) versus M_n relative to PMMA standards.

Regarding phase separation reversibility, all three terpolymers cited above showed irreversible phase separation. The value of (CPT – T_g) of each polymer/IL system was used earlier to represent the flexibility of the polymer chains at the start of re-dissolution process and the larger the value, the faster the mutual diffusion between polymer chains and IL ions and hence the re-dissolution process. Interestingly, the value of (CPT- T_g) of B80/M10/V10-15 (F_{MMA} = 9 mol%) was 17 °C, which was larger than the (CPT – T_g) of 6 °C for B50/M40/V10-40 (F_{MMA} = 29 mol%). However, B80/M10/V10-15 showed irreversible phase separation while the phase

separation for B50/M40/V10-40 was reversible. Therefore, one should be careful that the value of $(CPT - T_g)$ may be used to correlate to re-dissolution kinetics, but it cannot be used as an indicator for whether re-dissolution would occur or not. Since the only difference between the two terpolymers besides \bar{M}_n (and hence T_g) was their compositions, these results illustrated that although \bar{M}_n and T_g played important roles in the CPT of the terpolymers, sufficiently high concentration of solvophilic groups in the terpolymer was necessary to drive the re-dissolution process.

7.3.2.4 Reversibility of the phase separation and terpolymer fluorescent properties

After discovering incorporating a sufficient amount of solvophilic co-monomer could restore phase separation reversibility, verification of the reversibility under repeated heating and cooling was studied. IL solutions of B50/M40/V10-40 ($F_{BzMA} = 51$ mol%, $F_{MMA} = 29$ mol%, $F_{VBK} = 20$ mol%) and B83/O7/V10-40 ($F_{BzMA} = 81$ mol%, $F_{OEGMA} = 5$ mol% (eq. $F_{EG\ units} = 31$ mol%), $F_{VBK} = 14$ mol%) were heated above their CPT and then cooled to room temperature four times consecutively while the solution light transmittance was monitored. As shown in Figure 7-7, all heat/cool cycles appeared to be very similar. Slightly faster re-dissolution was observed during the first cooling compared to the consequent cycles for both terpolymers. Nonetheless, hysteresis stayed relatively constant with ± 1 °C variance during all the cycles for both terpolymers. Therefore, we concluded that the phase separation reversibility of both terpolymers was predictable and consistent for at least 4 heat/cool cycles.

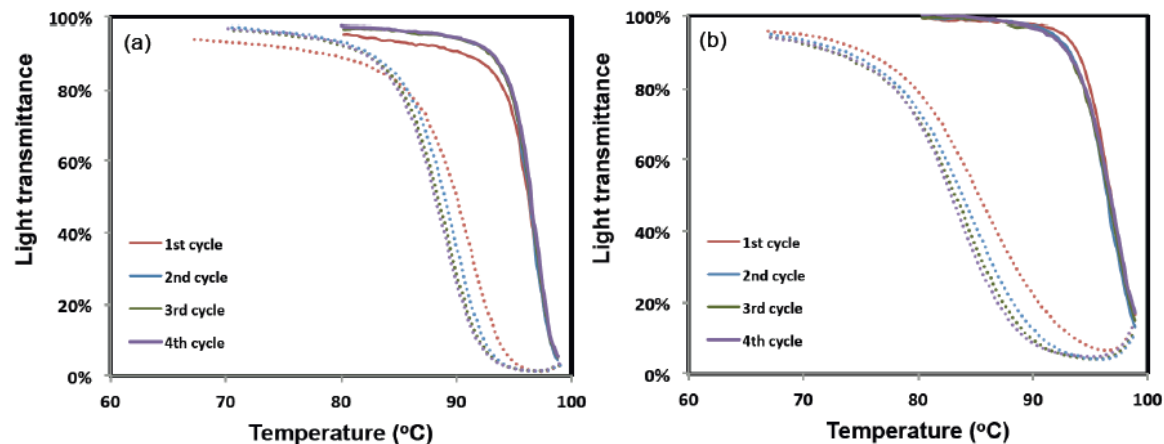


Figure 7-7. Light transmittance of (a) B50/M4/0M10-40 ($F_{BzMA} = 51 \text{ mol\%}$, $F_{MMA} = 29 \text{ mol\%}$, $F_{VBK} = 20 \text{ mol\%}$) and (b) B83/O7/V10-40 ($F_{BzMA} = 81 \text{ mol\%}$, $F_{OEGMA} = 5 \text{ mol\%}$, $F_{VBK} = 14 \text{ mol\%}$) in 3 wt% $[C_2mim][NTf_2]$ solutions during 4 consecutive heat/cool cycles (solid line represents heating and dotted line represent cooling).

In our previous study,¹⁴⁸ an interesting fluorescence phenomena was observed for BzMA/VBK random copolymers in $[C_2mim][NTf_2]$ where the fluorescence intensity of the solution increased sharply as the copolymer phase separated from the IL. It was attributed to the enhanced fluorescence resonance energy transfer (FRET) efficiency between BzMA and VBK after phase separation because of its strong dependency on the donor/acceptor distance.^{148,251} Since phase separation reversibility could be restored, fluorescence enhancement triggered by the phase separation was expected to be reversible as well. Therefore, the fluorescence intensity of B50/M40/V10-40 and B83/O7/V10-40 in $[C_2mim][NTf_2]$ was measured while the solution was heated and cooled for 3 consecutive cycles (Figure 7-8).

For B50/M40/V10-40, the maximum fluorescence intensity remained relatively constant as the solution was heated until the CPT of 95 °C, after which the intensity increased rapidly by about 2-fold. For B83/O7/V10-40, similar fluorescence enhancement at its CPT was observed to be about 5-fold during the first heating cycle and about 3-fold during the two consequent cycles. In

the previous study of BzMA/VBK copolymers, the enhancement was observed to be about 5-fold.¹⁴⁸ The decrease in enhancement for the terpolymers can be a result of the collisions between BzMA or VBK and MMA or OEGMA units, causing non-radiative relaxation.²⁷⁰

It was also noted that the fluorescence behaviour of the terpolymers was different during the first cycle compared to the two consequent cycles. The terpolymers were dissolved in the IL at temperature below their T_g s. Therefore, internal stresses may develop while the glassy polymer chains were changing their conformation in the viscous solutions.^{271,272} These stresses can be relaxed after the first heating, resulting in different polymer chain conformations and consequently different fluorescence properties for subsequent cycles.

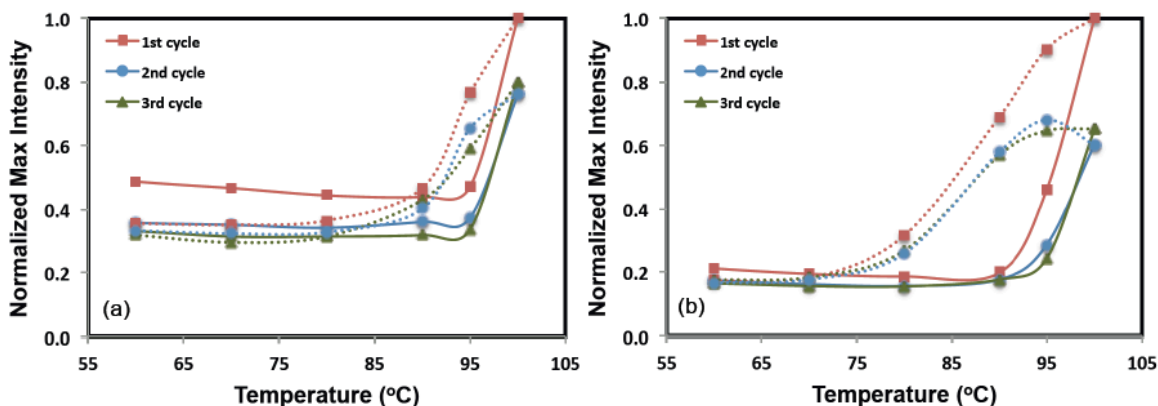


Figure 7-8. Normalized maximum fluorescence intensity (excitation at 330 nm) of (a) B50/M40/M10-40 ($F_{\text{BzMA}} = 51 \text{ mol}\%$, $F_{\text{MMA}} = 29 \text{ mol}\%$, $F_{\text{VBK}} = 20 \text{ mol}\%$) and (b) B83/O7/V10-40 ($F_{\text{BzMA}} = 80 \text{ mol}\%$, $F_{\text{OEGMA}} = 8 \text{ mol}\%$, $F_{\text{VBK}} = 12 \text{ mol}\%$) in 3 wt% $[\text{C}_2\text{mim}][\text{NTf}_2]$ solutions during 3 consecutive heat/cool cycles (solid line represents heating and dotted line represent cooling).

Lastly, the reduction in fluorescence intensity during cooling was observed to be more gradual than the enhancement during heating for all cycles. The hysteresis in fluorescence response can be explained by the much more rapid process of aggregation than re-dissolution for both

terpolymer systems studied.²⁶² The slow swelling process of the aggregates during cooling led to a gradual increase in distance between BzMA and VBK. Consequently, the FRET efficiency did not decrease as sharply during cooling as when it increased during phase separation. Thus, the fluorescence enhancement was confirmed to be essentially reversible and relatively consistent during the 3 consecutive heat/cool cycles for both of the selected BzMA/MMA/VBK and BzMA/OEGMA/VBK terpolymers.

7.4 Conclusions

Terpolymers of BzMA/MMA/VBK and BzMA/OEGMA/VBK were synthesized via NMP with fixed $f_{\text{VBK},0} = 10$ mol% and varying BzMA/MMA ($f_{\text{BzMA},0}:f_{\text{MMA},0} = 80:10$ to $50:40$) or BzMA/OEGMA ($f_{\text{BzMA},0}:f_{\text{OEGMA},0} = 87:3$ to $80:10$) compositions at 90 °C in a controlled manner.

The concentration of solvatophilic groups (ie. ester group in MMA and EG units in OEGMA) was illustrated to be the dominant factor affecting solubility and the extent of re-dissolution of the terpolymers in $[\text{C}_2\text{mim}][\text{NTf}_2]$. A minimum of 20 – 30 mol% solvatophilic groups was found necessary to facilitate complete re-dissolution for both terpolymer systems. Both increasing solution concentration and molecular weight resulted in decreased CPT. However, the solution concentration correlated weakly with the extent of re-dissolution and irreversible phase separation was observed for the lowest M_n (7.3 kg mol^{-1}) investigated.

Finally, the phase separation reversibility of the two terpolymer systems was demonstrated to be consistent and predictable for at least 4 consecutive heat/cool cycles. The fluorescence response was also shown to be reversible and relatively consistent within 3 heat/cool cycles.

In summary, the incorporation of the solvophilic content in the terpolymer with BzMA and VBK was successful in facilitating and accelerating the re-dissolution process of the terpolymer after its LCST phase separation in the IL. We showed that the solvophilicity can be quantified and tuned by adjusting the composition of solvophilic groups in the terpolymers. To our knowledge, this is the first time the effects of solvophilicity of polymers on the LCST phase separation and reversibility in IL solutions were studied quantitatively. The encouraging results represented an important step towards the development of robust and reusable fluorescence-based temperature sensitive devices based on polymer/IL solutions.

Acknowledgements

The authors are very grateful for the funding from the NSERC Postgraduate Scholarship, NSERC Discovery Grant and Canada Foundation for Innovation New Opportunities Fund. They also thank Prof. Bruce Lennox (Dept. of Chemistry, McGill University), for providing access to his temperature modulated UV-vis spectrometer. We also thank Arkema (Scott Schmidt and Noah Macy) for supplying BloBuilder and SG1.

References

Please refer to the global bibliography at the end of the thesis.

Chapter 8

Conclusions

8.1 Summary

The overall objective of this Ph.D. thesis is to illustrate the versatility of NMP as a synthetic technique for well-defined stimuli-responsive polymers and the various approaches to modify and fine-tune the properties of these “smart” polymers. All projects described in this thesis employed the methodology of using the commercially available alkoxyamine initiator BlocBuilder™ and a small amount of controlling co-monomer to yield methacrylate-rich polymers. The first part of the thesis (Chapter 3 and 4) details synthesis and characterization of copolymers based on 2-(dimethylamino)ethyl methacrylate (DMAEMA) which are pH and temperature-sensitive in aqueous solutions; the second part of the thesis (Chapter 5 – 7) focuses on benzyl methacrylate (BzMA)-rich copolymers (and terpolymers) which are thermo-responsive in ionic liquid (IL) solutions.

Styrene was initially used as the controlling co-monomer for DMAEMA. About 10 mol% styrene in the feed was found to be sufficient to yield copolymers with relatively narrow molecular weight distribution and ability to chain extend with a fresh batch of monomer (Chapter 3). The incorporation of styrene decreased the hydrophilicity of the DMAEMA/styrene copolymers and consequently lowered the LCST of the copolymers in aqueous solutions, as expected. The copolymers were completely water-soluble at pH 4 as DMAEMA was totally protonated; whereas at pH 10 when DMAEMA was neutral, copolymers with more than 15 mol% styrene was insoluble.

After confirming NMP was a valid technique to synthesize well-defined DMAEMA-rich copolymers, 2-vinylpyridine (2VP) was used as an alternative controlling co-monomer (Chapter 4). 2VP was shown to be effective in controlling copolymerizations with up to 98 mol% DMAEMA in the feed. Since 2VP was less hydrophobic than styrene, all copolymers synthesized ($F_{2VP} = 7 - 24$ mol%) were water-soluble from pH 7 – 11, which allowed fine-tuning of the copolymer LCST in the range of 14 – 75 °C. A block copolymer made by chain extension of a DMAEMA/2VP copolymer with a fresh batch of 2VP was illustrated to form pH-induced micelles due to the pH sensitivity of 2VP.

A modified alkoxyamine bearing a succinimidyl ester (NHS-BlocBuilder) made by coupling of BlocBuilderTM and *N*-hydroxysuccinimide was used in both of the DMAEMA studies. The succinimidyl ester can be used in pre- or post-polymerization conjugation to amine-containing compounds, which was demonstrated in Chapter 4 where amine-terminated poly(propylene glycol) (PPG) was coupled with NHS-BlocBuilder to yield an effective macroinitiator for the synthesis of doubly thermo-responsive PPG-*block*-P(DMAEMA/2VP) block copolymer.

Similar to the DMAEMA studies, BzMA was first copolymerized with varying amounts of styrene to validate NMP as the synthesis technique (Chapter 5) for well-defined BzMA-rich copolymers. The copolymerizations with as little as 10 mol% styrene in the feed showed linear increase in molecular weight with conversion and relatively narrow molecular weight distribution. However, chain extension was only successful when copolymers had at least 20 mol% styrene.

To reduce the necessary concentration of controlling co-monomer and impart additional functionality, 9-(4-vinylbenzyl)-9H-carbazole (VBK) was chosen to copolymerize with BzMA

(Chapter 6). As little as 2 mol% of VBK in the feed was shown sufficient for producing well-defined BzMA/VBK copolymers that were able to be the macroinitiator to form block copolymers with a fresh batch of monomer. The copolymers exhibited interesting phase separation-triggered fluorescence enhancements in the IL solutions, which resulted from the increased efficiency of fluorescent resonance energy transfer (FRET) between BzMA and VBK units during aggregation. However, the incorporation of solvophobic VBK also rendered the phase separation irreversible, making the temperature-sensitive fluorescence response less attractive.

In attempts to restore phase separation reversibility of BzMA/VBK copolymers in IL, varying amounts of solvophilic compound (methyl methacrylate (MMA) or oligo(ethylene glycol)methyl methacrylate (OEGMA)) were incorporated to obtain terpolymers of BzMA/MMA/VBK and BzMA/OEGMA/VBK (Chapter 7). A minimum of about 20 – 30 mol% of solvophilic groups (ester group for MMA or ethylene glycol group for OEGMA) in the terpolymers was found to be essential to obtain reversible phase separation. Molecular weight, glass transition temperature and solution concentration affected phase separation temperature significantly, but solvophilicity was shown to play the dominant role facilitating the redissolution process.

The use of functional controlling co-monomer for copolymerizations of methacrylates has been demonstrated as an effective way to yield functional and stimuli-responsive polymers via NMP. This thesis showcases NMP as a versatile synthesis technique for stimuli-responsive polymers and provides new insights to property tuning of these smart materials.

8.2 Statement of contributions

The projects involved in this Ph.D. thesis have resulted in the following contributions to the fields of experimental polymer synthesis and stimuli-responsive polymers:

1. I demonstrated that α -functional and stimuli-responsive DMAEMA-rich copolymers could be synthesized in a controlled manner by NMP using as little as 5 mol% styrene or 2 mol% 2VP as the controlling co-monomer and the modified alkoxyamine initiator bearing a succinimidyl ester (NHS-BlocBuilder) made by coupling of the commercially available initiator BlocBuilderTM and *N*-hydroxysuccinimide (Chapter 3 and 4). The effects of feed composition on kinetics and molecular weight increase with conversion were discussed in details. The “livingness” of the copolymers was illustrated by chain extension with a fresh batch of monomer(s). I also showed that unlike polymerizations initiated by BlocBuilderTM, additional free nitroxide was not necessary and posted no obvious benefits to synthesis control when using NHS-BlocBuilder (Chapter 4).
2. By employing 2VP as a controlling co-monomer for DMAEMA-rich copolymerizations, I reported for the first time that 2VP can be used as an effective controlling co-monomers for methacrylate-rich feeds by NMP (Chapter 4). The copolymerizations of DMAEMA with 2VP were performed at the same experimental conditions as the DMAEMA/styrene copolymerizations, thereby allowing side-by-side comparisons between the two controlling co-monomers. I found that the effects of styrene and 2VP on copolymerization kinetics and molecular weight distributions of the copolymers with similar composition were very similar.

3. I characterized the solution properties of DMAEMA/styrene copolymers using UV-Vis spectrometry and dynamic light scattering, establishing that the CPT of these copolymers can be effectively tuned by changing polymer composition (in the range of $F_{\text{styrene}} = 4 - 19$ mol%), pH (neutral or basic conditions), solution concentration (from 0.1 – 0.5 wt%) and molecular weight (in the range of 10 – 30 kg mol⁻¹) (Chapter 3).

4. I demonstrated the practicality of the succinimidyl ester group of the NHS-BlocBuilder by synthesizing a macroinitiator from conjugating NHS-BlocBuilder and amine-terminated poly(propylene glycol) (PPG), which was later initiated to form a doubly thermo-responsive PPG-*block*-DMAEMA/2VP block copolymer (Chapter 4).

5. I illustrated that pH (in the range of 7 – 10, when DMAEMA is partially ionized) played the dominant role on determining the cloud point temperature (CPT) and hysteresis of the DMAEMA/2VP copolymers in aqueous solutions. I also showed that the effect of polymer composition on CPT diminished as the degree of ionization of DMAEMA changed from 0 to 100% (Chapter 4).

6. I showed that block copolymers that form pH-induced micelles can be synthesized by NMP via chain extension of a statistical DMAEMA/2VP copolymer with 2VP, yielding a diblock copolymer DMAEMA/2VP-*block*-2VP. I demonstrated that this diblock

copolymer formed stable micelles with 2VP core and DMAEMA/2VP corona as pH increased above 5 in aqueous solutions at room temperature (Chapter 4).

7. I demonstrated that controlled synthesis of BzMA-rich copolymers could be done by NMP for the first time when a small amount of styrene was used as co-monomer. The kinetics, molecular weight increase with conversion, capability of the copolymers to form block copolymers, as well as reactivity ratios of BzMA and styrene were reported (Chapter 5).
8. I demonstrated that by using VBK as the controlling co-monomer, the product of average propagation rate constant and average equilibrium constant, $\langle k_p \rangle \langle K \rangle$, for BzMA/VBK copolymerizations was 2 orders of magnitude lower than that for BzMA/styrene copolymerizations with similar feed composition. The much slower kinetics allowed controlled synthesis of well-defined and “living” BzMA-rich copolymers with as little as 2 mol% VBK in contrast to 20 mol% styrene in the feed (Chapter 6).
9. I showed that the incorporation of VBK in the BzMA/VBK copolymers not only lowered the CPT of the copolymers in the IL $[\text{C}_2\text{mim}][\text{NTf}_2]$, but also rendered the phase separation completely irreversible. Using fluorescence spectrophotometer and Raman spectroscopy, I also demonstrated that the fluorescence signal for the BzMA/VBK copolymer was a result of fluorescence resonance energy transfer (FRET) from BzMA to

VBK, which led to 5-fold fluorescence enhancements during phase separation from heightened FRET efficiency between BzMA and VBK in close proximity (Chapter 6).

10. By characterizing terpolymers of BzMA/MMA/VBK and BzMA/OEGMA/VBK, I demonstrated that the re-dissolution process after phase separation was driven by the increasing amount of solvophilic groups, effectively restoring phase separation reversibility while maintaining thermo-responsiveness and fluorescent response of the terpolymers. I also established that molecular weight and solution concentration had significant effects on phase separation temperature but did not contribute significantly in facilitating the re-dissolution process within the studied range. (Chapter 7)

8.3 Recommendations for future work

While several advances to the synthesis and property tuning of stimuli-responsive polymers were made from this Ph.D. thesis, much possibilities in material designs remains unexplored. A few follow-up studies based on the results presented in this thesis merit consideration:

1. The pH sensitivity of 2VP could be further explored as a co-monomer with other pH-sensitive co-monomers such as methacrylic acid or acrylic acid to yield polyampholytes (polyelectrolytes bearing both cationic and anionic repeating groups) by NMP. The mechanical properties and pH sensitivities of these polyampholytes can be manipulated through controlling the polymer composition and microstructure. Polyampholytes can be useful for many applications, especially in the biomedical field.²⁷³ One should be able to tune the ranges of pH where such polyampholytes are soluble in aqueous solutions by

changing the copolymer composition. Di-block or tri-block copolymers with a polyampholyte block, a thermo- or pH-responsive block or a combination of these blocks could be used to create reverse micelles or self-assemble into more sophisticated microstructures. Hydrogels constructed using these polyampholytes can exhibit pH-sensitive swelling.

2. The use of the succinimidyl ester group of NHS-BlocBuilder can be further explored for hydrogel synthesis. This can be achieved by first conjugating NHS-BlocBuilder to poly(ethylene glycol) (PEG) with 2 amine-terminated ends, yielding a macroinitiator for synthesizing tri-block copolymers that contains two temperature- or pH-sensitive side blocks and a hydrophilic center block. The stimuli responsive blocks of such tri-block copolymers can switch between soluble and insoluble state in aqueous solutions, effectively facilitating reversible solution-to-gel transitions.
3. Further investigation into the fluorescence resonance energy transfer (FRET) between BzMA and VBK should be considered. It is known that *n*-butyl methacrylate (nBMA) also exhibits LCST behaviour in hydrophobic ILs.⁶³ Since nBMA should not have any fluorescence properties due to lack of any aromatic structures, the fluorescent emission and excitation wavelength ranges as well as intensity variance in response to temperature changes of copolymers of nBMA and VBK in IL solutions would result solely from VBK. These results would provide interesting comparison to those of BzMA/VBK copolymers and possibly further verify if BzMA and VBK are indeed a FRET donor/acceptor pair.

4. Triblock copolymers with a solvophilic central block such as PMMA or PEG and two thermo-responsive blocks such as BzMA/MMA/VBK terpolymers can be used to reversibly gel ILs into ion gels that also exhibit temperature-sensitive fluorescence response, which could be useful for applications such as fluorescent molecular thermometers. This can be achieved by the use of reversible addition-fragmentation chain transfer polymerization (RAFT) from a telechelic PEG precursor,^{23,267} or atom transfer radical polymerization (ATRP) with di-functional PMMA macroinitiator,²⁷⁴ or NMP with a telechelic macroinitiator made by conjugating NHS-BlocBuilder and di-functional PEG. The properties of these reversible ion gels can then be compared with ion gels made by either in situ polymerization of compatible polymers in ILs²³⁴ or cross-linking reaction between monomers and a cross-linker in ILs.²⁷⁵

Appendices

Appendix A

Controlled Synthesis of Water-soluble and Stimuli-responsive copolymers with small amount of styrene by NMP

A.1 Experimental Section

A.1.1 Materials

Styrene (99%), 2-(dimethylamino)ethyl methacrylate (DMAEMA, 98%), *N,N'*-dicyclohexylcarbodiimide (DCC, 99.9%), *N*-hydroxysuccinimide (NHS, 98%), basic alumina (Brockmann, Type I, 150 mesh), and calcium hydride (90-95% reagent grade) were purchased from Aldrich. Tetrahydrofuran (THF, 99.9%), pentane and hexane were obtained from Fisher; deuterated chloroform (CDCl₃) was obtained from Cambridge Isotope Laboratories Inc. *N*-(2-methylpropyl)-*N*-(1-diethylphosphono-2,2-dimethylpropyl)-*O*-(2-carboxylprop-2-yl) hydroxylamine, also known as BlocBuilder (99%), was obtained from Arkema and was used as received. Styrene and DMAEMA monomers were purified by passing through a column of basic alumina mixed with 5 wt% calcium hydride; they were stored in a sealed flask under a head of nitrogen in a refrigerator until needed. All other compounds were used as received.

A.1.2 Synthesis of *N*-hydroxysuccinimide functionalized BlocBuilder (NHS-BlocBuilder)

The following procedures for the synthesis of NHS-BlocBuilder was first described by Vinas et al. and adapted for use here as follows.¹⁷¹ BlocBuilder (15.0 g, 38 mmol) and *N*-hydroxysuccinimide (NHS, 5.43 g, 47 mmol) were dissolved in dry THF (60 ml) and placed in

an ice-water bath. In a separate flask, *N,N'*-dicyclohexylcarbodiimide (DCC) was dissolved in 15 ml of dry THF. Both solutions were degassed by bubbling ultra-pure N₂ gas for 30 min. The degassed DCC solution was then added to the NHS/BlocBuilder solution. After stirring the mixed solution at 0 °C for 90 min, the precipitated *N,N'*-dicyclohexylurea (DCU) was removed by filtration. The filtrate was concentrated under reduced pressure to about one third of its volume. The residual DCU was precipitated at -20 °C overnight and removed by filtration. Precipitation of NHS-BlocBuilder was done in pentane and the obtained white solid was washed with de-ionized water to remove residual NHS. After drying under vacuum at room temperature, NHS-BlocBuilder was obtained as a white powder (10.6 g, 22 mmol, 56% yield). The structure of the NHS-BlocBuilder was confirmed by ¹H NMR (400 MHz, CDCl₃, δ, ppm): 1.1 – 1.4 (24H), 1.6 – 1.9 (6H), 2.7 – 2.9 (4H), 3.2 – 3.4 (1H), 3.9 – 4.4 (4H).

A.1.3 Synthesis of statistical copolymers of 2-(dimethylamino)ethyl methacrylate and styrene (poly(DMAEMA-*stat*-styrene)) by NMP

Statistical copolymerizations of DMAEMA and styrene were performed in a 50 mL three-neck round-bottom glass flask equipped with a reflux condenser and a thermal well. Target molecular weight (number average molecular weight M_n at 100% conversion) of 30 kg · mol⁻¹ was used for all copolymerizations. A typical procedure is given as an illustration. The initiator, *N*-hydroxysuccinimidyl-functionalized BlocBuilder (NHS-BlocBuilder, 0.097 g, 0.20 mmol), was dissolved in the monomer mixture (6.0 g) with initial molar compositions with respect to DMAEMA (f_{DMAEMA}) varied from 85 to 95 mol% (Table A-1). Dissolved oxygen in the mixture was removed by purging with an ultra-pure nitrogen flow for 30 min prior to heating. The mixture was then heated by a heating mantle to 80 °C at a rate of about 8 °C · min⁻¹ while

maintaining a nitrogen purge. The time when the mixture reached 80 °C was taken as the start of the reaction ($t = 0$). Samples were taken periodically to determine conversion and molecular weight. Polymerization was stopped when the reaction mixture became too viscous to withdraw samples. The copolymers were precipitated in hexane, decanted and dried in vacuum at room temperature overnight; the copolymers were then re-dissolved in THF, re-precipitated in hexane, decanted and dried under vacuum to obtain the final purified copolymers.

Table A-1. Experimental conditions of the bulk copolymerizations of 2-(dimethylamino)ethyl methacrylate (DMAEMA) and styrene (S) at 80 °C using *N*-hydroxysuccinimidyl-functionalized BlocBuilder (NHS-BlocBuilder) as initiator.

Experiment ID	[NHS-BlocBuilder]	[DMAEMA]	[Styrene]	f_{DMAEMA}^a	$M_{n,\text{target}}^b$
	mol L ⁻¹	mol L ⁻¹	mol L ⁻¹	mol%	kg mol ⁻¹
DMAEMA/S-95/5	0.031	5.729	0.313	95%	30.2
DMAEMA/S-90/10	0.031	5.529	0.608	90%	30.2
DMAEMA/S-85/15	0.032	5.340	0.885	86%	29.7
DMAEMA/S-80/20	0.031	5.068	1.287	80%	30.2

^a Initial feed composition with respect to DMAEMA. ^b Molecular weight at 100% conversion

Two chain extension experiments were performed using the copolymers synthesized. The copolymers DMAEMA/S-90/10 and DMAEMA/S-80/20 were used as the macroinitiators (0.35 g, 0.03 mmol). The chain-extensions were performed using the same methods as described for the statistical copolymerizations. The macroinitiator was chain-extended with a mixture of DMAEMA and styrene (a total of 3.0 g) after purging with nitrogen for 30 minutes followed by heating up to 80 °C. The work-up was identical to that used for statistical copolymerizations. The detailed experimental conditions are listed in Table A-2.

Table A-2. Experimental conditions of the chain extension experiments at 80 °C in bulk.

Macroinitiator	[Macroinitiator]	[DMAEMA]	[Styrene]	$f_{\text{DMAEMA}}^{\text{a}}$	$M_{\text{n,target}}^{\text{b}}$
	mol L ⁻¹	mol L ⁻¹	mol L ⁻¹	mol%	kg mol ⁻¹
DMAEMA/S-80/20	0.010	5.718	0.328	95%	107.2
DMAEMA/S-90/10	0.010	5.573	0.542	90%	106.1

^a Molar composition with respect to DMAEMA in the monomer mixture. ^b M_n of block copolymer at 100% conversion

A.1.4 Polymer characterization using Gel permeation chromatography (GPC) and Nuclear magnetic resonance (NMR)

Monomer conversion and copolymer composition were determined by ¹H NMR with a 400 MHz Varian Gemini 2000 spectrometer using CDCl₃ as solvent. Conversion of DMAEMA was calculated using the two protons adjacent to the ester oxygen of the monomer ($\delta = 3.7 - 3.8$ ppm) and those corresponding to the polymer ($\delta = 3.9 - 4.1$ ppm). Styrene conversion was determined using the three vinyl protons ($\delta = 6.6 - 6.7$, $5.6 - 5.7$, and $5.1 - 5.2$ ppm) of the monomers and the five aromatic protons of both monomers and polymers ($\delta = 6.9 - 7.2$ ppm). Average conversion was then calculated using the composition of the copolymers with respect to DMAEMA (F_{DMAEMA} , mol%) determined by the same NMR spectra ($\text{Conv.}_{\text{ave}} = F_{\text{DMAEMA}} \times \text{Conv.}_{\text{DMAEMA}} + (1 - F_{\text{DMAEMA}}) \times \text{Conv.}_{\text{styrene}}$). Molecular weight and dispersity (\mathcal{D}) were characterized by GPC (Waters Breeze) using THF as the mobile phase. The GPC was equipped with three Waters Styragel HR columns (molecular weight measurement ranges: HR1: $10^2 - 5 \times 10^3$ g·mol⁻¹, HR2: $5 \times 10^2 - 2 \times 10^4$ g·mol⁻¹, HR3: $5 \times 10^3 - 6 \times 10^5$ g·mol⁻¹) and a guard column. The columns were operated at 40 °C and a mobile phase flow rate of 0.3 mL·min⁻¹ during analysis. The GPC was also equipped with both ultraviolet (UV 2487) and differential refractive index (RI 2410) detectors. The molecular weight measurements were calibrated relative to poly(styrene) narrow molecular weight standards in THF at 40 °C. The percentage of copolymer chains capped by SG1 was determined using ³¹P NMR with a 200 MHz Varian Gemini 2000

spectrometer using CDCl_3 as solvent and diethyl phosphite (DEP) as internal standard. In each sample, known amounts of copolymer and DEP were dissolved in CDCl_3 . The ratio of SG1-capped chains to DEP was calculated using the ^{31}P resonance at $\delta = 24 - 27$ ppm for SG1 and $\delta = 8 - 9$ ppm for DEP. This ratio was then compared to the molar ratio of copolymer to DEP in the sample to calculate the percentage of SG1-capped chains.

A.1.5 Transition temperature characterization using UV-Visible spectrometry and Dynamic light scattering (DLS)

The statistical copolymers and block copolymers were dissolved in de-ionized water and buffer solutions of pH 4 and 10 with 0.1, 0.3 and 0.5 wt% concentrations. Light transmittance of the solutions at various temperatures was measured using a Cary 5000 UV-Vis-NIR Spectrophotometer at 600 nm. The solutions were equilibrated for 10 min at the starting temperature and then heated at a rate of $0.5\text{ }^\circ\text{C min}^{-1}$. The transmittance was recorded every $0.5\text{ }^\circ\text{C}$.

The DLS measurements for these solutions were performed using a Malvern ZetaSizer (Nano-ZS). The instrument was equipped with a He-Ne laser operating at 633 nm and an avalanche photodiode detector. In a typical DLS measurement, the solution was filtered using a 0.2 μm pore size filter into a plastic cuvette. The cuvette was then placed in the temperature-controlled measurement cell and equilibrated at the starting temperature for at least 30 min. Measurements were then performed automatically for every degree Celsius after an equilibration time of 2 min. The first-order intensity correlation function, $g_1(t)$, was measured at a scattering angle of 173° using Non-Invasive Back-Scatter (NIBS) and analyzed by the method of cumulants²⁷⁶ to estimate the average decay rate, Γ , and the width of the decay, μ_2/Γ^2 .

Equation A-1

$$g_1(t) = \exp[-\Gamma t + (\mu_2/2)t^2 - (\mu_3/3!)t^3 + \dots]$$

The average decay rate Γ is given by:

Equation A-2

$$\Gamma = Dq^2$$

where D is the translational diffusion coefficient, and q is the magnitude of the scattering vector defined as:

Equation A-3

$$q = \frac{4\pi n}{\lambda} \sin\left(\frac{\theta}{2}\right)$$

where n is the refractive index of the solvent, λ is the wavelength of the light in vacuum and θ is the scattering angle.

In the limit of low concentrations, D can be approximated as the diffusion coefficient for spherical particles, D_0 , which is related to the hydrodynamic radii of the particles, R_h , by the Stokes-Einstein equation:

Equation A-4

$$R_h = \frac{k_B T}{6\pi\eta D_0}$$

where k_B is the Boltzmann constant, T is temperature in Kelvin and η is the viscosity of the solvent.

Appendix B

α -Functional Statistical Copolymers with Dual pH and Temperature Responsiveness Made by NMP using 2-Vinylpyridine as “Controlling” Comonomer

B.1 Experimental Section

B.1.2 Materials

2-Vinylpyridine (2VP, 97%), 2-(dimethylamino)ethyl methacrylate (DMAEMA, 98%), *N,N'*-dicyclohexylcarbodiimide (99.9%), *N*-hydroxysuccinimide (98%), poly(propylene glycol)-bis(2-aminopropyl ether) ($M_n \sim 2000 \text{ g mol}^{-1}$), basic alumina (Brockmann, Type I, 150 mesh), and calcium hydride (90-95% reagent grade) were purchased from Sigma-Aldrich. Tetrahydrofuran (THF, 99.9%), pentane and hexane (certified grade) were obtained from Fisher; deuterated chloroform (CDCl_3) was obtained from Cambridge Isotope Laboratories Inc. 2-[(*tert*-butyl)[1-(diethoxyphosphoryl)-2,2-(dimethylpropyl)amino]oxy]-2-methylpropionic acid, also known as BlocBuilderTM (99%, Scheme 1 (b)), was obtained from Arkema. 2VP and DMAEMA monomers were purified by passing through a column of basic alumina mixed with 5 wt% calcium hydride; they were stored in a sealed flask under a head of nitrogen in a refrigerator until needed. All other compounds were used as received.

B.1.3 Homopolymerization of 2-vinylpyridine (2VP) using NHS-BlocBuilder as initiator

The initiator NHS-BlocBuilder was synthesized via coupling of BlocBuilder and *N*-hydroxysuccinimide following procedures described previously.^{47,171} The homopolymerization

of 2VP was performed in a 50 mL three-neck round-bottom glass flask fitted with a reflux condenser, a magnetic stir bar, and a thermal well. The NHS-BlocBuilder (0.048 g, 0.10 mmol) was dissolved in 2VP monomer (3.0 g, $M_{n,target} = 30 \text{ kg mol}^{-1}$). The solution was then deoxygenated by nitrogen bubbling for 30 min at room temperature prior to heating to 120 °C using a heating mantle with a heat controller at a rate of about 8 °C min⁻¹ while maintaining a nitrogen purge. The time when the solution reached 120 °C was taken as the start of the reaction ($t = 0$). Samples were taken periodically to monitor conversion and molecular weight. The reaction was stopped when the mixture became too viscous to draw samples. The final polymer was precipitated in hexane, decanted and dried in vacuum at 40 °C overnight. The purified polymer (50% conversion) has number-average molecular weight (M_n) = 15.8 kg mol⁻¹ and dispersity (\mathcal{D}) = 1.29. Conversion was determined by ¹H NMR (400 MHz Varian Gemini 2000 spectrometer, CDCl₃) using the peak of the aromatic proton closet to the nitrogen of the monomer ($\delta = 8.5 - 8.6 \text{ ppm}$) and of the polymer ($\delta = 8.3 - 8.5 \text{ ppm}$). Molecular weight and \mathcal{D} of the samples were measured by GPC (Waters Breeze) relative to poly(styrene) standards (see *Gel Permeation Chromatography* section for full details).

B.1.2 Statistical copolymerization of 2-(dimethylamino)ethyl methacrylate (DMAEMA) and 2-vinylpyridine (2VP)

The same setup and experimental procedures as the homopolymerizations were used for the statistical copolymerizations of DMAEMA and 2VP except for the feed composition with respect to DMAEMA ($f_{DMAEMA,0}$) was varied from 80 – 99 mol% and the synthesis was conducted at 80 °C (detail experimental conditions can be found in Table B-1). Samples were taken periodically to determine conversion and molecular weight. Monomer conversion and copolymer composition were determined by ¹H NMR (400 MHz Varian Gemini 2000

spectrometer, CDCl₃). Conversion of DMAEMA was calculated using the two protons adjacent to the ester of the monomer ($\delta = 3.7 - 3.8$ ppm) and those corresponding to the polymer ($\delta = 3.9 - 4.1$ ppm). 2VP conversion was determined by using the proton adjacent to the nitrogen of the monomer ($\delta = 8.5 - 8.6$ ppm) and of the polymer ($\delta = 8.3 - 8.5$ ppm). Overall conversion was then calculated using the feed composition with respect to DMAEMA ($f_{DMAEMA,0}$, mol%, $Conv_{ave} = f_{DMAEMA,0} \times Conv_{DMAEMA} + (1 - f_{DMAEMA,0}) \times Conv_{2VP}$). Polymerization was stopped when the reaction mixture became too viscous to withdraw samples. The copolymers were precipitated in hexane, decanted and dried in vacuum at 40 °C overnight. Molecular weight and dispersity of the samples were measured by GPC (Waters Breeze) (see *Gel Permeation Chromatography* section for full details). The molecular weight stated for the copolymers was relative to poly(methyl methacrylate) standards. A homopolymerization of DMAEMA was also attempted with the same setup and procedures as the statistical copolymerizations. However, the polymerization was highly exothermic and the viscosity of the reaction mixture increased sharply as soon as the temperature reached 80 °C, which forbade any samples to be drawn. The mixture was diluted with THF and the final polymer was precipitated in hexane, decanted and dried in vacuum at 40 °C overnight. Molecular weight and dispersity of the PDMAEMA homopolymer was measured by GPC (Waters Breeze) relative to poly(methyl methacrylate) standards (see *Gel Permeation Chromatography* section for full details).

Table B-1. Experimental conditions for the bulk homopolymerization of 2-vinylpyridine (2VP) and 2-(dimethylamino)ethyl methacrylate (DMAEMA) as well as DMAEMA/2VP statistical copolymerizations using NHS-BlocBuilder as the initiator.

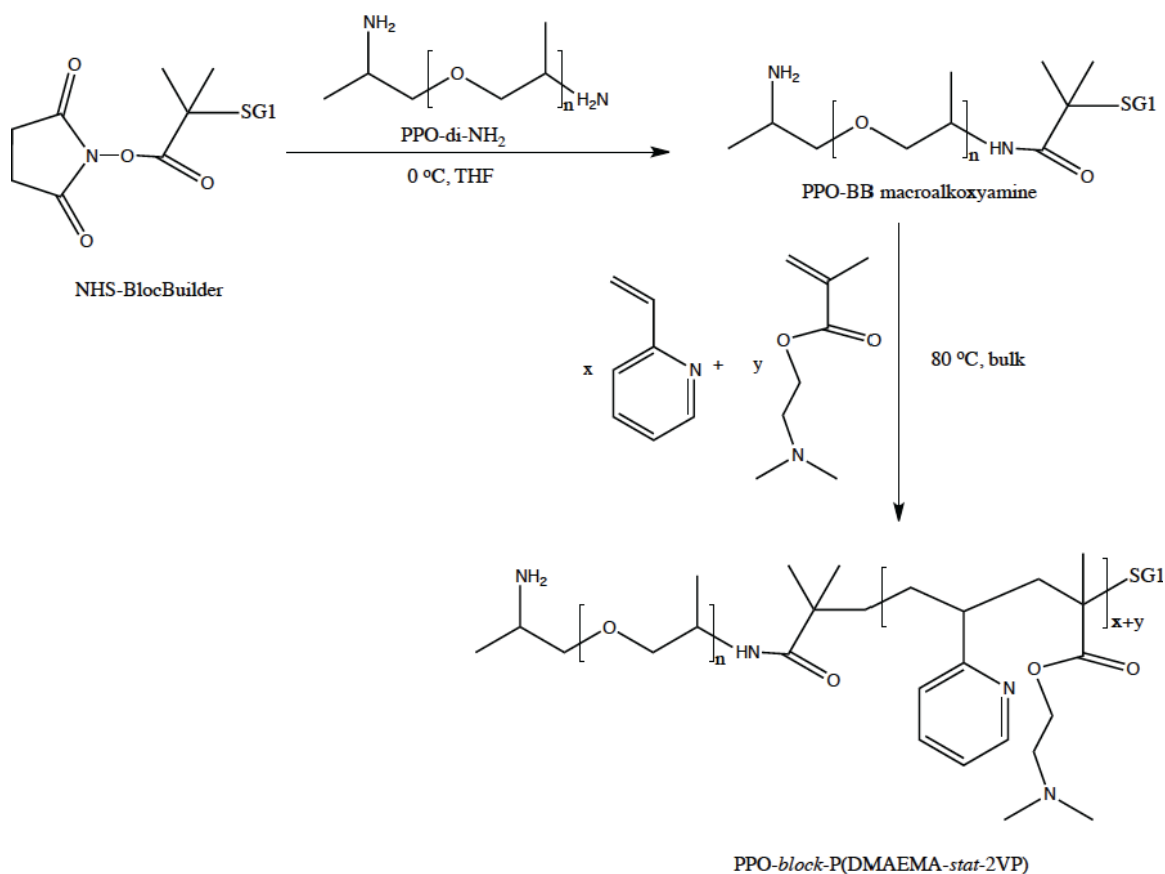
Experiment ID ^a	[initiator] (mol L ⁻¹)	[DMAEMA] (mol L ⁻¹)	[2VP] (mol L ⁻¹)	$f_{DMAEMA,0}$ (mol%) ^b	[SG1] (mol L ⁻¹)	$M_{n,target}$ (kg mol ⁻¹) ^c	T (°C)
P2VP	0.033	0	9.226	-	-	29.7	120
PDMAEMA	0.032	5.941	0	100%	-	30.0	80
D2VP-99	0.032	5.900	0.064	99%	-	30.1	80
D2VP-98	0.032	5.861	0.124	98%	-	30.0	80
D2VP-95	0.032	5.750	0.296	95%	-	29.9	80
D2VP-90	0.032	5.538	0.626	90%	-	30.1	80
D2VP-85	0.032	5.318	0.968	85%	-	30.0	80
D2VP-80	0.032	5.124	1.269	80%	-	30.2	80
D2VP-95s	0.031	5.744	0.306	95%	0.004	30.2	80
D2VP-99s	0.031	5.897	0.069	99%	0.003	30.3	80

^a Experimental identification (ID) for copolymers was given by D2VP-X, where D2VP = DMAEMA and 2VP; the number abbreviation refers to the feed composition with respect to DMAEMA. D2VP-95s and D2VP-99s were copolymerizations with additional SG1. ^b Feed composition with respect to DMAEMA. ^c Theoretical molecular weight at 100% conversion.

B.1.3 Synthesis of poly(propylene oxide)-coupled BlocBuilder (PPO-BB) macroalkoxyamine

The following procedures were adapted from Vinas et al.¹ with slight modifications to produce a BlocBuilder terminated PPO. NHS-BlocBuilder (0.50 g, 1.05 mmol) was dissolved in THF (16 mL) and bubbled with ultra-pure nitrogen for 15 min at 0 °C. Poly(propylene glycol)-bis(2-aminopropyl ether) (PPO-di-NH₂) $M_n \sim 2000$ g mol⁻¹ (4.20 g, 2.10 mmol) was then added to the degassed NHS-BlocBuilder solution. Then, 4 times excess amine functional group from PPO-di-NH₂ was added to ensure only one NHS-BlocBuilder was coupled to each PPO-di-NH₂. The mixture was stirred at 0 °C for 2 hours, then filtered to remove the precipitated *N*-hydroxysuccinimide and dried under reduced pressure to remove THF. The final product is a mixture of PPO-coupled BlocBuilder (PPO-BB, Scheme B-1) macroalkoxyamine and unreacted PPO-di-NH₂. ¹H NMR (400 MHz Varian Gemini 2000 spectrometer, CDCl₃, δ , ppm): 1.0 – 1.4

(3nH; CH₃ (PPO with degree polymerization of n) + 18H; 2 *tert*-butyl groups + 6H; 2 x (POCH₂CH₃) (BlocBuilder)), 1.6 – 1.9 (6H; (CH₃)₂CO (BlocBuilder)), 3.1 – 3.9 (3nH; OCH₂CH (PPO with degree polymerization of n)), 3.9 – 4.4 (4H; 2 x (POCH₂CH₃) (BlocBuilder)).



Scheme B-1. Synthesis route for a diblock copolymer containing a poly(propylene glycol) block and a DMAEMA/2VP statistical copolymer block by NMP.

B.1.4 Synthesis of statistical copolymer of DMAEMA and 2VP using PPO-BB macroalkoxyamine

The mixture of PPO-BB and residual PPO-di-NH₂ (0.85 g total, ~ 0.43 g or 2.12 mmol PPO-BB) was dissolved in a mixture of DMAEMA and 2VP monomers (total 6.0 g, $M_{n,target} = 30 \text{ kg mol}^{-1}$,

$f_{DMAEMA,0} = 95$ mol%). The same procedures as the random copolymerizations described earlier were followed. Samples were drawn periodically to monitor conversion and molecular weight. Monomer conversion and final polymer composition were determined by ^1H NMR (400 MHz Varian Gemini 2000 spectrometer, CDCl_3). All samples and the final polymer were precipitated in hexane where the monomers and the oligomeric PPO-di- NH_2 were soluble. The recovered block copolymer was then dried in an oven at 40 °C under vacuum. The final yield of the block copolymer was 0.8 g (32% conversion, low yield was mainly due to the loss from many samples drawn during the reaction) with $M_n = 21.5$ kg mol $^{-1}$ and $\text{Đ} = 1.78$ as determined by GPC (Waters Breeze) relative to poly(methyl methacrylate) standards (see *Gel Permeation Chromatography* section for full details). The composition of the DMAEMA/2VP block with respect to DMAEMA (F_{DMAEMA} , mol%) was 94% as determined by ^1H NMR.

B.1.5 Chain extension experiments

Selected DMAEMA/2VP statistical copolymers were chain-extended with 2VP at 120 °C in bulk. The setup and polymerization procedures were the same as the synthesis of homopolymer and statistical copolymers described earlier. The detailed experimental conditions can be found in Table B-2. The experiments were stopped after 3 hours and the polymer was precipitated in hexane, decanted and dried in an oven at 40 °C under vacuum. The chain-extended block copolymers were characterized by GPC (Waters Breeze) calibrated with poly(methyl methacrylate) standards (see *Gel Permeation Chromatography* section for full details).

Table B-2. Experimental conditions of the chain extension experiments.

Macroinitiator	[Macroinitiator] (mol L ⁻¹)	[2VP] (mol L ⁻¹)	M _{n,target} (kg mol ⁻¹) ^a	T (°C)
D2VP-95	0.010	9.226	102.0	120
D2VP-98	0.008	9.226	143.5	120
D2VP-99	0.011	9.226	99.5	120
PPO-D2VP-95	0.008	9.226	145.9	120

^a Theoretical molecular weight of the block copolymers at 100% conversion.

B.1.6 Gel permeation chromatography

Molecular weight and dispersity index (\bar{M}_w/\bar{M}_n) of all polymers were characterized by gel permeation chromatography (GPC) (Waters Breeze) using THF as the mobile phase at 40 °C in this study. The GPC was equipped with three Waters Styragel HR columns (molecular weight measurement ranges: HR1: $10^2 - 5 \times 10^3$ g mol⁻¹, HR2: $5 \times 10^2 - 2 \times 10^4$ g mol⁻¹, HR3: $5 \times 10^3 - 6 \times 10^5$ g mol⁻¹) and a guard column. The columns were operated at 40 °C and a mobile phase flow rate of 0.3 mL min⁻¹ during analysis. The GPC was also equipped with both ultraviolet (UV 2487) and differential refractive index (RI 2410) detectors. The molecular weight measurements were calibrated relative to poly(styrene) narrow molecular weight distribution standards for 2VP homopolymer and poly(methyl methacrylate) narrow molecular weight distribution standards for all other polymers in this study.

B.1.7 Characterization of the aqueous solutions of the statistical copolymers and block copolymers

The transition temperature of the statistical copolymers in buffer solutions from pH 7 – 11 at 0.5 wt% concentration was characterized using a Cary 5000 UV-vis-NIR Spectrophotometer. Light transmittance of the solutions was monitored at 600 nm while the solution is heated/cooled at a rate of 0.5 °C min⁻¹. The cloud point temperature is defined as the temperature where the

transmittance dropped to 50% during heating. Dynamic light scattering (DLS) was used to determine the hydrodynamic radius of the block copolymers in aqueous solutions at different pHs and temperatures using a Malvern ZetaSizer (Nano-ZS). The instrument was equipped with a He-Ne laser operating at 633 nm with a scattering angle of 173°, an avalanche photodiode detector, and a temperature-controlled cell. In all DLS measurements, the aqueous solutions were filtered using a 0.2 μm pore size filter and the filtered solutions were monitored in the temperature-controlled cell while heated at a rate of about 0.5 $^{\circ}\text{C min}^{-1}$. The pKas of the statistical copolymers and block copolymers were extrapolated from the titration curve obtained from an 888 Titrand automatic titrator with a pH probe calibrated with pH 4, 7, and 10 buffers. The copolymers were dissolved at pH 2 and titrated with a 0.05 mol L⁻¹ NaOH titrant.

B.2 Supporting Information

GPC chromatograms of intermediate samples taken during the copolymerization of DMAEMA with 2VP initiated by PPO-BB macroinitiator are presented in Figure B-1.

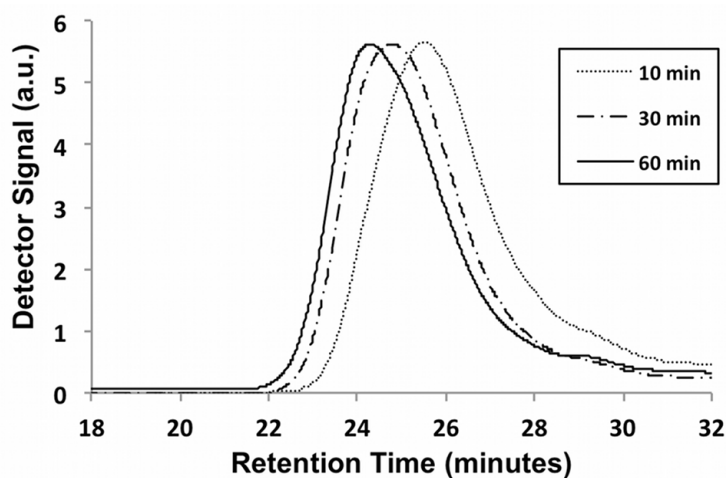


Figure B-1. GPC chromatograms of intermediate samples during the copolymerization of DMAEMA with 2VP initiated by a PPO-BB macroalkoxyamine.

The phase behaviour of the polymers in aqueous solutions was examined by UV-vis spectrometry. The results for solutions in pH 8 buffers are given as an example in Figure B-2.

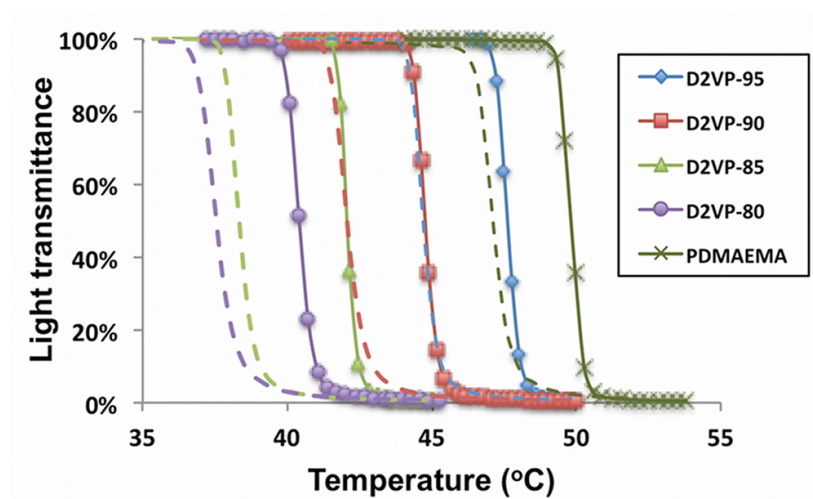


Figure B-2. Light transmittance of 0.5 wt% solutions of polymers with different compositions in pH 8 buffer measured by UV-visible spectrometry with heating/cooling rate of $0.5 \text{ }^\circ\text{C min}^{-1}$; solid lines are heating cycles and dashed lines are cooling cycles.

Appendix C

Controlled Synthesis of Benzyl Methacrylate-rich Copolymer via NMP using Styrene as “Controlling” Co-monomer

C.1 Experimental Section

C.1.1 Materials

Styrene (99%), benzyl methacrylate (BzMA) (96%), basic alumina (Brockmann, Type I, 150 mesh), and calcium hydride (90-95% reagent grade) were purchased from Aldrich. Methanol (99.8%) was obtained from Fisher. Both the styrene and BzMA monomers were purified by passing through a column of basic alumina mixed with 5 wt% calcium hydride and were stored in a sealed flask under a head of nitrogen in a refrigerator until needed. 2-((*tert*-butyl[1-(diethoxyphosphoryl)-2,2-(dimethylpropyl)amino]oxy)-2-methylpropionic acid, also known as BlocBuilder (99%), was purchased from Arkema and was used as received. (*tert*-butyl[1-(diethoxyphosphoryl)-2,2-dimethylpropyl]amino) oxidanyl, also known as SG1 (>85%), was kindly donated by Noah Macy of Arkema and used as received. Tetrahydrofuran (THF, 99.9%, Fisher) and deuterated chloroform (CDCl₃, Cambridge Isotope Laboratories Inc.) were used without any further purification.

C.1.2 Synthesis of BzMA/Styrene Random Copolymers

The random copolymerization approach described here has also been employed previously for a wide range of methacrylates.^{106,110,130,132} The copolymerization was performed in a 100 mL three-neck round-bottom glass flask equipped with a reflux condenser and a thermal well.

Formulations for various initial feed compositions ($f_{BzMA,0}$, 10 mol% to 90 mol% BzMA, in increments of 10 mol%) were followed. In all cases, the target molecular weight was about 32 kg·mol⁻¹ and was calculated based on the mass of monomers (total monomer mixture = 17 g) relative to the moles of BlocBuilder initiator (0.2 g, 0.53 mmol). 0.015 g of SG1 (10 mol% relative to BlocBuilder) was used to control the polymerization more easily. The initiator and SG1 were added to the flask with a stirrer which was then sealed with a rubber septum. A thermocouple was inserted into the temperature well and connected to a controller. The reflux condenser was connected to a chilling unit (Neslab 740) which constantly supplies water at 5 °C to reflux any vapors produced during the experiments and thus prevented loss of monomers due to evaporation. The previously purified BzMA and styrene monomers were injected into the flask using disposable 5 mL and 10 mL syringes to ensure precisely controlled feed compositions. Once all ingredients were added, the mixture was stirred and purged by an ultra-pure nitrogen flow for 30 minutes to remove all dissolved oxygen. The mixture was then heated by a heating mantle to 90 °C at a rate of about 8 °C·min⁻¹ while maintaining a nitrogen purge. The time when the mixture reached 90 °C was taken as the start of the reaction ($t = 0$). Reactions were stopped by removing the reactor from the heating mantle when the mixture became noticeably viscous. Reaction time varied greatly depending on the initial feed composition (440 min for $f_{BzMA,0} = 10$ mol% and 6 min for $f_{BzMA,0} = 90$ mol%). Also, since radical polymerization of BzMA is highly exothermic,³⁰ temperature control required special attention for polymerizations of BzMA rich mixtures. Temperature overshoots of more than 20 °C were observed for bulk polymerizations when $f_{BzMA,0} > 80$ mol%. Since reaction time for BzMA rich mixtures was very short as previously mentioned, large temperature overshoot could cause significant error in the analysis of polymerization kinetics. To minimize the temperature overshoot for BzMA rich ($f_{BzMA,0} > 80$

mol%) mixtures, the heating power was set at minimum when mixture temperature reached 80 °C and shut off as soon as 90 °C was reached. The power was turned back to minimum as soon as the temperature stopped increasing. Overshoots were minimized to about 2 to 3 °C in this manner. Samples were taken periodically during the polymerization. The samples as well as the final mixtures were precipitated in methanol and left to settle for several hours after which they were decanted and dried overnight in a vacuum oven at about 70 °C to remove any solvent or unreacted monomer.

C.1.3 Chain Extensions with Styrene

To examine the “livingness” of the copolymers, chain extensions with styrene were performed using the copolymers synthesized as described in the previous section as macroinitiators. For all chain extensions, the target molecular weight of the extended polymer was set at about 230 kg·mol⁻¹ to obtain clear molecular weight shifts. The amounts of the macroinitiator and styrene varied according to the molecular weight of the macroinitiators. The same set-up as the one for copolymer synthesis was used for chain extension experiments. A period of 30-minute bubbling was applied after both the macroinitiator and styrene were added to the reactor. The mixture was then heated to 110 °C and polymerization was run for 90 - 120 minutes. Samples were taken periodically and precipitated with methanol. The samples were then decanted and dried in a vacuum oven until constant mass was attained.

C.1.5 Characterization

The monomer conversion was determined gravimetrically. The molecular weight distribution was measured using gel permeation chromatography (GPC, Water Breeze) which used THF as the mobile phase. The GPC was equipped with three Waters Styragel HR columns (molecular weight measurement ranges: HR1: $10^2 - 5 \times 10^3 \text{ g}\cdot\text{mol}^{-1}$, HR2: $5 \times 10^2 - 2 \times 10^4 \text{ g}\cdot\text{mol}^{-1}$, HR3: $5 \times 10^3 - 6 \times 10^5 \text{ g}\cdot\text{mol}^{-1}$) and a guard column. The columns were operated at 40 °C and a mobile phase flow rate of $0.3 \text{ mL}\cdot\text{min}^{-1}$ was applied during analysis. The GPC was also equipped with both ultraviolet (UV 2487) and differential refractive index (RI 2410) detectors. The molecular weight measurements were calibrated based on narrow molecular weight poly(styrene) standards in THF at 40 °C. The copolymer molecular weights were corrected based on the following Mark-Houwink coefficients: $K_{PS} = 11.4 \times 10^{-5} \text{ dL}\cdot\text{g}^{-1}$ and $a_{PS} = 0.716$; $K_{PBzMA} = 10.8 \times 10^{-5} \text{ dL}\cdot\text{g}^{-1}$ and $a_{PBzMA} = 0.635$.²¹⁶ The copolymer compositions were analyzed by ^1H nuclear magnetic resonance (NMR). The ^1H NMR measurements were done with a 400 MHz Varian Gemini 2000 spectrometer using CDCl_3 as solvent.

Appendix D

Benzyl Methacrylate-rich Copolymers synthesized by NMP that are Fluorescent and Thermoresponsive in an Ionic Liquid

D.1 Experimental Section

D.1.1 Materials

N,N-Dimethylformamide (DMF, 99.8%), benzyl methacrylate (BzMA, 96%), methyl methacrylate (MMA, 99%), basic alumina (Brockmann, Type I, 150 mesh), and calcium hydride (90 - 95% reagent grade) were purchased from Sigma-Aldrich; tetrahydrofuran (THF, 99.9%), styrene (>99%) were obtained from Fisher; and deuterated chloroform (CDCl₃) was obtained from Cambridge Isotope Laboratories Inc. Poly(methyl methacrylate) narrow molecular weight distribution standards (molecular weight ranged from 875 to 1,677,000 g mol⁻¹) were purchased from Varian, Inc. BzMA, MMA, and styrene monomers were each purified by passing through a column of basic alumina mixed with 5 wt% calcium hydride and were stored in a sealed flask under a head of nitrogen in a refrigerator until needed. All other compounds were used as received.

2-((*tert*-butyl[1-(diethoxyphosphoryl)-2,2-(dimethylpropyl)amino]oxy)-2-methylpropionic acid, also known as BlocBuilderTM (99%), was obtained from Arkema; (*tert*-butyl[1-(diethoxyphosphoryl)-2,2-dimethylpropyl]amino) nitroxide (SG1, >85%) was kindly donated by Noah Macy from Arkema. Both were used as received and stored at 5 °C. Ionic liquid 1-ethyl-3-methylimidazolium bis(trifluoromethylsulfonyl)imide ([C₂mim][NTf₂], 99%) was purchased from Iolitec; it was used without further purification and stored in a desiccator to minimize moisture absorption. 9-(4-Vinylbenzyl)-9H-carbazole (VBK, >95%) was synthesized according to previous literature.²⁷⁷

D.1.2 Statistical copolymerization of benzyl methacrylate (BzMA) and 9-(4-Vinylbenzyl)-9H-carbazole (VBK)

The copolymerizations were performed in a 50 mL three-neck round-bottom glass flask fitted with a reflux condenser, a magnetic stir bar, and a thermal well. The amounts of initiator and monomers were calculated according to a target molecular weight ($M_{n,target}$, molecular weight at 100% conversion) of 30 kg mol^{-1} and feed composition relative to VBK ($f_{VBK,0}$, mol%) varied from 2 to 11 mol%; *N,N*-dimethylformamide (DMF) was also added (monomer concentration 20 wt%) to assist dissolution of VBK. A statistical copolymer of methyl methacrylate (MMA) and VBK was also synthesized in a similar manner. Detailed experimental conditions were summarized in Table D-1. Using the experiment B/V-8 as an example, a mixture of BlocBuilder (0.078 g, 0.20 mmol), SG1 (0.0067 g, 0.023 mmol), BzMA (5.30 g, 0.030 mol), VBK (0.70 g, 0.0026 mol), DMF (24.3 g) was added to the reactor. The solution was then deoxygenated by nitrogen bubbling for 30 min at room temperature prior to heating to $90 \text{ }^{\circ}\text{C}$ at a rate of about $8 \text{ }^{\circ}\text{C min}^{-1}$ while maintaining a nitrogen purge. The time when the solution reached $90 \text{ }^{\circ}\text{C}$ was taken as the start of the reaction ($t = 0$). Samples were taken periodically to determine conversion and molecular weight. Monomer conversion and copolymer composition was determined by ^1H NMR (400 MHz Varian Gemini 2000 spectrometer, CDCl_3). Conversion of BzMA was calculated using the two protons adjacent to the ester of the monomer ($\delta = 4.8 - 4.9 \text{ ppm}$) and those corresponding to the polymer ($\delta = 4.3 - 4.6 \text{ ppm}$). VBK conversion was determined by using the vinyl proton of the monomer ($\delta = 5.4 - 5.5 \text{ ppm}$) and of the 8 carbazole protons of the polymer ($\delta = 6.4 - 6.8 \text{ ppm}$, the NMR spectrum of a BzMA/VBK copolymer can be find in Section D.2 Supporting Information). Overall conversion was then calculated using the feed composition with respect to VBK ($f_{VBK,0}$, mol%, $\text{Conv.}_{overall} = f_{VBK,0} \times \text{Conv.}_{VBK} + (1 - f_{VBK,0}) \times \text{Conv.}_{BzMA}$). The copolymer products were precipitated in methanol, decanted and dried in

vacuum at 40 °C overnight to give 1.60 g of B/V-8 (yield = 27%, overall conversion = 29%, number-average molecular weight $M_n = 6.7 \text{ kg mol}^{-1}$ and dispersity $\mathcal{D} = 1.39$). A homopolymerization of BzMA was also attempted using similar procedures at 80 °C in bulk. The reaction mixture turned into a gel within a minute after temperature reached 80 °C. The homopolymer of BzMA was recovered by dilution with THF followed by precipitation in methanol. Molecular weight and dispersity of the samples and polymer products were measured using GPC (Waters Breeze) (see *Gel Permeation Chromatography* section for full details). The molecular weight stated for the copolymers was relative to poly(methyl methacrylate) standards in THF at 40 °C.

Table D-1. Experimental conditions for statistical copolymerization of benzyl methacrylate (BzMA) (or methyl methacrylate (MMA)) with 9-(4-vinylbenzyl)-9H-carbazole (VBK) in dimethylformamide (DMF) solution at 90 °C and homopolymerization of BzMA in bulk at 80 °C via nitroxide mediated polymerization with BlocBuilder.

Expt ID ^a	[BlocBuilder]	[SG1]	r^b	[BzMA] or [MMA]	[VBK]	$f_{\text{VBK},0}^c$	[DMF]	$M_{n,\text{target}}^d$
	mol L ⁻¹	mol L ⁻¹		mol L ⁻¹	mol L ⁻¹	mol%	mol L ⁻¹	kg mol ⁻¹
B/V-2	0.0065	0.0007	0.10	1.059	0.021	2%	10.7	29.9
B/V-5	0.0065	0.0007	0.10	1.019	0.054	5%	10.7	30.0
B/V-8	0.0066	0.0007	0.11	0.981	0.085	8%	10.8	29.8
B/V-11	0.0066	0.0007	0.11	0.937	0.115	11%	10.9	30.1
M/V-5	0.0098	0.0010	0.10	1.700	0.089	5%	10.9	20.1
PBzMA	0.0527	0.0051	0.10	5.909	-	-	-	20.1

^a The experiment ID B/V-X or M/V-X denotes the monomers used in the copolymerization (B for BzMA, M for MMA and V for VBK) and X represents the feed composition of VBK in mol%; ^b $r = [\text{SG1}]_0/[\text{BlocBuilder}]_0$; ^c Initial feed composition relative to VBK; ^d Number average molecular weight at 100% conversion.

D.1.3 Chain extension experiments

The chain extension experiments were performed using the same setup and polymerization procedures as the synthesis of the statistical copolymers described earlier. The detailed chain

extension experimental conditions were summarized in Table D-2. Using the experiment B/V5-M/S10 as an example, a mixture of macroinitiator B/V-5 ($M_n = 9.9 \text{ kg mol}^{-1}$ and $\text{Đ} = 1.42$, 0.55 g, 0.055 mmol), MMA (3.0 g, 0.030 mol), styrene (0.35 g, 0.0034 mol) and free SG1 (0.0019 g, 0.006 mmol) was added to the reactor. The solution was then deoxygenated by nitrogen bubbling for 30 min at room temperature prior to heating to 90 °C at a rate of about 8 °C min⁻¹ while maintaining a nitrogen purge. The time when the solution reached 90 °C was taken as the start of the reaction ($t = 0$). The reaction was stopped after 2 hours and the chain extended block copolymer was precipitated in methanol, decanted and dried in a vacuum oven at 40 °C overnight to give 0.50 g of B/V8-M/S10 ($M_n = 15.1 \text{ kg mol}^{-1}$ and $\text{Đ} = 1.47$). Note that the target M_n for M/V5-B/S10 was smaller compared to the other two chain extensions (~50 kg mol⁻¹ instead of ~70 kg mol⁻¹, Table D-2). This was done to minimize termination reaction through chain transfer to monomers as BzMA/styrene copolymerization was not very well controlled with only 10 mol% styrene in the feed.¹⁴² Fractionation was performed for the chain extended block copolymers in attempt to remove dead chains with lower molecular weight. The block copolymers were dissolved in a minimal amount of THF and then methanol was added dropwise while the solution was stirred until the solution turned cloudy and polymer precipitates were observed. The polymer was then collected and dried. The M_n and Đ of the chain-extended block copolymers were characterized by GPC (Waters Breeze) and were calibrated relative to poly(methyl methacrylate) standards (see *Gel Permeation Chromatography* section for full details). Polymer composition was determined by ¹H NMR (400 MHz Varian Gemini 2000 spectrometer, CDCl₃).

Table D-2. Experimental conditions for chain extension experiments using selected statistical copolymer of benzyl methacrylate (BzMA) (or methyl methacrylate (MMA)) with 9-(4-vinylbenzyl)-9H-carbazole (VBK) as macroinitiators at 90 °C.

Expt. ID ^a	[Macroinitiator]	[MMA] or [BzMA]	[Styrene] or [VBK]	[SG1]	$f_{St,0}$ or $f_{VBK,0}$ ^b	$M_{n,target}$ ^c	[DMF]
	mol L ⁻¹	mol L ⁻¹	mol L ⁻¹	mol L ⁻¹	mol%	kg mol ⁻¹	mol L ⁻¹
B/V5-M/S10	0.016	8.388	0.940	0.0017	10%	70.2	-
B/V8-M/S10	0.015	8.381	0.946	0.0018	10%	70.9	-
M/V5-B/S10	0.004	0.935	0.103	0.0004	10%	49.8	10.8

^a The experiment ID denotes the feed composition used to synthesize the macroinitiator followed by the feed composition used for the chain extension (B stands for BzMA, V for VBK, M for MMA and S for styrene; the numbers represent the feed composition of the controlling co-monomer (either styrene or VBK)); ^b Feed composition of styrene or VBK in the chain extensions; ^c Over all molecular weight for the block copolymer at 100% monomer conversion.

D.1.4 Gel permeation chromatography

Molecular weight and dispersity of all polymers were characterized by gel permeation chromatography (GPC) (Waters Breeze) using THF as the mobile phase at 40 °C in this study. The GPC was equipped with three Waters Styragel HR columns (molecular weight measurement ranges: HR1: $10^2 - 5 \times 10^3$ g mol⁻¹, HR2: $5 \times 10^2 - 2 \times 10^4$ g mol⁻¹, HR3: $5 \times 10^3 - 6 \times 10^5$ g mol⁻¹) and a guard column. The columns were operated at 40 °C and a mobile phase flow rate of 0.3 mL min⁻¹ during analysis. The GPC was also equipped with both ultraviolet (UV 2487) and differential refractive index (RI 2410) detectors. The results reported in this paper were obtained from the RI detector. All molecular weight measurements were calibrated with poly(methyl methacrylate) (PMMA) narrow molecular weight distribution standards.

D.1.5 Characterization of the statistical copolymers and block copolymers in ionic liquid solutions

The statistical copolymers and block copolymers were dissolved in the ionic liquid 1-ethyl-3-methylimidazolium bis(trifluoromethylsulfonyl)imide ([C₂mim][NTf₂]) with tetrahydrofuran

(THF) as the co-solvent. THF was subsequently evaporated at atmospheric pressure and room temperature for at least 24 hours followed by drying in vacuum at about 60 °C until constant weight. All solutions were initially prepared at a concentration of 3 wt% and they were stored in a desiccator to minimize exposure to moisture. The transition temperatures of the statistical copolymers in the ionic liquid were characterized using a Cary 5000 UV-vis-NIR Spectrophotometer. Light transmittance of the solutions was monitored at 600 nm while the solution is heated/cooled at a rate of 0.1 °C min⁻¹ or 1 °C min⁻¹. The cloud point temperature (CPT) was defined as the temperature where the transmittance dropped to 50% during heating. Fluorescence measurements were performed using a Cary Eclipse fluorescence spectrophotometer equipped with a xenon flash lamp and a Peltier thermostatted multi-cell holder with a temperature controller. Solutions were excited at a wavelength of 330 nm in quartz cuvettes at various temperatures and their emission spectra were recorded. Thermo Scientific DXR Raman Microscope was used to obtain Raman spectra of the ionic liquid solutions before and after phase separation at 532 nm. The Raman spectra of the solutions were corrected by subtracting the Raman spectrum of the neat ionic liquid.

D.2 Supporting Information

The proton NMR spectrum of B/V-5 ($F_{VBK} = 4$ mol%) was shown in Figure D-1 as an example of the statistical copolymer of benzyl methacrylate (BzMA) and 9-(4-vinylbenzyl)-9*H*-carbazole (VBK). The compositions of the copolymers were calculated using the two methoxy protons (peak a) as the marker for BzMA and the two protons between benzyl and carbazole groups (peak d) as the marker for VBK.

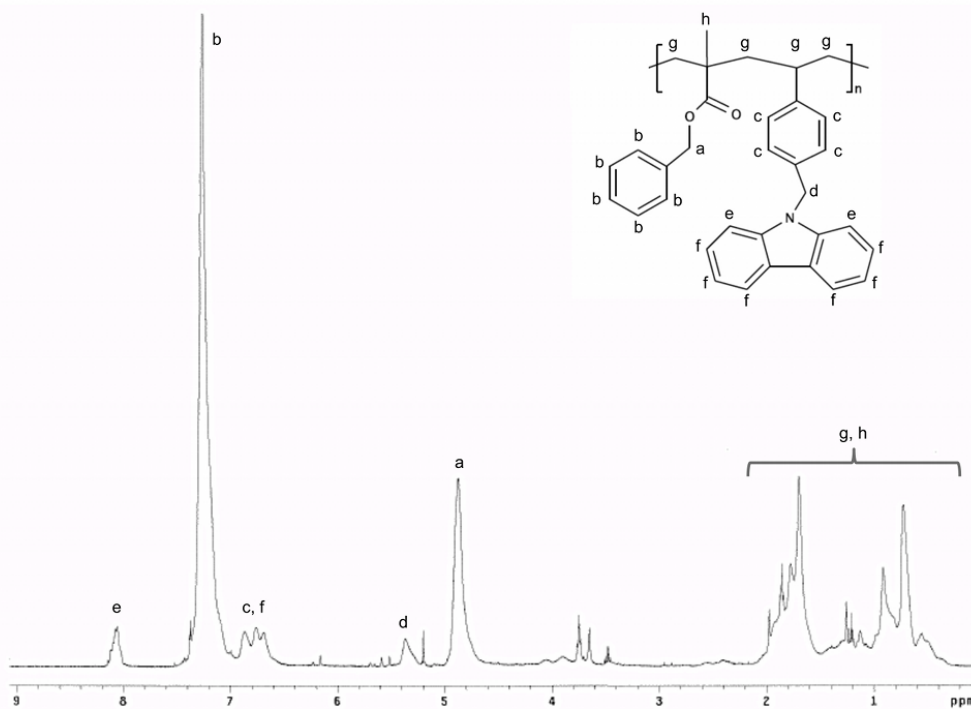


Figure D-1. Proton NMR spectrum of a statistical copolymer of benzyl methacrylate (BzMA) and 9-(4-vinylbenzyl)-9H-carbazole (VBK) (B/V-5 ($F_{VBK} = 4$ mol%).

Semi-logarithmic kinetic plots ($\ln((1-\text{conversion})^{-1})$ versus time) for copolymerizations of BzMA and VBK ($f_{VBK,0} = 2 - 11$ mol%) were shown in Figure D-2. the copolymerizations of BzMA with VBK demonstrated first-order kinetics during the early stage of the copolymerizations (below 20% conversion) followed by decreasing polymerization rates. The extent of deviation from first-order kinetics diminished with increasing amount of VBK in the feed. When the feed contained only 2 mol% VBK, polymerization rate started to decrease significantly after ~25% conversion, whereas the copolymerization with 11 mol% VBK in the feed followed first-order kinetics throughout the polymerization up to 34% conversion. The non-first-order kinetics observed indicated significant decrease in radical concentration, (i.e. formation of significant amount of dead chains due to irreversible termination).

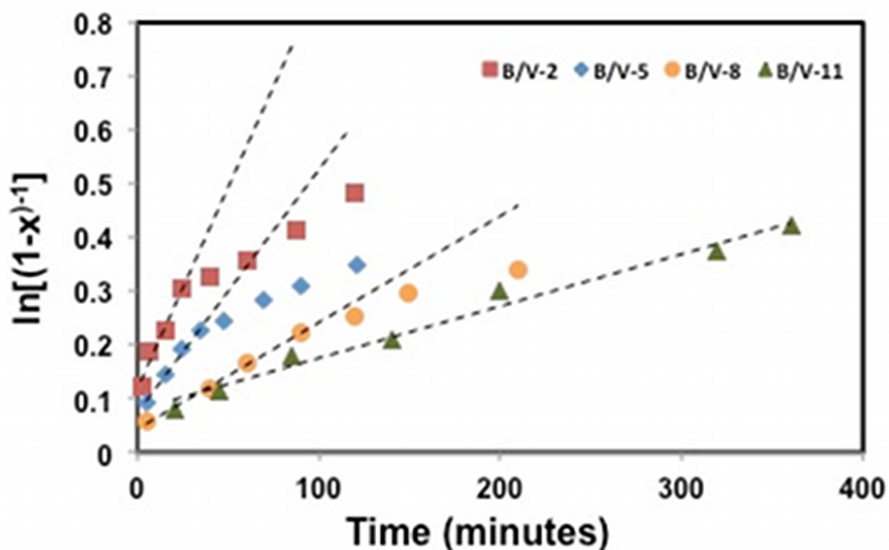


Figure D-2. Semi-logarithmic kinetic plots of statistical copolymerization of benzyl methacrylate (BzMA) and 9-(4-vinylbenzyl)-9H-carbazole (VBK) at 90 °C via NMP with BlocBuilder™ (symbols: B/V-2 ($f_{VBK,0} = 2$ mol%): red squares, B/V-5 ($f_{VBK,0} = 5$ mol%): blue diamonds, B/V-8 ($f_{VBK,0} = 8$ mol%): orange circles, B/V-11 ($f_{VBK,0} = 11$ mol%): green triangles).

Sharp increase in particle size followed by relatively constant particle size as the BzMA-rich block phase separated from the ionic liquid was illustrated in Figure D-3 for M/V5-B/S10 block copolymer. Combining with the narrow particle distribution ($\mu_w/\Gamma^2 < 0.1$), the results shown in Figure D-3 demonstrated the formation of micelles with BzMA-rich block core and MMA-rich block corona.

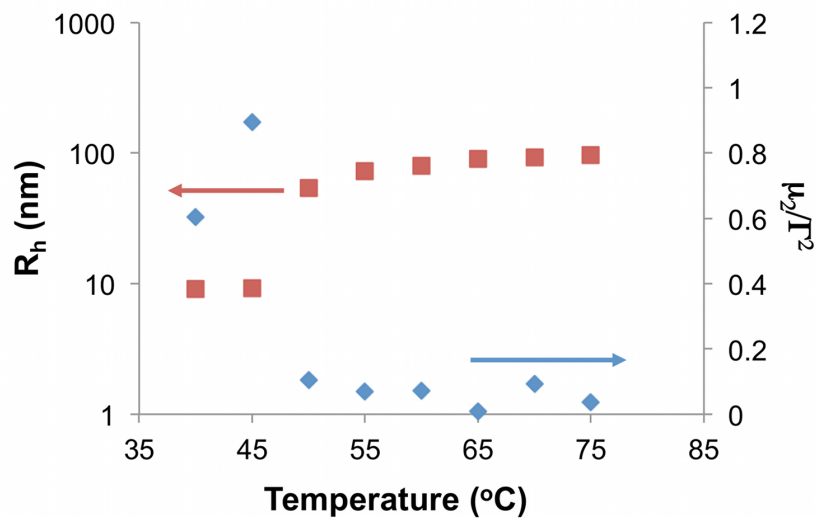


Figure D-3. Hydrodynamic radius (R_h , red square) and particle distribution index (μ_2/Γ^2 , blue diamond) versus temperature measured by dynamic light scattering for block copolymer M/V5-B/S10.

Appendix E

Effects of solvatophilicity of statistical terpolymers on phase separation and reversibility in an ionic liquid

E.1 Experimental section

E.1.1 Materials

N,N-Dimethylformamide (DMF, 99.8%), benzyl methacrylate (BzMA, 96%), methyl methacrylate (MMA, 99%), oligo(ethylene glycol) methyl ether methacrylate (OEGMA, average molecular weight = 475 g mol⁻¹), basic alumina (Brockmann, Type I, 150 mesh), and calcium hydride (90-95% reagent grade) were purchased from Sigma-Aldrich; tetrahydrofuran (THF, 99.9%) was obtained from Fisher; deuterated chloroform (CDCl₃) was obtained from Cambridge Isotope Laboratories Inc. BzMA, and MMA monomers were purified by passing through a column of basic alumina mixed with 5 wt% calcium hydride; they were stored in a sealed flask under a head of nitrogen in a refrigerator until needed. All other compounds were used as received.

2-((*tert*-butyl[1-(diethoxyphosphoryl)-2,2-(dimethylpropyl)amino]oxy)-2-methylpropionic acid, also known as BlocBuilder™ (99%), was purchased from Arkema; (*tert*-butyl[1-(diethoxyphosphoryl)-2,2-dimethylpropyl]amino) nitroxide (SG1, >85%) was kindly donated by Noah Macy from Arkema, both were used as received and stored at 5 °C. Ionic liquid 1-ethyl-3-methylimidazolium bis(trifluoromethylsulfonyl)imide ([C₂mim][NTf₂], 99%) was purchased from Iolitec; it was used without further purification and stored in a desiccator to minimize moisture exposure. 9-(4-Vinylbenzyl)-9H-carbazole (VBK, >95%) was synthesized according to previous literature.²⁷⁷

E.1.2 Terpolymerization of benzyl methacrylate (BzMA), methyl methacrylate (MMA) or oligo(ethylene glycol) methyl ether methacrylate (OEGMA), and 9-(4-Vinylbenzyl)-9H-carbazole (VBK)

The terpolymerizations were performed in a 50 mL three-neck round-bottom glass flask fitted with a reflux condenser, a magnetic stir bar, and a thermal well. The amounts of initiator and monomers were calculated according to a target molecular weight ($M_{n,target}$, theoretical molecular weight at 100% conversion) of 15, 40 or 80 kg mol⁻¹. Feed composition of VBK ($f_{VBK,0}$, mol%) was fixed at 10 mol% while the feed composition of BzMA ($f_{BzMA,0}$, mol%) was varied from 50 to 80 mol% for BzMA/MMA/VBK terpolymerizations and varied from 80 to 87 mol% for BzMA/OEGMA/VBK terpolymerizations; *N,N*-dimethylformamide (DMF) was also added (solution concentration 20 wt%) to assist dissolution of VBK. Detailed experimental conditions were summarized in Table E-1. Using the experiment B80/M10/V10-40 as an example, a mixture of BlocBuilder (0.0576 g, 0.15 mmol), SG1 (0.0044 g, 0.015 mmol), BzMA (4.75 g, 0.027 mol), MMA (0.35 g, 0.0035 mol), VBK (0.90 g, 0.0034 mol) and DMF (24.3 g) was added to the reactor. The solution was then deoxygenated by nitrogen bubbling for 30 min at room temperature prior to heating to 90 °C at a rate of about 8 °C min⁻¹ while maintaining a nitrogen purge. The time when the solution reached 90 °C was taken as the start of the reaction ($t = 0$). Samples were taken periodically to determine conversion and molecular weight. Monomer conversion was estimated gravimetrically. ¹H NMR was not used to determine conversion because of overlapping peaks of the three monomers. Terpolymer composition was determined by ¹H NMR (400 MHz Varian Gemini 2000 spectrometer, CDCl₃). The ¹H NMR spectra of a BzMA/MMA/VBK terpolymer (using B60/M30/V10-40 as example) and a BzMA/OEGMA/VBK terpolymer (using B85/O5/V10-40 as example) are shown in Figure E-1. The terpolymer product was precipitated in methanol, decanted and dried in vacuum at 40 °C overnight to give 1.68 g of B80/M10/V10-40 (yield = 28% (low yield mainly due to loss of

polymers in samples), overall conversion = 39%, number-average molecular weight $M_n = 13.2$ kg mol⁻¹ and dispersity $\bar{D} = 1.35$). Molecular weight and dispersity of the samples were measured using GPC (Waters Breeze) (see *Gel Permeation Chromatography* section for full details). The molecular weight stated for the terpolymers was relative to poly(methyl methacrylate) standards in THF at 40 °C. The glass transition temperatures (T_g) of the terpolymers were determined using differential scanning calorimetry (DSC). The measurements followed a standard heat/cool/heat protocol where sample was first heated to 150 °C, then cooled to -20 °C and finally heated to 150 °C again, at a rate 10 °C/min in all cycles. The T_g was defined as the inflection point on the heating curve during the second heating.

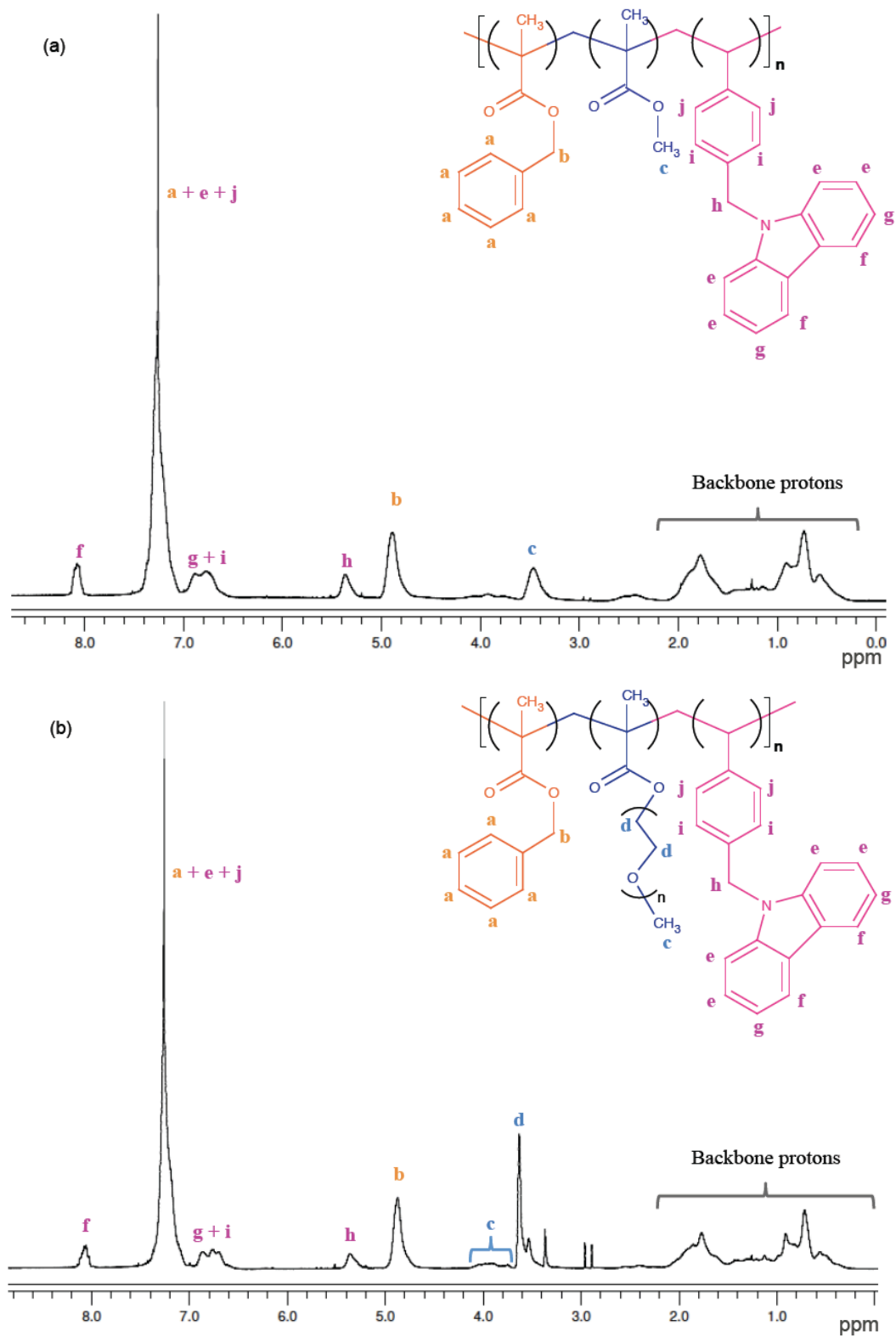


Figure E-1: ^1H NMR spectrum of (a) B60/M30/V10-40 as an example of BzMA/MMA/VBK terpolymer and (b) B85/O5/V10-40 as an example of BzMA/OEGMA/VBK terpolymer.

E.1.3 Gel permeation chromatography

Molecular weight and dispersity (\mathcal{D}) of all polymers were characterized by gel permeation chromatography (GPC) (Waters Breeze) using THF as the mobile phase at 40 °C in this study. The GPC was equipped with three Waters Styragel HR columns (molecular weight measurement ranges: HR1: $10^2 - 5 \times 10^3$ g mol⁻¹, HR2: $5 \times 10^2 - 2 \times 10^4$ g mol⁻¹, HR3: $5 \times 10^3 - 6 \times 10^5$ g mol⁻¹) and a guard column. The columns were operated at 40 °C and a mobile phase flow rate of 0.3 mL min⁻¹ during analysis. The GPC was also equipped with both ultraviolet (UV 2487) and differential refractive index (RI 2410) detectors. The results reported in this paper were obtained from the RI detector. All molecular weight measurements were calibrated with poly(methyl methacrylate) narrow molecular weight distribution standards in THF at 40 °C.

Table E-1. Experimental conditions for terpolymerizations of benzyl methacrylate (BzMA), methyl methacrylate (MMA) or oligo(ethylene glycol)methyl methacrylate (OEGMA) and 9-(4-vinylbenzyl)-9H-carbazole (VBK) in dimethylformamide (DMF) solution at 90 °C via NMP.

Expt. ID ^a	[BlocBuilder]	[SG1]	[BzMA]	[MMA] or [OEGMA]	[VBK]	[DMF]	$M_{n,target}$
	mmol L ⁻¹	mmol L ⁻¹	mol L ⁻¹	mol L ⁻¹	mol L ⁻¹	mol L ⁻¹	kg mol ⁻¹
B80/M10/V10-40	4.9	0.5	0.883	0.115	0.109	10.9	40.1
B70/M20/V10-40	5.0	0.5	0.812	0.228	0.115	10.9	40.1
B60/M30/V10-40	5.0	0.5	0.725	0.360	0.121	10.9	39.9
B50/M40/V10-40	5.0	0.5	0.632	0.508	0.127	10.9	39.9
B80/M10/V10-15	13.5	1.3	0.883	0.115	0.097	10.9	14.9
B80/M10/V10-80	2.5	0.3	0.888	0.111	0.109	10.9	78.1
B87/03/V10-40	4.9	0.5	0.877	0.031	0.100	10.9	40.2
B85/05/V10-40	4.9	0.5	0.831	0.051	0.097	10.9	40.1
B83/07/V10-40	4.9	0.5	0.784	0.065	0.096	10.9	40.1
B80/010/V10-40	4.9	0.5	0.724	0.094	0.091	10.9	40.2

^a The experiment ID Bx/My/Vz-m (or Bx/Oy/Vz-m) denotes feed composition in mol% of BzMA (B), MMA (M) or OEGMA (O) and VBK (V) with x, y, z, with respectively, m represents the target molecular weight which is the number average molecular weight at 100% conversion

E.1.4 Characterization of the ionic liquid solutions of the terpolymers

The terpolymers were dissolved in the ionic liquid 1-ethyl-3-methylimidazolium bis(trifluoromethylsulfonyl)imide ($[\text{C}_2\text{mim}][\text{NTf}_2]$) with THF as the co-solvent. THF was subsequently evaporated at atmospheric pressure and room temperature for 24 hours followed by drying in vacuum at about 60 °C until constant weight was measured. Solution concentration was varied from 1 - 10 wt% and the solutions were stored in a desiccator to minimize exposure to moisture. The transition temperature of the terpolymer solutions was characterized using a Cary 5000 UV-vis-NIR Spectrophotometer. Light transmittance of the solutions was monitored at 600 nm while the solution is heated/cooled at a rate of 1 °C min⁻¹. The cloud point temperature is defined as the temperature where the transmittance dropped to 50% during heating. Fluorescence measurements were performed using a Cary Eclipse fluorescence spectrophotometer equipped with a xenon flash lamp and Peltier thermostated multi-cell holder with a temperature controller. Solutions were excited at a wavelength of 330 nm in quartz cuvettes at various temperatures and their emission spectra were recorded.

References

1. Gandhi, M. V.; Thompson, B. S. *Smart materials and structures*; Chapman & Hall: London, **1992**.
2. Lutz, J.-F.; Andrieu, J.; Üzgün, S.; Rudolph, C.; Agarwal, S. *Macromolecules* **2007**, *40*, 8540-8543.
3. Schmaljohann, D. *Adv. Drug Delivery Rev.* **2006**, *58*, 1655-1670.
4. Ward, M. A.; Georgiou, T. K. *Polymers* **2011**, *3*, 1215-1242.
5. Zhang, J.; Wu, L.; Meng, F.; Wang, Z.; Deng, C.; Liu, H.; Zhong, Z. *Langmuir* **2011**, *28*, 2056-2065.
6. Yan, Q.; Xin, Y.; Zhou, R.; Yin, Y.; Yuan, J. *Chem. Commun.* **2011**, *47*, 9594-9596.
7. Zhao, Y. *Macromolecules* **2012**, *45*, 3647-3657.
8. Lin, S.; Theato, P. *Macromol. Rapid Commun.* **2013**, *34*, 1118-1133.
9. Han, D.; Tong, X.; Boissière, O.; Zhao, Y. *ACS Macro Lett.* **2011**, *1*, 57-61.
10. Levy, D.; Einhorn, S.; Avnir, D. *J. Non-Cryst. Solids* **1989**, *113*, 137-145.
11. Stewart, R. F.; Patent, U. S., Ed.; Landec Corporation: United States, **1993**.
12. Kessler, D.; Theato, P. *Macromol. Symp.* **2007**, 424-430.
13. Heksins, M.; Guillet, J. E. *J. Macromol. Sci. Chem.* **1968**, *2*, 1441-1455.
14. Xue, W.; Champ, S.; Huglin, M. B. *Polymer* **2001**, *42*, 2247-2250.
15. Monji, N.; Hoffman, A. *Appl. Biochem. Biotechnol.* **1987**, *14*, 107-120.
16. Kubota, K.; Fujishige, S.; Ando, I. *J. Phys. Chem.* **1990**, *94*, 5154-5158.
17. Kaneko, Y.; Yoshida, R.; Sakai, K.; Sakurai, Y.; Okano, T. *J. Membr. Sci.* **1995**, *101*, 13-22.

18. Yoshida, R.; Kaneko, Y.; Sakai, K.; Okano, T.; Sakurai, Y.; Bae, Y. H.; Kim, S. W. *J. Controlled Release* **1994**, *32*, 97-102.
19. Kokufuta, E. In *Responsive Gels: Volume Transitions II*, **1993**, p 157-177.
20. Lee, J.; Panzer, M. J.; He, Y.; Lodge, T. P.; Frisbie, C. D. *J. Am. Chem. Soc.* **2007**, *129*, 4532-4533.
21. Ueki, T.; Watanabe, M. *Macromolecules* **2008**, *41*, 3739-3749.
22. Wang, Z.-S.; Koumura, N.; Cui, Y.; Miyashita, M.; Mori, S.; Hara, K. *Chem. Mater.* **2009**, *21*, 2810-2816.
23. He, Y.; Lodge, T. P. *Chem. Commun.* **2007**, 2732-2734.
24. Marsh, K. N.; Boxall, J. A.; Lichtenthaler, R. *Fluid Phase Equilib.* **2001**, *219*, 93-98.
25. Huddleston, J. G.; Willauer, H. D.; Swatoski, R. P.; Visser, A. E.; Rogers, R. D. *Chem. Commun.* **1998**, 1765-1766.
26. Suarez, P. A. Z.; Dullius, J. E. L.; Einloft, S.; Desouza, R. F.; Dupont, J. *Polyhedron* **1996**, *12*, 1217-1219.
27. Tokuda, H.; Hayamizu, K.; Ishii, K.; Susan, M. A. B. H.; Watanabe, M. *J. Phys. Chem. B* **2004**, *108*, 16593-16600.
28. Tokuda, H.; Hayamizu, K.; Ishii, K.; Susan, M. A. B. H.; Watanabe, M. *J. Phys. Chem. B* **2005**, *109*, 6103-6110.
29. Tokuda, H.; Ishii, K.; Susan, M. A. B. H.; Tsuzuki, S.; Hayamizu, K.; Watanabe, M. *J. Phys. Chem. B* **2006**, *110*, 2833-2839.
30. Branco, L. C.; Rosa, J. N.; Ramos, J. J. M.; Afonso, C. A. M. *Chem. Eur. J.* **2002**, *8*, 3671-3677.
31. Park, S.; Kazlauskas, R. J. *J. Org. Chem.* **2001**, *66*, 8395-8401.

32. Swatloski, R. P.; Spear, S. K.; Holbrey, J. D.; Rogers, R. D. *J. Am. Chem. Soc.* **2002**, *124*, 4974.
33. Mouthrop, J. S.; Swatloski, R. P.; Moyna, G.; Rogers, R. D. *Chem. Commun.* **2005**, 1557.
34. Remsing, R. C.; Swatloski, R. P.; Rogers, R. D.; Moyna, G. *Chem. Commun.* **2006**, 1271.
35. Xie, H. B.; Li, S. H.; Zhang, S. B. *Green Chem.* **2005**, *7*, 606.
36. Fukushima, T.; Kosaka, A.; Ishimura, Y.; Yamamoto, T.; Takigawa, T.; Ishii, N.; Aida, T. *Science* **2003**, *300*, 2072.
37. Welton, T. *Chem. Rev.* **1999**, *99*, 2071-2083.
38. Ryan, J.; Aldabbagh, F.; Zetterlund, P. B.; Yamada, B. *Macromol. Rapid Commun.* **2004**, *25*, 930-934.
39. Kubisa, P. *Prog. Polym. Sci.* **2004**, *29*, 3-12.
40. Siegmann, R.; Jeličić, A.; Beuermann, S. *Macromol. Chem. Phys.* **2010**, *211*, 546-562.
41. Johnston-Hall, G.; Harjani, J. R.; Scammells, P. J.; Monteiro, M. J. *Macromolecules* **2009**, *42*, 1604-1609.
42. Flory, P. J. *J. Chem. Phys.* **1942**, *10*, 51.
43. Huggins, M. L. *Ann. N.Y. Acad. Sci.* **1942**, *42*, 1.
44. Huggins, M. L. *J. Phys. Chem.* **1942**, *46*, 151.
45. Huggins, M. L. *J. Am. Chem. Soc.* **1942**, *64*, 1712.
46. Winnik, F. M. *Macromolecules* **1992**, *25*, 6007-6017.
47. Zhang, C.; Maric, M. *Polymers* **2011**, *3*, 1398-1422.
48. Lessard, B.; Marić, M. *J. Polym. Sci. A: Polym. Chem.* **2011**, *49*, 5270-5283.
49. Lutz, J.-F.; Akdemir, Ö.; Hoth, A. *J. Am. Chem. Soc.* **2006**, *128*, 13046-13047.
50. Lessard, B. H.; Ling, E. J. Y.; Marić, M. *Macromolecules* **2012**, *45*, 1879-1891.

51. Eggenhuisen, T. M.; Becer, C. R.; Fijten, M. W. M.; Eckardt, R.; Hoogenboom, R.; Schubert, U. S. *Macromolecules* **2008**, *41*, 5132-5140.
52. Savelyeva, X.; Lessard, B. H.; Marić, M. *Macromol. React. Eng.* **2012**, *6*, 200-212.
53. Lessard, B.; Savelyeva, X.; Maric, M. *Polymer* **2012**, *53*, 5649-5656.
54. Liu, H. Y.; Zhu, X. X. *Polymer* **1999**, *40*, 6985-6990.
55. Laschewsky, A.; Rekaï, E. D.; Wischerhoff, E. *Macromol. Chem. Phys.* **2001**, *202*, 276-286.
56. Jeong, B.; Gutowska, A. *Trends Biotechnol.* **2002**, *20*, 305-311.
57. Xu, F.-J.; Li, H.; Li, J.; Zhang, Z.; Kang, E.-T.; Neoh, K.-G. *Biomaterials* **2008**, *29*, 3023-3033.
58. Ueki, T.; Watanabe, M. *Chem. Lett.* **2006**, *35*, 964.
59. Ueki, T.; Watanabe, M.; Lodge, T. P. *Macromolecules* **2009**, *42*, 1315-1320.
60. Ueki, T.; Karino, T.; Kobayashi, Y.; Shibayama, M.; Watanabe, M. *J. Phys. Chem. B* **2007**, *111*, 4750-4754.
61. Ueki, T.; Arai, A. A.; Kodama, K.; Kaino, S.; Takada, N.; Morita, T.; Nishikawa, K.; Watanabe, M. *Pure Appl. Chem.* **2009**, *81*, 1829-1841.
62. Fujii, K.; Ueki, T.; Niitsuma, K.; Matsunaga, T.; Watanabe, M.; Shibayama, M. *Polymer* **2011**, *52*, 1589-1595.
63. Lee, H.-N.; Lodge, T. P. *J. Phys. Chem. B* **2011**, *115*, 1971-1977.
64. Lee, H.-N.; Lodge, T. P. *J. Phys. Chem. Lett.* **2010**, *1*, 1962-1966.
65. Jin, H.; O'Hare, B.; Dong, J.; Arzhantsev, S.; Baker, G. A.; Wishart, J. F.; Benesi, A. J.; Maroncelli, M. *J. Phys. Chem. B* **2007**, *112*, 81-92.

66. Santos, L. M. N. B. F.; Canongia Lopes, J. N.; Coutinho, J. A. P.; Esperanca, J. M. S. S.; Gomes, L. R.; Marrucho, I. M.; Rebelo, L. P. N. *J. Am. Chem. Soc.* **2006**, *129*, 284-285.
67. Swiderski, K.; McLean, A.; Gordon, C. M.; Vaughan, D. H. *Chem. Commun.* **2004**, 2178-2179.
68. Lee, S. H.; Lee, S. B. *Chem. Commun.* **2005**, 3469-3471.
69. Liu, Q.; Yu, Z.; Ni, P. *Colloid Polym. Sci.* **2004**, *282*, 387-393.
70. Lessard, D. G.; Ousalem, M.; Zhu, X. X. *Can. J. Chemistry* **2001**, *79*, 1870-1874.
71. Winnik, F. M.; Ringsdorf, H.; Venzmer, J. *Macromolecules* **1990**, *23*, 2415-2416.
72. Schild, H. G.; Muthukumar, M.; Tirrell, D. A. *Macromolecules* **1991**, *24*, 948-952.
73. Liu, X.-M.; Wang, L.-S.; Wang, L.; Huang, J.; He, C. *Biomaterials* **2004**, *25*, 5659-5666.
74. Patterson, D. *Macromolecules* **1969**, *2*, 672-677.
75. Xia, Y.; Yin, X.; Burke, N. A. D.; Stöver, H. D. H. *Macromolecules* **2005**, *38*, 5937-5943.
76. Creutz, S.; Teyssié, P.; Jérôme, R. *Macromolecules* **1997**, *30*, 6-9.
77. Bütün, V.; Armes, S. P.; Billingham, N. C. *Polymer* **2001**, *42*, 5993-6008.
78. Flory, P. J. *J. Am. Chem. Soc.* **1936**, *58*, 1877-1885.
79. Xue, W.; Huglin, M. B.; Jones, T. G. J. *Macromol. Chem. Phys.* **2003**, *204*, 1956-1965.
80. Laukkanen, A.; Valtola, L.; Winnik, F. M.; Tenhu, H. *Macromolecules* **2004**, *37*, 2268-2274.
81. Otake, K.; Inomata, H.; Konno, M.; Saito, S. *Macromolecules* **1990**, *23*, 283-289.
82. Schild, H. G.; Tirrell, D. A. *J. Phys. Chem.* **1990**, *94*, 4352-4356.
83. Tong, Z.; Zeng, F.; Zheng, X.; Sato, T. *Macromolecules* **1999**, *32*, 4488-4490.
84. Fujishige, S.; Kubota, K.; Ando, I. *J. Phys. Chem.* **1989**, *93*, 3311-3313.

85. Aoshima, S.; Oda, H.; Kobayashi, E. *J. Polym. Sci. A: Polym. Chem.* **1992**, *30*, 2407-2413.
86. Szwarc, M.; Levy, M.; Milkovich, R. *J. Am. Chem. Soc.* **1956**, *78*, 2656-2657.
87. Mays, J. W.; Hadjichristidis, N. *Polym. Bull.* **1989**, *22*, 471.
88. Conlon, D. A.; Crivello, J. V.; Lee, J. L.; O'Brien, M. J. *Macromolecules* **1989**, *22*, 509.
89. Konigsberg, I.; Jagur-Grodzinski, J. *J. Polym. Sci. Polym. Chem. Ed.* **1983**, *21*, 2535.
90. Fetters, L. J.; Morton, M. *Macromolecules* **1969**, *2*, 453.
91. Young, R. N.; Quirk, R. P.; Fetters, L. J. *J. Adv. Polym. Sci.* **1984**, *56*, 1.
92. Blondin, D.; Regis, J.; Prud'homme, J. *J. Macromolecules* **1974**, *7*, 187.
93. Suzuki, T.; Tsuji, Y.; Tagekami, Y.; Harwood, H. J. *Macromolecules* **1979**, *12*, 234.
94. Hatada, K.; Kitayama, T.; Ute, K. *Prog. Polym. Sci.* **1988**, *13*, 189.
95. Yuki, H.; Hatada, K. *Adv. Polym. Sci.* **1979**, *31*, 1.
96. Allen, R. D.; Long, T. E.; McGrath, J. E. *Polym. Bull.* **1986**, *15*, 127.
97. Luxton, A. R.; Quig, A.; Delxaux, M.-J.; Fetters, L. J. *J. Polymer* **1978**, *19*, 1320.
98. Muller, M.; Lenz, R. W. *Makromol. Chem.* **1989**, *190*, 1153.
99. Kricheldorf, H. R.; Berl, M.; Scharnagl, N. *Macromolecules* **1988**, *21*, 286.
100. Hadjichristidis, N.; Iatrou, H.; Pispas, S.; Pitsikalis, M. *J. Polym. Sci. A: Polym. Chem.* **2000**, *38*, 3211-3234.
101. Greszta, D.; Mardare, D.; Matyjaszewski, K. *Macromolecules* **1994**, *27*, 638-644.
102. Spanswick, J.; Pike, B. In *Controlled/Living Radical Polymerization: Progress in ATRP*; American Chemical Society: Washington DC, **2009**, p 385-396.
103. Couvreur, L.; Lefay, C.; Belleney, J.; Charleux, B.; Guerret, O.; Magnet, S. *Macromolecules* **2003**, *36*, 8260-8267.

104. Charleux, B.; Nicolas, J.; Guerret, O. *Macromolecules* **2005**, *38*, 5485-5492.
105. Diaz, T.; Fischer, A.; Jonquieres, A.; Brembilla, A.; Lochon, P. *Macromolecules* **2003**, *36*, 2235-2241.
106. Dire, C.; Charleux, B.; Magnet, S.; Couvreur, L. *Macromolecules* **2007**, *40*, 1897-1903.
107. Farcet, C.; Charleux, B.; Pirri, R. *Macromolecules* **2001**, *34*, 3823-3826.
108. Gibbons, O.; Carroll, W. M.; Aldabbagh, F.; Yamada, B. *J. Polym. Sci. Part A: Polym. Chem.* **2006**, *44*, 6410-6418.
109. Guillaneuf, Y.; Gigmes, D.; Marque, S. R. A.; Astolfi, P.; Greci, L.; Tordo, P.; Bertin, D. *Macromolecules* **2007**, *40*, 3108-3114.
110. Lessard, B.; Graffe, A.; Maric, M. *Macromolecules* **2007**, *40*, 9284-9292.
111. Matyjaszewski, K.; Xia, J. *Chemical Reviews* **2001**, *101*, 2921-2990.
112. Wang, J.-S.; Matyjaszewski, K. *J. Am. Chem. Soc.* **1995**, *117*, 5614-5615.
113. Matyjaszewski, K.; Wei, M.; Xia, J.; McDermott, N. E. *Macromolecules* **1997**, *30*, 8161-8164.
114. Wang, J.-S.; Matyjaszewski, K. *Macromolecules* **1995**, *28*, 7901-7910.
115. Chiefari, J.; Chong, Y. K.; Ercole, F.; Krstina, J.; Jeffery, J.; Le, T. P. T.; Mayadunne, R. T. A.; Meijs, G. F.; Moad, C. L.; Moad, G.; Rizzardo, E.; Thang, S. H. *Macromolecules* **1998**, *31*, 5559-5562.
116. Mayadunne, R. T. A.; Rizzardo, E.; Chiefari, J.; Krstina, J.; Moad, G.; Postma, A.; Thang, S. H. *Macromolecules* **2000**, *33*, 243-245.
117. Perrier, S.; Davis, T. P.; Carmichael, A. J.; Haddleton, D. M. *Eur. Polym. J.* **2003**, *39*, 417-422.
118. Dubois, P.; Jerome, R.; Senninger, T.; Teyssie, P. *Macromolecules* **1998**, *31*, 545-547.

119. Barner-Kowollik, C.; Perrier, S. *J. Polym. Sci. Part A: Polym. Chem.* **2008**, *46*, 5715-5723.
120. Matyjaszewski, K.; Pintauer, T.; Gaynor, S. *Macromolecules* **2000**, *33*, 1476-1478.
121. Honigfort, M. E.; Brittain, W. J.; Bosanac, T.; Wilcox, C. S. *Macromolecules* **2002**, *35*, 4849-4851.
122. Willcock, H.; O'Reilly, R. K. *Polym. Chem.* **2010**, *1*, 149-157.
123. Marestin, C.; Noel, C.; Guyot, A.; Claverie, J. *Macromolecules* **1998**, *31*, 4041-4044.
124. Gabaston, L. I.; Jackson, R. A.; Armes, S. P. *Macromolecules* **1998**, *31*, 2883-2888.
125. Benoit, D.; Chaplinski, V.; Braslau, R.; Hawker, C. J. *J. Am. Chem. Soc.* **1999**, *121*, 3904-3920.
126. Benoit, D.; Grimaldi, S.; Robin, S.; Finet, J.-P.; Tordo, P.; Gnanou, Y. *J. Am. Chem. Soc.* **2000**, *122*, 5929-5939.
127. Lessard, B.; Schmidt, S. C.; Maric, M. *Macromolecules* **2008**, *41*, 3446-3454.
128. Benoit, D.; Harth, E.; Fox, P.; Waymouth, R. M.; Hawker, C. J. *Macromolecules* **2000**, *33*, 363-370.
129. Tang, C.; Kowalewski, T.; Matyjaszewski, K. *Macromolecules* **2003**, *36*, 1465-1473.
130. Nicolas, J.; Dire, C.; Mueller, L.; Belleney, J.; Charleux, B.; Marque, S. R. A.; Bertin, D.; Magnet, S.; Couvreur, L. *Macromolecules* **2006**, *39*, 8274-8282.
131. Chenal, M.; Mura, S.; Marchal, C.; Gigmes, D.; Charleux, B.; Fattal, E.; Couvreur, P.; Nicolas, J. *Macromolecules* **2010**, *43*, 9291-9303.
132. Nicolas, J.; Couvreur, P.; Charleux, B. *Macromolecules* **2008**, *41*, 3758-3761.
133. Grubbs, R. B. *Polym. Rev.* **2011**, *51*, 104-137.
134. Nagai, K. *Appl. Catal. A: Gen.* **2001**, *221*, 367-377.

135. Lekisvili, N. V. J. S. *Polymers and polymeric materials for fiber and gradient optics*; VSP: Utrecht, **2002**.
136. Moad, G.; Anderson, A. G.; Ercole, F.; Johnson, C. H. J.; Krstina, J.; Moad, C. L.; Rizzardo, E.; Spurling Thomas, H.; Thang San, H. *ACS Symp. Ser.* **1998**, *685*, 332-360.
137. Dire, C.; Belleney, J.; Nicolas, J.; Bertin, D.; Magnet, S.; Charleux, B. *J. Polym. Sci. A: Polym. Chem.* **2008**, *46*, 6333-6345.
138. Guillaneuf, Y.; Gigmes, D.; Marque, S. R. A.; Tordo, P.; Bertin, D. *Macromol. Chem. Phys.* **2006**, *207*, 1278-1288.
139. Ananchenko, G. S.; Souaille, M.; Fischer, H.; LeMercier, C.; Tordo, P. *J. Polym. Sci. A: Polym. Chem.* **2002**, *40*, 3264-3283.
140. Nicolas, J.; Mueller, L.; Dire, C.; Matyjaszewski, K.; Charleux, B. *Macromolecules* **2009**, *42*, 4470-4478.
141. Lessard, B.; Maric, M. *J. Polym. Sci. A: Polym. Chem.* **2009**, *47*, 2574-2588.
142. Zhang, C.; Lessard, B.; Maric, M. *Macromol. React. Eng.* **2010**, *4*, 415-423.
143. Nicolas, J.; Brusseau, S.; Charleux, B. *J. Polym. Sci. A: Polym. Chem.* **2010**, *48*, 34-47.
144. Brusseau, S.; Belleney, J.; Magnet, S.; Couvreur, L.; Charleux, B. *Polym. Chem.* **2010**, *1*, 720-729.
145. Becer, C. R.; Kokado, K.; Weber, C.; Can, A.; Chujo, Y.; Schubert, U. S. *J. Polym. Sci. A: Polym. Chem.* **2010**, *48*, 1278-1286.
146. Lessard, B.; Ling, E. J. Y.; Morin, M. S. T.; Marić, M. *J. Polym. Sci. A: Polym. Chem.* **2011**, *49*, 1033-1045.
147. Lessard, B.; Guillaneuf, Y.; Mathew, M.; Liang, K.; Clement, J.-L.; Gigmes, D.; Hutchinson, R. A.; Maric, M. *Macromolecules* **2013**.

148. Zhang, C.; Maric, M. *J. Polym. Sci. Part A: Polym. Chem.* **2013**, *51*, 4702-4715.
149. Zhang, C.; Maric, M. *J. Polym. Sci. Part A: Polym. Chem.* **2012**, *50*, 4341-4357.
150. Greene, A. C.; Grubbs, R. B. *Macromolecules* **2010**, *43*, 10320-10325.
151. Chenal, M.; Boursier, C.; Guillaneuf, Y.; Taverna, M.; Couvreur, P.; Nicolas, J. *Polym. Chem.* **2011**, *2*, 1523-1530.
152. Ahn, S.-k.; Kasi, R. M.; Kim, S.-C.; Sharma, N.; Zhou, Y. *Soft Matter* **2008**, *4*, 1151-1157.
153. Alarcon, C. d. l. H.; Pennadam, S.; Alexander, C. *Chem. Soc. Rev.* **2005**, *34*, 276-285.
154. Hoffman, A. S. *Macromol. Symp.* **1995**, *98*, 645-664.
155. Lutz, J.-F. *J. Polym. Sci. Part A: Polym. Chem.* **2008**, *46*, 3459-3470.
156. Gohy, J.-F.; Antoun, S.; Jerome, R. *Macromolecules* **2001**, *34*, 7435-7440.
157. Fournier, D.; Hoogenboom, R.; Thijs, H. M. L.; Paulus, R. M.; Schubert, U. S. *Macromolecules* **2007**, *40*, 915-920.
158. Emileh, A.; Vasheghani-Farahani, E.; Imani, M. *Eur. Polym. J.* **2007**, *43*, 1986-1995.
159. Feil, H.; Bae, Y. H.; Feijen, J.; Kim, S. W. *Macromolecules* **1992**, *25*, 5528-5530.
160. Krasia, T. C.; Patrickios, C. S. *Polymer* **2002**, *43*, 2917-2920.
161. Matyjaszewski, K. *Curr. Opin. Solid State Mater. Sci.* **1996**, *1*, 769-776.
162. Zhang, X.; Xia, J.; Matyjaszewski, K. *Macromolecules* **1998**, *31*, 5167-5169.
163. Lee, S. B.; Russell, A. J.; Matyjaszewski, K. *Biomacromolecules* **2003**, *4*, 1386-1393.
164. Monge, S.; Darcos, V.; Haddleton, D. M. *J. Polym. Sci. Part A: Polym. Chem.* **2004**, *42*, 6299-6308.
165. Perrier, S.; Takolpuckdee, P. *J. Polym. Sci. Part A: Polym. Chem.* **2005**, *43*, 5347-5393.
166. Alam, M. N.; Zetterlund, P. B.; Okubo, M. *Polymer* **2008**, *49*, 3428-3435.

167. Beuermann, S.; Buback, M. *Prog. Polym. Sci.* **2002**, *27*, 191-254.
168. Anderson, G. W.; Zimmerman, J. E.; Callahan, F. M. *J. Am. Chem. Soc.* **1964**, *86*, 1839-1842.
169. Lecolley, F.; Tao, L.; Mantovani, G.; Durkin, I.; Lautru, S.; Haddleton, D. M. *Chem. Commun.* **2004**, 2026-2027.
170. Bathfield, M.; D'Agosto, F.; Spitz, R.; Charreyre, M.-T.; Delair, T. *J. Am. Chem. Soc.* **2006**, *128*, 2546-2547.
171. Vinas, J.; Chagneux, N.; Gignes, D.; Trimaille, T.; Favier, A.; Bertin, D. *Polymer* **2008**, *49*, 3639-3647.
172. Moayeri, A.; Lessard, B.; Maric, M. *Polym. Chem.* **2011**.
173. Lokaj, J.; Vlcek, P.; Kriz, J. *Macromolecules* **1997**, *30*, 7644-7646.
174. Zhang, X.; Matyjaszewski, K. *Macromolecules* **1999**, *32*, 1763-1766.
175. Burguiere, C.; Dourges, M.-A.; Charleux, B.; Vairon, J.-P. *Macromolecules* **1999**, *32*, 3883-3890.
176. Moad, G.; Anderson Albert, G.; Ercole, F.; Johnson Charles, H. J.; Krstina, J.; Moad Catherine, L.; Rizzardo, E.; Spurling Thomas, H.; Thang San, H. In *Controlled Radical Polymerization*; ACS Symp.Ser., **1998**, p 332-360.
177. Marque, S.; Le Mercier, C.; Tordo, P.; Fischer, H. *Macromolecules* **2000**, *33*, 4403-4410.
178. Lessard, B.; Maric, M. *Macromolecules* **2008**, *41*, 7870-7880.
179. Lutz, J.-F.; Hoth, A. *Macromolecules* **2006**, *39*, 893-896.
180. Okabe, S.; Seno, K.-i.; Kanaoka, S.; Aoshima, S.; Shibayama, M. *Macromolecules* **2006**, *39*, 1592-1597.
181. Huang, J.; Matyjaszewski, K. *Macromolecules* **2005**, *38*, 3577-3583.

182. Hua, F.; Jiang, X.; Li, D.; Zhao, B. *J. Polym. Sci. Part A: Polym. Chem.* **2006**, *44*, 2454-2467.
183. Schild, H. G. *Prog. Polym. Sci.* **1992**, *17*, 163-249.
184. Taylor, L. D.; Cerankowski, L. D. *J. Polym. Sci.: Polym. Chem. Ed.* **1975**, *13*, 2551-2570.
185. Braun, D.; Czerwinski, W.; Disselhoff, G.; Tüdös, F.; Kelen, T.; Turcsányi, B. *Die Angewandte Makromolekulare Chemie* **1984**, *125*, 161-205.
186. Park, J.-S.; Kataoka, K. *Macromolecules* **2006**, *39*, 6622-6630.
187. Park, J.-S.; Kataoka, K. *Macromolecules* **2007**, *40*, 3599-3609.
188. Burillo, G.; Bucio, E.; Arenas, E.; Lopez, G. P. *Macromol. Mater. Eng.* **2007**, *292*, 214-219.
189. Van Beylen, M.; Bywater, S.; Smets, G.; Szwarc, M.; Worsfold, D.; Springer Berlin / Heidelberg, **1988**, p 87-143.
190. Schumers, J.-M.; Fustin, C.-A.; Can, A.; Hoogenboom, R.; Schubert, U. S.; Gohy, J.-F. *J. Polym. Sci. A: Polym. Chem.* **2009**, *47*, 6504-6513.
191. Greszta, D.; Matyjaszewski, K. *Macromolecules* **1996**, *29*, 7661-7670.
192. Barker, I. C.; Cowie, J. M. G.; Huckerby, T. N.; Shaw, D. A.; Soutar, I.; Swanson, L. *Macromolecules* **2003**, *36*, 7765-7770.
193. Lokaj, J.; Holler, P. *J. App. Polym. Sci.* **2001**, *80*, 2024-2030.
194. Chalari, I.; Pispas, S.; Hadjichristidis, N. *J. Polym. Sci. A: Polym. Chem.* **2001**, *39*, 2889-2895.
195. Martin, T. J.; Procházka, K.; Munk, P.; Webber, S. E. *Macromolecules* **1996**, *29*, 6071-6073.

196. Borchert, U.; Lipprandt, U.; Bilanz, M.; Kimpfler, A.; Rank, A.; Peschka-Süss, R.; Schubert, R.; Lindner, P.; Förster, S. *Langmuir* **2006**, *22*, 5843-5847.
197. Bekturov, E. A.; Bimendina, L. A. *J. Macromol. Sci. C: Polym. Rev.* **1997**, *37*, 501-518.
198. Harrisson, S.; Couvreur, P.; Nicolas, J. *Polym. Chem.* **2011**, *2*, 1859-1865.
199. Buback, M.; Gilbert, R. G.; Hutchinson, R. A.; Klumperman, B.; Kuchta, F.-D.; Manders, B. G.; O'Driscoll, K. F.; Russell, G. T.; Schweer, J. *Macromol. Chem. Phys.* **1995**, *196*, 3267-3280.
200. Beuermann, S.; Buback, M.; Davis, T. P.; Gilbert, R. G.; Hutchinson, R. A.; Kajiwara, A.; Klumperman, B.; Russell, G. T. *Macromol. Chem. Phys.* **2000**, *201*, 1355-1364.
201. Bengough, W. I.; Henderson, W. *Faraday Soc.* **1965**, *61*, 141-149.
202. Zetterlund, P. B.; Saka, Y.; McHale, R.; Nakamura, T.; Aldabbagh, F.; Okubo, M. *Polymer* **2006**, *47*, 7900-7908.
203. Lacroix-Desmazes, P.; Lutz, J. F.; Chauvin, F.; Severac, R.; Boutevin, B. *Macromolecules* **2001**, *34*, 8866-8871.
204. Teoh, R. L.; Guice, K. B.; Loo, Y.-L. *Macromolecules* **2006**, *39*, 8609-8615.
205. Puterman, M.; Koenig, J. L.; Lando, J. B. *J. Macromol. Sci., B* **1979**, *16*, 89-116.
206. López-Pérez, P. M.; da Silva, R. M. P.; Pashkuleva, I.; Parra, F.; Reis, R. L.; San Roman, J. *Langmuir* **2010**, *26*, 5934-5941.
207. Hoogeveen, N. G.; Stuart, M. A. C.; Fleer, G. J.; Frank, W.; Arnold, M. *Macromol. Chem. Phys.* **1996**, *197*, 2553-2564.
208. Kirsh, Y. E.; Komarova, O. P.; Lukovkin, G. M. *Eur. Polym. J.* **1973**, *9*, 1405-1415.
209. Wang, X.; Qiu, X.; Wu, C. *Macromolecules* **1998**, *31*, 2972-2976.
210. Lee, A. S.; Gast, A. P.; Bütün, V.; Armes, S. P. *Macromolecules* **1999**, *32*, 4302-4310.

211. Alexandridis, P.; Holzwarth, J. F.; Hatton, T. A. *Macromolecules* **1994**, *27*, 2414-2425.
212. Ueki, T.; Watanabe, M. *Langmuir* **2007**, *23*, 988-990.
213. Schierholz, K.; Givehchi, M.; Fabre, P.; Nallet, F.; Papon, E.; Guerret, O.; Gnanou, Y. *Macromolecules* **2003**, *36*, 5995-5999.
214. Moad, G.; Solomon, D. H. *The Chemistry of Radical Polymerization*, 2nd Ed.; Gulf Professional Publishing, **2006**.
215. Mchale, R.; Aldabbagh, F.; Zetterlund, P. B. *J. Polym. Sci. A: Polym. Chem.* **2007**, *45*, 2194-2203.
216. Hutchinson, R. A.; Beuermann, S.; Paquet, D. A.; McMinn, J. H.; Jackson, C. *Macromolecules* **1998**, *31*, 1542-1547.
217. Tamura, S.; Ueki, T.; Ueno, K.; Kodama, K.; Watanabe, M. *Macromolecules* **2009**, *42*, 6239-6244.
218. Lu, J.; Yan, F.; Texter, J. *Prog. Polym. Sci.* **2009**, *34*, 431-448.
219. Singh, B.; Sekhon, S. S. *J. Phys. Chem. B* **2005**, *109*, 16539-16543.
220. Zetterlund, P. B.; Yamazoe, H.; Yamauchi, S.; Yamada, B. In *Advances in Controlled/Living Radical Polymerization*; American Chemical Society, **2003**, p 72-85.
221. Coote, M. L.; Johnston, L. P. M.; Davis, T. P. *Macromolecules* **1997**, *30*, 8191-8204.
222. Coote, M. L.; Davis, T. P. *Macromolecules* **1999**, *32*, 3626-3636.
223. Mayo, F. R., Lewis, F.M. *J. Am. Chem. Soc.* **1944**, *66*, 1594-1601.
224. Fineman, M.; Ross, S. D. *J. Polym. Sci.* **1950**, *5*, 259-262.
225. Kelen, T.; Tüdös, F. *Reaction Kinetics and Catalysis Letters* **1974**, *1*, 487-492.
226. Tidwell, P. W. M., G.A. *J. Polym. Sci. A* **1965**, *3*, 369.
227. Takayuki, O., Toshio, I., Minoru, I. *Polymer Letters* **1965**, *3*, 113-117.

228. Mott, G.; TH Darmstadt, **1973**.
229. Beaudoin, E.; Bertin, D.; Gigmes, D.; Marque, S. R. A.; Siri, D.; Tordo, P. *Eur. J. Org. Chem.* **2006**, *2006*, 1755-1768.
230. Wei, D.; Ivaska, A. *Anal. Chim. Acta* **2008**, *607*, 126-135.
231. Hara, K.; Wang, Z.-S.; Cui, Y.; Furube, A.; Koumura, N. *Energy Environ. Sci.* **2009**, *2*, 1109-1114.
232. He, Y.; Boswell, P. G.; Buhlmann, P.; Lodge, T. P. *J. Phys. Chem. B* **2006**, *111*, 4645-4652.
233. Kitazawa, Y.; Ueki, T.; Niitsuma, K.; Imaizumi, S.; Lodge, T. P.; Watanabe, M. *Soft Matter* **2012**, *8*, 8067-8074.
234. Susan, M. A. B. H.; Kaneko, T.; Noda, A.; Watanabe, M. *J. Am. Chem. Soc.* **2005**, *127*, 4976-4983.
235. Harner, J. M.; Hoagland, D. A. *J. Phys. Chem. B* **2010**, *114*, 3411-3418.
236. Dong, B.; Gao, Y. Ä.; Su, Y.; Zheng, L.; Xu, J.; Inoue, T. *J. Phys. Chem. B* **2009**, *114*, 340-348.
237. Burns, C. T.; Lee, S.; Seifert, S.; Firestone, M. A. *Polym. Adv. Technol.* **2008**, *19*, 1369-1382.
238. Kodama, K.; Nanashima, H.; Ueki, T.; Kokubo, H.; Watanabe, M. *Langmuir* **2009**, *25*, 3820-3824.
239. Oter, O.; Ertekin, K.; Topkaya, D.; Alp, S. *Sens. Actuators, B* **2006**, *117*, 295-301.
240. Li, J.; Huang, M.; Liu, X.; Wei, H.; Xu, Y.; Xu, G.; Wang, E. *Analyst* **2007**, *132*, 687-691.
241. Zhou, Y.; Guo, W.; Cheng, J.; Liu, Y.; Li, J.; Jiang, L. *Adv. Mater.* **2012**, *24*, 962-967.

242. Brandrup, J.; Immergut, E. H.; Grulke, E. A.; Abe, A.; Bloch, D. R. *Polymer Handbook* (4th edition); John Wiley & Sons. Inc., **1999**.
243. Lessard, B. H.; Guillaneuf, Y.; Mathew, M.; Liang, K.; Clement, J.-L.; Gimes, D.; Hutchinson, R. A.; Maric, M. *Macromolecules* **2013**, *46*, 805-813.
244. Tsuda, R.; Kodama, K.; Ueki, T.; Kokubo, H.; Imabayashi, S.-i.; Watanabe, M. *Chem. Commun.* **2008**, 4939-4941.
245. Cheng, H.; Shen, L.; Wu, C. *Macromolecules* **2006**, *39*, 2325-2329.
246. Chen, H.; Li, J.; Ding, Y.; Zhang, G.; Zhang, Q.; Wu, C. *Macromolecules* **2005**, *38*, 4403-4408.
247. Hunter, C. A.; Sanders, J. K. M. *J. Am. Chem. Soc.* **1990**, *112*, 5525-5534.
248. Suzuki, I.; Nakayama, C.; Ui, M.; Hirose, K.; Yamauchi, A. *Analytical Sciences : the International Journal of the Japan Society for Analytical Chemistry* **2007**, *23*, 249-251.
249. Idziak, I.; Avoce, D.; Lessard, D.; Gravel, D.; Zhu, X. X. *Macromolecules* **1999**, *32*, 1260-1263.
250. Samanta, A. *J. Phys. Chem. B* **2006**, *110*, 13704-13716.
251. Förster, T. *Discuss. Faraday Soc.* **1959**, *27*, 7-17.
252. Clapp, A. R.; Medintz, I. L.; Mattoussi, H. *ChemPhysChem* **2006**, *7*, 47-57.
253. Chiu, Y.-C.; Kuo, C.-C.; Hsu, J.-C.; Chen, W.-C. *ACS Appl Mater Interface* **2010**, *2*, 3340-3347.
254. Nagai, A.; Kokado, K.; Miyake, J.; Cyujo, Y. *J. Polym. Sci. A: Polym. Chem.* **2010**, *48*, 627-634.
255. Bawa, P.; Pillay, V.; Choonara, Y. E.; Toit, L. C. d. *Biomed. Mater.* **2009**, *4*, 1-15.
256. Harrison, S.; Mackenzie, S. R.; Haddleton, D. M. *Macromolecules* **2003**, *36*, 5072-5075.

257. He, Y.; Li, Z.; Simone, P.; Lodge, T. P. *J. Am. Chem. Soc.* **2006**, *128*, 2745-2750.
258. Hawker, C. J.; Bosman, A. W.; Harth, E. *Chem. Rev.* **2001**, *101*, 3661-3688.
259. Nicolas, J.; Guillaneuf, Y.; Lefay, C.; Bertin, D.; Gigmes, D.; Charleux, B. *Prog. Polym. Sci.* **2013**, *38*, 63-235.
260. Gota, C.; Okabe, K.; Funatsu, T.; Harada, Y.; Uchiyama, S. *J. Am. Chem. Soc.* **2009**, *131*, 2766-2767.
261. Cui, K.; Zhu, D.; Cui, W.; Lu, X.; Lu, Q. *J. Phys. Chem. C* **2012**, *116*, 6077-6082.
262. Gota, C.; Uchiyama, S.; Ohwada, T. *Analyst* **2007**, *132*, 121-126.
263. Uchiyama, S.; Matsumura, Y.; de Silva, A. P.; Iwai, K. *Anal. Chem.* **2003**, *75*, 5926-5935.
264. Horton, J. M.; Bao, C.; Bai, Z.; Lodge, T. P.; Zhao, B. *Langmuir* **2011**, *27*, 13324-13334.
265. Adam, G.; Gibbs, J. H. *J. Chem. Phys.* **1965**, *43*, 139-146.
266. Horton, J. M.; Bai, Z.; Jiang, X.; Li, D.; Lodge, T. P.; Zhao, B. *Langmuir* **2010**, *27*, 2019-2027.
267. He, Y.; Lodge, T. P. *Macromolecules* **2008**, *41*, 167-174.
268. Hoogenboom, R.; Popescu, D.; Steinhauer, W.; Keul, H.; Möller, M. *Macromol. Rapid Commun.* **2009**, *30*, 2042-2048.
269. Hiemenz, P. C.; Lodge, T. P. *Polymer Chemistry*; CRC Press: United States, **2007**.
270. Link, S.; El-Sayed, M. A. *Int. Rev. Phys. Chem.* **2000**, *19*, 409-453.
271. Crank, J. *J. Polym. Sci.* **1953**, *11*, 151-168.
272. Rouse, P. E. *J. Chem. Phys.* **1953**, *21*, 1272-1280.
273. Zurick, K. M.; Bernards, M. *J. Appl. Polym. Sci.* **2014**, *131*, n/a-n/a.
274. Zhang, S.; Lee, K. H.; Frisbie, C. D.; Lodge, T. P. *Macromolecules* **2011**, *44*, 940-949.

275. Klingshirn, M. A.; Spear, S. K.; Subramanian, R.; Holbrey, J. D.; Huddleston, J. G.; Rogers, R. D. *Chem. Mater.* **2004**, *16*, 3091-3097.
276. Koppel, D. E. *J. Chem. Phys.* **1972**, *57*, 4814-4820.
277. Babazadeh, M. *Polym. Degrad. Stab.* **2006**, *91*, 3245-3251.